Optimisation of a Power Distribution Network's Active Power Loss and Reliability Performance

Jiansong Ding

BEng (Honours)

Submitted for the Degree

of

Doctor of Philosophy

Institute for Energy and Environment

Department of Electronic and Electrical Engineering

University of Strathclyde

Glasgow G1 1XW

United Kingdom

June 2013

Acknowledgements

I would like to express my deep gratefulness to my supervisor Dr. K.R.W. Bell and for his continuous guidance, encouragement, helpful comments, kind advice and capable supervision throughout my PhD study.

I also wish sincerely to thank Dr. S.Strachan, Dr. I. Elders, Prof G.W.Ault, Prof. S.D.McArthur and D.Kadar, J.McWillam, C.Bayfield, J.Kirkwood of Scottish Power Energy Networks for their help and support in research aspects.

The Scottish Power Advanced Research Centre (SPARC) at the University of Strathclyde is acknowledged for the financial support for this research

Finally, I would like to thank my parents, Xiaoping Ding, Qiuyang Hu for their love, support and encouragement throughout my PhD study.

Abstract

The deregulation of UK power distribution market started in 1990. Due to the drivers from the regulator, DNOs need to invest appropriately and optimise network operation by innovations to satisfy the targets set by the industry regulator, the Office of Gas and Electricity Markets (Ofgem). Reduction of network losses and improvement of reliability of supply to customers are extremely important for distribution network operators (DNOs) to take into account when designing and operating their networks. They are important because of the need to minimise wasted energy and carbon emissions and to provide customers with an adequate level of service. Moreover, in Great Britain, Ofgem has implemented financial incentives with respect to these things.

This thesis describes an investigation of methods these have been developed to help DNOs improve their performance with respect to two particular incentives. The first relates to network losses; the second relates to reliability of supply to consumers.

A new loss optimisation algorithm by feeder reconfiguration based on graph theory and topology search techniques is developed in this thesis. By means of a directed exhaustive search of network configurations (and unlike a number of previous methods in the literature that rely on heuristics), this algorithm can find the global optimal result. In addition the results of the algorithm can be readily used in the solution of a multiobjective optimisation problem (optimisation both of *P* loss and reliability in this thesis). A new reliability evaluation and optimisation algorithm developed in this thesis is based on topology search techniques. This algorithm can not only calculate the reliability indices but, unlike previous approaches emerging from the academic literature, also determines the restoration method of each fault affected bus for a specific fault which is critical to determining the restoration time following a fault. The loss and reliability optimisation is developed to optimise both network's *P* loss and reliability performance. It can also provide a number of options regarding the configuration of the network, and suggests which are optimal with respect to either incentive or to both of them combined. An analytical tool developed to perform these algorithms is described. Case studies are presented to illustrate how

DNOs can use the analytical methods and tool developed in this thesis to accurately calculate the impacts of design or operation decisions on losses and reliability and thereby help in the identification of cost-effective network operation actions and longer-term investments.

Table of Contents

List of Figures

List of Tables

Abbreviations

CI	Customer interruptions
CML	Customer minutes lost
CB	Circuit breaker
cust	Customer
DisOPT	Distribution Network Optimisation Computer Program
h.	Hours
int.	Interruptions
IIS	Interruptions Incentive Scheme
mins.	Minutes
MVA	Mega Volt Amperes
MW	Megawatt
MVAr	Mega volt-ampere reactive
MWh	Megawatt Hours
Ofgem	Office of the Gas and Electricity Markets
P	Active power
Q	Reactive power
RC	Remote control switch
SPEN	Scottish Power Energy Networks
yr.	Year

Chapter 1 Introduction

Since the deregulation of UK power distribution market started in 1990, Distribution Network Operators (DNOs) have more pressures on their business [1]. Due to the drivers from the regulator, DNOs need to invest appropriately and optimise network operation by innovations to satisfy the targets set by the industry regulator. The chapter first briefly introduces the structure of the UK electricity distribution network and the role of the regulator. The remainder of this chapter provides background on the aims of the research described in this thesis.

1.1 Introduction to UK Electricity Distribution Networks

An electric power system has three main parts: generation, transmission and distribution [2]. The generation plant generates electricity from other energy, like wind, hydro, nuclear, etc. [3]. The transmission system transfers the electricity from generation plants to Grid Supply Points which are the connection points to the distribution network [4]. The electricity distribution network delivers energy from Grid Supply Points to customers except some very large ones that are directly connected to the transmission system [4]. The voltage levels of UK electricity distribution networks are 33kV and 22kV (EHV), 11kV and 6.6kV (HV) and 400 volts and 230 volts (LV) [4]. The lines of a distribution network can be cable or overhead line. Taking the networks of Scottish Power Distribution Ltd, as an example, the urban EHV circuits mainly consist of standard sized underground cables and the rural circuits are mainly overhead lines of three-phase wood pole construction without earth conductor; the urban HV networks mainly use standard size underground cables and the rural HV networks mainly use overhead line constructed as “a series of three phase main lines with radial spur lines branched off” [4]. For an urban LV network, the cable used can be 4-core separate earth cable (these generally correspond to earlier installations), 3-core combined neutral/earth cable (in later years), 3-core waveform distributor cable and concentric service cable [4]. The winding configurations of 33kV/11kV and 11kV/0.415kV transformers are both Dy11 [4]. Both urban and rural HV (11kV and 6.6kV) networks are operated radially [4]. The radial configuration is simple and has low cost [5]. The magnitude

of fault current in radial network decreases as the distance from the substation increases so the protection system can be coordinated in an effective way [6, 7]. For example, the protection equipment is segregated so that it can only trip the circuit it is associated with and a rural distribution area can be protected with non-directional time graded overcurrent protection scheme [8, 9]. But any fault on a radial connection completely disconnects customer downstream of the nearest circuit breaker whereas with a meshed arrangement, there would generally be another path that could continue to feed most customers without interruption. However, the latter arrangement would require more sophisticated protection to correctly identify the location of faults and more switches capable of interrupting fault current if the continuity of supply benefits are to be realised. Therefore, the practice of building distribution networks in mesh but operating them radially by normally open points is widely adopted [10].

1.2 The Regulator of UK Electricity Distribution Market

The liberalisation and privatisation of UK energy markets (gas and electricity) was begun in the 1980s [11]. Currently, the Office of Gas and Electricity Markets (Ofgem) is the UK government regulator which regulates the UK's electricity and gas markets [12]. The target of Ofgem is to protect the interests of customer and secure the energy supply of UK [12]. The electricity distribution sector is regulated by Ofgem as well. There are 14 electricity distribution network operator (DNO) areas for which there are distribution licences to operate in UK [13]. Their names (full and abbreviation) and locations in 2010-2011 are shown in Figure 1.1 [13].

All DNOs are subject to the electricity distribution price control by Ofgem. The price control sets the total revenues that DNOs may recover from their customers. The services and standards provided by DNOs must satisfy with those set out in their licences. The previous price control was Distribution Price Control Review 4 (DPCR4) which ran from 1st April 2005 to 31st March 2010 [14]. The recent price control is Distribution Price Control Review 5 (DPCR5) from 1st April 2010 to 31st March 2015 [15, 16]. Ofgem also sets some incentive schemes on DNOs [15]. Under these schemes, DNOs get rewards when their actual performance is better than the target. Otherwise, they need to pay penalties. Ofgem believes these schemes will

cause DNOs to provide better services to customers. This thesis studies power loss and the reliability of electricity distribution networks. The Losses Incentive Mechanism [1] and Interruption Incentive Scheme (IIS) are two of the incentive schemes, which set the loss and reliability targets respectively. These two schemes are briefly introduced in the next subsections. The thesis describes an investigation of methods which have been developed to help DNOs improve their performance with respect to these two particular incentives as they are the focus of the research in this thesis. The first relates to network losses; the second relates to reliability of supply to consumers.

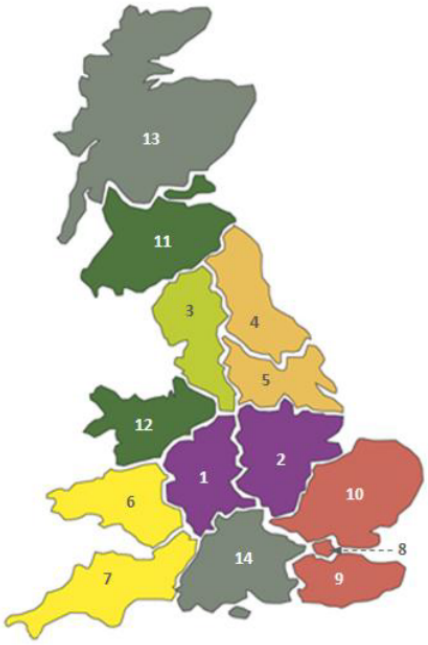

1. Central Networks[5]: West (CN West), now Western Power Distribution: West Midlands (WMID)
2. Central Networks[5]: East (CN East), now Western Power Distribution: East Midlands (EMID)
3. Electricity North West Limited (ENWL)
4. CE Electric UK[6]: Northern Electric Distribution Limited (NEDL), now Northern Powergrid: Northeast Ltd (NPGN)
5. CE Electric UK[6]: Yorkshire Electricity Distribution plc (YEDL), now Northern Powergrid: Yorkshire Plc (NPGY)
6. Western Power Distribution: South Wales (SWALES)
7. Western Power Distribution: South West (SWEST)
8. UK Power Networks[7]: London Power Networks (LPN)
9. UK Power Networks: South East Power Networks (SPN)
10. UK Power Networks: Eastern Power Networks (EPN)
11. Scottish Power: Distribution (SPD)
12. Scottish Power: Manweb (SPMW)
13. Scottish & Southern Energy: Hydro (SSEH)
14. Scottish & Southern Energy: Southern Electric Power Distribution (SSES).

Figure 1.1 Map of the 14 Distribution Network Operators' Location in UK [13]

[1] In 16th November 2012, Ofgem said it decided not to activate the Losses Incentive Mechanism in the Fifth Distribution Price Control (DPCR5) [16]. However, the work described in the thesis is based on the situation that prevailed up to November 2012. Moreover, the principle that network losses should be minimised remains valid, even if, given DNO's access to monitoring to date, it has been difficult to validate and, as this thesis shows, it should be considered alongside other incentives.

1.2.1 Losses Incentive Mechanism

The total electrical distribution loss (GWh) percentages in Great Britain from 2000 to 2010 are shown in Figure 1.2 based on the data in [17]. The electricity loss of distribution networks represents approximately 1.5% cent of total Great Britain greenhouse gas (GHG) emissions [18].

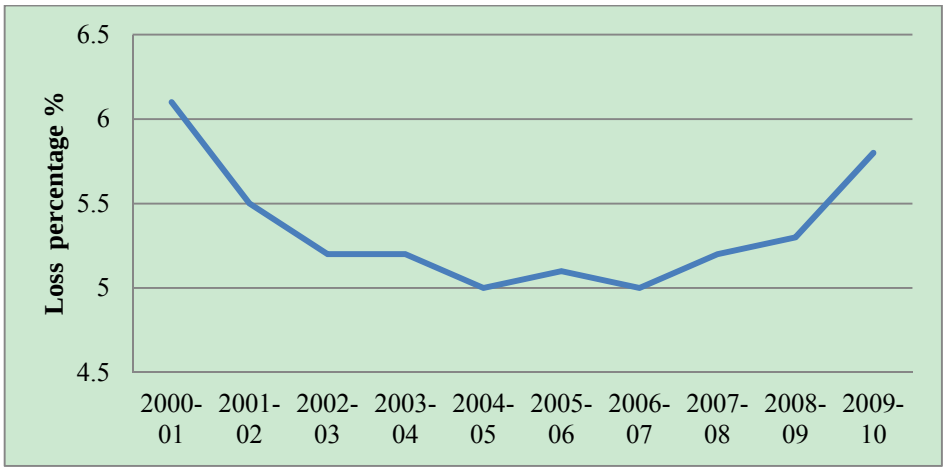

Figure 1.2 GB electricity distribution loss variations

In order to reduce GHG emissions and save energy, Ofgem has set a losses incentive mechanism to all 14 UK DNOs from April 2005 [19]. The losses incentive mechanism is a part of distribution price control [20]. Each DNO has its own loss target set by Ofgem and this target remains constant during an electricity price control period which rolls every five years [21]. The electricity distribution loss percentage of each DNO from 2000-2010 is set out in Table 1-1 [17]. The variation in each DNO's *P* loss is caused by the different nature of the networks, for example, very rural covering a large area, or more concentrated and urban, different loading level, etc. That is why Ofgem sets different *P* loss targets for different DNOs.

The losses targets for DNOs in DPCR 4 is shown in Table 1-2 [22]. The losses targets in DPCR 5 are still being set by Ofgem [23]. If DNOs' actual performance is better than the reference value, they receive rewards. Otherwise, they need to pay a penalty. In DPCR5, the loss incentive value is £60/MWh [24]. Ofgem believes it can incentivise DNOs to reduce the network loss by making new investments, optimising network operation, etc. [24].

Table 1-1 Electricity Distribution Loss Percentages by DNO Area [17]

DNOs	2000-01	2001-02	2002-03	2003-04	2004-05	2005-06	2006-07	2007-08	2008-09	2009-10
CN West	5.1	3.3	4.2	4.2	4.3	4.7	3.8	4.3	5.2	5.2
CN East	5.6	5.6	4.9	4.6	4.8	4.7	4.9	3.9	3.8	4.4
Electricity North West	5.8	3.9	5.4	5.5	4.4	4.4	4.5	4.8	4.8	6.5
CE NEDL	4.9	4.9	4.4	4.3	5.2	4.6	4.3	5	4.7	6.3
CE YEDL	6	4.7	5.6	5.3	4.8	3.5	3.7	5.5	5	7
WPD S Wales	5.3	4.6	2.4	4.5	4.6	4.7	5	5.1	4.4	5
WPD S West	7.2	6.3	6	6.2	5.7	5.4	5.4	6.3	6.2	6.2
EDFE LPN	6.6	6.1	5.8	5.8	5.2	5.3	5	5.5	5.5	5.2
EDFE SPN	6.3	6.2	6.2	5.8	5.3	5.6	5.3	5.6	5.6	4.9
EDFE EPN	6.3	6.1	4.4	4.9	4.3	4.4	4.2	3.7	5	6
EDFE EPN	6.3	6.1	4.4	4.9	4.3	4.4	4.2	3.7	5	6
SP Distribution	6	6.1	4.4	3.9	4.3	5.7	5.8	5.3	6.2	5.8
SP Manweb	7.3	5.7	4.9	4.6	4.9	5.8	5.5	6.6	6.2	6
SSE Hydro	8.2	8.3	8.2	8.2	8.2	8.1	8	8.1	7.8	7.7
SSE Southern	6.4	6.4	6.4	6.4	6.4	6.1	6.2	6.2	6.1	5.9

Table 1-2 Losses targets [22]

DNO	Losses Target(%)
CN – Midlands	4.96
CN - East Midlands	5.69
United Utilities	5.68
CE – NEDL	5.2
CE – YEDL	5.9
WPD - South West	6.96
WPD - South Wales	4.94
EDF – LPN	6.54
EDF – SPN	6.54
EDF – EPN	6.32
SP Distribution	6.45
SP Manweb	7.52
SSE – Hydro	8.73
SSE - Southern	6.74

1.2.2 Interruption Incentive Scheme

Ofgem has applied Interruption Incentive Scheme (IIS) to all Distribution Network Operators (DNOs) in United Kingdom electricity market from April 2002 [25]. The purpose of this scheme is to incentivise DNOs to improve customer service through reducing the frequency and duration of power supply interruptions. Under this scheme, the reliability performance of the DNOs is evaluated by Customer Interruptions (*CI*) per 100 customers and the number of Customer Minutes Lost (*CML*). If the duration of losing electricity supply caused by a fault event is equal to or greater than 3 minutes, this fault event is defined as an "interruption" and included in *CI* and *CML* evaluation [26]. If the loss of supply of electricity caused by a fault event is "up to but excluding 3 minutes", this fault event is considered as a "short interruption" and not included in the *CI* and *CML* evaluation [27]. Each DNO has its own *CI* and *CML* target set by Ofgem. The actual annual performances of *CI* and *CML* are evaluated independently by Ofgem. When its actual annual performance is better than the reference value, a DNO receives the reward. Otherwise, the DNO needs to pay the penalty. Each DNO's performance, rewards and penalties of *CI* and *CML* during 2010-2011 are set out in Table 1-3 [13]. In the penalty/reward (£million) column, a negative value means a penalty and is coloured in red. From this table, it can be seen that EDFE EPN, which is now part of UK Power Networks, pays a

penalty for its *CI* performance and three DNOs, UK Power Networks: London Power Networks (LPN), UK Power Networks: Eastern Power Networks (EPN) and Scottish & Southern Energy: Hydro (SSEH), pay penalties for their *CML* performance.

Table 1-3 2010-2011 DNOs' Rewards and penalties for *CI* and *CML* [13]

	Customer interruptions 2010-11			Customer minutes lost 2010-11		
DNO	**Target**	**Performance**	**Penalty/ reward (£ million)**	**Target**	**Performance**	**Penalty/ reward (£ million)**
WMID	109.9	102.2	0.8	97	89.5	3
EMID	75.7	61.7	1.7	69	54.9	5.9
ENWL	52.9	47.8	0.6	55.6	47.3	4.6
NPGN	68.3	65.2	0.2	71.3	71.1	0
NPGY	75.3	69.9	0.5	76	68.2	2.9
S	79.5	58.4	1.1	44.6	32.4	2.2
S West	73.6	61.5	0.8	51	42.6	2.1
LPN	33.4	24.4	2.7	41	42.4	-0.5
SPN	85	76.9	0.8	87.6	73.2	5.2
EPN	76.1	86	-1.6	71.1	72.4	-0.8
SPD	60.1	50.7	0.8	65.5	49.4	5.3
SPMW	45.6	39.3	0.4	61.1	47.5	2.8
SSEH	77	74	0.1	75.1	78.4	-0.5
SSES	73.8	63.6	1.3	69.1	64.1	2.4
GB			10.3			34.6
GB			0.7			2.5

1.3 The Objectives of this Thesis

The main objectives of the thesis are to optimise *P* loss and evaluate reliability of the medium voltage distribution network by developing innovative methods. Doing so will provide a DNO with the facilities to quantify the likely impact, for given situations, of interventions such as network reconfiguration, installation of new remote control points or network reinforcement. These facilities will be particularly important in helping to evaluate the costs and benefits of possible interventions with respect to the losses and reliability incentive schemes. In order to achieve the objectives, the following steps are required:

1. To investigate the nature of the losses that can be found on a realistic medium voltage distribution network

2. To explore how to make full use of DNOs' existing devices to minimise *P* loss and find the global optimisation result.
3. To estimate the network reliability performance when subject to fault conditions, in particular the restoration time, by considering the protection system, automation system and the operation of manual switches for service restoration.
4. To investigate whether *P* loss and reliability performance of a network need to be optimised at the same time or separately.
5. To develop a tool to help DNOs to quantify the impact of different decisions or operational actions, for example, network reconfiguration through changing the location of open points, and the effects of such actions on network losses and the reliability of supply to end users of electric power.

1.4 Main Contributions

The main contributions of this study are:

1. To enable understanding of which devices make the most contribution to the *P* loss by building a realistic medium size 11kV distribution simulation model.
2. By means of a directed, exhaustive search of network configurations (and unlike a number of previous methods in the literature that rely on heuristics), an algorithm is proposed that can find the globally optimal result in respect of minimization of network losses. In addition the results of the algorithm can be readily used in the solution of a multiobjective optimisation problem.
3. A new reliability evaluation based on graph theory and topology search techniques is developed. Unlike many previous approaches emerging from academic literature, this evaluation makes an accurate estimate of restoration time. That is, the restoration method of each fault affected bus for a specific fault interruption can be determined automatically.
4. Unlike anything identified by the author in the literature, an algorithm that can optimise the *P* loss and reliability performance separately or at the same is developed. This algorithm can be used to investigate P loss and reliability

performance together, the result being driven by whichever is more important in respect of regulatory network performance incentives.

5. A analytical tool is developed to perform the *P* loss optimisation, reliability evaluation and loss-reliability optimisation algorithms. This tool can help DNOs to accurately calculate the impacts of design or operation decisions on losses and reliability.

1.5 Thesis Structure

This thesis has seven chapters, the contents of which are briefly outlined as follows:

Chapter 1 introduces the background and motivations of this thesis.

Chapter 2 describes the *P* loss of distribution network. A small part of the realistic 11kV distribution network is modelled in Digsilent Power Factory. The *P* loss of a three-phase four-wire system and the application of load balancing techniques are discussed.

Chapter 3 describes a new algorithm of network reconfiguration for *P* loss optimisation. This algorithm is based on graph theories, e.g. Breadth-First Search, Depth-First Search, Spanning Tree. No network approximation is required in this algorithm and a global optimisation result can be guaranteed. This algorithm is implemented in an analytical tool known as DisOPT which is described in Appendix C.

Chapter 4 describes the basic reliability theory and briefly introduces distribution network automation. Service restoration processing under fault conditions considering the network protection and automation system is discussed.

Chapter 5 describes a new reliability evaluation algorithm which considers network protection, automation and load transfer. This algorithm is designed especially for *CI* and *CML* calculation. The network reliability optimisation algorithm is presented as well.

Chapter 6 presents seven case studies to illustrate how DNOs can use the analytical tool developed in this thesis to accurately calculate the impacts of design or operation decisions on losses and reliability.

Chapter 7 presents the conclusions of this thesis and suggestions for future work.

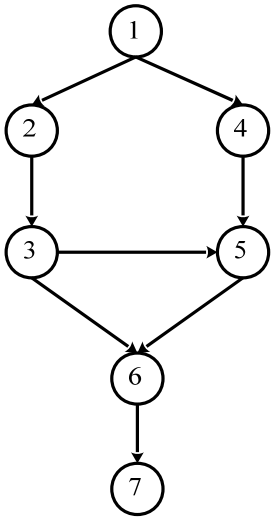

Figure 1.3 Interrelation of chapters

The interrelation of chapters is illustrated in Figure 1.3.

1.6 Publications and Reports

Ding Jiansong, K. R. W. Bell, and S. M. Strachan, "Study of Low Voltage System Losses," in *Universities Power Engineering Conference (UPEC), 2010 45th International*, 2010, pp. 1-6

Ding Jiansong, "Report on 11kV model of Glasgow Urban Network Losses.", Technical report, University of Strathclyde,01/2009.

1.7 Summary

This chapter has briefly introduced the UK distribution network and the regulator's (Ofgem) incentives schemes with rewards and penalties for the loss and reliability

performance of DNOs. This research provides a valuable tool to help the distribution network planners make decisions on how to optimise the network P loss and improve the network reliability performance.

Chapter 2 Distribution Network *P* Loss Analysis

The previous chapter introduced the aims of this research. In this chapter, the *P* loss of a realistic 11kV distribution network is studied first. The methods of reducing *P* loss are introduced. By comparing different techniques, network reconfiguration is chosen to optmise the network *P* loss. The summary of previous on *P* loss minimisation by network reconfiguration is presented.

2.1 Introduction

It is estimated that Distribution losses in the UK are typically 5% of energy distributed [17]. The network has been designed to some extent to accommodate these losses; however, as it has evolved over time, network extensions, new generation and increasing load demand mean that new measures are required to manage these system losses.

In order to optimise the *P* loss, the best method to calculate the *P* loss needs to be determined first. Then, the devices having the main contribution to the network's total *P* loss need to be located. Finally, a suitable technique needs to be chosen to optimise the *P* loss. These issues are addressed in the following sections.

2.2 Load Flow in Three-Phase Four-Wire System

Three-phase distribution networks can be connected in three-wire or four-wire configurations [28]. Both of these two structures have three wires carrying the three phases (R,Y,B). Four-wire systems have an extra neutral line connected to the neutral point of the transformer so that single phase loads can be connected between one phase and the neutral line [7]. The three-wire system in Figure 2.1 is used when the loads don't require a neutral line, e.g., motors [29]. The four-wire system in Figure 2.2 is widely used in LV distribution networks which have many single phase loads [30].

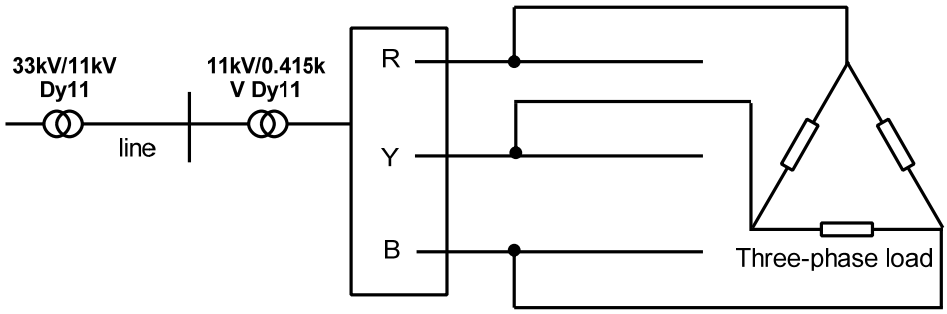

Figure 2.1 Three-phase three-wire system

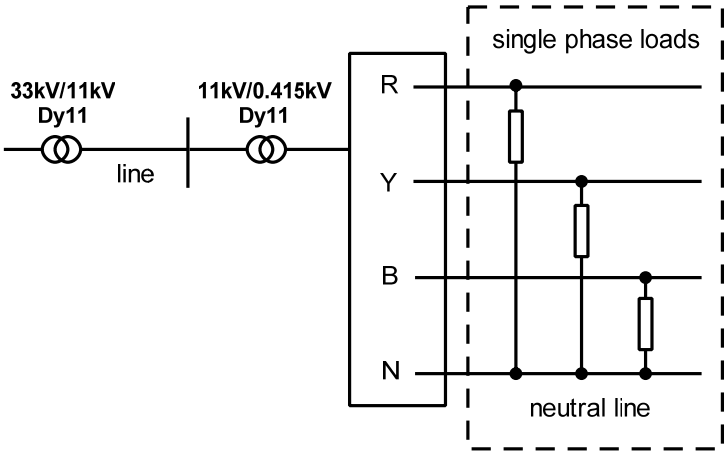

Figure 2.2 Three-phase four-wire system

Due to the unbalanced load condition, extra loss will be caused in neutral line. So the current in neutral line is important for the loss analysis of three-phase four-wire systems. In most power system simulation tools, the load flow analysis functions are designed for three-wire systems and merge the neutral line into phases by applying Kron's reduction [30]. The details of Kron's reduction are introduced in the following section by using line segments of three-phase three-wire and three-phase four-wire systems in Figure 2.3 and Figure 2.4 respectively[31]. The meanings of symbols used for this introduction are:

$U_{A,}\ U_{B}, U_{C,}\ U_{N}$: the phase voltages at the sending end of the line

$U'_{A}, U'_{B}, U'_{C}, U'_{N},$: the phase voltages at the receiving end of the line

Z_{AA}: the impedance of Phase A

Z_{AB}: the impedance between Phase A and Phase B

Z_{AC}: the impedance between Phase A and Phase C

Z_{AN}: the impedance between Phase A and neutral line

Z_{BA}: the impedance between Phase B and Phase A

Z_{BB}: the impedance of Phase B

Z_{BC}: the impedance between Phase B and Phase C

Z_{BN}: the impedance between Phase B and neutral line

Z_{CA}: the impedance between Phase C and Phase A

Z_{CB}: the impedance between Phase C and Phase B

Z_{CC}: the impedance of Phase C

Z_{CN}: the impedance between Phase C and neutral line

I_A, I_B, I_C, I_N: the phase currents

Taking the line segment of three-phase three-wire system in Figure 2.3 for example [31]; the node equation of line segment is:

$$\vec{U}_{ABC} = \vec{U}'_{ABC} + \vec{Z}_{ABC}\vec{I}_{ABC} \tag{2.1}$$

where:

$$\vec{U}_{ABC} = \begin{bmatrix} U_A \\ U_B \\ U_C \end{bmatrix} \tag{2.2}$$

$$\vec{U}'_{ABC} = \begin{bmatrix} U'_A \\ U'_B \\ U'_C \end{bmatrix} \tag{2.3}$$

$$\vec{Z}_{ABC} = \begin{bmatrix} Z_{AA} & Z_{AB} & Z_{AC} \\ Z_{BA} & Z_{BB} & Z_{BC} \\ Z_{CA} & Z_{CB} & Z_{CC} \end{bmatrix} \tag{2.4}$$

$$\vec{I}_{ABC} = \begin{bmatrix} I_A \\ I_B \\ I_C \end{bmatrix} \tag{2.5}$$

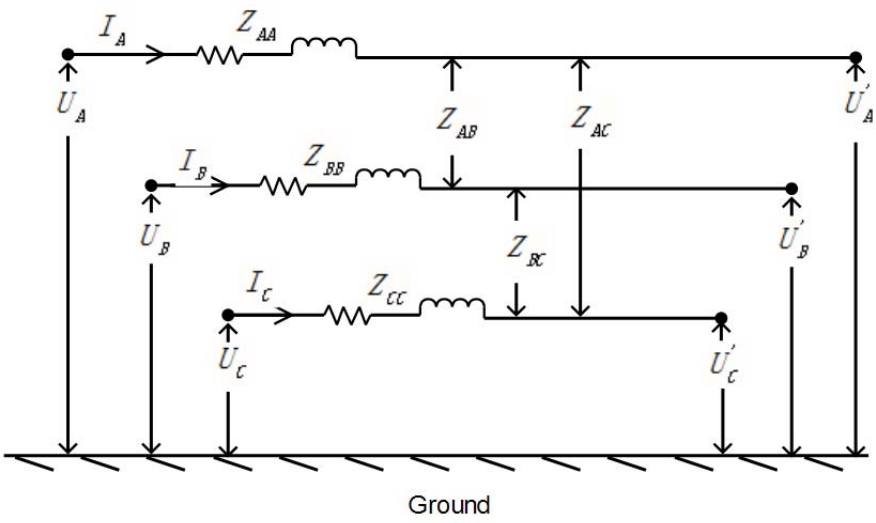

Figure 2.3 Line segement of three-phase three-wire [31]

For a three-phase four-wire system, the node equation of line segment in Figure 2.4 is [31]:

$$\vec{U}_{ABCN} = \vec{U}'_{ABCN} + \vec{Z}_{ABCN}\vec{I}_{ABCN} \tag{2.6}$$

where:

$$\vec{U}_{ABCN} = \begin{bmatrix} U_A \\ U_B \\ U_C \\ U_N \end{bmatrix} \tag{2.7}$$

$$\vec{U}'_{ABCN} = \begin{bmatrix} U'_A \\ U'_B \\ U'_C \\ U'_N \end{bmatrix} \tag{2.8}$$

$$\vec{Z}_{ABCN} = \begin{bmatrix} Z_{AA} & Z_{AB} & Z_{AC} & Z_{AN} \\ Z_{BA} & Z_{BB} & Z_{BC} & Z_{BN} \\ Z_{CA} & Z_{CB} & Z_{CC} & Z_{CN} \\ Z_{NA} & Z_{NB} & Z_{NC} & Z_{NN} \end{bmatrix} \tag{2.9}$$

$$\vec{I}_{ABCN} = \begin{bmatrix} I_A \\ I_B \\ I_C \\ I_N \end{bmatrix} \tag{2.10}$$

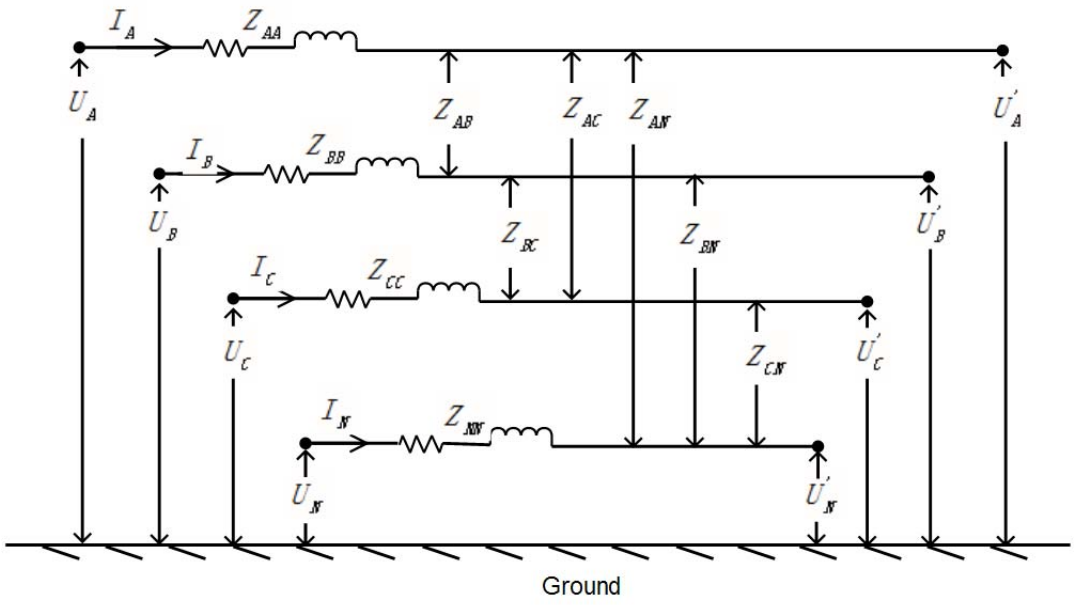

Figure 2.4 Line segment of three-phase four-wire system [31]

Comparing $\vec{Z}_{ABCN}$ (2.9) with $\vec{Z}_{ABC}$ (2.4), $\vec{Z}_{ABCN}$ is a 4×4 matrix but the dimension of $\vec{Z}_{ABC}$ is 3×3. As a consequence, the load flow algorithm of a three-wire system cannot be applied on four-wire system directly. Kron's reduction method can solve this problem [31]. In order to apply the Kron reduction method, (2.6) is rewritten as:

$$\begin{bmatrix} \vec{U}_{ABC} \\ \vec{U}_N \end{bmatrix} = \begin{bmatrix} \vec{U}'_{ABC} \\ \vec{U}'_N \end{bmatrix} + \begin{bmatrix} \vec{Z}_{ABC} & \vec{Z}_{ABC-N} \\ \vec{Z}_{N-ABC} & \vec{Z}_{NN} \end{bmatrix} \begin{bmatrix} \vec{I}_{ABC} \\ \vec{I}_N \end{bmatrix} \tag{2.11}$$

where:

$$\vec{U}_{ABC} = \begin{bmatrix} U_A \\ U_B \\ U_C \end{bmatrix} \tag{2.12}$$

$$\vec{U}_N = [U_N] \tag{2.13}$$

$$\vec{U}'_{ABC} = \begin{bmatrix} U'_A \\ U'_B \\ U'_C \end{bmatrix} \tag{2.14}$$

$$\vec{U}'_N = [U'_N] \tag{2.15}$$

$$\vec{Z}_{ABC} = \begin{bmatrix} Z_{AA} & Z_{AB} & Z_{AC} \\ Z_{BA} & Z_{BB} & Z_{BC} \\ Z_{CA} & Z_{CB} & Z_{CC} \end{bmatrix} \tag{2.16}$$

$$\vec{Z}_{N-ABC} = [Z_{NA} \quad Z_{NB} \quad Z_{NC}] \tag{2.17}$$

$$\vec{Z}_{ABC-N} = \begin{bmatrix} Z_{AN} \\ Z_{BN} \\ Z_{CN} \end{bmatrix} \tag{2.18}$$

$$\vec{Z}_{NN} = [Z_{NN}] \tag{2.19}$$

$$\vec{I}_{ABC} = \begin{bmatrix} I_A \\ I_B \\ I_C \end{bmatrix} \tag{2.20}$$

$$\vec{I}_N = [I_N] \tag{2.21}$$

When the neutral is grounded, U_N and U'_N are equal to zero. Substituting $U_N = U'_N = 0$ into (2.11) and expanding it as:

$$\vec{U}_{ABC} = \vec{U}'_{ABC} + \vec{Z}_{ABC}\vec{I}_{ABC} + \vec{Z}_{ABC-N}\vec{I}_N \tag{2.22}$$

$$0 = 0 + \vec{Z}_{N-ABC}\vec{I}_{ABC} + \vec{Z}_{NN}\vec{I}_N \tag{2.23}$$

From (2.23), $\vec{I}_N$ can be calculated:

$$\vec{I}_N = -\vec{Z}_{NN}^{-1}\vec{Z}_{N-ABC}\vec{I}_{ABC} \tag{2.24}$$

Substitute (2.24) into (2.22):

$$\vec{U}_{ABC} = \vec{U}'_{ABC} + \vec{Z}_{new}\vec{I}_{ABC} \tag{2.25}$$

where:

$$\vec{Z}_{new} = \vec{Z}_{ABC} - \vec{Z}_{ABC-N}\vec{Z}_{NN}^{-1}\vec{Z}_{N-ABC} \tag{2.26}$$

(2.26) is the form when the process of Kron reduction is finished. Now, the dimension of new line impedance matrix $\vec{Z}_{new}$ is 3×3. Though the load flow of a 4-wire system can be calculated now, the neutral line and ground currents are unknown. Especially when the loads are unbalanced, these two values are important for loss analysis. A load flow algorithm for four-wire distribution system is presented in [30]. This algorithm is based on a backward-forward technique instead of Newton-Raphson. Not only the neutral line but also the ground impedance are represented and no matrix reduction is required. So the *P* loss of four-wire system calculated by this algorithm is more accurate.

2.3 *P* Loss of a realistic 11kV Distribution Network

A small part of a three-wire unbalanced urban 11kV SP distribution network associated with a set of particular Grid Supply Points (GSPs) has been built in Digsilent Power Factory [32] to assist in analysing the potential benefits of moving NOPs for loss minimization. The details of this model can be found in [33]. The problems of building this model and simulation results are discussed in the following subsections.

2.3.1 Construction of the Simulation Model

In order to analyse a power network using simulation tools, an accurate and complete network simulation model needs to be built first. The complete network model contains:

- 5 primary substations (33kV/11kV)
- 11 interconnected feeder pairs
- 110 11kV/0.415kV secondary substations (loads are unbalanced and their data are monitored at the LV fuse board (0.415kV) and based on measured load phase current magnitudes)
- 722 cable sections (three-phase cables without neutral)

Due to a distribution network's inherent characteristics such as very low monitoring level, lack of asset information due to their varying ages and characteristics, it is difficult to build a realistic and complete model. So there are some challenges presented to a network modeller and they are outlined below:

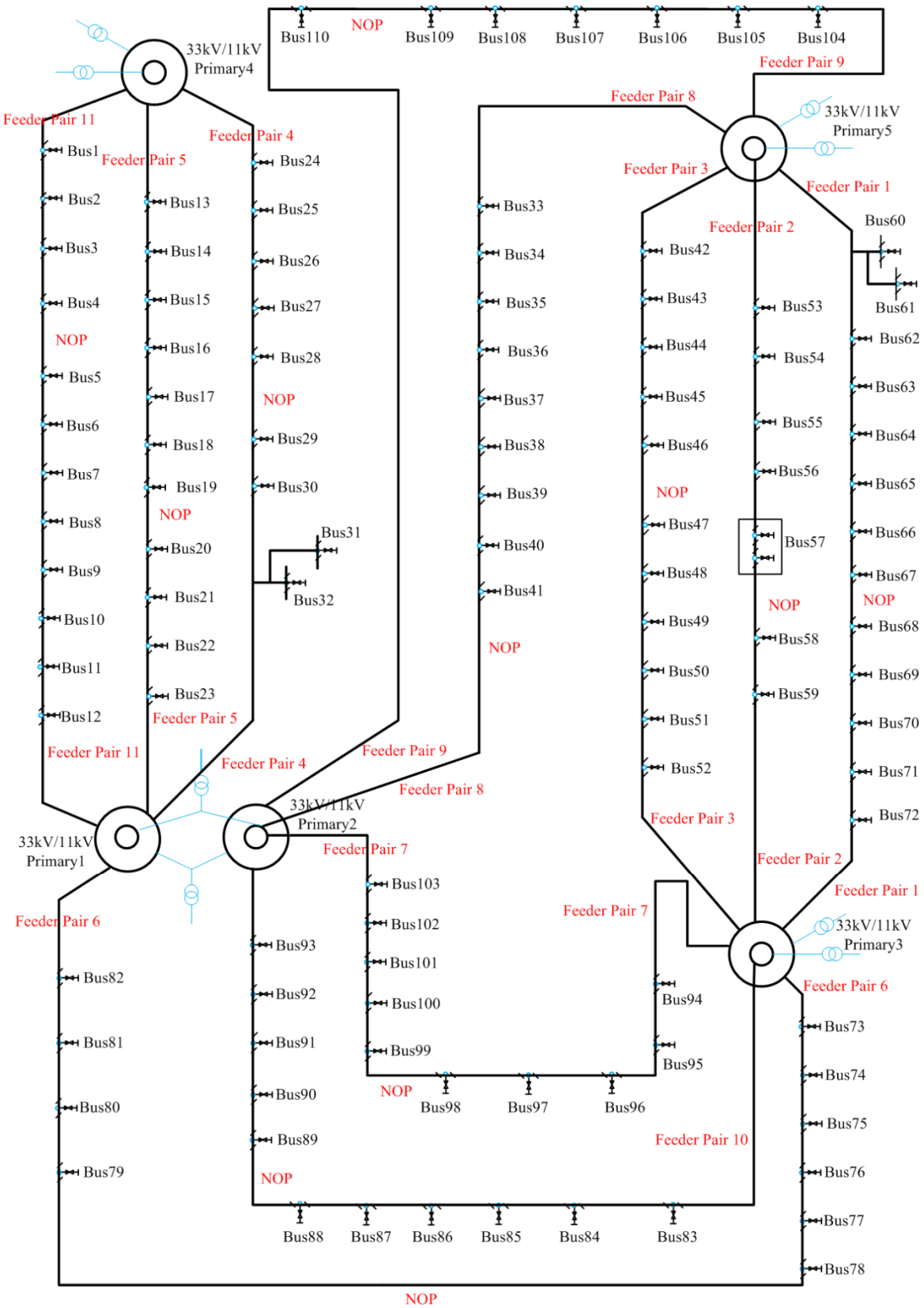

Figure 2.5 The diagram of network built in Digsilent Power Factory

1) Building an Impedance Map of the Network

The link between two substations is generally made up of several cable sections. Information on these cable sections, such as cable type and cable length, is typically stored in a Geographic Information System (GIS). When building a network model, the first step is to extract the information needed from the GIS system, which is normally done manually. In contrast to the Transmission and EHV systems, DNOs typically have little in the way of 11kV/LV network models, mainly due to the network size and gaps in network data. Ideally, a link would exist between power system simulation software and the GIS database, enabling extraction of network details from the GIS database to automatically build an initial version of the model; however, in practice this was not possible for the case study described here.

2) Dealing with Unknown Equipment Information

Even when the network simulation tool does have a facility for importing GIS data (as is the case with Digsilent Power Factory) [32], gaps in available network data require manual intervention and assumptions to provide estimates for missing parameters. For example:

- 11/0.415kV transformers - Many 11/0.415kV transformers, in particular, are old and their precise electrical characteristics are not recorded. However, transformer losses comprise a high proportion of the whole system loss making this missing information quite significant.
- Cable sections of unknown type - Some cable section data is not recorded in the GIS system, which means cable impedance and thermal rating is unknown

3) Dealing with Limited Load Information

Measurements at LV are typically quite sparse, and even the phase to which domestic customers are connected may be unknown. Until more complete information becomes available (such as may be mandated by government or regulator intervention under ‘advanced metering infrastructure’ (AMI) or ‘smart meter’ initiatives) [34], network modellers need to make some prudent assumptions. These include taking the available measurements, relating them to

the time of year at which they were believed to have been taken, and applying feeder by feeder scaling to estimate a set of reference loads for a condition such as the annual peak demand for the grid supply point as a whole.

2.3.2 *P* loss Simulation Results

After the network model has been built, the whole system's losses can be calculated for different loading conditions. When the total demand is 28,633kW, the *P* loss percentage of this network is 1.1%. With use of a typical load duration curve [35], the annual network loss is estimated to be 3827MWh. The whole system can be divided into 11 feeder pairs and each feeder pair whose general configuration is shown in Figure 2.6 has two grid infeeds. Table 2-1 shows the *P* losses of each feeder pair for estimated peak load condition. Figure 2.7 represents the line loss and transformer loss of each feeder pair in a bar chart to show the contrast of these two losses. There are eleven feeder pairs and the positions of these eleven feeder pairs are marked in Figure 2.5. The differences of each feeder pair's *P* loss shown in Figure 2.7 are caused by differences in each feeder pair's cable length, number of substations and loading level.

Figure 2.6 The schematic of Feeder pair

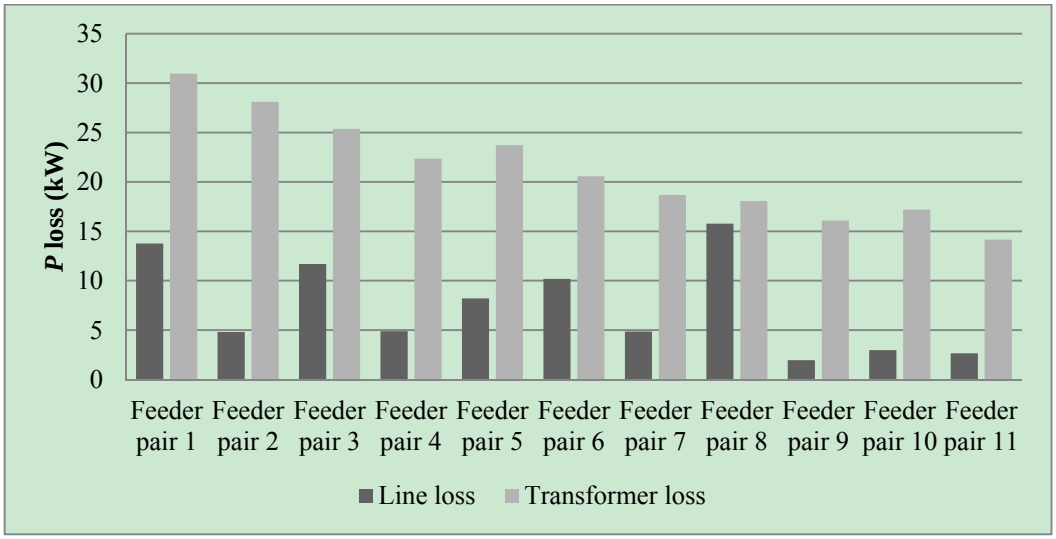

Figure 2.7 Line and transformer losses of each feeder pair

Table 2-1 Loss information of each feeder pair

Interlink	Total infeed(kW)	Load demand(kW)	Total loss(kW)	Line loss(kW)	Transformer loss(kW)	Loss%
Feeder pair 1	3582.57	3537.91	44.71	13.76	30.95	1.25
Feeder pair 2	3545.24	3512.35	32.9	4.8	28.1	0.93
Feeder pair 3	3452.78	3415.74	37.06	11.69	25.37	1.07
Feeder pair 4	2810.43	2783.19	27.25	4.89	22.36	0.97
Feeder pair 5	2757.63	2725.69	31.94	8.21	23.73	1.16
Feeder pair 6	2658.39	2627.65	30.76	10.19	20.57	1.16
Feeder pair 7	2243.15	2219.65	23.52	4.85	18.68	1.05
Feeder pair 8	2133.87	2100.04	33.85	15.78	18.06	1.59
Feeder pair 9	2111.17	2093.15	18.03	1.95	16.08	0.85
Feeder pair 10	2005.22	1985.04	20.18	2.98	17.2	1.01
Feeder pair 11	1649.92	1633.12	16.81	2.65	14.16	1.02

Due to a lack of precise data for the modelled secondary transformers, a full load loss of 6.5kW and no load loss of 1.95kW are assumed, based on the datasheet for an Alstom 1000kVA 11kV/415V transformer [36]. Figure 2.8 shows that transformers contribute 74% to the whole system loss and line loss is only 26% in the peak load condition.

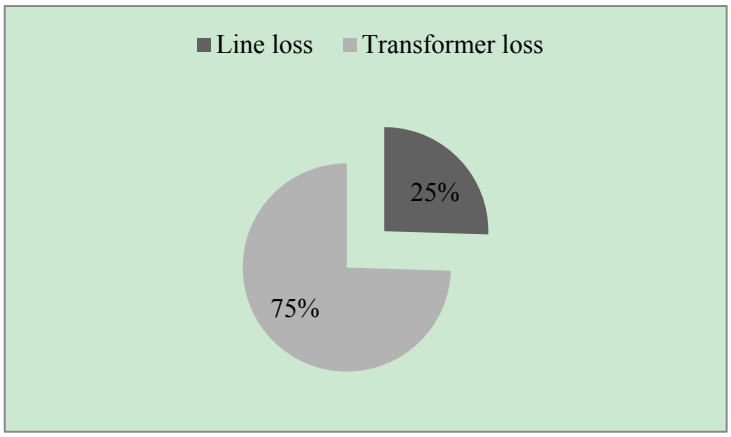

Figure 2.8 The proportions of line and transformer losses

This result shows that the transformer loss is much higher than the line loss. In addition, the transformer used in the simulation model is a modern type of transformer. In reality, the age profile of transformers in the LV distribution network suggests that they will have higher losses [37]. Therefore, an affordable means of reducing transformer loss could present a useful means of reducing network loss.

2.4 Methods of Minimising Network's *P* Loss

Load balancing and network reconfiguration are two major methods of distribution network *P* loss minimisation [38-42]. Brief introductions to these two methods are presented below.

Load Balancing

The LV distribution network has a large amount of single phase load connected from phase conductor to neutral conductor. Normally, despite attempts to balance customer connections and loads between the phases, some unbalance, usually small, results in some neutral current and unwanted neutral line losses. Details of how to calculate *P* loss caused by load unbalance are presented below:

Assuming the line resistance of each phase conductor is R, when the load current is balanced, the total *P* loss of the line is:

$$P = 3I^2R \tag{2.27}$$

where *I* is the magnitude of the phase current.

In order to analyse the *P* loss of line under unbalanced condition, the load phase currents $\dot{I}_A$, $\dot{I}_B$, $\dot{I}_C$ need to be converted to sequence domain as below [43]:

$$\dot{I}_{0A} = \frac{1}{3}\left(\dot{I}_A + \dot{I}_B + \dot{I}_C\right) \tag{2.28}$$

$$\dot{I}_{1A} = \frac{1}{3}\left(\dot{I}_A + \alpha\dot{I}_B + \alpha^2\dot{I}_C\right) \tag{2.29}$$

$$\dot{I}_{2A} = \frac{1}{3}\left(\dot{I}_A + \alpha^2\dot{I}_B + \alpha\dot{I}_C\right) \tag{2.30}$$

where:

$\alpha = \angle 120^{\circ}$

$\dot{I}_{0A}$: the current of Phase A in zero sequence

$\dot{I}_{1A}$: the current of Phase A in positive sequence

$\dot{I}_{2A}$: the current of Phase A in negative sequence

The positive and negative sequence currents do not inject into neutral line and so only produce losses in the phase wire which are:

$$\dot{I}_{1A} + \dot{I}_{1B} + \dot{I}_{1C} = 0 \tag{2.31}$$

$$\dot{I}_{2A} + \dot{I}_{2B} + \dot{I}_{2C} = 0 \tag{2.32}$$

where:

$\dot{I}_{1A}, \dot{I}_{1B}, \dot{I}_{1C}$: phase currents in positive sequence

$\dot{I}_{2A}, \dot{I}_{2B}, \dot{I}_{2C}$: phase currents in negative sequence

So they don't inject into neutral line and only produce loss of phase wire which are:

$$P_1 = 3\left|\dot{I}_{1A}\right|^2 R \tag{2.33}$$

$$P_2 = 3\left|\dot{I}_{2A}\right|^2 R \tag{2.34}$$

where:

P_1: the P loss caused by phase currents in positive sequence

P_2: the P loss caused by phase currents in negative sequence

For zero sequence currents, their summation $\dot{I}_{0-sum}$ is :

$$\dot{I}_{0-sum} = \dot{I}_{0A} + \dot{I}_{0B} + \dot{I}_{0B} = 3\dot{I}_{0A} = \dot{I}_A + \dot{I}_B + \dot{I}_C \tag{2.35}$$

Since $\dot{I}_A, \dot{I}_B, \dot{I}_C$ are unbalanced, $\dot{I}_{0-sum}$ is not equal to zero. The loss of the neutral line produced by the unwanted non-zero $\dot{I}_{0-sum}$ is:

$$P = \left|\dot{I}_{0-sum}\right|^2 R_n \tag{2.36}$$

where R_n is the resistance of the neutral line.

Comparing with the balanced condition, zero sequence currents, negative sequence currents and the imaginary part of the positive sequence current produce the

additional *P* loss of line. The load unbalance not only increases the line copper power loss, but also has an adverse effect on the system's reliability and security [44]. For example, the unbalanced loads cause unbalanced phase currents which represent non-zero currents in the zero and negative sequences. Negative sequence currents can increase transformer losses and be harmful to synchronous generators, while zero sequence currents affect the protection equipment [45].

Some load balancing techniques have been published in [38-41]. One technique is to balance the load by applying appropriate amounts of reactive power produced by static VAr compensators (SVC) to each phase. In this technique, a *Y*- connected SVC is used to eliminate the zero sequence currents and the imaginary part of the positive sequence currents while the negative sequence currents are eliminated by a Δ-connected SVC [38]. The schematic diagram of applying these two SVCs is shown in Figure 2.9 [38].

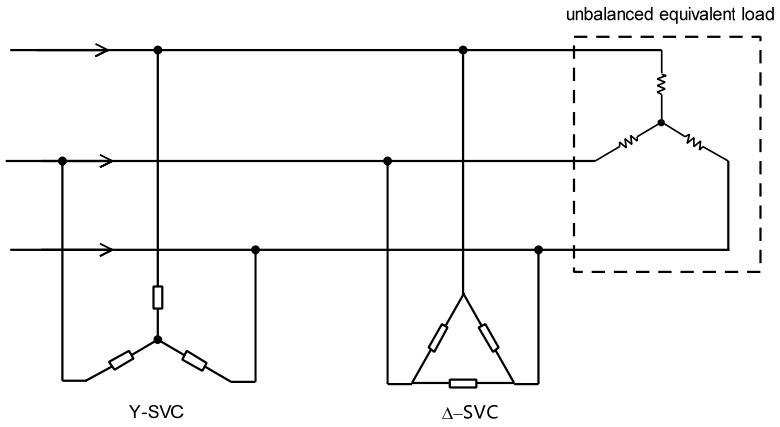

Figure 2.9 A four-wire system with *Y*-SVC and Δ-SVC [38]

Monitoring of unbalanced conditions in order to actively and dynamically balance the load across the phases may offer a useful means of minimizing system loss. Some manufacturers provide products to achieve dynamic load balancing, for example, Alstom's STATCOM [46]. STATCOM (static synchronous compensator) is a device based on a voltage source converter [47]. The STATCOM used in distribution system is also named as DSTATCOM. The DSTATCOM can not only balance the load but also correct the power factor and regulate the voltage [48].

Network reconfiguration

When a distribution network is built in mesh and operated in a radial configuration, its topology can be changed by moving the position of NOPs. Varying the topology varies, the *P* loss of the network varies as well. Consider a two-feeder network example similar to that in [49], which has two feeders (A and B) seven branches (br1-br7), 6 nodes (b1-b6), 6 loads (L1-L6) and one NOP. The loads of this network can be connected to either feeder A or feeder B by different positions of NOP. When the NOP moves from branch br1 to br7, the variations of network's *P* loss is shown in Figure 2.11(a). The *P* loss of branch is calculated by (2.27). So if the NOP could be moved continuously along the branch, the shape of *P* loss in Figure 2.11(a) could be approximated to a "U" shape in Figure 2.11(b) [50].

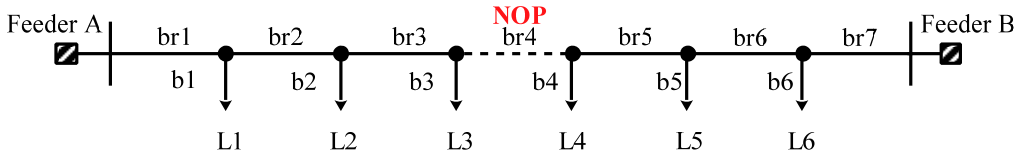

Figure 2.10 Example two-feeder network [49]

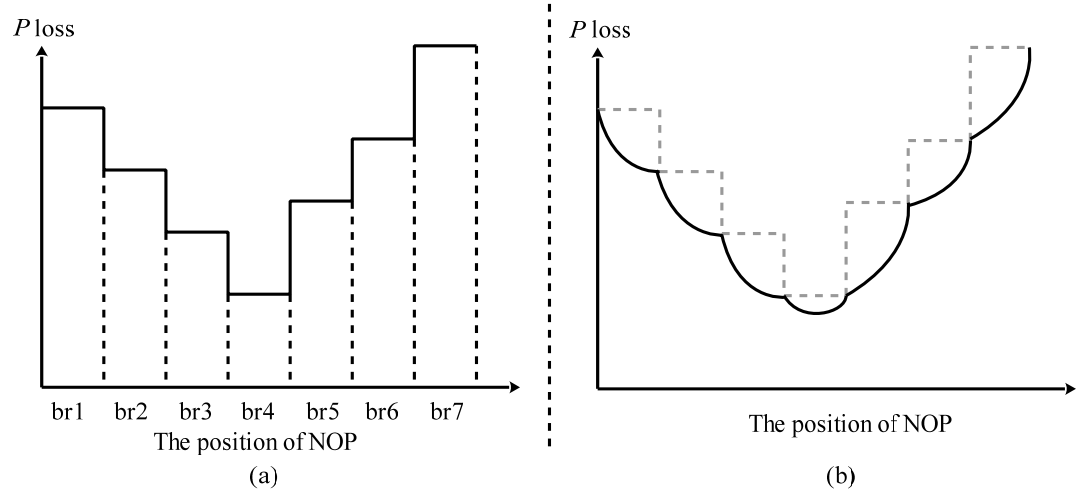

Figure 2.11 The variation of *P* loss when topology is changed [49, 50]

Based on Figure 2.11, it can be concluded that when topology is changed, the *P* loss of the network changed in a discrete, non-linear way. So the *P* loss optimisation by network reconfiguration is a discrete, non-linear optimisation problem.

The current SPEN distribution network has already had some remote control points and a large number of manual switches installed. The switch devices make the operation of network reconfiguration possible. Furthermore, these switch devices are mainly used for restoring the power supply under fault conditions and changing the network topology for planned outages. Using remote control and manual switches to minimise loss can make full use of existing devices and gain extra benefits. So the method of network reconfiguration is chosen to minimise distribution network *P* loss in this thesis.

2.5 Summary of Previous Works on *P* Loss Minimisation by Load Balancing and Network Reconfiguration

Load Balancing

Some algorithms of power distribution network *P* loss optimisation by load balancing have been published [38-40, 51]. San-Yi and Chi-Jui develop a new reactive power compensation method to balance the load [38]. Leszek S et al. analyse the control range and frequency properties of the compensator susceptances used for load balancing [51]. Wei-Neng and Kuan-Dih introduce how to design the distribution level static compensator for load balancing purposes [39]. Adrian et al. validate the method of load balancing by using variable susceptances in a distribution network [40]. In order to perform the load balancing, the distribution network needs to be well monitored. Due to the current level of monitoring, the load balancing technique is not widely used in the real network.

Network Reconfiguration

Various algorithms of power distribution network *P* loss optimisation by network reconfiguration have been published [6, 42, 49, 50, 52-70]. These algorithms can be divided into three main categories [61]: 1) Heuristic methods; 2) Artificial intelligence methods; 3) Deterministic methods.

For heuristic methods, Merlin and Black first use the method of network reconfiguration to minimise *P* loss [58]. Shirmohammadi and Hong develop the

optimal flow pattern to improve the method developed by Merlin and Black [52]. Civanalar et al. develop a new heuristic method based on the concept of switch pairs [49]. Baran and Wu introduce the Dist-Flow equations to calculate the loss reduction instead of the equation developed by Civanalar et al. [68]. Goswami and Basu improve Shirmohammadi and Hong's method and get a better *P* loss for the network model used in Baran and Wu's method [57]. Raju and Bijwe present a two-stage method which uses the real power sensitivity by considering the impedances of the candidate branches in the first stage and performs the branch exchange in the second stage [54]. Schmidt et al. use best-first search to find the best *P* loss topology whose branch current is calculated by the standard Newton method [70]. Gomes et al. use optimal power flow to find the best configuration [69]. The major weakness of these heuristic methods is that the global optimum result cannot be guaranteed.

For artificial intelligence methods, simulated annealing [71-73], genetic algorithms [65], ant colony optimisation [74], artificial neural networks [75] and expert systems [76] have been applied to solve the network reconfiguration problem. Genetic algorithms (GAs) are one of the most popular techniques [62-67]. Nara first applied GAs to minimise *P* loss by network reconfiguration [65]. The results of this paper demonstrated that GAs are a useful technique to solve the network reconfiguration problem. Yin extended GAs to solve multiobjective network reconfiguration problems which optimises both *P* loss and voltage drop [66]. In [62], a method is developed to generate a radial topology for the initial population which can improve the efficiency of GA to find the optimum results. The advantages of a GA are that it can find the result close to the global optimum result and can handle multiobjective optimisation. But when the network is large, the length of the string may be very long. This feature may decrease a GA's search efficiency [64].

For deterministic methods, Ramos et al. develop a new approach based on "path-to-node" concept and conventional mixed-integer linear programming [62]. Khodr et al improve the method of Ramos et al. by using an exact model to present network *P* loss [77]. Rabih et al. develop a new exact mixed integer nonlinear programming approach to solve the network reconfiguration problem by considering the distributed

generation [61]. The major weakness of deterministic methods is that the network needs to be represented by a mathematical model and some approximations are required. The global optimum solution cannot be guaranteed by these approximations.

The details of some typical methods used for network reconfiguration are outlined below.

1. Branch Exchange Method

This heuristic method is developed by Civanlar et al. [49]. In this method, loads are modelled as constant currents and switches are operated in pairs, which means closing one first and then opening one. So the topology of the initial network must be radial. The approximated amount of *P* loss change when loads are transferred from feeder *N* to feeder *O* is

$$\Delta P_{loss} = P_{new} - P_{old} = Re\left\{2\left(\sum_{i\in D} I_i\right)(E_o - E_n)^*\right\} + R_{loop}\left|\sum_{i\in D} I_i\right|^2 \quad (2.37)$$

where:

P_{old}: the *P* loss of the old network topology

P_{new}: the *P* loss of the new network topology

$\sum_{i\in D} I_i$: The sums of the total transferred buses' injected currents

R_{loop}: Series resistance of the path connecting two feeders via the closure of the normally open point

E_o: Voltage of the node *o* powered by feeder *O* and connected to one side of the original normally open point

E_n: Voltage of the node *n* powered by feeder *N* and connected to the other side of the original normally open point

Equation (2.37) expresses the change in losses when the initially open branch between nodes *o* and *n* is closed. The equation suggests that the change in losses is negative, i.e. losses reduce, if the magnitude of E_n in the initial state is higher than E_o. After performing the load flow of the initial network, the switch operation pairs that

make minimise equation (2.37) form the required result. The calculation speed of this method is very fast since only the load flow of the initial network is required in the whole processing. But the initial topology of the network will affect the final result and a globally optimal result cannot be guaranteed. Furthermore, the (2.37) is not always true in any case [68]. While equation (2.37) given in [49] suggests that the normally open point between nodes *n* and *o* should be closed if the initial voltage at node *n* is higher than that at node *o*; an example is given in [68] that showed a counter case. The error arising from simple application of equation (2.37) could be because the post-switching voltages are different from the pre-switching voltages but this approximated equation does not take that into account.

2. Optimal Flow Pattern

Reconfiguring the distribution network by optimal flow pattern is first proposed by Shirmohammadi and Hong [52]. The steps of this algorithm are:

- Step 1: Compute the load current of the original network by AC load flow
- Step 2: Close all normally open points. Closure of each normally open point creates an additional loop path.
- Step 3: Choose a loop, replace each branch's impedance by its corresponding resistance and then calculate the current in the branches that make up the loop by optimal flow pattern. The optimal flow pattern is defined as: represent the branch impedance only by resistance and consider the load current as an injected current source, then calculate the current flows in each branch by KVL and KCL equations of the network [52].
- Step 4: Open the branch that has a minimum current value.
- Step 5: Go back to Step 3 until the network restores the radial structure.

Goswami and Basu improved Shirmohammadi and Hong's method in 1992 [57]. Instead of closing all normally open points, Goswami and Basu's algorithm only closes one original normally open point and then opens one switch found by this algorithm. There are three options to determine which normally open point to close: 1) choose the normally open point that has the maximum voltage difference across it;

2) choose the normally open point that has the minimum voltage difference across it; 3) choose the normally open point randomly. The final network configuration is the same in the three options. This algorithm provides a network topology with better *P* loss than Shirmohammadi and Hong's algorithm [57].

The advantages of this heuristic algorithm are that the final result does not depend on the initial positions of the normally open points and the computing speed is fast. However, the global optimal result cannot be guaranteed when the network has more than one loop and these loops have mutual parts with others since only one branch is opened in solving an optimal flow pattern.

3. Genetic Algorithm

Genetic algorithm (GA) is an artificial intelligence optimisation technique which simulates the natural evolution process [78]. Since GA solves the problem by coding it in a binary code string, it is suitable for solving the network reconfiguration problem in which switch states are either 'open' or 'closed'. The approach of applying GA to *P* loss minimisation by network reconfiguration is introduced below [64]:

- Step 1: Determine the target function:

  The target function of *P* loss minimisation can be presented as follows [79]:

$$Min. \sum_{k=1}^{Nt} R_k I_k^2 \tag{2.38}$$

  Subject to:

$$I_k \leq I_k^{max} \tag{2.39}$$

$$V_j^{min} \leq V_j \leq V_j^{max} \tag{2.40}$$

  where:

  Nt: the total number of branches

  k: the branch k

  R_k: the resistance of branch k

  I_k: the current of branch k

  $I_k \leq I_k^{max}$: the thermal limits of branch k

$V_j^{min} \leq V_j \leq V_j^{max}$: the voltage limits of bus j

- Step 2: Determine the format of topology's binary code

  The target of applying a GA to solve the network reconfiguration is to determine the positions of normally open points. So the normally open points of a topology are coded in binary format. Consider a network that has 4 normally open points (NOPs) which are numbered as 1, 2, 3, 4 respectively. The binary numbers for these NOPs are 0001, 0010, 0011, 0100 [80]. Take the normally open point whose number is 4 for example, the relationship between the number and binary code is: $4 = 0 \times 2^0 + 0 \times 2^1 + 1 \times 2^2 + 0 \times 2^2$. The binary code of this network is shown in Figure 2.2 [80].

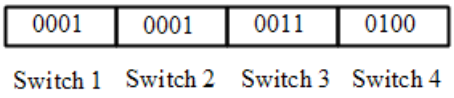

Figure 2.12 The binary code of the network [80].

- Step 3: Generate initial population

  Based on the coding method introduced in Step 2, generate an initial population which has M individuals randomly. Different problems may have different population size.

- Step 4: Selection

  The operation of selection selects the individuals from the population generated in Step 3 for crossover and mutation operations [81]. Whether the best individuals are selected has significant effects on the convergence of GA [82]. The common selection techniques are: roulette wheel selection, tournament selection, truncation selection, exponential ranking selection, etc. [81]. Taking "roulette wheel selection" for example, the area of each string on the wheel is calculated by target function defined in Step 1[80].

- Step 5: Crossover and mutation

  Crossover and mutation are two major genetic operators [80]. The target of these

two operators is to generate new individuals. The brief introductions of these two techniques are introduced below:

i) Crossover

The operation of crossover in GA produces new individuals by exchanging information among individuals [78]. It can be achieved by various techniques, like: one-point crossover, two-point crossover, uniform crossover, etc. Taking one-point crossover for example, its process is illustrated in Figure 2.13 [83]. First, two individuals are chosen as parents. Second, the code strings of these two parents are divided into two parts from the exchange point selected randomly. Finally, the code strings of two new individual are generated by exchanging the tail parts of two parents.

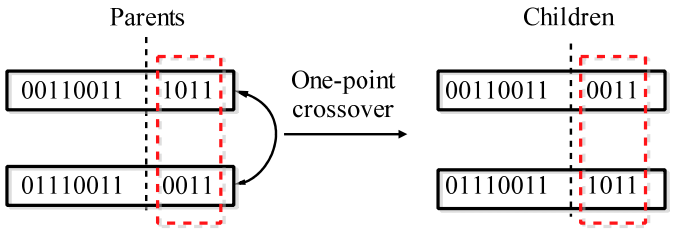

Figure 2.13 One-point crossover [83]

ii) Mutation

The operation of mutation in GA produces new individuals by reversing at least the value of one binary code [81]. The techniques of achieving the mutation are: bit string mutation, flip bit, boundary, uniform, etc. [81]. Taking the bit string technique for example, a new individual is generated by choosing one binary code from the code string of the parent and reversing it. An example of using bit string to achieve mutation is shown in Figure 2.14 [83].

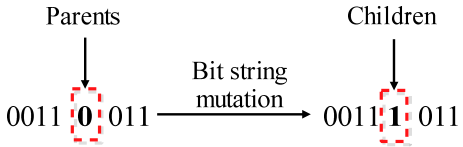

Figure 2.14 Bit string mutation [83]

- Step 6: A new population has been generated when steps 2-5 have been finished. This population is the new parent generation and some bad individuals are deleted. The process now goes back to step 4 unless the maximum generation is reached.

4. Mixed-Integer Programming.

The total resistance loss of network's branches can be written as [56]:

$$P_{Total\ loss} = \sum_{i=1}^{n} R_i\left(\frac{P_i^2 + Q_i^2}{|V_i|}\right) \tag{2.41}$$

where:

The current flows from bus i to bus $i+1$

R_i: resistance of the branch that connects bus i and bus $i+1$

P_i, Q_i: real and reactive powers flow out of bus i

V_i: voltage of bus i

Mixed-integer programing can be used to find the minimum value of (3.2) under the following constraints whose mathematical models are illustrated in [61]:

1) The network must be radial and without islands
2) Real and reactive power injection constraints
3) Voltage magnitude limits
4) Line current ratings

Applications of mixed-integer programing in network reconfiguration for P loss minimisation are introduced in [56, 61, 62]. Ramos et al. present how to apply mixed-integer linear programming on network reconfiguration for loss minimisation [62]. Rabih et al. present a new mixed-integer nonlinear programing model which considers distribution connected generators [61].

2.6 Summary

The scope for DNOs to respond positively to incentives to reduce losses is limited by the nature of legacy assets, their configuration, interactions with other incentives and

the cost-effectiveness of possible actions. However, limited availability of detailed network data required to model 11kV networks and perform load flow analysis, in order to assess these loss minimisation options, makes the modelling process onerous and demands certain assumptions to be made. An example from an urban network has been described and the various issues associated with building an accurate network model outlined. The future development of smart grids will improve the network monitoring level when more smart meters and network monitoring points are installed [84].

Chapter 3 Distribution Network *P* Loss Minimisation by Network Reconfiguration

In the previous chapter, the *P* loss of realistic 11kV distribution networks was studied first. After comparing with different published *P* loss optimisation methods and considering the existing devices DNOs have, the network reconfiguration method was chosen to optimise the *P* loss of distribution network. The configuration of the distribution network can be changed by moving the positions of the normally open points. Since different topologies may have different *P* loss, distribution network *P* loss optimisation can be solved by network reconfiguration. In this chapter, a new network reconfiguration algorithm based on graph theory is developed. This method does not require a network equivalent and can guarantee the global optimal result.

3.1 Introduction

The topology with minimum *P* loss can be obtained by calculating all possible pure radial topologies. But for a network that has *N* branches which can be opened, the number of all possible topologies is 2^N. When *N* is large, for example, when *N*=100, $2^{100} = 1.2676506 \times 10^{30}$: the load flow computing time of these 2^N is too long even by high speed computer. The *P* loss minimisation algorithm presented in this thesis can only handle pure radial distribution networks without islands (unconnected loads). So the topologies with loops and islands among the 2^N are invalid topologies for executing the loss minimisation algorithm. A topology generation algorithm which can generate all possible radial topologies without islands is developed in this thesis. The details of this algorithm are introduced in section 3.5. But the amount of these valid topologies is still large. In order to solve this problem, the network is divided into sub zones further. Instead of generating the valid topologies of the whole network, the valid topologies of each zone are generated. The details of the zone generation algorithm are introduced in section 3.4.1. When each zone's topology which has the minimum *P* loss is obtained, the whole network topology that has minimum *P* loss can be obtained by putting these topologies together.

3.2 Network Representation

Networks are modelled in different ways for different applications. For example, the admittance matrix is used to model the network for load flow calculation; the single line diagram is used to represent the structure of the network [43]. Graph algorithms introduced in Section 3.4 are used to search the network topology and generate all radial topologies. Graph theory is more appropriate to apply graph algorithms than the admittance matrix and the single diagram because graph algorithms are based on graph theory and they are much faster and use less memory, it is used to represent the network topology in this thesis. In graph theory, a graph consists of nodes and edges. Nodes can be linked with or without direction. If the edges have direction, the graph is a directed graph. Otherwise, it is an undirected graph. If a path whose start node and end node are the same, this path is defined as loop. A specific graph that has no loops and has a path between any two nodes is defined as a tree. A tree can be a directed or undirected graph [85]. When the topology of the distribution network is represented by a graph, a busbar is represented by a node and a branch is represented by an edge. All devices (e.g. transformers, loads) connected to the busbars are ignored. If the number of a graph's unconnected nodes is increased by removing an edge, this edge is defined as a "bridge" of this graph [85]. Consider an original graph named "*G*". A spanning tree of *G* is a directed graph whose direction is the direction of the current flows through the edges and in which all nodes are connected [86]. The topology of a distribution network operated in a pure radial structure is a spanning tree. When all open branches of the distribution network are closed, its topology is an undirected graph that has some loops. Different combinations of open branches generate different spanning trees. Comparing each possible spanning tree with *G*, the edges in *G* but not in the spanning tree represent the open branches of the distribution network.

Although representing a graph by a picture is convenient for visualizing it, it is not suitable for a programming language to deal with. The adjacency matrix and adjacency list are two widely used data structures for storing the graph linking information [87]. A $n \times n$ adjacency matrix $\vec{M}$ represents a graph with n nodes. The value of the matrix element can be 1 or 0. For undirected graphs, if there is an edge that links node i and node j, the elements $m_{ij} = m_{ji} = 1$. Otherwise, $m_{ij} = m_{ji} = 0$.

For directed graph, if there is an edge whose direction is from node *i* to node *j*, the element $m_{ij} = 1$. Otherwise, $m_{ij} = 0$. For the adjacency list, the adjacent nodes and edges of each node are represented by a list [87]. The adjacency matrix of the undirected graph in Figure 3.1 is shown in Figure 3.2. In order to make the figure simple, only the name of the node is shown on the figure in this thesis. The rule for naming an edge is: when an edge links node *a* and node *b*, its name is *a*-*b* or *b*-*a*. Comparing these two data structures, the adjacency matrix has many elements whose value is 0 because only relatively few nodes have branches between them in a radial network, and typical meshed power networks also have lots of zeros in the adjacency matrix, i.e. the matrix is sparse. When the graph has a large number of nodes, the adjacency matrix requires a large memory to store the data. So, the adjacency list used in this thesis is more efficient than the adjacency matrix when the graph is large and radial.

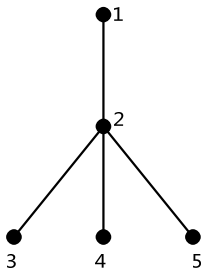

Figure 3.1 Example graph

$$\vec{M} = \begin{array}{c} \\ 1 \\ 2 \\ 3 \\ 4 \\ 5 \end{array} \begin{array}{c} \begin{array}{ccccc} 1 & 2 & 3 & 4 & 5 \end{array} \\ \begin{bmatrix} 0 & 1 & 1 & 1 & 1 \\ 1 & 0 & 1 & 1 & 1 \\ 0 & 1 & 0 & 0 & 0 \\ 0 & 1 & 0 & 0 & 0 \\ 0 & 1 & 0 & 0 & 0 \end{bmatrix} \end{array}$$

Figure 3.2 The adjacency matrix

3.3 The Algorithm of *P* Loss Minimisation by Network Reconfiguration Based on Graph Theory and Topology Search Techniques

A new algorithm of *P* loss minimisation by network reconfiguration is developed in this thesis. This algorithm is based on graph theory and topology search techniques. The main steps of this algorithm shown in Figure 3.3 are: 1) Step 1: closing all open

branches of a network whose original topology must be radial; 2) Step 2: dividing the whole network into independent sub-networks; 3) Step 3: finding all spanning trees of each sub-network; 4) Step 4: calculating each spanning tree's *P* loss and finding the spanning tree with the minimum *P* loss in every sub-network. 5) Step 5: choosing the minimum *P* loss topology of each sub-network to form a whole network topology. This new topology is the minimum *P* loss topology of the whole network.

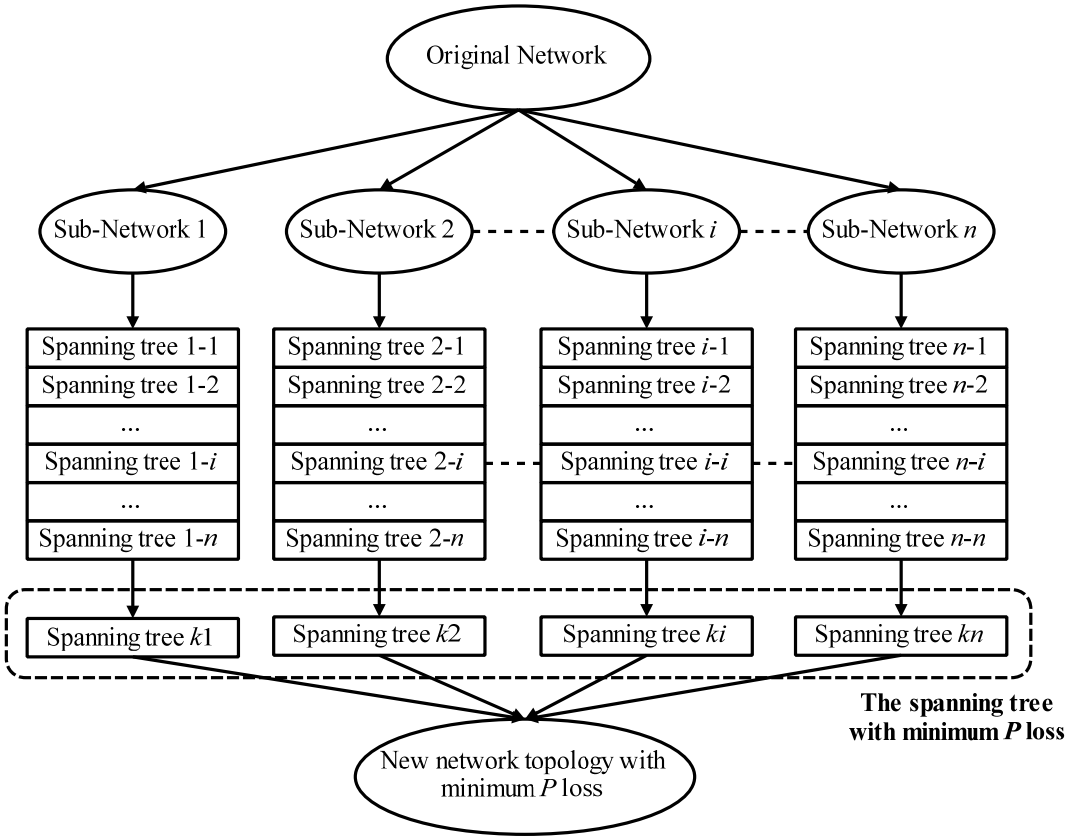

Figure 3.3 The new *P* loss optmisaton by network reconfiguration developed in this thesis

Since this *P* loss optimisation algorithm performs an exhaustive search, the global optimal results. The algorithms to find the sub-networks of a whole network and all spanning trees of each sub network are the most important parts of the *P* loss optimisation algorithm. In order to implement these two algorithms, the following concepts and techniques are applied:

- **The Concepts of Upstream and Downstream**

  When the graph of a distribution network is considered as a directed graph, the direction of the edge is defined as the direction of the current flow through it. In this case, the concepts of upstream and downstream are used to illustrate the position relations of the elements [88]. Taking node B2 in Figure 3.4 for example, the nodes and edges in the current flow direction are defined as downstream parts of the node B2. Otherwise, they are defined as the upstream parts.

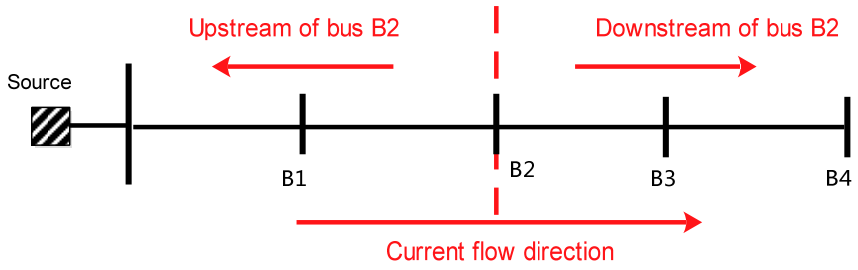

Figure 3.4 Definiton of upstream and downstream

- **The Concepts of PV Node, PQ Node and PV Edge**

  The naming convention of PV node, PQ node and PV edge have been developed by the author of this thesis. A node connected to a source (e.g. generator, grid infeed) is named as a PV node in this thesis. In Figure 3.5(a), node 1 is a PV node. A node that does not have a connected source is named as a PQ node in this thesis. As shown in Figure 3.5(a), nodes 2, 3, 4 and 5 are PQ nodes. All edges directly connected to a PV node are named as PV edge in this thesis. In Figure 3.5(b), edge 1-2 is a PV edge.

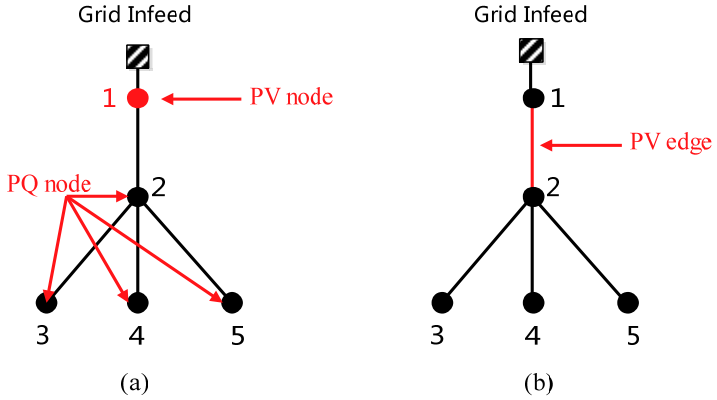

Figure 3.5 PV node, PQ node and PV edge

- **Topology Search Techniques**

There are two general techniques for traversing a graph: Breadth-First Search (BFS) and Depth-First Search (DFS) [89]. Both of BFS and DFS need a root node to start the search. In a BFS, all nodes connected to the root node are found. Then all newly found nodes are used as root node to find a further set of nodes [89]. In a DFS, the search starts from the root node and goes as far as possible. Figure 3.6 is used to illustrate the difference between BFS and DFS for the same graph. The orders of nodes searched in BFS and DFS are shown in Figure 3.6(a) and Figure 3.6(b) respectively.

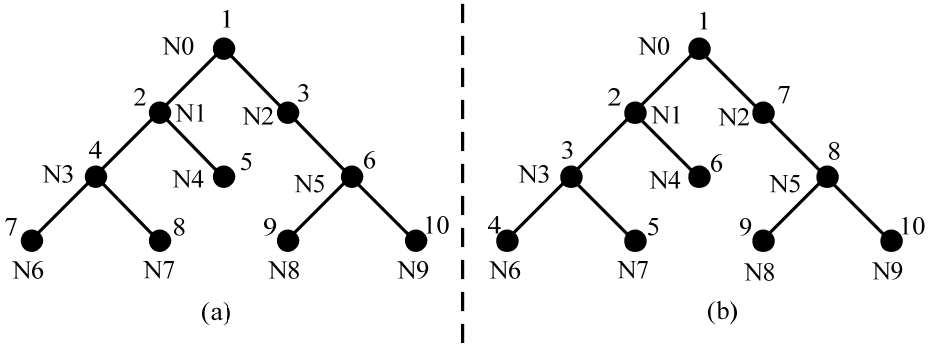

Figure 3.6 BFS and DFS

The concept of layers introduced in [52] is used in BFS. Consider Figure 3.7 for example. BFS starts from node 1 which is the root of the graph. Nodes 2 and 3 are connected to node 1 and form the 1st layer. Nodes 4 and 5 are connected to node 2 and node 3 is connected to node 5. These three nodes form the 2nd layer. Similarly, the nodes forming the 3rd layer are nodes 7, 8, 9 and 10.

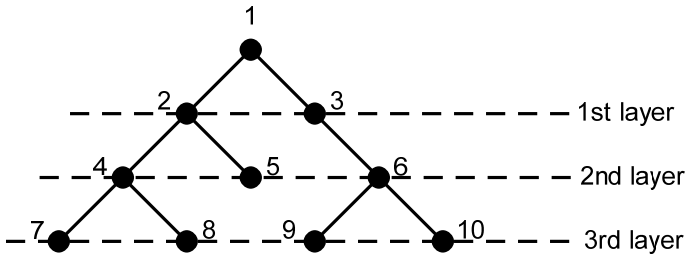

Figure 3.7 Layers of BFS

The reason for using breadth-first search (BFS) rather than depth-first search (DFS) in this thesis is that successive layers must be identified and these can

readily be generated by using BFS. Furthermore, the BFS algorithm developed in this thesis generates the layers, the paths from source to each node, and each node's upstream and downstream edges at the same time.

The flowchart of the BFS is shown in Figure 3.8 in which the variables used in the flowchart are:

- ***Pre***: vector holds nodes of the previous layer
- ***Nex***: vector holds nodes of the next layer
- ***TN***: vector holds searched nodes

The flowchart means that the vector ***Pre*** is initialized by adding all nodes on the first layer. After all unsearched nodes connected to the nodes in the vector ***Pre*** have been added to the vector ***Nex***, set ***Pre***=***Nex*** and empty ***Nex***. So one layer formed by nodes in ***Pre*** has been found. Keep on running this process to find the next layer until no node is connected to the present vector ***Pre***.

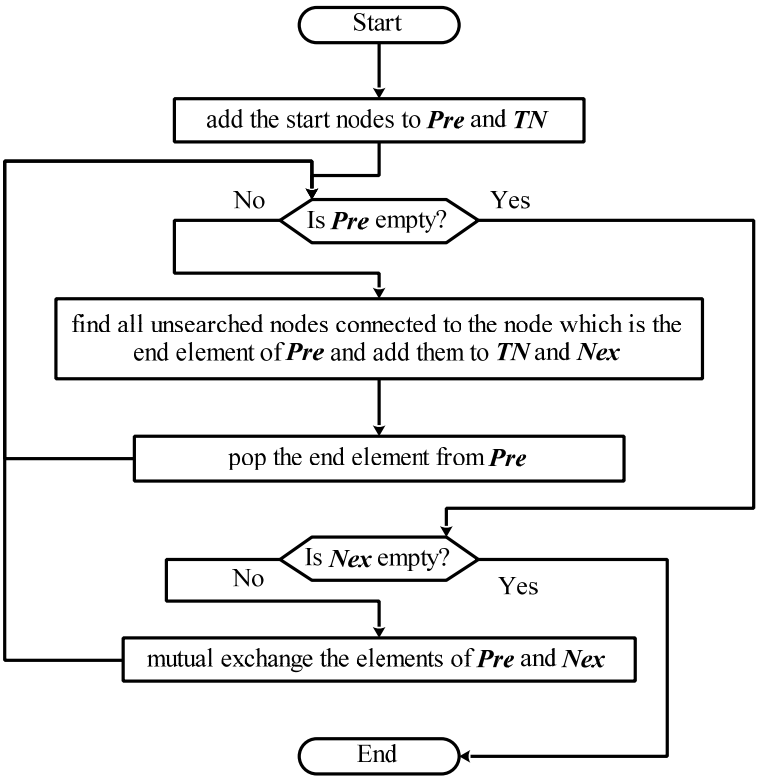

Figure 3.8 Flowchart of BFS [90]

3.4 Preprocessing of Network Topology

In order to reduce the time of generating all spanning trees of a graph and prepare the graph data used in loss minimisation and reliability evaluation analysis, preprocessing of the network needs to be performed on the graph. The preprocessing includes the following steps:

1. Dividing the network into separate zones
2. Determining the direction of each edge and finding the Upstream and Downstream edges of each node
3. Finding the edges which must be in closed status
4. Merging all PV nodes into one node

The details of each step are presented in the next subsections.

3.4.1 Dividing the Network into Separate Zones

The concept of a zone used here is developed by the author of this thesis. A zone is defined as: If a zone has N PV nodes (where $N \geq 1$), PQ nodes belonging to this zone can only be transferred among these PV nodes. A PV node can belong to more than one zone. A PQ node can only belong to one zone. Thus, a zone can be thought of as a set of PQ nodes associated with a single set of PV nodes; even when closing all normally points, no path exists between a PQ node in one zone and a PQ node in another zone except via one or more PV nodes. (The concepts of PV and PQ nodes were introduced in Section 3.3).

The algorithm of zone generation used here is developed by the author of this thesis. The BFS is applied in dividing the network into separate zones. PQ nodes are permitted to only belong to one zone and PV nodes may belong to more than one zone.

The flowchart of the process of network zone division is shown in Figure 3.9. In the zone identification process, the graph is considered as an undirected graph no matter if its original property is directed or undirected, and all edges are closed. Before starting the BFS to find a zone, all nodes are marked as “unsearched”. The BFS

search starts from a randomly chosen PV node. This chosen PV node is marked as “searched”. It should be noted that PV nodes are only marked as “searched” on the initial step of a BFS. If an unsearched PV node is found during BFS, its status remains “unsearched”. During the BFS, when an unsearched PQ node is found, it is marked as “searched”, added to the relevant zone and considered as a new start node of BFS to find the next connected node. When an unsearched PV node is found, it is added to the relevant zone as well but not considered as a new start node of BFS and not marked as “searched”. The BFS does not proceed past this PV node. When no new start node of the BFS can be found, all nodes of a zone have been found. The algorithm chooses the next unsearched PV node to find other zones until no unsearched PV node is left.

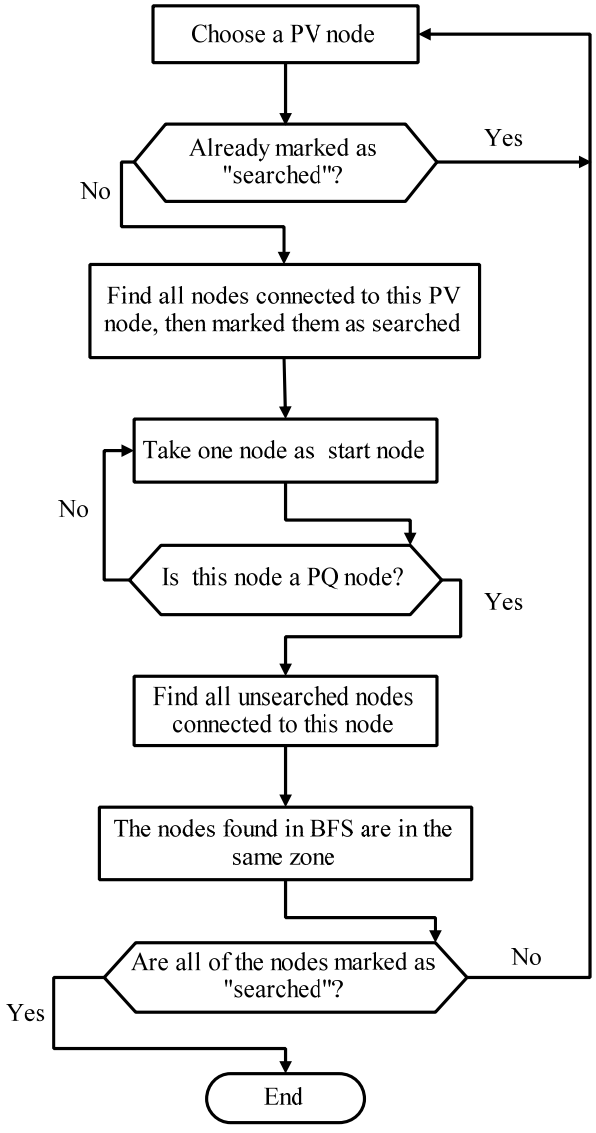

Figure 3.9 Flowchart of zone dividing

Figure 3.10 is used to illustrate this process. Here, the PV nodes of this graph are nodes b1, b2, b3, b4 and b5. The BFS starts from node b1 chosen randomly from these five PV nodes and continues until nodes b2 and b3 are searched. Since b2 and b3 are PV nodes, the BFS of these two nodes are stopped. All searched nodes b6, b7, b8, b9, b10, b11, b12,b b13, b14, b15, b16 are treated as being in the same zone whose name is zone 1. Similarly, the nodes b17-b21 are in zone 2. When this processing has finished, the closed edges whose original status is open need to be opened again.

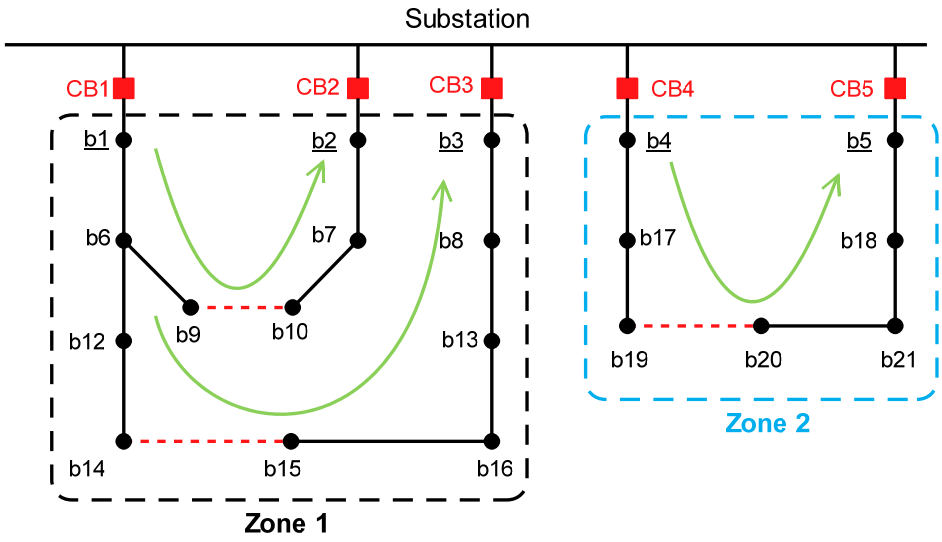

Figure 3.10 Dividing the network in to separate zones

3.4.2 Determining the Direction, and the Upstream and Downstream Edges of Each Node

The concept of a layer was introduced in Section 3.2. After keeping the original open edges in open status and finishing the BFS which starts from the PV nodes of the graph, each node has a layer number. Since the current flows from the upstream layers to the downstream layers, the direction of the edge is from the node with smaller layer ID to the node with larger layer ID. The concepts of upstream and downstream have been introduced in section 3.2. When the direction of each edge has been identified, the upstream and downstream edges of each node can be determined. Due to the characteristic of a radial network, each node has only one upstream edge connected to it except the root node which has no upstream edge connected to it because it is the start node of the graph. There is no limit on the

number of the connected downstream edges. Consider the graph in Figure 3.11 for example. The upstream edge of node 1 is edge 0-1 and the downstream edges are edges 1-2, 1-3 and 1-4.

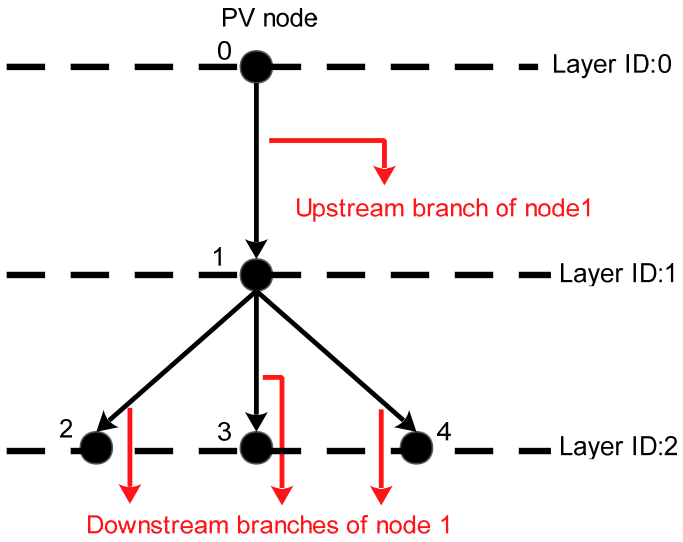

Figure 3.11-The upsteam and downsteam parts of a bus

3.4.3 Finding the Edges Which Must be in Closed Status

Even if every edge of the graph could be opened, some edges must always remain in a closed status so that the constraints of the distribution network topology can be satisfied. Since these edges are closed in every spanning tree of the graph, they can be deleted from the original graph so that the size of the candidate edges used to generate spanning trees can be reduced. The processing of finding these edges has two steps:

Step 1: Finding the path from the nodes which the open edge links to the PV node

After generating the upstream branch of each node, the path between any two nodes which are connected to the same primary feeder can be found quickly by using this information. The flowchart of finding the path between two nodes is shown in Figure 3.12 in which the variables used in the flowcharts are:

- ***S***: The start node of the path
- ***E***: The end node of the path (the layer ID of *E* must be larger than *S*'s)
- ***UE***: The upstream edge of *S*

- ***PEV***: The vector holding all the edges of the path

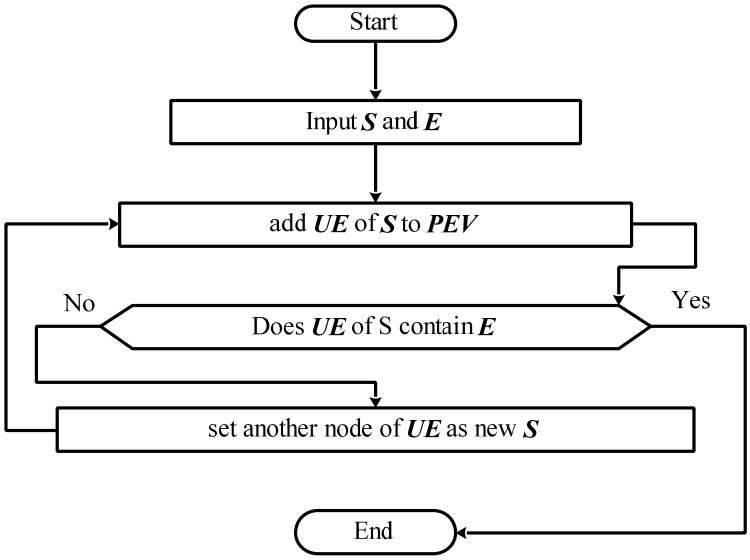

Figure 3.12 The flowchart of path search algorithm

Taking the graph in Figure 3.13(a) as an example, this graph has two PV nodes which are nodes 0 and 1 and one open edge which is edge 4-5. The edge 4-5 links two nodes: nodes 4 and 5. So the edges of the path from node 4 to node 0 are edges 2-4 and 0-2; the edges of the path from node 5 to node 1 are edges 5-3 and 3-1. Any edges in the path from the nodes of the open edge to the PV nodes are marked as "tree" and used to generate the spanning tree. Otherwise, the edges are marked as "lateral" and deleted from the graph. As shown in Figure 3.13(b), the number of edges is reduced from 9 to 5. In this way, the number of candidate edges used to generate the spanning tree is reduced.

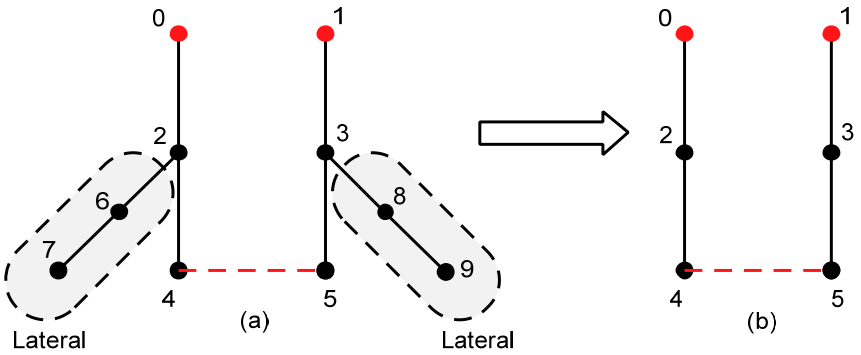

Figure 3.13 Graph with laterals

Step 2: Finding the bridges of the Graph

In order to check whether a "tree" edge is a bridge, delete this edge from the graph then run the BFS from the PV nodes. All branches marked as "lateral" in the previous step are not included in this step since it is obvious that all laterals are bridges of the graph. If all nodes of the graph can be found in a search that uses only the edges that remain within the graph, i.e. closed branches, this edge is not a bridge. Otherwise, it is a bridge. The flowchart of finding the bridges in a graph whose lateral edges are deleted is shown in Figure 3.14. The variables used in the flowchart are listed as follows:

- ***G***: The graph of the network
- ***EV*****:** The vector that holds the edges of *G*
- ***RV*****:** The vector that holds the PV nodes of *G*
- ***DE***: The edge that needs to be checked whether it is a bridge
- ***BV*****:** The vector that holds the bridges of *G*

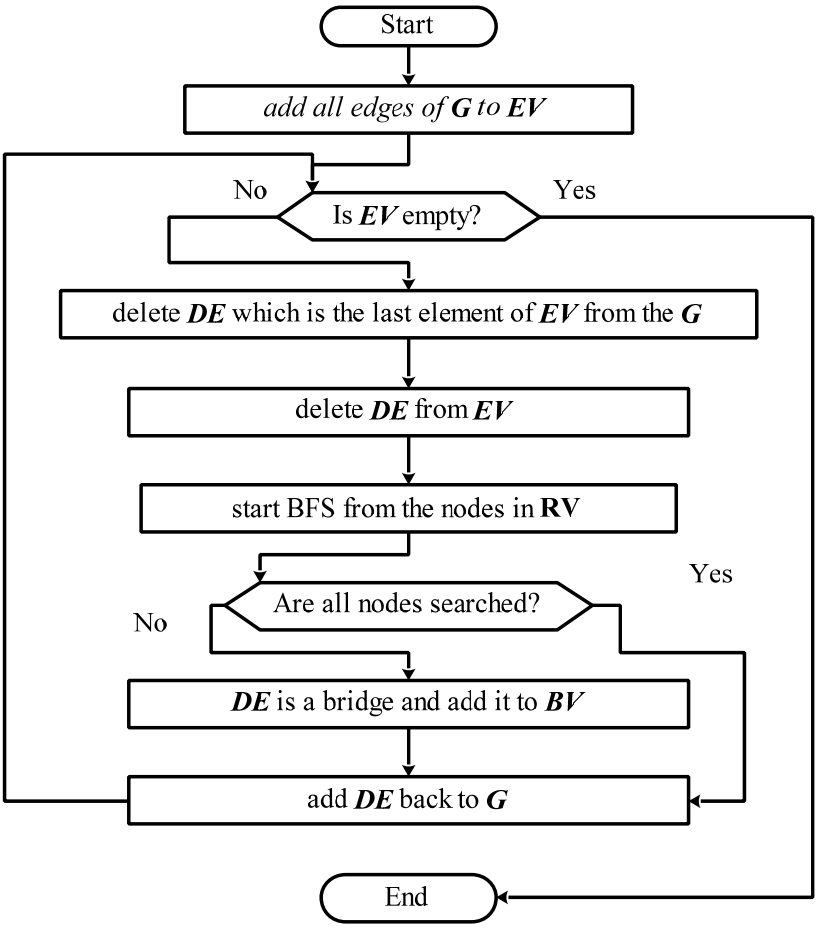

Figure 3.14 Flowchart of finding the bridges of the Graph

Unlike the edges marked as “lateral”, the edges marked as “bridge” are, like the edges marked as “tree”, candidate edges for generating the spanning tree. But they must appear in every spanning tree of the graph.

3.4.4 Merging all PV Nodes into One Node

When all PV nodes are found, spanning trees will start to grow from these nodes. But in the spanning tree generation algorithm, one graph can only have one root node. In order to solve this problem, when a graph has more than one PV node, these nodes are merged into one node. This new PV node is the root node of the graph for spanning tree generation. The network in Figure 3.13(b) has two PV nodes – nodes 0 and 1. When these two nodes are merged, node 1 is the root node of new graph in Figure 3.15(b).

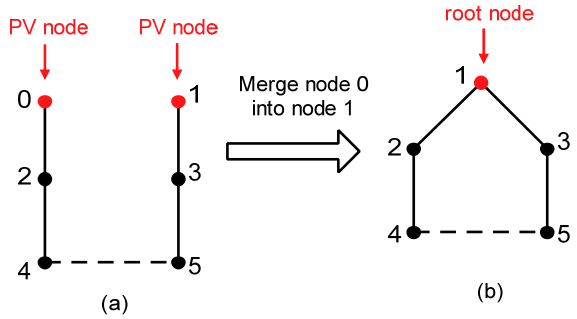

Figure 3.15 Merging the PV nodes of the graph

When all spanning trees are generated, the root node of each spanning tree needs to be split into the original separated nodes. Figure 3.16 illustrates this process. The graph in Figure 3.16(a) is one spanning tree of the graph in Figure 3.15(a). The dashed line means the open edge. Figure 3.16(a) shows the PV-nodes-merged state of the spanning tree and Figure 3.16(b) shows PV-nodes-split state of the spanning tree.

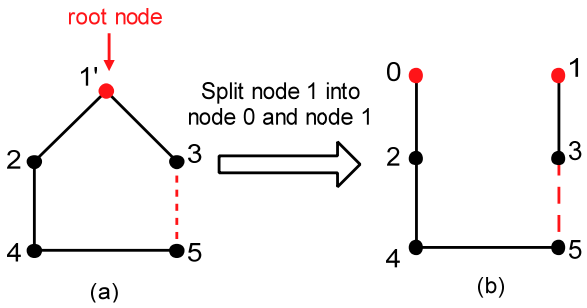

Figure 3.16 Splitting the root node into the original separated nodes

3.5 Generating all Spanning Trees of a Graph

Different algorithms to generate all the spanning trees of a graph have been introduced in [91-93]. The algorithm presented in [91] has been used in this thesis. This algorithm uses the concepts of stacking and recursion (introduced in Appendix B.1) to control the growth of a spanning tree. In the algorithm, there is only one global stack to control the tree growth depth first and the local stack that corresponds to recursion is used to reconstruct the global stack. The global stack has the first priority to add the new edge to the tree. When the global stack is empty and the local stack has elements, the local stack swaps its elements with the global stack. If both of them are empty, the growth process ends. The flowchart of this algorithm is shown in Figure 3.17. The main variables used in the flowchart are listed below:

- ***G*:** The graph of the distribution network
- ***GS***: The global stack that holds candidate edges
- ***LS***: The local stack that holds candidate edges
- ***VE***: The vector that holds the edges
- ***VS***: The vector that holds the spanning trees of the graph
- ***r***: The root node
- ***TN*:** The vector that holds the nodes of the tree, all nodes in this vector are marked as "searched node"
- ***TE***: The vector that holds the edges of the tree, all edges in this vector are marked as "searched edges"
- ***n*:** The new node added to *TN*

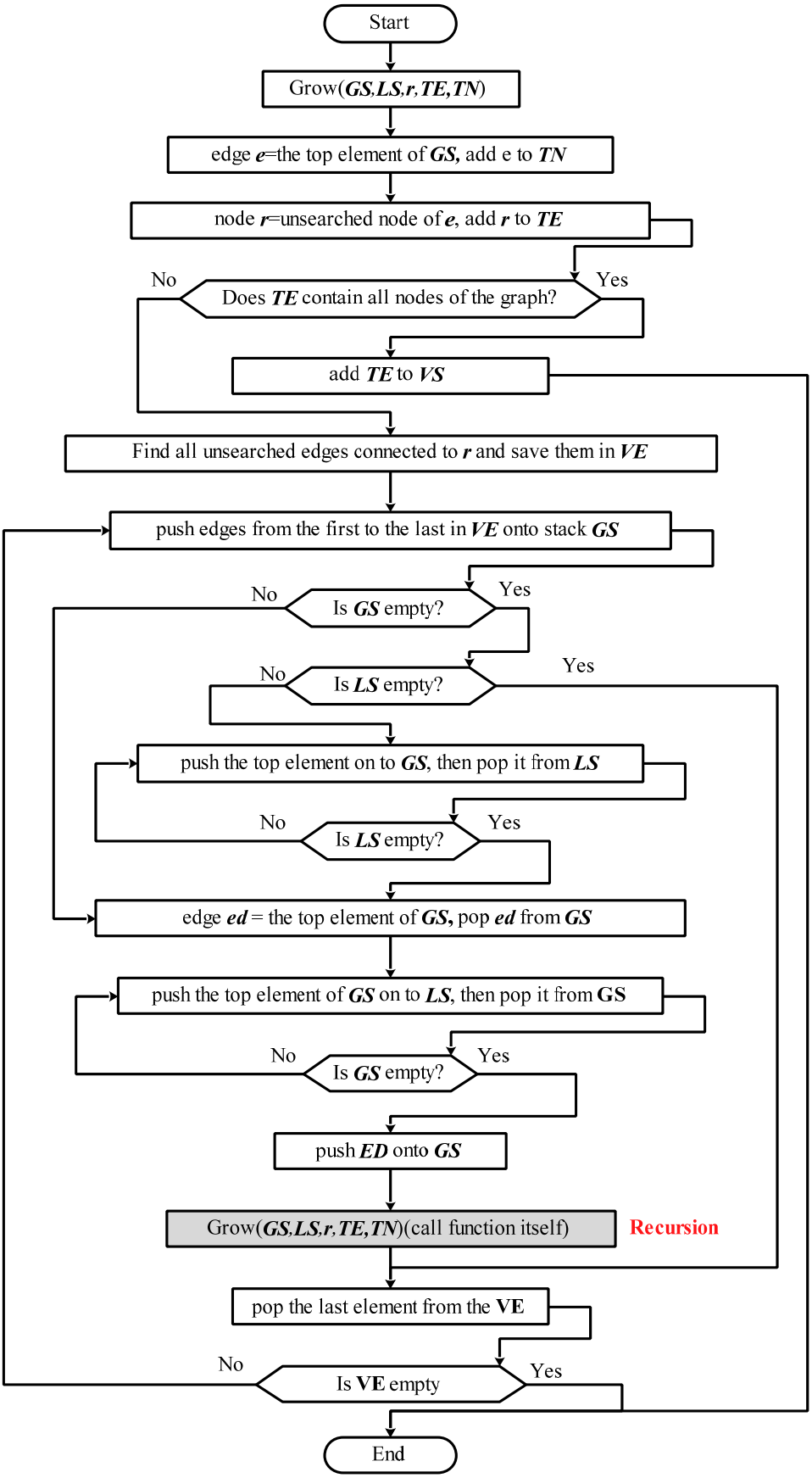

Figure 3.17 Flowchart of the spanning tree generation algorithm

When the graph in Figure 3.13(a) represents the topology of a distribution network, all spanning trees of *G* can be generated by applying the spanning tree generation algorithm introduced above. As shown in Figure 3.18, the open branches of this network's all valid radial topologies are edges 1-3, 3-5, 4-5, 2-4 and 1-2 respectively. The branches represented by dashed lines show the positions of normally open points. The detailed process of generating these spanning trees is introduced in Appendix B.2.

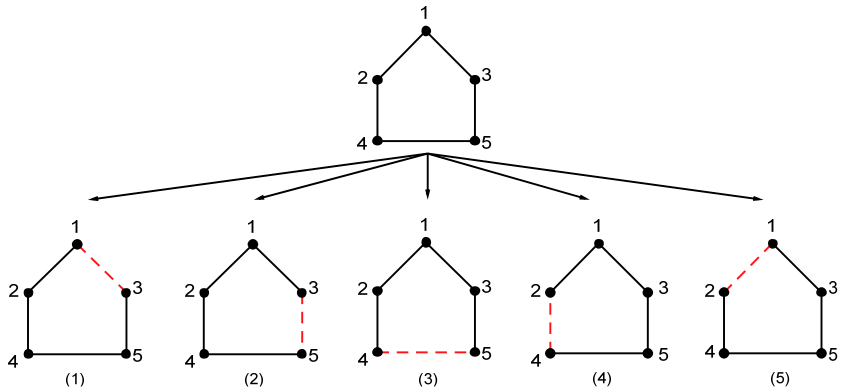

Figure 3.18 All spanning trees of *G*

3.6 Final Network Reconfiguration Results Evaluation

When all valid topologies of each zone have been generated, each topology's *P* loss is calculated by running a load flow. Among these topologies, the load flow of some topologies might not converge so they are ignored for the next step calculation in order to reduce total number of candidate topologies. The remaining topologies are named as "valid candidate topologies". The load flow engine used in thesis is based on the Newton-Raphson method so it is not guaranteed to always converge for any network. The networks with non-converged Newton-type load flow solutions are considered as voltage unstable [94]. The reasons for non-converged network topology in these are that the feeder is loaded heavily and some loads are far from the source leading to an unacceptably high voltage drop.

In order to illustrate how to get the network minimum *P* loss topology after the *P* loss of each zone's valid candidate topologies have been obtained, the network used in section 3.4.1 is reused here. As shown in Figure 3.19, the example network has

two zones: zone 1 and zone 2. The locations of the various branches dictate that load points in zone 1 can only be transferred among the PV nodes in zone 1 which are busbars b1, b2 and b3. Similarly, transfer of the load points in zone 2 is limited to be within zone 2. So when the minimum *P* loss topologies of these two zones are found individually, the normally open points of the whole network's minimum *P* loss topology can be obtained by putting the normally open points of each zone's minimum *P* loss topologies together. The minimum *P* loss topology of each zone can be obtained by sorting all topologies of the zone from the lowest to the highest *P* loss. The process of how to obtain the minimum *P* loss topology of a network with *i* zones and where each zone has N_i valid candidate topologies is shown in Figure 3.20.

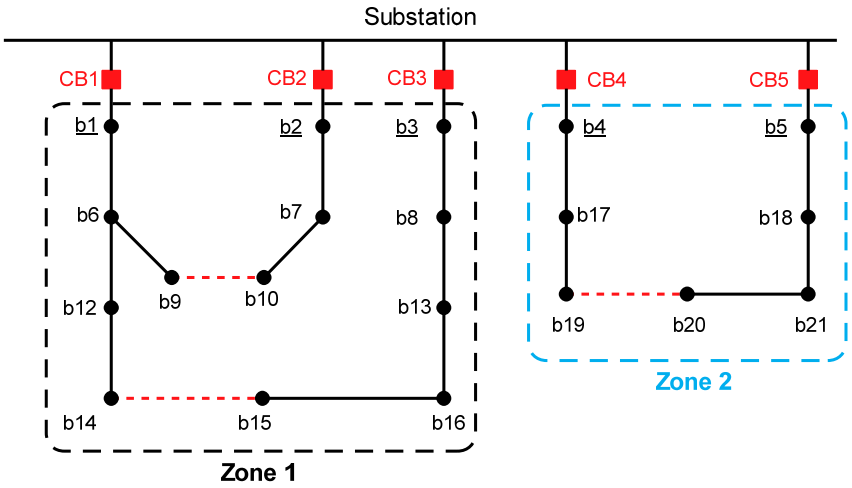

Figure 3.19 The example network with two zones

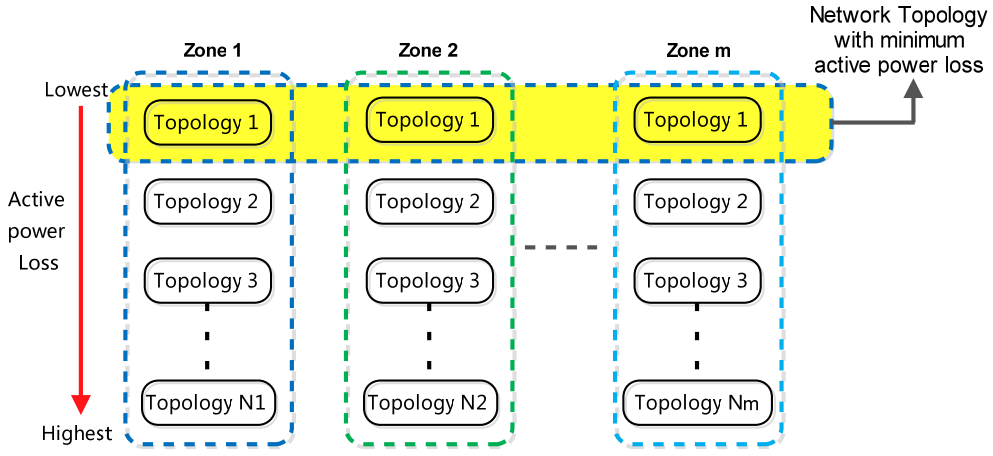

Figure 3.20 Valid topologies of each zone

Since the load flow engine used in this thesis is based on Newton-Raphson method, the load flow results of a network are not exactly the same when the positions of busbars in the admittance matrix used for load flow calculation are different due to the different sequences of adding load points to the load flow engine and different numbers of busbars. Taking a network *G* with two zones Z_1 and Z_2 for example, in the algorithm of *P* loss optimisation by feeder reconfiguration, the *P* losses of Z_1 and Z_2 are calculated separately first and then added together to get the total *P* loss of the whole network *G*. Let $P_{sep-loss}$ represent the *P* loss of *G* calculated in this way. Another way to calculate *G*'s *P* loss is consider the *G* as whole network so that its *P* is represented by $P_{tog-loss}$. The values of $P_{sep-loss}$ and $P_{tog-loss}$ may not be exactly the same when using the Newton-Raphson method to calculate the load flow. When the number of output topologies is *F*, the sequences of these *F* topologies sorted from lowest to highest $P_{sep-loss}$ may be different from the sequences sorted by $P_{tog-loss}$ since one topology's $P_{sep-loss}$ and $P_{tog-loss}$ are not exactly the same. The difference between $P_{sep-loss}$ and $P_{tog-loss}$ and the impacts of this difference on the feeder reconfiguration results is evaluated in section 6.2. In order to reduce the impact of the potential error caused by calculating the whole network's *P* loss by separated zones, more candidate topologies of the whole network are generated by a rule introduced below. Instead of calculating *P* loss in separate zones, these topologies are considered as a whole network to calculate their *P* loss by load flows to check whether their *P* loss is smaller than the loss of the network topology which consists of each zone's minimum *P* loss topologies directly. The rule of generating these network topologies are is outlined in the following section.

The topology of a network consists of choosing one topology from each zone. When a network has *N* zones and the number of valid candidate topologies in zone i is $K_i (i = 1,2, \dots N)$, the number of all possible radial network topologies T_{Ntotal} is:

$$T_{Ntotal} = K_1 \times K_2 \times \dots\dots \times K_N \tag{3.1}$$

Theoretically, the minimum *P* loss network topology can be obtained by calculating the load flow of all T_{Ntotal} topologies and sorting them from lowest to highest *P* loss. But when T_{Ntotal} is very large, the calculation speed is very slow. T_o is taken to

represent the network topology that consists of each zone's own minimum *P* loss topology. For the topologies whose total *P* loss estimated as the summation of the separate zone losses are higher than T_o, for example, 1.5 times T_o's *P* loss, their *P* loss as a single, combined network does not need to be calculated again. In order to reduce the potential error on *P* loss optimisation by feeder reconfiguration caused by calculating network *P* loss in separate zones, the tool developed in thesis provides two modes to find the final result. These two modes are: 1) when the calculation time of all T_{Ntotal} topologies is acceptable to the user, the algorithm re-calculates the *P* loss of all T_{Ntotal} topologies by considering them as a whole network instead of separate zones. 2) when the calculation time of all T_{Ntotal} topologies is long, the algorithm will only generate *M* topologies of the whole network to calculate their *P* loss by considering them as a whole network instead of separated zones. The maximum topology number threshold T_{max} and a weight σ which are both positive integral values chosen by user are used to make the algorithm choose the appropriate mode. By comparing the value of T_{total} and $(1+\sigma)T_{max}$, the appropriate mode can be chosen as follows:

- When $T_{total} > (1+\sigma)T_{max}$

  In this scenario, it should be impractical to run the load flow of all *T* topologies because of the long calculation time. So the algorithm will generate *M* valid network topologies to check whether there is a topology whose *P* loss is lower than T_o's. In order to limit the size of *M*, only the first and second minimum *P* loss topologies of each zone are used to generate the topologies combination of the whole network. So *M* is not a fixed value but depends on the number of zones in the network. These *M* whole network topologies are generated by the following coding method:

  Taking a network with *Z* zones for example, its topology can be represented by the code string shown in Figure 3.21. The position of each value in the code string is marked as 1 to *N* from left to right. The value of each position can be zero or one. As shown in Figure 3.22, zero means the chosen topology of this zone is the second minimum *P* loss topology. If this zone only has one topology,

this sole topology is used instead. One means the chosen topology of this zone is the first minimum *P* loss topology.

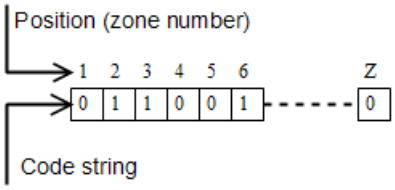

Figure 3.21 Code string of network topology

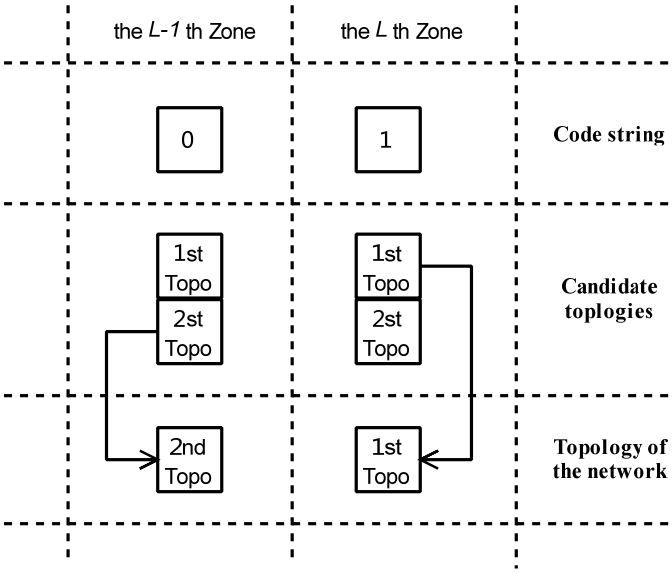

Figure 3.22 Processing of generating new network topologies

T_a, which is the total number of all possible network topologies generated by the rule introduced above, is:

$$T_a = C_Z^0 + C_Z^1 + C_Z^2 + \cdots + C_Z^i + \cdots + C_Z^{Z-1} + C_Z^Z = \sum_{i=0}^{Z} \frac{Z!}{i!\,(Z-i)!} \tag{3.2}$$

where:

i: the number of zones whose 2nd minimum *P* loss topology are chosen.

Z: the total number of zones.

So *M* is equal to T_a in this mode.

- When $T_{Ntotal} \leq (1+\sigma)T_{max}$

  In this scenario, the load flow calculation time of all T_{Ntotal} topologies should be acceptable. So M is equal to T_{Ntotal}.

At this point, the process of finding the minimum P loss topology by feeder reconfiguration is complete. The flowchart of this process is shown in Figure 3.23.

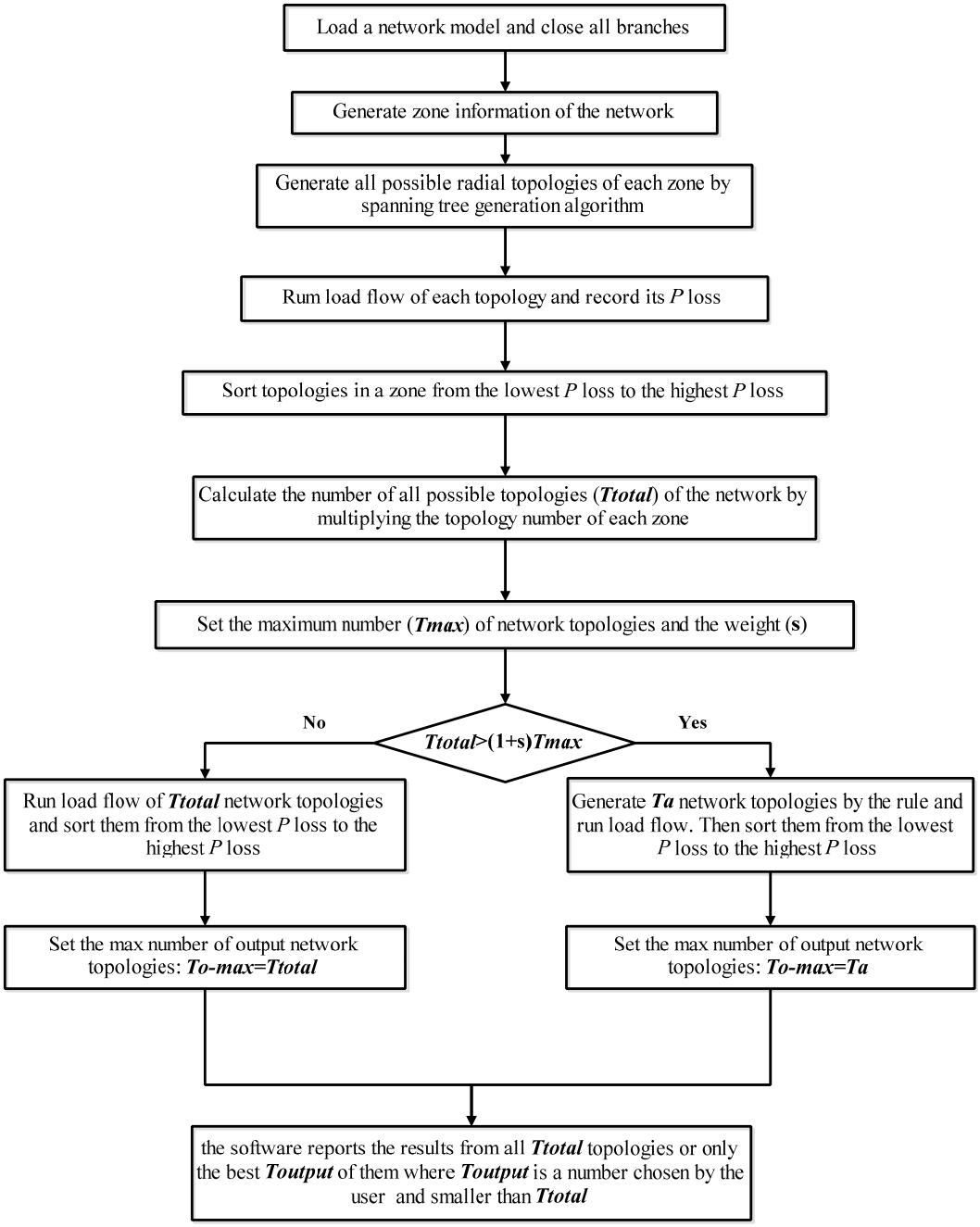

Figure 3.23 Flowchart of network loss minimisation by network reconfiguration

The value of T_{max} is defined by the user since it is dependent on the size of the calculation network, the speed of the computer, the acceptable calculation time, etc. The weight σ is used to determine whether it is still acceptable to run the load flow of T_{Ntotal} topologies even when $T_{Ntotal} > T_{max}$. For example, when T_{Ntotal} is equal to 2000 and T_{total} is equal to 1000, it may still be acceptable to run the load flow of T_{Ntotal} topologies. One method for the user to determine the values of T_{max} and σ is to try different values according to the topologies of different zones. Further methods of finding the appropriate value of σ are discussed in section 7.2 under future work.

Though the rule discussed here may not always work for any network, it still provides a way to further check the output results and can provide more than one output topology with good *P* loss.

3.7 Validation of the Spanning Tree Generation and *P* Loss Optimisation by Implementations of the Network Reconfiguration Algorithms

In this section, the implementations of the spanning tree generation and *P* loss optimisation by network reconfiguration algorithms introduced in this chapter are validated. The graph of the network model in Figure 3.24 is used in each validation [49].. The reason for choosing this model is that it is widely used in the study of distribution network reconfiguration for loss minimisation [49, 54, 56, 69, 74, 95].

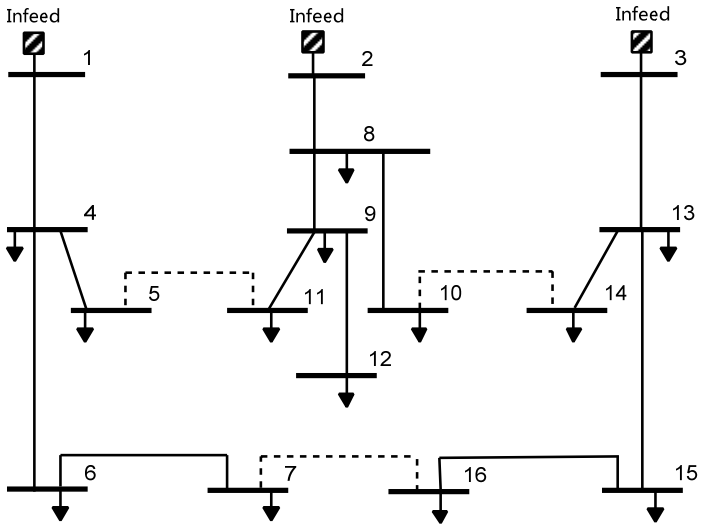

Figure 3.24 16-bus network model [49]

This network model has three feeders, sixteen busbars, and thirteen loads. All branches have switches on them so that they can be used to perform the network reconfiguration. The network needs three open branches in appropriate positions to make the network structure radial while ensuring that all loads are powered by a single source. The initial open branches of this network are branches 10-14, 11-5 and 7-16.

3.7.1 Validation of the Spanning Tree Algorithm's Implementation

The spanning tree generation algorithm introduced in Section 3.5. This algorithm was developed by Gabow et al. [91]. In order to validate the accuracy of this algorithm's implementation in DisOPT, a case study of calculating all spanning trees of a graph by a different algorithm is presented in this section. In order to distinguish these two spanning tree algorithms, the algorithm used in this section for validation is named as "Algorithm2" while the algorithm introduced in Section 3.5 is named as "Algorithm1".

Algorithm 2 is used to generate all spanning trees of the network in Figure 3.24 first, then Algorithm1 is applied to the same graph. Unlike Algorithm1, which is suitable for any graph, Algorithm2 is developed by the author of this thesis and designed for the network in Figure 3.24 especially. The details of how to use Alogrithm2 are presented below:

The example network in Figure 3.24 has three infeeds. Which infeeds are chosen to energize the loads depends on status of branches 1-4, 2-8 and 3-13 (e.g. open or closed) connected directly to the infeeds. For example, there is no load connected to the infeed on busbar 1 when the branch 1-4 is open. Before starting to calculate all spanning trees of this network, the branches 1-4, 2-8 and 3-13 that are connected directly to infeeds need to be divided into the following seven combinations shown in Table 3-1 by their status.

Table 3-1 Status combinations of the branches 1-4, 2-8 and 3-13

Topology ID	The status combinations of branches		
	1-4	2-8	3-13
1	Close	Open	Open
2	Open	Close	Open
3	Open	Open	Close
4	Open	Close	Close
5	Close	Open	Close
6	Close	Close	Open
7	Open	Open	Open

Since these seven combinations represent seven different initial topologies, duplicated spanning trees can be avoided. The next step of finding the remaining open branch or branches is illustrated below. The open branches are shown by red dashed lines in the figures.

1) No.1: Open branches: 2-8, 3-13 Close branch: 1-4

In order to find the remaining open branch in this scenario, one path from busbar 4 (coloured red) to busbar 4 is defined and shown in Figure 3.25. This path is named "Path 1" for this infeed scenario and contains 12 branches which are 4-6, 6-7, 7-16, 16-15, 15-13, 13-14, 14-10, 10-8, 8-9, 9-11, 11-5 and 4-5. So, twelve different topologies can be found by choosing one branch from these twelve candidate branches in Path 1.

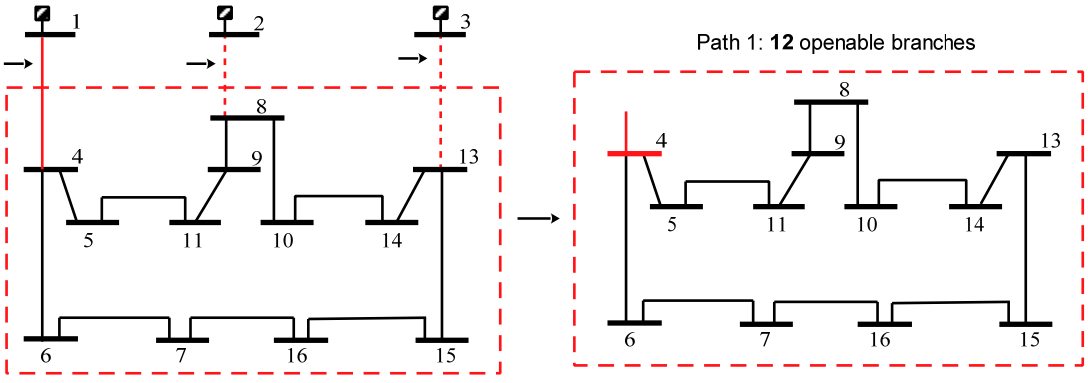

Figure 3.25 Paths in Combination No.1

2) No.2: Open branches:1-4, 3-13 Close branch:2-8

In order to find the remaining open branch in this scenario, one path from busbar 8 to busbar 4 coloured with red is defined and shown in Figure 3.26. This path is named

"Path 1" and contains 12 branches which are 8-9, 9-11, 11-5, 5-4, 4-6, 6-7, 7-16, 16-15, 15-13, 13-14, 14-10 and 10-8. So, twelve topologies can be found by choosing one branch from twelve candidate branches in Path 1.

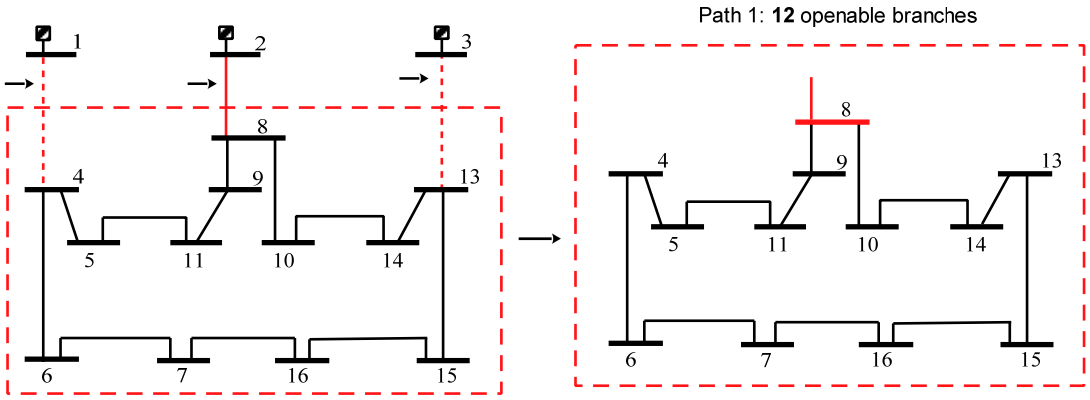

Figure 3.26 Paths in Combination No.2

3) No.6: Open branches:1-4, 2-8 Close branch: 3-13

In order to find the remaining open branch in this scenario, one path from busbar 13 to busbar 4 coloured with red is defined and shown in Figure 3.27. This path is named "Path 1" and contains 12 branches which are 4-6, 6-7, 7-16, 16-15, 15-13, 13-14, 14-10, 10-8, 8-9, 9-11, 11-5 and 4-5. So, twelve topologies can be found by choosing one branch from twelve candidates in Path 1.

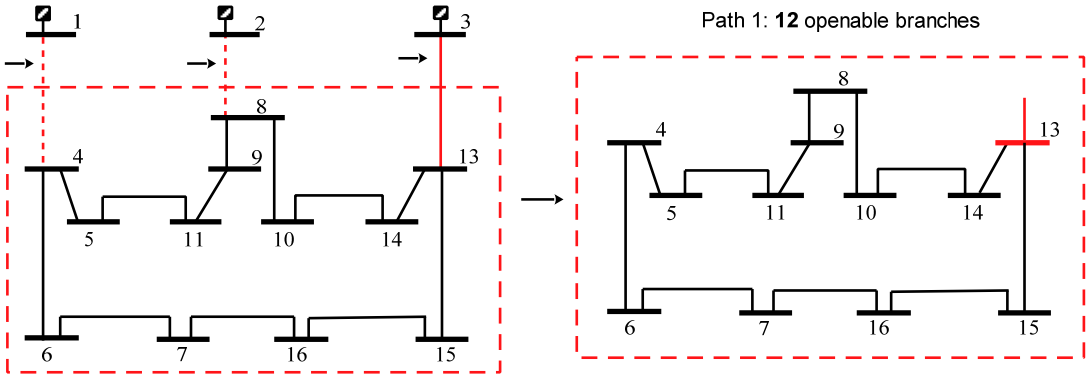

Figure 3.27 Paths in Combination No.6

4) No.4: Open branch: 1-4 Close branches:2-8, 3-13

In order to find the remaining two open branches in this scenario, two paths from busbar 8 to busbar 13 are defined and shown in Figure 3.28. The path containing the 3 branches 8-10, 10-14 and 14-13 is named "Path 1". The path containing the 9 branches 8-9, 9-11, 11-5, 5-4, 4-6, 6-7, 7-16, 16-15 and 15-13 is named as "Path 2".

So, twenty-seven topologies can be found by choosing one branch from three candidate branches in Path 1 and one branch from nine candidate branches in Path 2.

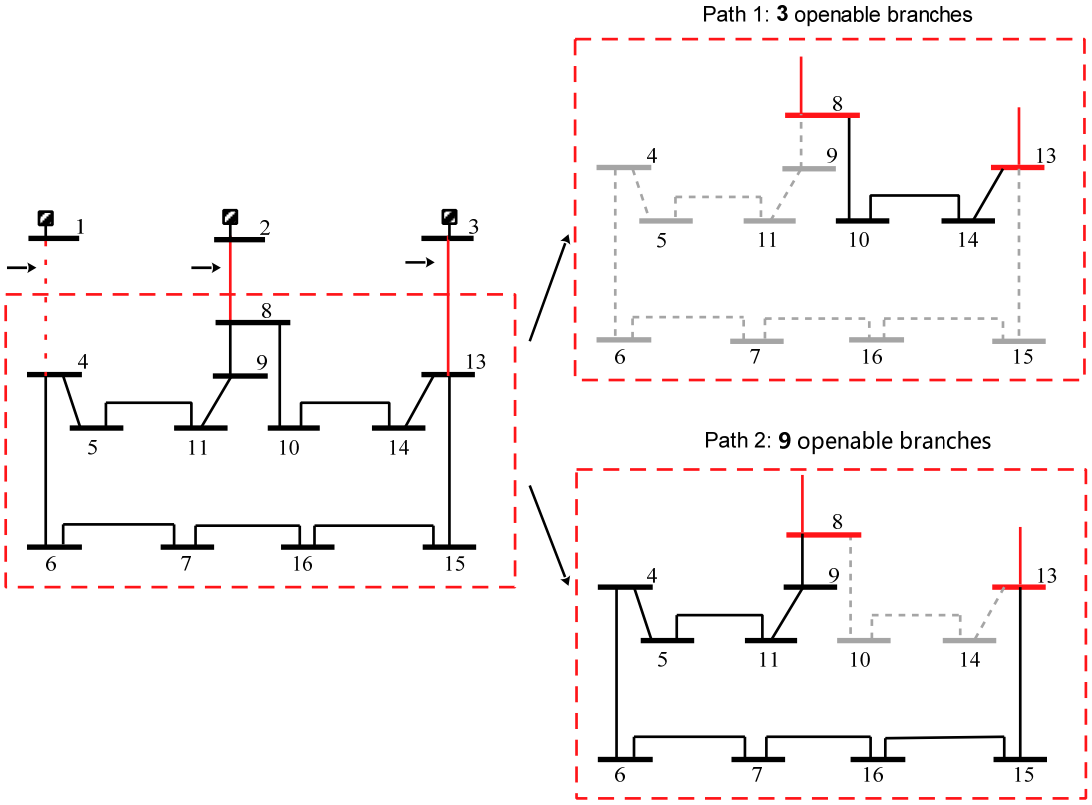

Figure 3.28 2 Paths in Combination No.4

5) No.5: Open branch: 2-8 Close branches:1-4, 3-13

In order to find the remaining two open branches in this scenario, two paths from busbar 4 to busbar 13 are defined and shown in Figure 3.29. The path containing the 7 branches 4-5, 5-11, 11-9, 9-8, 8-10, 10-14 and 14-13 is named “Path 1”. The path containing the 5 branches 4-6, 6-7, 7-16, 16-15 and 15-13 is named “Path 2”. So, thirty-five topologies can be found by choosing one branch from the seven candidate branches in Path 1 and one branch from the five candidates in Path 2.

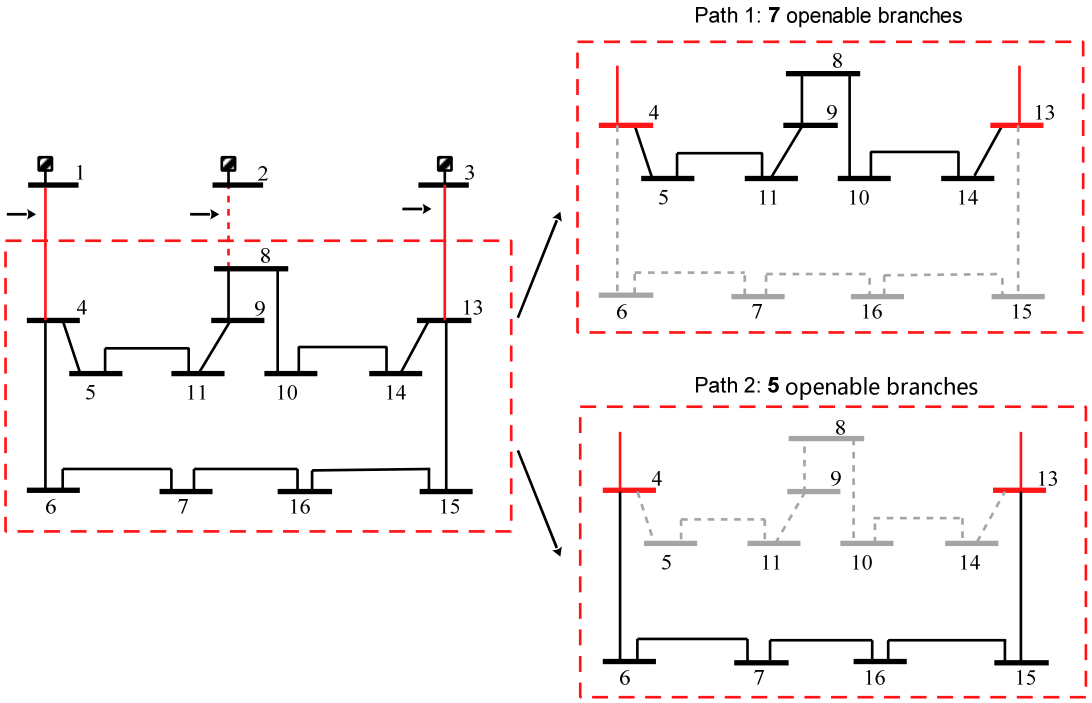

Figure 3.29 Paths in Combination No.5

6) No.6: Open branch: 3-13 Close branches:1-4, 2-8

In order to find the remaining two open branches in this scenario, two paths from busbar 4 to busbar 8 are defined and shown in Figure 3.30. The path containing the 4 branches 4-5, 5-11, 11-9, 9-8 is named “Path 1”. The path containing the 8 branches 4-6, 6-7, 7-16, 16-15, 15-13, 13-14, 14-10 and 8-10 is named “Path 2”. So, thirty-two topologies can be found by choosing one branch from the four candidate branches in Path 1 and one branch from the eight candidate branches in Path 2.

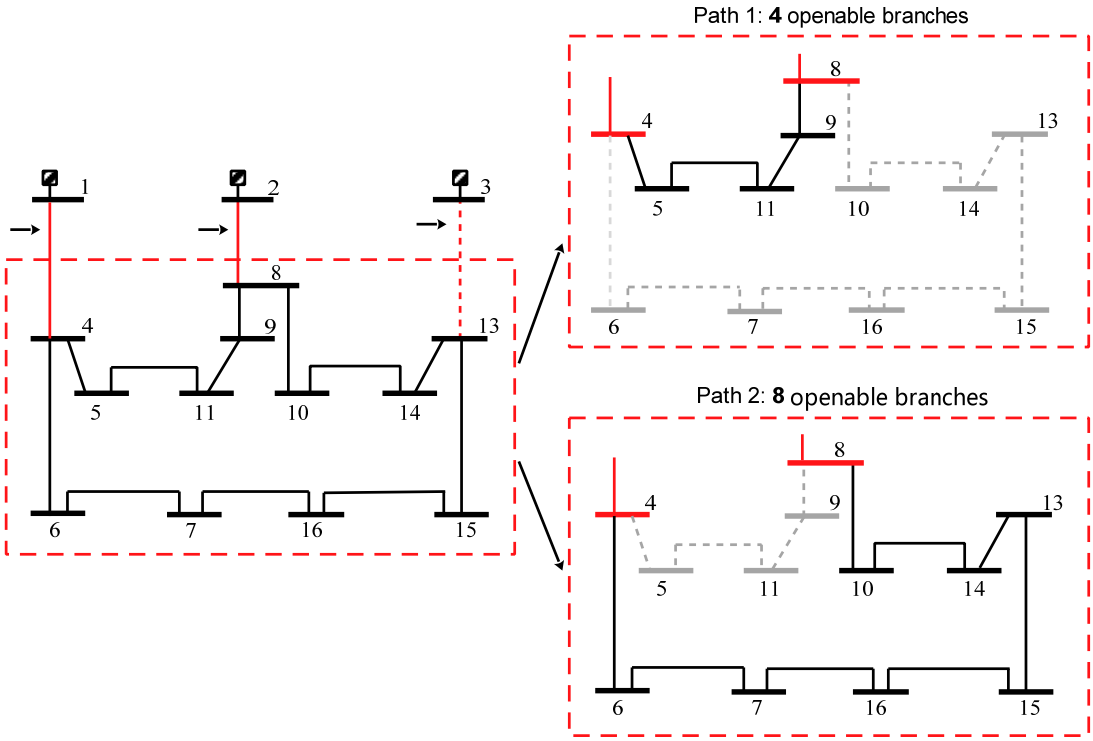

Figure 3.30 Paths in Combination No.6

7) No.7: close branches: 1-4, 3-8, 3-13

In order to find the remaining three open branches in this scenario, three paths which are from busbar 4 to busbar 13, from busbar 4 to busbar 8 and from busbar 8 to busbar 13 respectively are defined and shown in Figure 3.31. The path containing the 4 branches 4-5, 5-11, 11-9 and 9-8 is named “Path 1”. The path containing the 3 branches 8-10, 10-14 and 14-13 is named “Path 2”. The path containing the 5 branches 4-6, 6-7, 7-16, 16-15 and 15-13 is “Path 3”. So, sixty topologies can be found by choosing one branch from the four candidate branches in Path 1, one branch from the three candidate branches in Path 2 and one branch from the five candidates in Path 3.

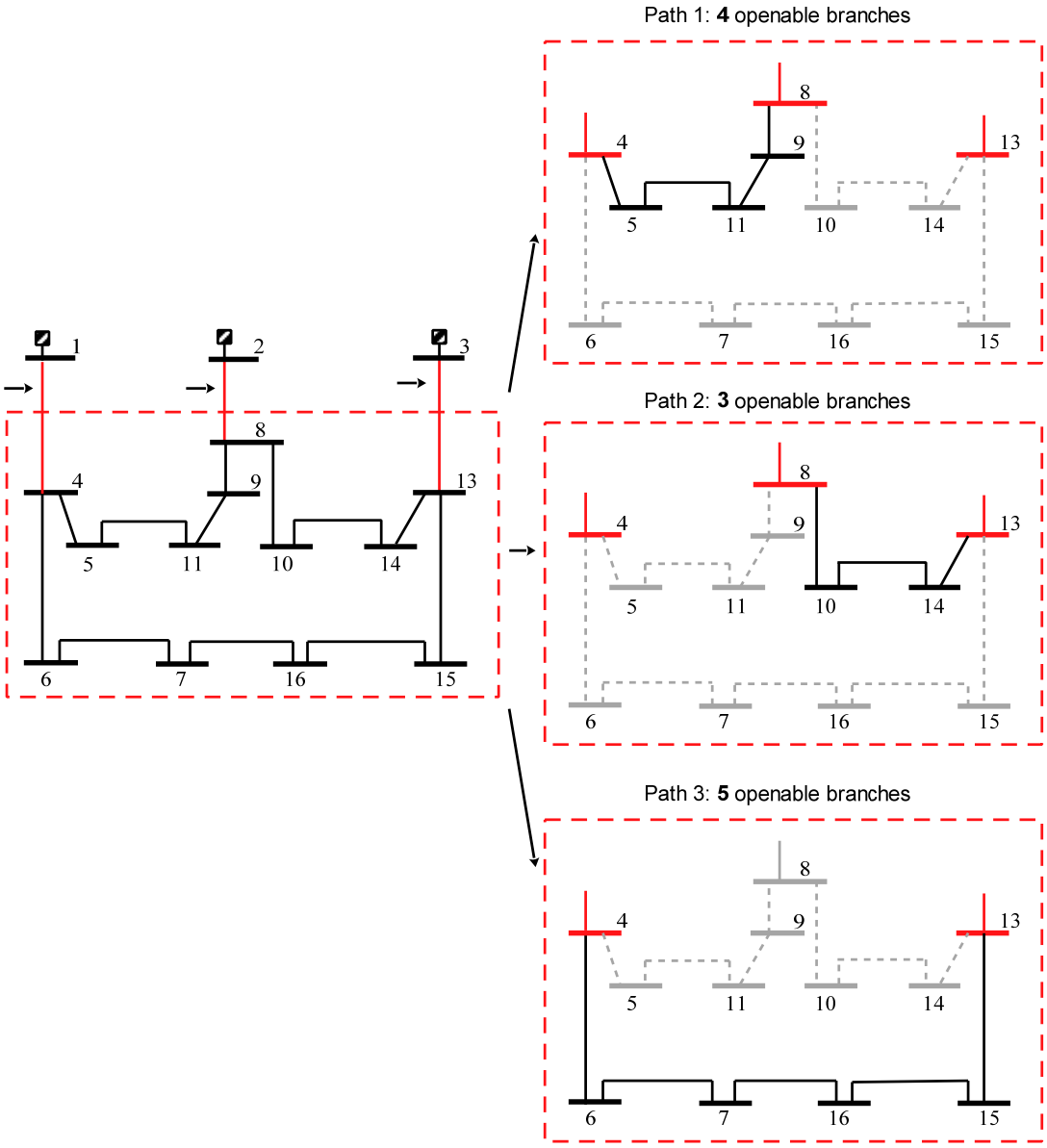

Figure 3.31 Paths in Combination No.7

Based on the above calculation, the total number of spanning tree is:

$$27 + 35 + 32 + 12 + 12 + 12 + 60 = 190$$

The number of total spanning tree calculated by Algorithm1 implemented in DisOPT is 190 too. The open branches of each spanning tree are shown in Appendix A.1.2. The results of Algorithm1 and Algorithm2 are the same. So the implementation of Algorithm 1 in DisOPT works correctly.

3.7.2 Validation of the Network Reconfiguration for *P* Loss Minimisation Algorithm's Implementation

The network reconfiguration for *P* loss minimisation introduced in the previous sections of this chapter is implemented in DisOPT. The branch and load data of this network are listed in Appendix A.1.1[49]. In order to observe more output results, the number of output topologies is set to 10. These output topologies are sorted from the lowest to the highest *P* loss. The *P* loss optimisation results calculated by DisOPT are shown in Table 3-2. The open branches of these topologies are listed in Table 3-3. Since only seven topologies' *P* loss is lower than or equal to that of the initial network topology, only seven network topologies are shown here. According to Table 3-2 and Table 3-3, the topology TopoID 1 whose open branches are 11-9, 8-10 and 7-16 has the minimum *P* loss. The set of open branches of the topology (Topo ID 1) having the minimum *P* loss calculated by DisOPT is the same as the result in [49].

Since the *P* loss optimisation algorithm used in this study evaluates the *P* loss of all possible topologies whose structures are radial and supply all load, the lowest *P* loss topology found by this algorithm is indeed the correct one. Furthermore, its result is the same as the results in [49]. As a consequence, it is concluded that the *P* loss minimisation algorithm developed in Chapter 3 succeeds in finding the lowest *P* loss topology for a valid operating condition.

Table 3-2 Loss optimisation results

Topo ID	Original Loss(MW)	Final Loss(MW)	Saving	
			(MW)	%
1	0.536	0.501	0.035	6.56
2	0.536	0.518	0.019	3.49
3	0.536	0.518	0.018	3.37
4	0.536	0.518	0.018	3.35
5	0.536	0.528	0.008	1.57
6	0.536	0.53	0.007	1.28
7	0.536	0.536	0	0

Table 3-3 Open branches of output topologies

TopoID	Open branches		
1	11-9	8-10	7-16
2	11-9	10-14	7-16
3	11-9	6-7	8-10
4	8-10	11-5	7-16
5	11-9	16-15	8-10
6	11-9	6-7	10-14
7	10-14	11-5	7-16

3.8 Long Period *P* Loss Optimisation by Network Reconfiguration Simulation

Another important aspect of network reconfiguration is how often to perform it. Long period network reconfiguration simulation can give advice on the frequency of network reconfiguration for *P* loss optimisation. Besides still using the network *P* loss minimisation reconfiguration algorithm developed in this thesis, this simulation uses a load duration curve or load profile instead of a single load value for each load point. In order to analyse load behaviour, the load demand value can be sampled in a certain interval which can be measured in minutes, hours or days, etc. A load duration curve is derived by sorting these values from the highest to the lowest [96]. Figure 3.32 illustrates the procedure of generating a load duration curve, and a typical annual Great Britain load duration curve is shown in Figure 3.33[97, 98].

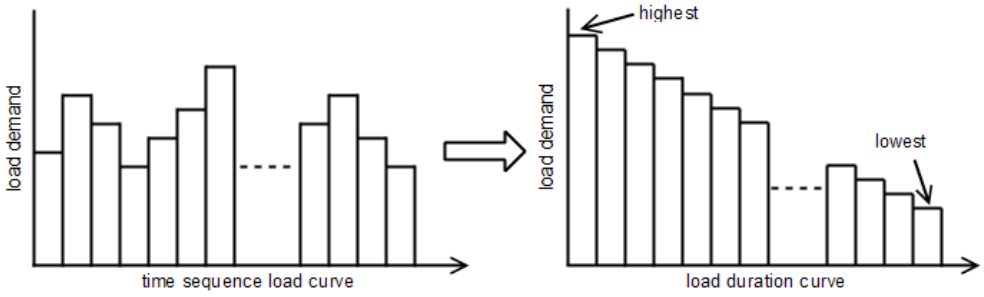

Figure 3.32 Load duration curve [97]

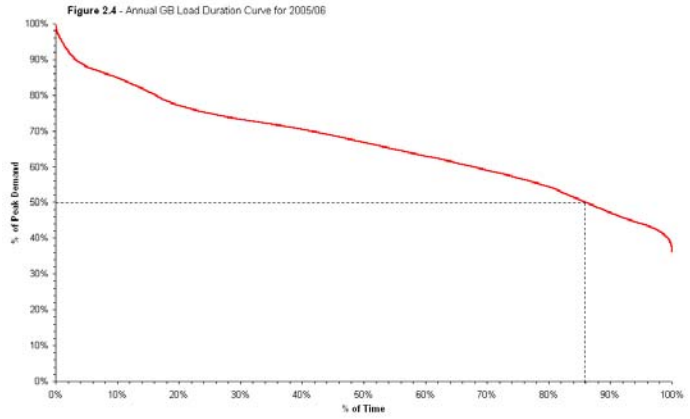

Figure 3.33 Annual GB load duration Curve [98]

A load profile is derived by sorting these values into time sequence [96]. The end-users of a distribution network can be categorized as: residential, commercial and industrial [99]. The typical load profiles of these three types of customers are shown in Figure 3.34 [99]. The shapes of different customer types are different. Residential load is the major type of loads in the LV distribution network so its load profile is very important for loss analysis. The load curve in Figure 3.35 is an average daily load profile for a household whose peak demand is 0.85kW [100]. Some papers on how to formulate load duration curves and load profiles have been published [101-104].

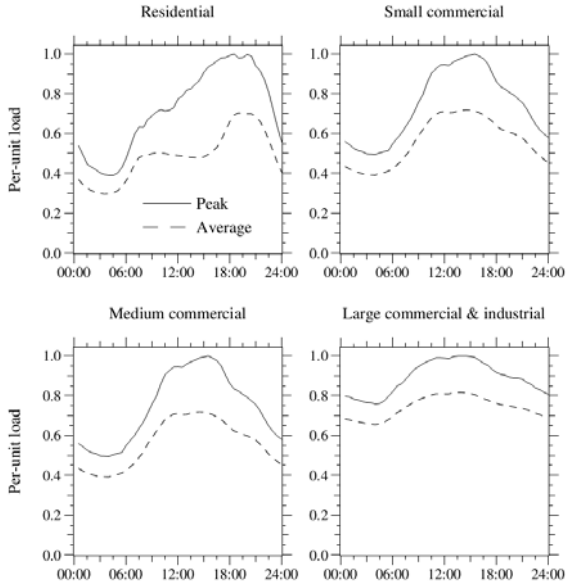

Figure 3.34 Daily load profiles of different customer types [99]

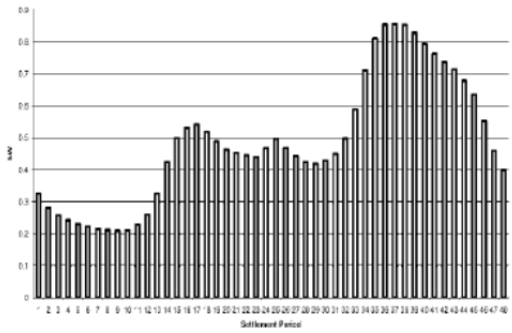

Figure 3.35 Average domestic load profile [100]

The format of load profile used in the algorithm is shown in Figure 3.36. The x-axis of the curve is time of the load point and the y-axis is the load scale factor. For example, if the load scale factor at time t is a and the peak demand is bkW, the demand at time t is abkW. In the case of a load profile which is a time series of load values, when a reconfiguration might happen from one topology to another, and also when a switching action might be needed to reconfigure it back again could be observed. This would help to determine how much burden there would be on the operator to carry out switching actions.

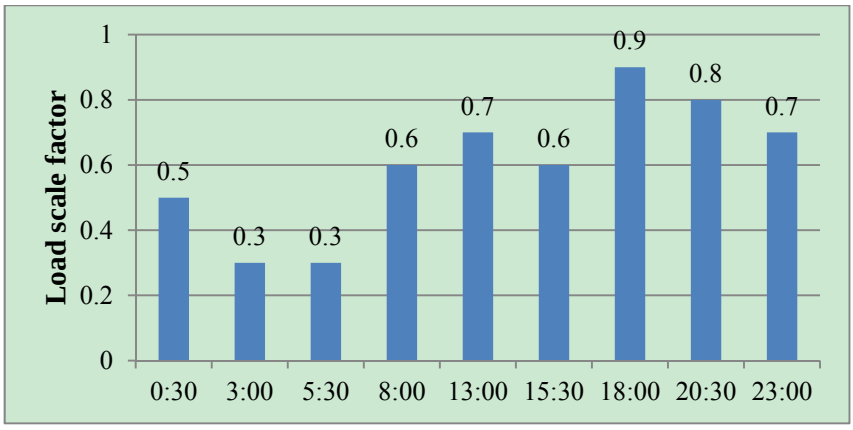

Figure 3.36 Format of load profile used in this thesis

In principle, by stepping through a load duration curve it is possible to find the number of different states of the network. However, in reality, it is very unlikely that each load in the network will have the same load duration curve; use of a single load duration curve for the whole network will imply some errors in the loads relative to what would really occur at different locations simultaneously. Whether by using a load profile or a load duration curve, by looking at which switches are opened or

closed, it would be possible to identify those switches that would be good candidates for remote control if they are not already so equipped.

3.9 Summary

A distribution network *P* loss minimisation reconfiguration method using graph theory has been developed in this chapter. This method can find the globally optimal result. Though some techniques like lateral cut, zone dividing introduced in Section 3.4 have been used to reduce the size of the solution space, the solution space is still very large when the network is complex. Some future works on this network reconfiguration method based on spanning tree generation algorithm are discussed in section 8.2.2.

Chapter 4 Distribution Network Reliability Evaluation

The previous section introduced the algorithm of *P* loss optimisation by network reconfiguration. In this chapter, the basic theories of reliability evaluation are introduced and the effects of the overcurrent protection system and network control points operation on the reliability performance of the distribution network are discussed.

4.1 Introduction

In this thesis, a tool for evaluating a purely radial distribution reliability performance has been developed. A pure radial system means there is no parallel connection between any two nodes and only one path from the source point to any load point. Any failure of an element on the path causes the load point to lose its power supply. As was explained in Chapter 1, most distribution networks are normally operated in a radial manner. This means that loads connected on a particular radial feeder are vulnerable to failure of any one element in that radial connection. However, down to certain voltages (e.g. 33-11kV distribution network of SPEN) [4], there are normally also alternative paths available that could be utilised to restore at least some of the load with suitable reconfiguration of the open points. This chapter is concerned with the principles used in estimating the probability of such loss of load conditions arising and how long it would normally take for load to be restored. Then in chapter 5, the implementation of reliability evaluation algorithm is described.

4.2 Key Definitions

Standard IEEE and Ofgem definitions for terms relevant to distribution system reliability have been used in this thesis. They are given as follows:

Failure: “The inability of an item to carry out the work that is designed to perform within specified limits of performance.” [105]

Interruption: “The loss of supply of electricity to one or more customers due to an incident but excluding voltage quality and frequency abnormalities, such as dips, spikes or harmonics." [106]

Outage: “The state of a component when it is not available to perform its intended function due to some event directly associated with that component. Notes: 1. An

outage may or may not cause an interruption of service to customers, depending on system configuration. 2. This definition derives from transmission and distribution applications and does not apply to generation outages." [107]

Scheduled outage: "A loss of electric power that results when a component is deliberately taken out of service at a selected time, usually for the purposes of construction, preventative maintenance, or repair." [107]

Restoration duration: "The period (measured in seconds, or minutes, or hours, or days) from the initiation of an interruption to a customer or other facility until service has been restored to that customer or facility." [107]

4.3 Reliability Indices

The performance of power system reliability is assessed by reliability indices. Normally, the reliability evaluation is based on the system historical reliability data so that the reliability indices are average values. Reliability indices are used to not only assess system past performance but also to predict system future performance for planning purposes. These indices can be divided into two categories: load point indices and system indices [108]. The details of them are presented in the following sub sections.

4.3.1 Load Point Indices

Load point indices are used to indicate the impact of system behaviour on the customers connected to the load points under fault conditions. The customer-based indices used for a load point *i* are listed as follows [109]:

- failure rate λ_i: [frequency/year]
- average annual outage duration U_i: [hours/yr]
- average outage duration r_i: [hours]

The details of how to calculate these indices are discussed in section 4.6 and the implementation of the tool to do so in Chapter 5.

4.3.2 System Indices

System indices describe the whole system reliability behaviour. The evaluation of the system indices is based on the value of the load point indices. In North America and

some other countries around the world, system average interruption frequency index (SAIFI) and system average interruption frequency index (SAIDI) are the two main system indices widely used in reliability evaluation [110, 111]. The equations of these two indices are shown as follows [107]:

- System average interruption frequency index (SAIFI) [interruptions/yr/cust]:

$$SAIFI = \frac{\text{Total number of customers interrupted}}{\text{Total number of customers Served}} \tag{4.1}$$

- System average interruption duration index (SAIDI) [hours/yr/cust]

$$\text{SAIDI} = \frac{\text{Total Customer interruption durations}}{\text{Total number of customers Served}} \tag{4.2}$$

In the United Kingdom, Customer Interruptions (*CI*) and Customer Minutes Lost (*CML*) are used instead of SAIFI and SAIDI. The equations to calculate these two indices are shown as follows [112]:

- Customer interruptions (*CI*) [int./100cust.yr.]: the number of customers affected by interruption per 100 customers per year.

$$CI = \frac{\text{No. of Customers involved in an incident} \times 100}{\text{Total No. of Customers in DNO}} \tag{4.3}$$

- Customer Minutes Lost (*CML*) [mins./cust.yr.]: the duration of interruptions to supply per year.

$$CML = \frac{\text{No. of Customers off} - \text{supply} \times \text{Time of Supply (minutes)}}{\text{Total No. of Customers in DNO}} \tag{4.4}$$

4.4 Reliability Evaluation Methods

The method of reliability evaluation can be divided into two main categories: analytical methods and Monte Carlo simulation methods. The analytical methods are based on mathematical modelling techniques and the simulation methods evaluate the system reliability performance by simulating its actual process and random behaviour [113]. The overview of the analytical methods and the simulation methods is described in the following sections [114].

4.4.1 Analytical Method

Before applying the analytical method, the system needs to be represented by mathematical models. Based on these models, the analytical method can evaluate the reliability indices directly. The techniques used for this method include failure modes and effects analysis (FMEA), event trees and fault trees [108, 115, 116]. Brief overviews of these techniques are given below.

- **Failure Modes and Effects Analysis (FMEA) Method**

  The failure modes and effects analysis (FMEA) method analyses independent failure states of every single component and identifies the effects on the system [116]. FMEA is a simple method of evaluating a system's reliability performance, but it is difficult to evaluate the effects of multiple failures directly [108].

- **Event-Tree Analysis Method**

  The event-tree analysis method analyses how the system will develop from an initial state. It is an inductive technique and an initial state must be provided. When the relationships among all states are represented in a graph, each state looks like a branch of a tree. By use of an event-tree, the states between the initial state and the chosen state are known. So the probability of entering the chosen state from the initial state can be calculated [116].

- **Fault-Tree Analysis Method (FTA)**

  The fault-tree analysis (FTA) method identifies the effects of all possible combinations of failures that may occur on the system. FTA chooses a failure first and then looks for what caused it [117]. The fault tree is represented by logic symbols (e.g. event symbols, gate symbols, transfer symbols) [116]. In order to apply the fault-tree analysis method, a particular failure event needs to be taken as the root of the logic fault tree. Then all combinations of other failures or events causing the root event can be identified and represented by logic symbols on the fault tree [118]

The computation time of the analytical method is relatively short and the calculation results are always the same for each calculation. However, for large systems, assumptions are usually necessary to simplify the model which will cause the analysis of the results to lose its significance [113].

4.4.2 Monte Carlo Simulation Methods

Monte Carlo simulation methods can simulate the system planning and operation events, such as outages, element failures and replacement, load variations as a series of experiments [108]. When Monte Carlo simulation method samples randomly from one or more probability distributions, the system behaviour during the simulation time can be predicted [114]. Monte Carlo simulation method has three basic types: state sampling approach, state duration sampling approach and system state transition sampling approach [119]. The features of these three methods are:

- **State sampling approach**

  The state sampling approach is also named as non-sequential Monte Carlo method [108, 120]. The system state consists of each component's state. Take a system with N components as an example to illustrate how to evaluate system reliability by using state sampling approach. Assume each component of this system has two states which are the normal operation state and the failure state and that the failure of each individual component is assumed as an independent event. The state S_i that the component i is in for a given random number N_r distributed uniformly between [0,1] can be presented as [119]:

$$S_i = \begin{cases} 1 & N_r \geq P_{fi} \\ 0 & 0 \leq N_r < P_{fi} \end{cases} \tag{4.5}$$

  where:

  $S_i = 1$: the component is in the normal operation state

  $S_i = 0$: the component is in the failure state

  P_f: the failure probability of the component

The system state can be expressed as:

$$S_{sys} = [S_1 \quad S_2 \quad \cdots \quad S_i \quad \cdots \quad S_m] \tag{4.6}$$

When generating K random numbers N_r distributed uniformly between [0,1] and recording all occurred states, the probability of a state occurring in these K samples can be calculated. If a system state i occurred $k(sys-i)$ times, its probability P_{sys-i} is [119]:

$$P_{sys-i} = \frac{k(sys-i)}{K} \tag{4.7}$$

Assuming the probability in S_{sys} is $P(S_{sys})$ and the corresponding reliability index in S_{sys} is $I(S_{sys})$, the expectation of the index function of all system states E_{sys} is [119]:

$$E_{sys} = \sum_{S_{sys} \in M} I(S_{sys}) \frac{k(sys-i)}{K} \tag{4.8}$$

where:

M: the set of all system states

Though this approach has a simple sampling method and the only required basic reliability data are the probabilities of component-state, the actual frequency index cannot be calculated by this method [119].

- **State duration sampling approach**

  The state duration sampling approach is also called as the sequential Monte Carlo method [108, 120]. In this approach, the probability distribution of the component state duration is sampled by using a chronological state transition process [119]. The steps of applying the state duration sampling approach are summarised as follows [119]:

  1) Determine the initial state of each component. Normally, this state is the normal operation state.
  2) Sample the duration of each component remaining in its present state.
  3) Repeat Step 2 in a given period, for example, a year. Record sampling values of all states of each component.

4) The chronological state transition process of the whole system can be derived by combining every component's chronological state transition process. Figure 4.1 illustrates how to apply this step to a two-element system [119].

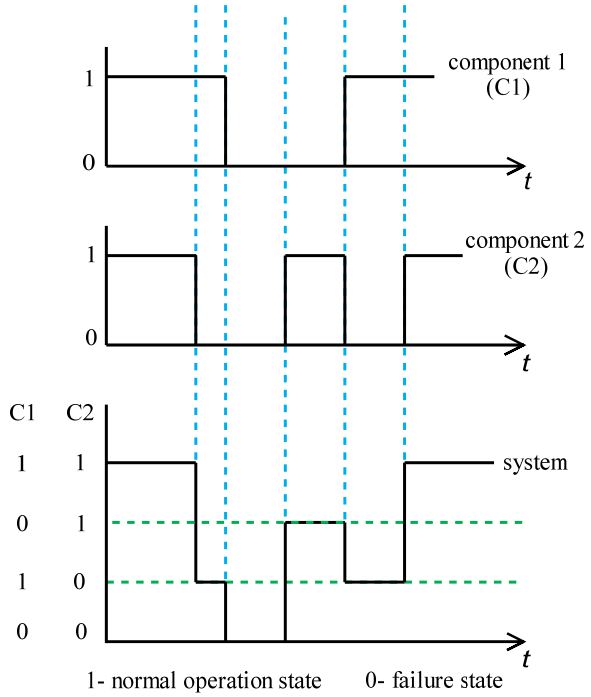

Figure 4.1 Generate chronological system state transition process [119]

5) Based on a chronological system state transition process, (4.8) can be calculated.

Comparing to the state sampling approach, though the actual frequency index can be calculated for any state duration distribution by this approach, more computing time and storage are required to generate a random variable for each component by following its distribution and to store the chronological component state transition of all components over a long time duration [119].

- **System state transition sampling approach**

  The system state transition sampling approach samples the system state transition process by creating the system state transition sequence directly [120]. The actual frequency index can be calculated directly without an additional enumeration procedure [120]. Compared with the state duration

sampling approach which samples the time at which a component's state changes, the system state transition sampling approach samples whether a component has changed state or not. In order that the system state transition sampling approach can be applied, the state duration of each system component must be assumed to meet an exponential distribution [119]. The system state space *SS* of a *n*-state system can be defined as [119]:

$$SS = \{S_1 \quad S_2 \quad \cdots \quad S_i \quad \cdots \quad S_n\} \tag{4.9}$$

Assuming the current system state is S_i ($S_i = 1$) and the transition rate of each component corresponding to S_i is λ_i, the probability P_k of the system state transiting from S_i to S_{i+1} can be expressed as [119]:

$$P_k = \frac{\lambda_k}{\sum_{j=1}^{n} \lambda_j} \tag{4.10}$$

where:

k: the component *k* causes the system state transition from S_i to S_{i+1}

n: the number of system components

The next system state can be determined by the following two steps [119]:
1) Generating a uniformly distributed random number *R* between [0,1] [119].
2) As shown in Figure 4.2 [119], since the value of P_k calculated by (4.10) is between $[0,1]$, the segment of P_k that R falls into means the system will transit into next state by the component *k*.

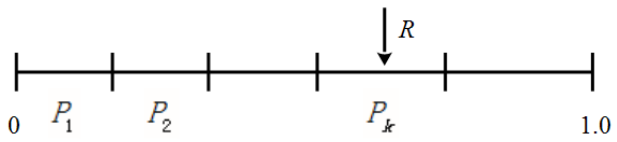

Figure 4.2 Explanation of how to determine the next state [119]

This approach only needs one random number to generate a system state instead of generating *n* random number to get a *n*-component system's state in the state sample approach [119]. Comparing to the state duration sampling approach, it can calculate the frequency index without sampling the distribution function of each component and generating chronological state

transition processes [119]. But only the system whose component state durations satisfy the exponential distribution can be analysed using the system state transition sampling approach [119].

4.5 Markov Modelling

A system's state consists of the different combinations of its elements' states. Markov modelling is a useful method to analyse the transitions between system states. A system which is suitable for using Markov modelling needs to satisfy two requirements: First, the system has no memory of the previous state. Second, the transition rate is a constant value [121]. Markov models can be divided into two categories: discrete models and continuous models. Though the model of a distribution network is a continuous Markov model, the discrete model is introduced first to help understand the continuous model [121].

4.5.1 Discrete Markov Chain

As shown in Figure 4.3, a single element system has two states: state 1 and state 2 [117]. After a time interval *t*, the system will remain in the previous state or transfer to a new state. The probability of transferring from state 1 to state 2 is P_1, so the probability of remaining in state 1 is $1 - P_1$. Similarly, the probabilities of transferring from state 2 to state 1 and remaining in state 2 are P_2 and $1 - P_2$ respectively.

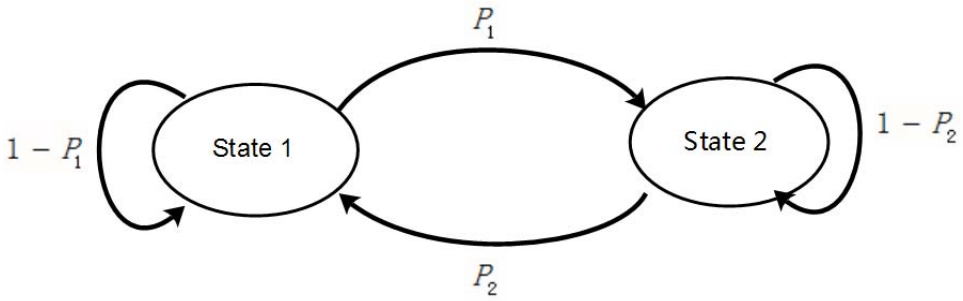

Figure 4.3 Two-state single element system [117]

Assuming the initial state of the element is state 1, the probability of an element being in a chosen state after three time intervals can be solved by the discrete Markov chain shown in Figure 4.4 [121].

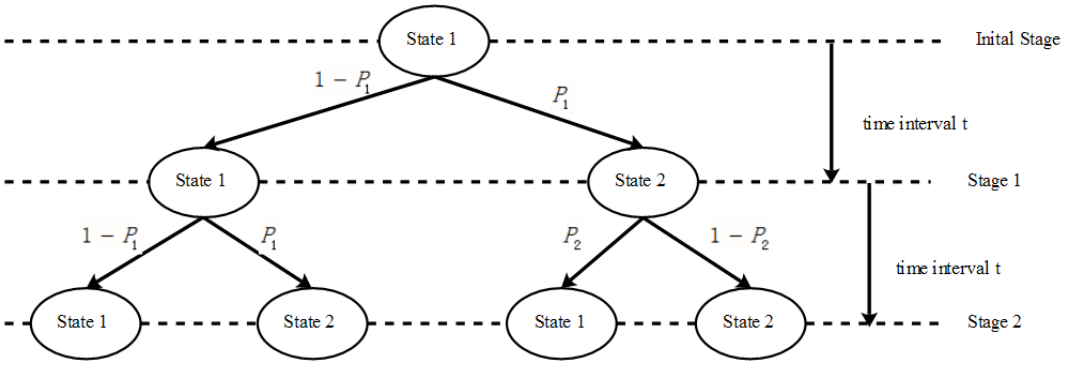

Figure 4.4 Discrete markov chain of two state system [121]

So after three steps, the probabilities of system being in state 1 are $[(1-P_1)(1-P_1)+P_1P_2]$ and $[(1-P_1)P_1+P_1(1-P_2)]$.

Transitional probability Matrix

When the number of transition steps is large, it is not realistic to use the tree diagram shown in Figure 4.4 to calculate the state probability after *n* stages. The transitional probability matrix can solve this problem [117]. Taking an *n*-state system for example, its transition probability matrix $\vec{\varepsilon}$ is shown in (4.11) [117]:

$$\vec{\varepsilon} = \begin{bmatrix} P_{11} & P_{12} & \dots & P_{1j} & \dots & P_{1n} \\ P_{21} & P_{22} & \dots & P_{2j} & \dots & P_{2n} \\ \vdots & \vdots & \vdots & \vdots & \vdots & \vdots \\ P_{i1} & P_{i2} & \cdots & P_{ij} & \cdots & P_{in} \\ \vdots & \vdots & \dots & \vdots & \vdots & \vdots \\ P_{n1} & P_{n2} & \cdots & P_{nj} & \dots & P_{nn} \end{bmatrix} \tag{4.11}$$

Here, $\vec{\varepsilon}$ is a $n \times n$ matrix. Since the system has *n* states, the row number *i* means the current state that the system is in at the start of the time interval and the column number *j* means the state that the system will transit to after a time interval. So the matrix element P_{ij} means the probability of the system moving from the state *i* to state *j* when *i* is not equal to *j*. When *i* is equal to *j*, P_{ij} means the probability that the system remains in the current state. Since each row of the matrix represents all possible states that the system could move into from the current state, the summation of all matrix elements in the same row must be equal to 1. The mathematical equation of this characteristic is shown in (4.12).

$$\sum_{j=1}^{n} P_{ij} = 1(i = 1,2, \dots n) \tag{4.12}$$

When the transition matrix is known, the system state probabilities after K time intervals can be calculated by (4.13), which is [117]:

$$\begin{bmatrix} P_1(K) \\ P_2(K) \\ \vdots \\ P_i(K) \\ \vdots \\ P_n(K) \end{bmatrix}^T = \begin{bmatrix} P_1(0) \\ P_2(0) \\ \vdots \\ P_i(0) \\ \vdots \\ P_n(0) \end{bmatrix}^T \begin{bmatrix} P_{11} & P_{12} & \dots & P_{1n} \\ P_{21} & P_{22} & \dots & P_{2n} \\ \vdots & \vdots & \dots & \vdots \\ P_{i1} & P_{i2} & \dots & P_{in} \\ \vdots & \vdots & \vdots & \vdots \\ P_{n1} & P_{n2} & \cdots & P_{nn} \end{bmatrix}^K \tag{4.13}$$

where:

$P_i(K)$=the probability that the system is in state i after K(K>0) time intervals

$P_i(0)$ is the probability of the system in the initial state.

$P_i(0) = 1$ and $P_k(0) = 0(k \in [1,n]\ and\ k! = i)$ when the initial state 0 is already known.

4.5.2 Continuous Time Markov Process

The theory described in this section is based on that given in [117]. For a continuous time Markov process, its time interval t is a continuous value rather than the discrete value in the discrete Markov chain. Unlike the discrete-time Markov chains introduced in section 4.5.1, state transitions in a Markov process occur continuously [121]. The conception of transition rate is used here instead of transition probability. The details of the transition rate will be introduced as follows:

System States

Network elements can be in different states. The state space diagram represents the transitions among these states. As shown in Figure 4.5, the basic state space diagram of a single repairable element has two states: the normal operation state and the fault state.

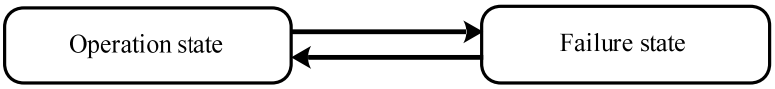

Figure 4.5 Two-state diagram

If planned outages are considered, the element has three states and the state space diagram is shown in Figure 4.6.

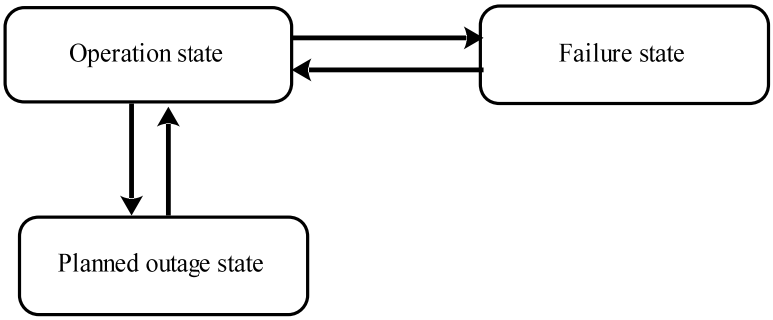

Figure 4.6 Three-state diagram

In this thesis, a planned outage condition is not modelled as a separate state and all elements have two states (operation state and failure state). The first purpose of the tool developed here is to assess the reliability of different given initial conditions in an operational timeframe, though the analytical tool can be also used for design; each possible planned outage state is an additional initial condition that the user can define. The reliability estimate would then relate to the period for which the planned outage is expected to last. If an element is in an initial "planned outage" condition, the "emergency return to service time" should be taken into account when assessing the restoration following a transition of any other elements to a failure condition due to a fault. This would be just like any other reconfiguration action, but the time that each option would take is a key to what action would actually be taken and what the restoration time for an interrupted load would be. Restoration is discussed further in section 4.8.3 below. The planned outage conditions could be treated as a set of different initial conditions via a loop wrapped around the evaluation of different states when used as a design tool. However, when used as an operational tool, the initial conditions include whether any element is in an initial out of service state. It can be treated either as having no option to be changed to an in-service state, or that it can be put into service but would take at least the defined "emergency return to service time".

Since all elements are connected in series in a purely radial distribution network, whether the power can be transferred from one point to another point depends on all elements being in service. Take the network in Figure 4.7 for example. This network

has two branches br1 and br2. Both of these two branches must be in service so that the power can be distributed from one end to the other.

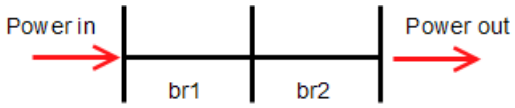

Figure 4.7 Two-branch series network

The diagram of a general two element series system is shown in Figure 4.8. This system has four states when each element has two states as shown in Figure 4.5. In order to make a series system fulfil its function for some given period of time, all of its elements must be in the normal operation condition during that period [113].

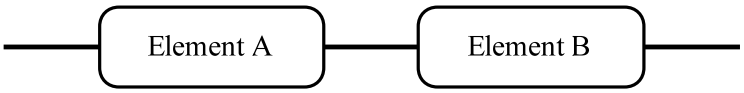

Figure 4.8 Two element series system

The diagram in Figure 4.9 named as state space diagram represents the transitions between all possible system states.

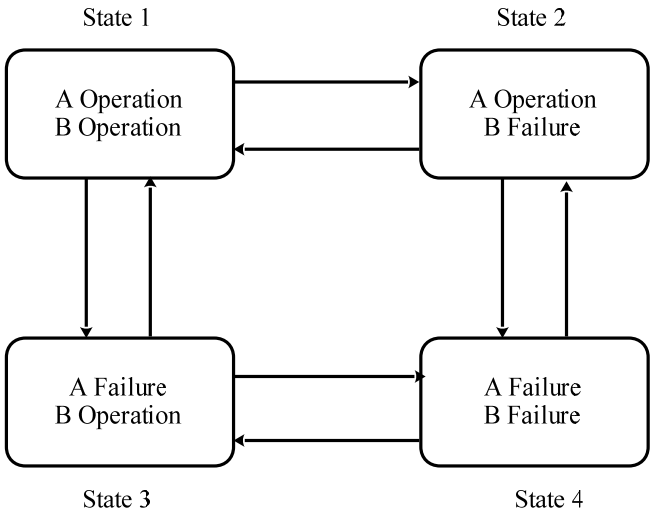

Figure 4.9 State space diagram of two-element series system

Transition rate

Unlike in a discrete Markov process, the transitions between two states are described by the transition rate. The definition of the transition rate is [117]:

$$\text{transition rate} = \frac{\text{number of times a transtion occurs from a given state}}{time\ spent\ in\ that\ state} \quad (4.14)$$

A system considered to exhibit a continuous Markov process must satisfy: 1) the probability function of the system in a given state at time t must meet an exponential distribution; 2) the transition rate must be a constant value. The probability of system in being state i is defined as:

$$P_i(t) = e^{-\eta t} \quad (4.15)$$

where:

$t \geq 0$

η is a constant value.

So the probability density of (4.15) is:

$$d(t) = \frac{dP_i(t)}{dt} = \eta e^{-\eta t} = \eta P_i(t) \quad (4.16)$$

The transition rate of the system transition from the current state to the other state can be calculated as:

$$\text{transition rate} = \frac{d(t)}{P(t)} = \eta \quad (4.17)$$

The (4.17) explains why the transition rate is constant when the probability function is an exponential distribution function. For a two-state element shown in Figure 4.10, the following are defined:

$P_O(\mathrm{t})$: Probability function that the element is in operation state at time t

$P_f(\mathrm{t})$: Probability function that the element is in failure state at time t

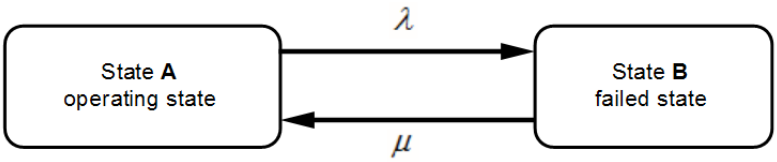

Figure 4.10 State diagram of two-state system

When $P_O(\mathrm{t})$ and $P_f(\mathrm{t})$ meet the requirements of exponential distribution, their probability density functions are:

$$d_O(t) = \eta_o e^{-\tau_0 t} \quad (4.18)$$

$$d_f(t) = \eta_f e^{-\tau_f t} \tag{4.19}$$

Since the element only has two states, η_O is referred to as the transition rate that the system transits from the operation state to the failure state. η_f is referred to the transition rate that the system transits from the failure state to the operation state. Normally, η_O is named as the failure rate and represented by λ. η_f is named as the repair rate and represented by μ.

The above parts describe how to get failure rate and repair rate from the probability function. It is a mathematical method. But in practice, the failure rate (λ) and repair rate (μ) are calculated from historical fault event records data and the equations to calculate them are:

$$\lambda = \frac{\text{number of failures in the given period of time}}{\text{total period of time the component was operating}} \tag{4.20}$$

$$\mu = \frac{\text{number of repairs in the given period of time}}{\text{total period of time the component was being repaired}} \tag{4.21}$$

State Probability

The steady-state ($t \to \infty$)probabilities of a system that has limited states can be calculated by a coefficient matrix [117]. This part illustrates how to apply this technique.

The format of a coefficient matrix is similar to that of the transition matrix introduced in section 4.5.1. The matrix element β_{ij} ($i \neq j$) represents the transition rate of the system transit from state *i* to state *j*. The differences between them are: the elements in the coefficient matrix are transition rates and the summation of each row is equal to zero whereas the elements in the transitional probability matrix are probabilities and the summation of each row is equal to 1. So the transition rate of remaining in the current state is calculated by (4.22), that is:

$$\beta_{ii} = -\sum_{j=2}^{n} \beta_{ij} \tag{4.22}$$

The equation to calculate the system state probability at time t is [117]:

$$\begin{bmatrix} dP_1/dt \\ dP_2/dt \\ \vdots \\ dP_i/dt \\ \vdots \\ dP_n/dt \end{bmatrix}^T = \begin{bmatrix} P_1(t) \\ P_2(t) \\ \vdots \\ P_i(t) \\ \vdots \\ P_n(t) \end{bmatrix}^T \begin{bmatrix} \beta_{11} & \beta_{12} & \dots & \beta_{1n} \\ \beta_{21} & \beta_{22} & \dots & \beta_{2n} \\ \vdots & \vdots & \dots & \vdots \\ \beta_{i1} & \beta_{i2} & \dots & \beta_{in} \\ \vdots & \vdots & \vdots & \vdots \\ \beta_{n1} & \beta_{n2} & \cdots & \beta_{nn} \end{bmatrix} \tag{4.23}$$

$$\sum_{i=1}^{n} P_i(t) = 1 \tag{4.24}$$

where:

$P_i(t)$ is the probability that the system is in state i at time t.

When the left part of (4.23) is set equal to zero, it can be rewritten as:

$$\begin{bmatrix} 0 \\ 0 \\ \vdots \\ 0 \\ \vdots \\ 0 \end{bmatrix}^T = \begin{bmatrix} P_1 \\ P_2 \\ \vdots \\ P_i \\ \vdots \\ P_n \end{bmatrix}^T \begin{bmatrix} \beta_{11} & \beta_{12} & \dots & \beta_{1n} \\ \beta_{21} & \beta_{22} & \dots & \beta_{2n} \\ \vdots & \vdots & \dots & \vdots \\ \beta_{i1} & \beta_{i2} & \dots & \beta_{in} \\ \vdots & \vdots & \vdots & \vdots \\ \beta_{n1} & \beta_{n2} & \cdots & \beta_{nn} \end{bmatrix} \tag{4.25}$$

where:

P_i is the probability of the system being in state i when $t \to \infty$.

The solutions of (4.24) and (4.25) are the steady state ($t \to \infty$) results for the Markov process [121]. λ and μ must be in the same time domain in the transition matrix $\vec{\beta}$, since the state probability must satisfy:

$$0 \ll P(t) \ll 1 \tag{4.26}$$

Normally, the unit of λ is failures/year, the unit of μ is 1/hour. In order to change the unit of λ from failures/year to failures/hour, the value of λ needs to be divided by 8760, i.e. $\frac{\lambda}{8760}$.

Taking the element in Figure 4.10 for example, the following terms are defined:

$P_A(t)$: the probability of the element being in state A at time t

$P_B(t)$: the probability of the element being in state B at time t

When $t \to \infty$, the steady state probabilities of the system being in state A and state B are:

$$P_A = P_A(\infty) \tag{4.27}$$

$$P_B = P_B(\infty) \tag{4.28}$$

So the transition matrix of the system in Figure 4.10 is:

$$\vec{\beta} = \begin{bmatrix} \beta_{11} & \beta_{12} \\ \beta_{21} & \beta_{22} \end{bmatrix} \tag{4.29}$$

where:

β_{11}: transition rate to state A to state A (remain in state A): $-\lambda$

β_{12} : transition rate to state A to state B: λ

β_{21}: transition rate to state B to state A: μ

β_{22}: transition rate to state B to state B (remain in state B): $-\mu$

So,

$$\vec{\beta} = \begin{bmatrix} -\lambda & \lambda \\ \mu & -\mu \end{bmatrix} \tag{4.30}$$

From (4.24) and (4.25):

$$[0 \quad 0] = [P_A \quad P_B] \begin{bmatrix} -\lambda & \lambda \\ \mu & -\mu \end{bmatrix} \tag{4.31}$$

$$P_A + P_B = 1 \tag{4.32}$$

So the results of P_A and P_B are:

$$P_A = \frac{\mu}{\lambda + \mu} \tag{4.33}$$

$$P_B = \frac{\lambda}{\lambda + \mu} \tag{4.34}$$

When P_A and P_B are known, the next step is to calculate the reliability indices from the state probabilities. Before starting to calculate the reliability indices, the load points affected by each state need to be determined first. When this step is finished, each load point interrupted in which states is known also.

The example network in Figure 4.11 is used to illustrate how to apply a Markov process to a radial distribution network reliability analysis [121]. This network consists of two feeders (Feeder 1, Feeder 2), one circuit breaker (CB1), two branches

(br1,br2), two manual switches (MSW1, MSW2), two load points (L1, L2). For the two manual switches, MSW1 is normally closed while MSW2 is normally open.

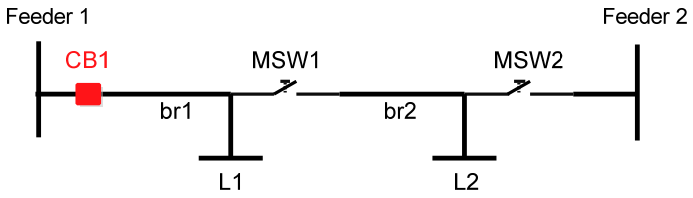

Figure 4.11 Example network for markov process analysis [121]

Assume that only branches of this network will experience failure. The failure rate and repair rate of br1 and br2 are λ_1, μ_1 and λ_2, μ_2 respectively. The switch rate of MSW1 and MSW2 are σ_1 and σ_2 respectively. Here, the switch rate is equal to $\frac{1}{Mean\ time\ to\ switch}$. So the Markov model of this network in Figure 4.12 can be derived [121].

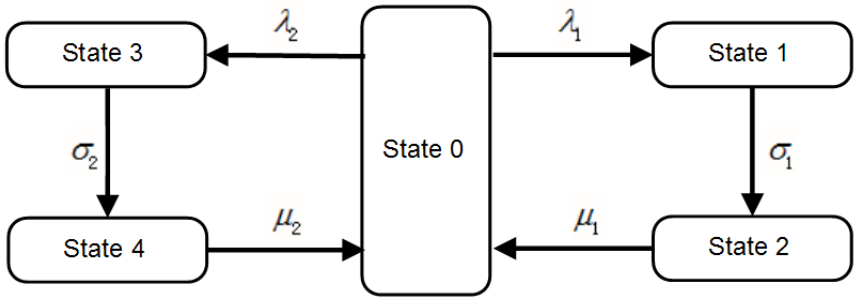

Figure 4.12 Markov model of example network [121] (State 0 is the initial state of the system)

Based on the Markov model in Figure 4.12 and (4.24) – (4.25), the following equations can be derived:

$$\begin{bmatrix}0\\0\\0\\0\\0\end{bmatrix}^T = \begin{bmatrix}P_0\\P_1\\P_2\\P_3\\P_4\end{bmatrix}^T \begin{bmatrix}-(\lambda_1+\lambda_2) & \lambda_1 & 0 & \lambda_2 & 0\\ 0 & -\sigma_1 & 0 & 0 & 0\\ \mu_1 & 0 & \sigma_1 & 0 & 0\\ 0 & 0 & -\mu_1 & -\sigma_2 & \sigma_2\\ \mu_2 & 0 & 0 & 0 & -\mu_2\end{bmatrix} \tag{4.35}$$

$$P_0 + P_1 + P_2 + P_3 + P_4 = 1 \tag{4.36}$$

where:

P_i: the probability that the system is in state i when $t \to \infty$

When $P_0 \sim P_4$ are worked out by solving (4.35) and (4.36), the average annual outage duration of each load point can be calculated. Taking load point L1 for example, the power supply of L1 will be interrupted in:

- State 1: br1 has failure, MSW1 is closed MSW2 is open.
- State 2: br1 has failure, MSW1 is open, MSW2 is closed.
- State 3: br2 has failure, MSW1 is closed, MSW2 is open.

So the annual average outage time of L1 is $(P_1 + P_2 + P_3) \times 8760$

4.6 Approximate Evaluation method

If a system has n components and each component has two states, the state space diagram of this system has 2^n states. When n is large, the state space diagram is hard to build. So the precise Markov model introduced in section 4.5.2 is not suitable to evaluate large and complex systems, even by using a digital computer. In order to solve this problem, the approximate techniques introduced in this section are used to simplify the precise Markov model of a series system. A simple two-element series system in Figure 4.8 is used to illustrate the development of the approximate evaluation method. This system has two series elements: element A and element B. Each element has two states: the operation state and the failure state. The failure rates of A and B are λ_A and λ_B. Their repair rates are μ_A and μ_B respectively. So the state space diagram of this system is shown in Figure 4.13.

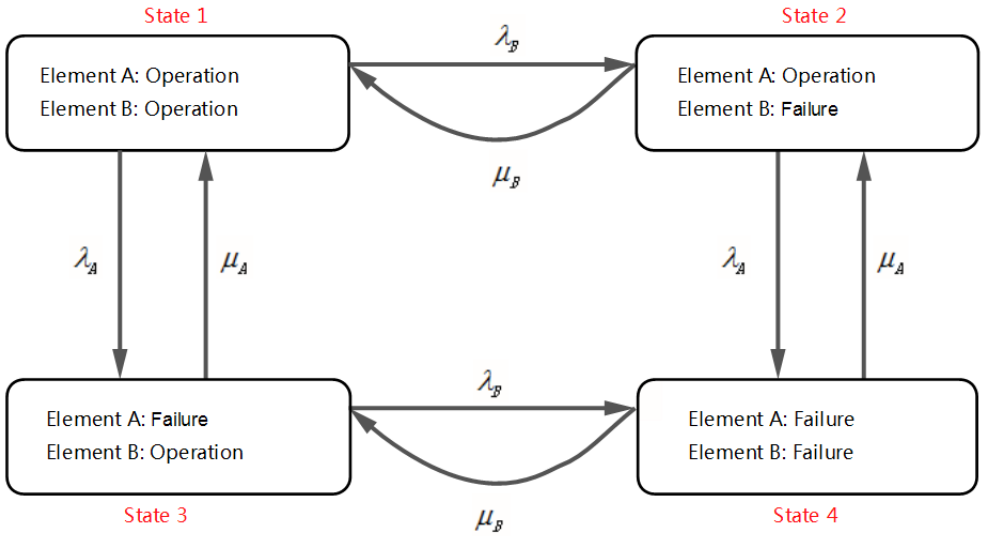

Figure 4.13 State space diagram

According to (4.22), the transition probability matrix of the above four-state state space diagram $\vec{\beta}$ is [117]:

$$\vec{\beta} = \begin{array}{c} \\ 1 \\ 2 \\ 3 \\ 4 \end{array} \begin{array}{c} \begin{array}{cccc} 1 & 2 & 3 & 4 \end{array} \\ \begin{bmatrix} -(\lambda_A + \lambda_B) & \lambda_B & \lambda_A & 0 \\ \mu_B & -(\lambda_A + \mu_B) & 0 & \lambda_A \\ \mu_A & 0 & -(\mu_A + \lambda_B) & \lambda_B \\ 0 & \mu_A & \mu_B & -(\mu_A + \mu_B) \end{bmatrix} \end{array} \tag{4.37}$$

The steady state probability of the system in being state i is $P_i(i = 1,2,3,4)$, so the probability matrix $\vec{P}$ is:

$$\vec{P} = [P_1 \quad P_2 \quad P_3 \quad P_4] \tag{4.38}$$

From (4.24) and (4.25),

$$[0 \quad 0 \quad 0 \quad 0] = \vec{P} \times \vec{\beta} \tag{4.39}$$

$$P_1 + P_2 + P_3 + P_4 = 1 \tag{4.40}$$

So the probability of this system being in state 1 $P_1(original)$ is:

$$P_1(original) = \frac{\mu_A \mu_B}{(\lambda_A + \mu_A)(\lambda_B + \mu_B)} \tag{4.41}$$

Assuming the single element system in Figure 4.14(b) is equivalent to the two elements series system in Figure 4.14(a), its failure rate and repair rate are λ_e and μ_e respectively. Based on its state diagram in Figure 4.10, the probability of this system in normal operation state $P_1(equivalent)$ is:

$$P_1(equivalent) = \frac{\mu_e}{\lambda_e + \mu_e} \tag{4.42}$$

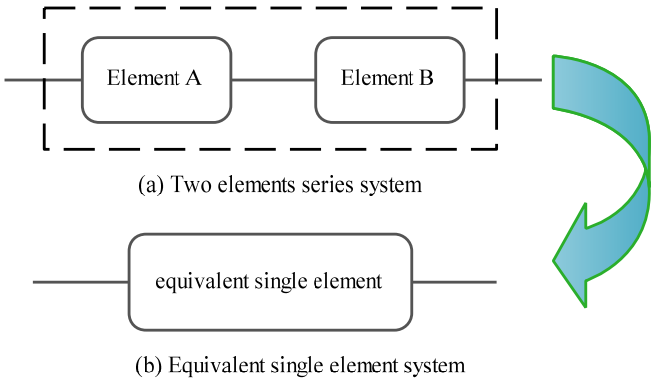

Figure 4.14 Equivalent single element system

For the two element series system in Figure 4.14(a), only state 1 represents the system in the normal operation state with both elements in service; the summation of the transition rate from state 1 to other states is: $\lambda_1 + \lambda_2$. For the single element equivalent system in Figure 4.14(b), the summation of the transition rate from the normal operation state to other states is λ_e. Since these two systems are equivalent, it can be concluded that:

$$\lambda_e = \lambda_A + \lambda_B \tag{4.43}$$

$$P_1 = P_{operation} \Rightarrow \frac{\mu_A \mu_B}{(\lambda_A + \mu_A)(\lambda_B + \mu_B)} = \frac{\mu_e}{\lambda_e + \mu_e} \tag{4.44}$$

Substituting (4.43) in to (4.44) gives,

$$\frac{1}{\frac{\lambda_A \lambda_B}{\mu_A \mu_B} + \frac{\lambda_A \mu_B}{\mu_A \mu_B} + \frac{\lambda_B \mu_A}{\mu_A \mu_B} + 1} = \frac{1}{\frac{\lambda_e}{\mu_e} + 1} \tag{4.45}$$

Rewriting the (4.45) as:

$$\frac{1}{\mu_e} = \frac{\frac{\lambda_A \lambda_B}{\mu_A \mu_B} + \frac{\lambda_A}{\mu_A} + \frac{\lambda_B}{\mu_B}}{\lambda_A + \lambda_B} \tag{4.46}$$

The repair rate μ can be represented by the repair time r as:

$$\mu = \frac{1}{r} \tag{4.47}$$

Substituting (4.47) into (4.46) and gives:

$$r_e = \frac{\lambda_A \lambda_B r_A r_B + \lambda_A r_A + \lambda_B r_B}{\lambda_A + \lambda_B} \tag{4.48}$$

Normally, the value of λr is very small. So the value of $\lambda_A r_A \lambda_B r_B$ is much smaller than $\lambda_A r_A$and $\lambda_B r_B$. So it makes sense to neglect $\lambda_A r_A \lambda_B r_B$

$$r_e = \frac{1}{\mu_e} \approx \frac{\lambda_A r_A + \lambda_B r_B}{\lambda_A + \lambda_B} \tag{4.49}$$

It can be concluded that the fault rate λ_e and average repair time r_e of a two-element series system are:

$$\lambda_e = \lambda_A + \lambda_B \tag{4.50}$$

$$r_e \approx \frac{\lambda_A r_A + \lambda_B r_B}{\lambda_A + \lambda_B} \tag{4.51}$$

Though (4.51) is an approximate equation, it is an accurate equation when state 4 in Figure 4.13 does not arise [117]. State 4 means both of the components have failed. In practice, when the first component has failed, that the remaining healthy components stop working has a very low probability of occurring which means the transition rate of entering the state 4 in which both of the two elements are failed almost decreases to zero [117]. So ignoring the state 4 has few effects on the final reliability evaluation results [117].

According to the above derivation for a two-element series system, the calculation steps of *n*-element series system are can be made as follows; Figure 4.15 visualizes the following steps:

- Step 1: Represent the first two series elements as a single equivalent element.
- Step 2: If the system still has an element connected to the single equivalent element in series, add this element to this single equivalent element to give a new two-element series system, and then return to Step 1. Otherwise, go to Step 3.
- Step 3: End

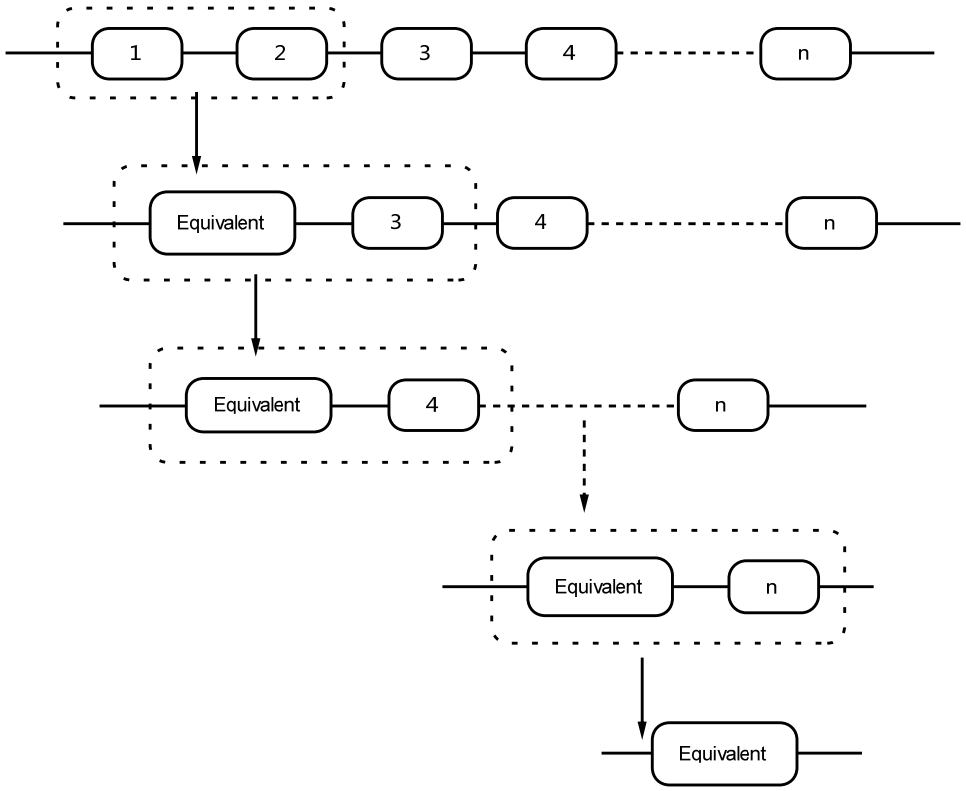

Figure 4.15 Calculation steps of n-element system

So after applying the approximate techniques, the failure rate (λ_e) and average outage duration (r_e) of the n-element series system is:

$$\lambda_e = \sum_{i=1}^{n} \lambda_i \text{ [interruptions/year]} \tag{4.52}$$

$$r_e = \frac{\sum_{i=1}^{n} \lambda_i r_i}{\sum_{i=1}^{n} \lambda_i} \text{ [hours]} \tag{4.53}$$

where:

λ_i: The fault rate of the element i.

r_i: The average repair time of the element i.

4.7 Modelling of Failure Events in Distribution Networks

Each network component has a risk of failure which is caused by internal or external factors. The internal factors can include the component's age and the external factors can be environmental conditions and human behaviour [109]. The aim of a reliability evaluation is to estimate the probability that the system fails to fulfil its function [116]. To do this, the rate of occurrence of faults and the system's and operators' responses to them must be assessed. So the precise nature of the failure event model is important. The details of how to model fault events are presented in the following subsections.

4.7.1 Active Failure and Passive Failure

Depending on whether a component failure can cause the operation of protection devices, failure modes can be divided into two basic types: passive failures and active failures [122]. The definitions of these two types of failure are [109, 123, 124]:

i) **Active failure:**

An active failure causes the operation of the primary protection zone around the failed component. Other healthy components may be outaged as well due to the operation of protection devices. The component which has an active failure needs to be isolated by switching actions so that some or all of the disconnected customers can be reconnected. The only way to restore the

failed component itself to normal operation condition is to repair or replace it.

ii) **Passive failure**

A passive failure does not cause any operation of protection devices. Open circuits and unintended opening of breakers are examples of passive failures.

Theoretically, each component will have both an active failure rate and a passive failure rate. However, for network components which are not switchable, like cables, overhead lines, etc., the main failure type is the active failure and the passive failure rate is negligible [124]. For self-switchable devices, like remote controlled switch, relay control circuit breaker, etc., the passive failure rate refers to the frequency of unwanted operation. It should be noted that the passive failure rate of manual switches whose value is close to zero is negligible [124]. In this thesis, only the active failure rates of cables, overhead lines and transformers are considered in the reliability evaluation. The significance of neglecting passive faults is discussed in the future work section. The algorithm for evaluating the effects of the failure of self-switchable devices will be implemented in future work.

4.7.2 Single Independent Failure and Multiple Independent Failures

Depending on the number of the failures occurring at the same time, types of failure can be defined as single failures or multiple failures. All failures are treated as independent in this thesis. In other words, such common failure modes as flooding, earthquakes or plane or vehicle crashes are neglected since experience suggests that the probabilities of such events are very low and therefore very hard to quantify. However, even if these events are not modelled in a reliability quantification, the designer of power network facilities should take account of the possibility of such events and decide whether the value of the service the facility provides would justify any investment in defence against those possibilities, e.g. flood barriers. The single independent failure refers a situation in which to only one component has a failure at the same time. Multiple independent failures means that more than one component has failed at the same time. In this thesis, only single independent failures are considered and the effects of multiple faults are discussed in future work.

4.7.3 Temporary Failure and Permanent Failure

A temporary failure does not need a manual repair. Some temporary failures can be cleared by themselves. For example, the branches of a tree are temporarily blown so close to an overhead line that a short circuit occurs but this is often naturally interrupted. In addition, if the overhead line is struck by lightning, service can be restored when the insulator has returned to its full insulting strength [125]. A permanent failure needs to be repaired manually and the repair time will vary from hours to days. As introduced in Section 1.2.2, since any temporary fault whose duration is less than three minutes will not affect the system reliability indices, only permanent failures are considered in the reliability evaluation discussed in this thesis.

4.7.4 Protection Failure

When a fault occurs in the network, the protection devices which should respond to this fault are assumed to operate to clear it as quickly as possible. However, the protection device's operation may fail sometimes. For example, a relay may fail to send a tripping signal to a circuit breaker once or twice per 100 demands and a circuit breaker will fail to operate less than once per 1000 demands [126]. In order to ensure that the system is still protected when a protection relay or a switching device does not operate as intended, back-up protection needs to be provided. Back-up protection may include: remote backup protection, substation local backup protection, and circuit local backup protection [126]. The example network in Figure 4.16 is one arrangement of back-up protection [127]. There are four relay-controlled circuit breakers: CB1, CB2, CB3 and CB4. CB1 and CB3 have auto reclose capability. So if CB3 fails to clear the fault, the back-up protection device CB1 needs to operate.

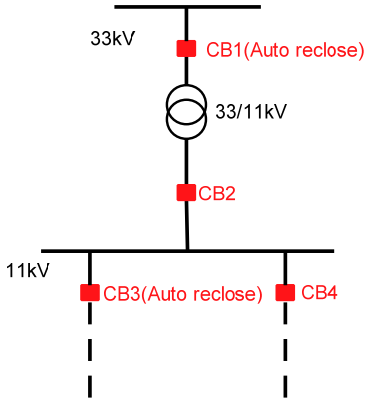

Figure 4.16 Back-up protection

Another condition of the protection failure is unwanted operation of a protection device where the device which should not operate in respond to a particular fault is tripped by that fault [128]. This protection failure will expand the fault-affected area. As a result, more customers will be affected by the fault. In this thesis, the reliability indices are evaluated assuming all overcurrent protection devices operate correctly at all times. The simulation of protection failure effects is discussed in the future work.

4.7.5 Planned Maintenance and Planned Outages

When network components need maintenance, these components should be disconnected from the source. A planned outage caused by maintenance cannot be considered as one of the random fault events discussed in the previous sections, since it is planned in advance to minimise its impact on the customer service supply. Normally, the network is designed so that maintenance can be executed without interrupting the customer electricity services. For example, the components of the feeder with an alternative source or a component with a parallel backup can achieve this target. So the planned maintenance can be ignored in reliability evaluation. However, a reconfiguration to facilitate a maintenance outage could often result in a less than ideal configuration which could mean that more customers are interrupted by a fault at a particular location than would have been the case without the reconfiguration for the planned outage. So if a permanent fault occurs during maintenance, the maintenance will affect the network restoration ability. In this thesis, all elements are assumed in normal operating condition before a permanent fault occurs. The implementation of simulating a permanent fault overlapping with a

planned maintenance condition will be discussed in the future work section. The analytical tool developed in this thesis can be used as an operational tool in which a maintenance outage would be represented as part of the initial condition.

4.8 Distribution Network Protection and Service Restoration under Fault Conditions

In a realistic network, more factors affect the network reliability performance. Among these factors, the impact of the overcurrent protection system is the most important. The overcurrent protection system can be tripped automatically to clear the fault. The network control points are used to reconfigure the network during the post fault condition. Many of these switches are operated manually, so the maintenance crew need to be sent to the switch position and the operation time is normally in hours. But the application of a remote controlled switch can reduce the switch time significantly. Since it can be operated remotely, its switch time is normally in minutes. Though the number of remote controlled switches is much lower than manual switches, it still plays an important role in network reliability performance and its number will continue to increase as DNOs will invest more on network automation in future [129, 130]. The distribution network protection system including protection devices and protection coordination are first introduced in section 4.8.1 and section 4.8.2 respectively. The service restoration process under fault conditions is introduced in section 4.8.3.

4.8.1 Distribution Network Protection Devices

The purpose of network protection in a power system is to detect unsafe operating conditions and prevent them from persisting. When such conditions are detected, the affected part of the network should be automatically removed from service. The different types of network protection, how they operate and where they are located are therefore extremely important in the evaluation of both the frequency of interruption of each customer's supply and the time that would normally be taken to restore it.

The types of electricity distribution network protection include: overcurrent protection, earth fault protection, unit and distance protection devices [131]. The overcurrent protection of distribution networks is different from the transmission system since it is usually operated in radial configuration. The protection of the transmission system consists of various types of relays, whereas the distribution overcurrent protection devices include: fuses, overcurrent relays, circuit breakers, reclosers, sectionalisers, etc. [7]. The fault between one phase and earth is a common fault in distribution networks [131]. The responsibility of an earth-fault relay is to clear the earth-fault current as quickly as possible. Unit protection relays only operate if faults occur in their protection zone [128]. They are used in interconnected systems and are used to protect transformers as well [131]. Distance protection is mainly used in HV systems [131].

The UK government has stated that 15% of the UK's total energy consumption should be supplied from renewable sources by 2020 [132]. The economics of different types of renewable electricity generation suggest that at least some of it will be connected into the distribution system [133]. The existing non-directional overcurrent and earth fault protection have very limited capability to solve the protection problems caused by connecting generation embedded within the distribution network, i.e. "distributed generation" (DG) [5, 134, 135]. Distance protection is an effective approach to solve these problems [127, 133, 136]. The UK 11kV distribution networks are mainly protected by non-directional overcurrent protection and earth fault protection [133].

In this thesis, the effects of overcurrent protection devices on system reliability are evaluated. The target of the overcurrent protection system is to minimize the fault duration and the number of customers affected by the fault. The overcurrent protection devices installed on the low voltage (11kV-415V) distribution network are automatic circuit breakers, reclosers, sectionalisers and fuses [137]. The network control points are the switches used to change the network configuration. Quick service restoration can be achieved by the operation of the network control points during the post fault condition. A brief introduction of these devices is presented as

follows and the symbols of them used in single line diagrams are illustrated in Figure 4.17 [138].

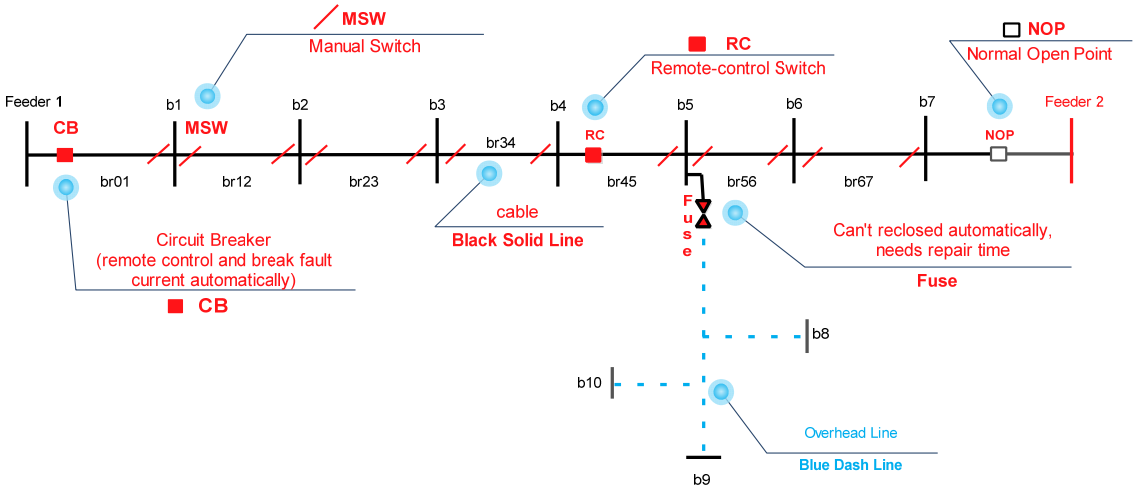

Figure 4.17 The symbols of the protection devices [138]

Circuit Breaker

Circuit breakers are normally installed at the start of the primary substation's feeder and coordinated with the protective relay. When the relay detects fault current in its protection zone, it will send an "open" signal to the circuit breaker. If the circuit breaker is tripped successfully, the fault location will be disconnected from the source and the fault current can be cleared. After the fault has been repaired, the circuit breaker can be reset to normal operation condition by a remote control signal or manual operation [131].

Recloser

When the fault location is far from the source, the fault current will be not large enough to trip the automatic circuit breaker. At these locations, a recloser can be used instead of the automatic circuit breaker. The main difference between the recloser and the relay-controlled circuit breaker installed at the substation is that the recloser has less interrupting capability and is cheaper [7]. For the areas whose distances are far from the substation, their fault currents may be too low for a relay-controlled circuit breaker. Reclosers have been used in these area historically [121]. The recloser can not only break fault current but also be closed automatically after a preset time interval, i.e. auto-reclosing. The main benefit of this feature is: a lot of

faults are only transient faults, e.g. lightning strikes on overhead lines, the system can be returned to normal operation condition automatically when the recloser recloses after the transient fault disappeared [121]. If the fault still exists when the recloser is closed, the recloser will open again. When the number of the reclose operations reaches the preset value (usually three or four times), the recloser remains in the open condition and stops reclose operation. The diagram of the time domain reclose sequence is shown in Figure 4.18 [121]. The time delay values (t_1 and t_2) of the recloser are adjustable and are normally less than one second [139, 140]. So if the temporary fault can be cleared by itself before the recloser returns to a closed condition, the network can be returned to normal operation state quickly and automatically.

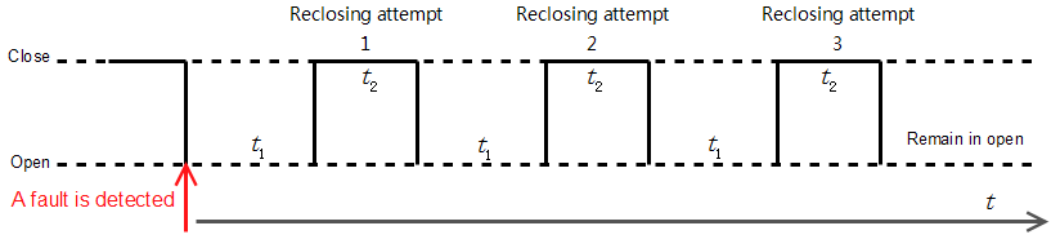

Figure 4.18 The reclosing sequence of the Recloser [121]

Fuse

Unlike automatic circuit breakers and reclosers which have a switch mechanism, a fuse has a fusible mechanism. The fusible component is normally made of a metal strip and has a maximum current rating. When the current that flows through the fuse is larger than its rating, the fusible component will be melted to disconnect it after the specified duration. The melted fusible component needs to be replaced so that the circuit can be reconnected. In an electricity distribution network, the fuse cutout which combines a fuse and a switch is used in networks whose voltage level is above 600V [141]. The fuse cutout is widely used in overhead line lateral protection and small capacity transformer protection [141].

Sectionaliser

The sectionaliser is an overcurrent protection device. It cannot break fault current and, in respect of short circuits, can only be used along with a circuit breaker or recloser [121, 137]. Protection coordination schemes determine the operation

sequence of the automatic circuit breaker, recloser and fuse. The settings of these devices are based on the time duration after the device detects a fault current. But the operation setting of the sectionaliser is based on the number of interruptions caused by its associated circuit breaker or recloser. This preset number is usually two or three [137]. The Figure 4.19 illustrates how a sectionaliser works [121, 137].

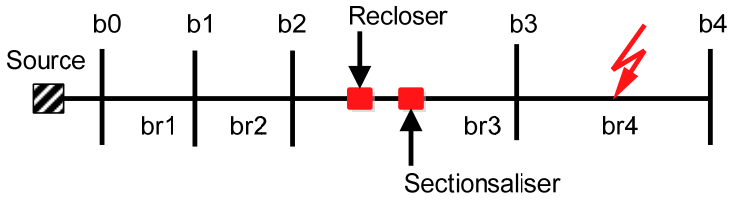

Figure 4.19 Example network for illustrating how sectionaliser works

Assuming that the preset number of the sectionaliser is 2, when there is a fault on branch br4 (downstream of the sectionaliser), the recloser opens and the count of sectionaliser is changed from 0 to 1. The recloser will close after a preset time. If the fault still exists, the recloser will open again and the count of sectionaliser is changed from 1 to 2. When the count of the sectionaliser reaches its preset number, it will automatically open to isolate the fault. The recloser will reclose again and remain in closed status. So the customers connected to buses b1 and b2 which are upstream of the recloser can be reenergized.

Based on this feature, a sectionaliser is easily operated in coordinatation with other protection devices to provide additional protection to the network without changing the existing protection coordination scheme. For example, a sectionaliser can be installed between the recloser and the fuse without changing the existing operation settings of the recloser and the fuse.

Network Control Point Devices

Network control points can be used to reconfigure the network to perform quick service restoration during the post fault condition. The types of network control point can be divided into two groups: manual switches and remote controlled switches. A manual switch, such as an air break switch, needs to be operated manually. It should be noted that some manual switches, like load disconnect switches, can only break normal load current. They do not have the ability to break fault current so they are not included in network protection devices, but instead are used as part of the

restoration or reconfiguration process in real networks. This thesis makes use of them. The remote controlled switch, such as a radio tele-control switch, can be operated not only manually but also by a remote control signal sent from the control room. A remotely controlled operation can be finished in minutes. Meanwhile, the operation time of the manual switch depends on how quickly the crew can reach the switch location and is normally in hours. So the application of remote controlled switches can significantly reduce the switch operation time, and the customer service down time can be minimised as well.

4.8.2 Protection Coordination

The protection device operation sequence under fault conditions is very important in reliability evaluation. The protection coordination scheme makes sure that each protection device works properly. The aim of the protection coordination is to make the protection devices coordinate with each other means of a communication channel or their fault clearance times [142]. Using the communication channel, the operated device sends a signal to lock other protection devices. If a communication channel is not available, the coordination is achieved by devices' different fault interruption times. Some devices can have a delay to open when they have detected the fault. One example of them is the relay-control device. Its fault clearance time consists of two parts: the relay delay time and the switch operation time [143]. The relay delay time is: when the device detects the fault, it can send the open signal to the switch mechanism after a time delay and the value of the time delay is modifiable [143]. So when a fault is detected by more than one device at the same time, the device operation sequence can be determined by their different fault clearance times.

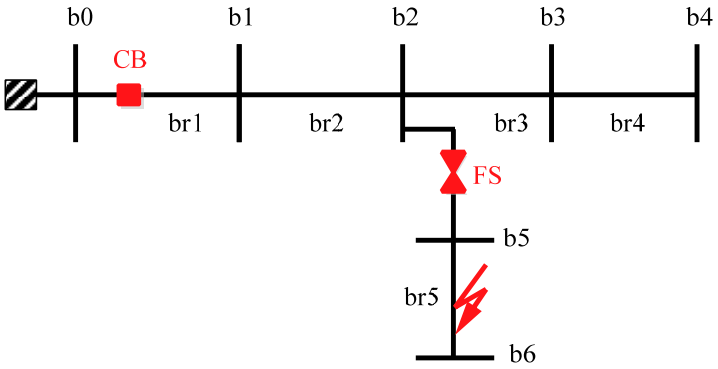

Figure 4.20 Example network for illustrating network protection coordination

The example network in Figure 4.20 is used to briefly illustrate the contribution of the well-coordinated protection system to the system reliability performance. When there is a fault on branch br5, all customers' power supply will be lost if the circuit breaker CB is opened. The fuse FS needs to be opened before the CB so that only the customers connected to buses b5 and b6 will lose power supply. In the thesis, a fault is assumed to be cleared by the nearest protection device on the path from the source to the fault location.

4.8.3 Service Restoration Process

When the protection device has been successful in isolating the fault, the control room will receive the fault indication signal sent by the device or reported by the customer. After the fault point has been located, engineers will be dispatched to repair the fault. The fault repair duration may vary from hours to days. Before starting to repair the fault, the control room will try to disconnect the faulted component from the source by the network control points, so that some customers' power supply can be restored in advance. The example network in Figure 4.21 is used to illustrate the process of the service restoration. In Figure 4.22, a dashed line for a branch means it is isolated and a dashed circle around a switch (e.g. breakers, remote controlled points and manual switches) means it is open. This network contains one automatic circuit breaker, one remote controlled switch, two manual switches and one normally open point.

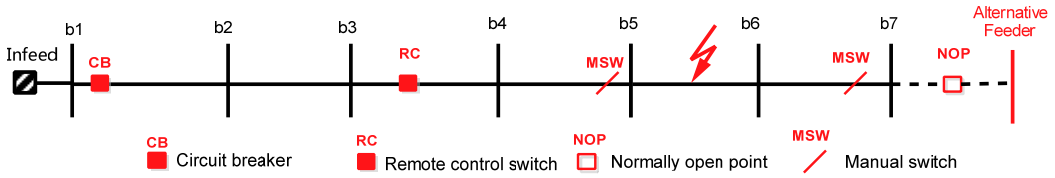

Figure 4.21 Example network with protection devices

If a permanent fault has occurred on branch br-56, the relay-control circuit breaker CB1 is tripped to open the circuit. As shown in Figure 4.22(A), all customers connected to this feeder lose their power supply although the fault current is cleared. Based on network reconfiguration, part of these customers' power supply can be restored before the fault has been repaired. As shown in Figure 4.22(B) the customers connected to busbar b2 and b3 are reconnected when remote control switch RC is opened and circuit breaker CB is closed. Then, by opening the manual switch MSW1 and reclosing remote control switch RC, the busbar b4 in Figure 4.22(C) is reenergized. The busbars restored on the previous steps are on the upstream side of the faulted branch. The busbars on the downstream side of the faulted branch can be transferred to the alternative feeder to restore their service. As shown in Figure 4.22(D), the busbar b7 can be reenergized by opening the manual switch MSW2 and closing the normally open point NOP. Supply to the busbars b5 and b6 can be restored when the fault has been repaired.

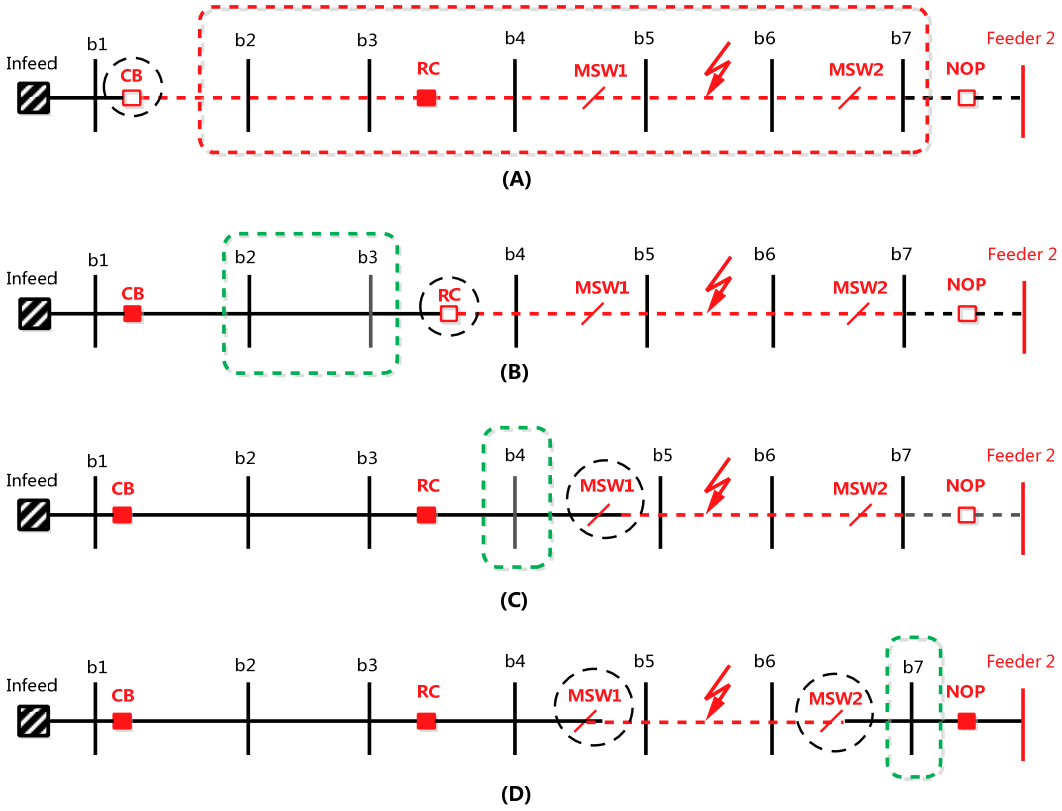

Figure 4.22 Service restoration process

4.9 Summary

This chapter has introduced the application of reliability theories to distribution networks. The overcurrent protection system and its impact have been discussed. The restoration process in reality has been illustrated by a simple example network. In the next chapter, how to implement the reliability evaluation algorithm is illustrated..

Chapter 5 Implementation of the Reliability Evaluation Algorithm

The previous chapter described the principles of distribution reliability assessment and the processes by which distribution service is restored following a fault outage. Based on these ideas, the fault duration of each load point can be obtained. But for a large and complex system, it is hard to evaluate the system reliability performance by the analytical method. So it is necessary to develop an algorithm which can perform this analysis automatically. In this chapter, the details of how to implement the reliability evaluation algorithm which can make an accurate estimate of restoration time are presented.

5.1 Introduction

As described in section 4.4, reliability evaluation methods can be divided into analytical methods and simulation methods. The Monte Carlo simulation methods are widely used in the reliability evaluation of power generation systems, transmission networks and substations [144-151]. The analytical methods are more popular in distribution network reliability analysis [152]. For example, EPRI developed the first distribution network reliability analysis tool based on analytical methods [153]; RELRAD developed by EFI in Norway is based on this method as well [154]; DS-RADS developed by the University of Washington is based on Hierarchical Markov modelling [152]; RADPOW and Racal developed by KTH are based on analytical methods [155, 156]. The protection system plays a very important role in distribution network reliability performance. Some previous publications have studied the effects of the protection system on distribution network reliability performance [157-159]. But they do not consider the effects of network automation devices, like remote control switches. A technique of evaluating the distribution reliability by considering both protection and automation systems is introduced in [142]. However, the restoration by manual switching is not considered in [142]. The reliability evaluation algorithm developed in this thesis considers the service restoration not only by remote control switches, but also by manual switches. The effects of the protection system are considered as well.

The basic flowchart of this algorithm is shown in Figure 5.1. In order to calculate the reliability indices in the final step, the first step is loading the input data. Besides the topology data used for loss minimization, the extra failure model data is required. Before staring the reliability indices calculation, the steps of network topology navigation and protection zone generation need to be executed first. These two steps preprocess the input data to generate the necessary data used in the step of restoration process simulation. The details of each step are illustrated in the next sections.

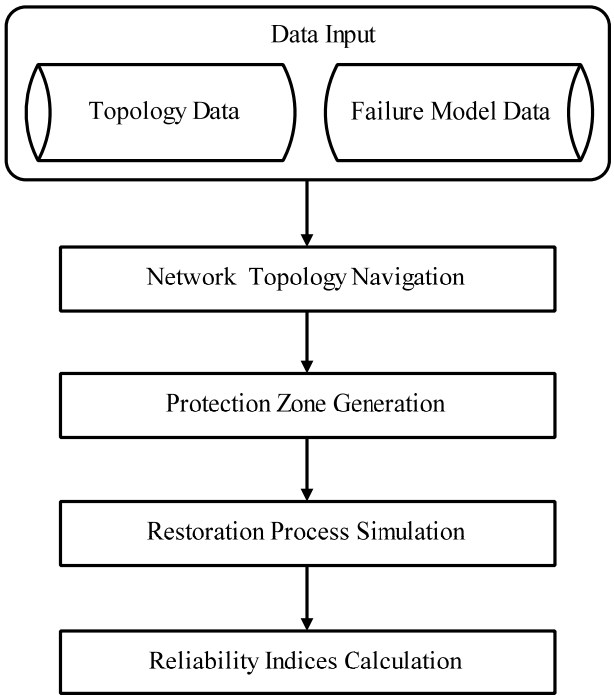

Figure 5.1 Basic flowchart of reliability evaluation algorithm

5.2 Input Data for Reliability Evaluation

The basic input data for reliability evaluation consists of two parts: network topology data and device failure data. The network topology data contains the element position data, and the device failure data describes the device's failure behaviour. The details of these data are described in the following subsections.

5.2.1 Network Topology Data

Besides the topology data required for loss minimisation analysis (described in chapter 3), extra topology information on the switch and protection devices is required for the reliability evaluation. Based on the characteristics of the device,

protection devices and remote controlled devices use the same data format while the manual switch has its own data format. The details of these data are illustrated below.

Manual Switch Data

The ring main unit is widely used in the secondary substations of the SPEN 11kV network [28, 160]. The symbol for a ring main unit used by SPEN's Distribution Management system is shown in Figure 5.2 [161]. It has manual switches at both line-in and line-out sides so the network will have a large number of manual switches. These switches can be used to reconfigure the network for service restoration under post fault conditions.

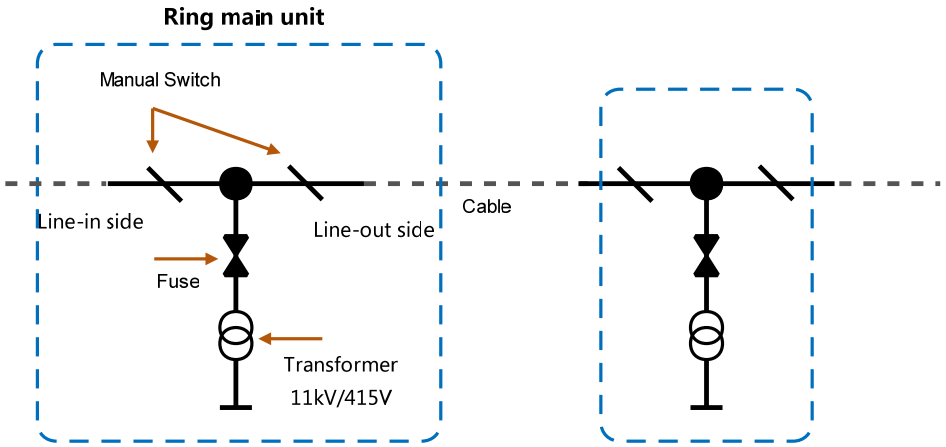

Figure 5.2 Structure of the ring main unit

In the default case, both ends of the branch have a manual switch. Based on this default case, the job of modelling the manual switch can be reduced since the number of the branches which have manual switches is much larger than the number of the branches without manual switches.

Protection Device and Remote Control Switch Data

Compared with manual switches, the number of protection devices and remote controlled switches is much smaller, but more data is required to describe their behaviour. So unlike manual switches, protection devices (e.g. auto circuit breaker, fuse) and remote controlled switches are modelled as a standalone 'class' [162]. As shown in Figure 5.3, the required parameters of locating the device are: the branch

and busbar which it is connected to. The related branch also contains the 'pointer' of this device so that the protection device data can be accessed effectively [162].

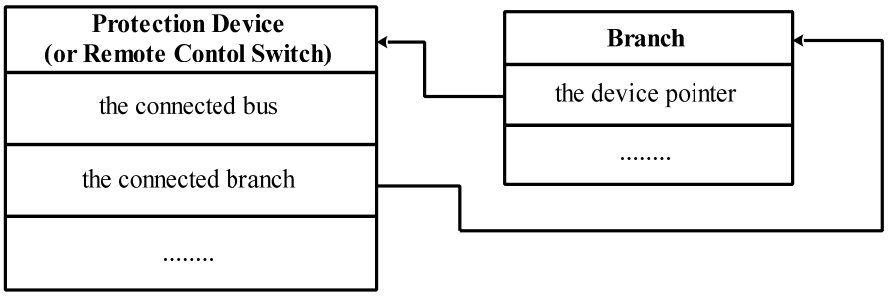

Figure 5.3 Topological modelling relationships for protection devices and remote controlled switches

5.2.2 Device Failure Model Data

The device failure model describes the device's failure behaviour; the parameters of this model are used for calculation of reliability indices. The main parameters used to define the failure model are the failure rate and the repair rate [117]. Besides these two rates, the switch rate which is equal to $\frac{1}{Mean\ time\ to\ switch}$ is used for switchable devices. Sometimes, the above three rate values are required to be rewritten in the format of a duration which are shown as follows (the unit of the rate is 1/year) [117]:

- Mean time to failure=8760/failure rate [hours]= 525600/failure rate [mins]
- Mean time to repair=8760/repair rate [hours]= 525600/repair rate [mins]
- Mean time to switch=8760/switch rate [hours]= 525600/switch rate [mins]

Referring to Chapter 4, the failure rate and repair rate are constant in value since the failure model used in this thesis is a continuous Markov model. The constant failure rate ideally applies when the occurrence of failures in time can be described by an exponential distribution, and assumption of constant failure rates for components in distribution network is generally good [163]. Though the failure rates, especially for overhead lines, are higher in adverse weather, it still can be considered as constant by ignoring the different weather conditions. Repair time and switch time generally do not match the exponential distribution as well as the failure rate [164, 165]. But modelling them as constant values only causes a small error in the final results [147].

The parameters of different device failure models may be not the same. Besides the three rates mentioned above, some devices need extra parameters to describe their failure model. According to [117], the minimum required data for each element for basic reliability computation are presented below.

Branch

- Failure rate
- Repair rate
- Length

The unit of length is normally the kilometre (km). The unit of the rate is frequency/year.km. So for a given branch, its final value of the rate is equal to the rate per length multiplied by the length. For branches that are series connections of sections of different types, they are modelled as separate branches with an artificial "bus" in between.

Bus

- Customer numbers
- Average load demand (kW/per customer)

Switch

- Failure rate
- Repair rate
- Mean time to switch
- Switch Type

For a remote controlled switch, it may fail to open when required. In addition, a short-circuit fault may happen on the switch itself. When these failures are ignored, the switch failure rate and repair rates are not used in reliability evaluation. Under this condition, the necessary parameters of the switch are the switch rate and switch type. In this thesis, the type of the switch is either manual or remote controlled.

Protection device

- Failure rate

- Repair rate
- Mean time to switch
- Device type

A protection system includes both the detection of a fault and the opening of appropriate switches to isolate it. A failure can be due to an error in fault detection, a failure of communication from the detection device to the switch or a failure of the switch to open when it should. The way in which a "protection device" is modelled should be consistent with the way a switch is modelled, e.g. there should not be double counting of failure modes. When the protection failure is ignored, only the switch rate is necessary for reclosable protection devices, like circuit breakers and reclosers. But for non-reclosable devices, like fuses, the repair rate is also necessary. The protection devices modelled in this thesis are auto-circuit breakers, reclosers and fuses.

5.3 Network Topology Navigation Module

The network topology navigation module generates the data which is necessary for the calculation of reliability indices. This is based both on the physical structure of the network and knowledge of which switches are initially open and closed. The following data is generated by this module:

- All elements connected to the same primary feeder
- The sending and receiving buses of each branch
- The upstream and downstream branches of each busbar

Further illustrations of the above data are presented below.

All Elements Connected to the Same Feeder

Before starting the reliability analysis, the network needs to be divided into sub networks defined by the feeders. As shown in Figure 5.4, the example network with three feeders is divided into three sub networks.

When network dividing has finished, information on each element belonging to each feeder is generated. So when a fault has occurred on a branch, the feeder which the

fault branch belongs to can be determined quickly. The following information relating to the feeder helps to determine how to restore the power supply of fault affected busbars:

- The locations of the protection devices and the switch devices on the feeder
- The locations of the normally open points on the feeder

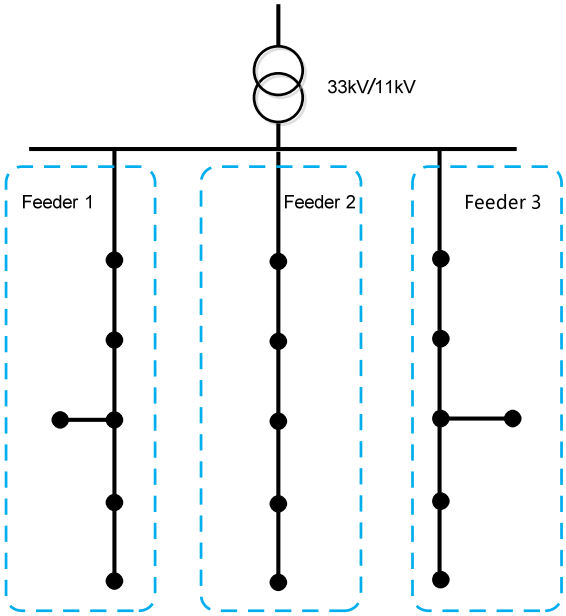

Figure 5.4 Original network is divided into sub networks

The Sending and Receiving Buses of Each Branch

The topology of the electricity distribution network is a directed graph and its direction is the current flow direction in the branch. This direction is very important in the breadth-first search. So in order to illustrate the direction of a branch, the two buses of the branch are defined as the sending busbar and the receiving busbar. Whether a bus is marked as "sending" or "receiving" depends on the particular operation condition. When looking at a number of operation conditions, such as when doing the load profile, load duration curve analysis, *P* loss optimisation analysis and reliability optimisation analysis, etc., particular nodes might change from being "sending" to "receiving" in different sub-cases. So the sending and receiving buses of each branch need to be redefined when the network topology is changed. As shown in Figure 5.5, the current flows from the sending busbar to the

receiving busbar. After determining the sending and receiving buses of each branch, the upstream parts and downstream branches of each busbar can be found quickly.

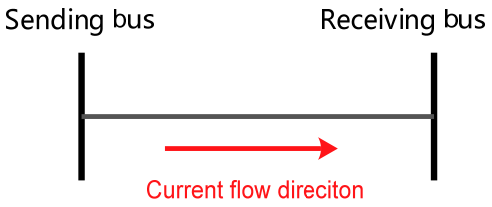

Figure 5.5 Direction of the branch

This process is performed by the algorithm introduced in section 3.4.2, which is only suitable for radial networks. If the connection of DG requires the network to be operated in mesh, this algorithm is no longer available. Under this condition, a load flow needs to be run to determine the direction of current flow in each branch.

The Upstream and Downstream Branches of Each Bus

The definition of a busbar's upstream and downstream branches is illustrated by Figure 5.6. Due to the characteristic of the radial network, each node has only one upstream branch connected to itself (except the root node) and there is no limit on the number of the connected downstream branches.

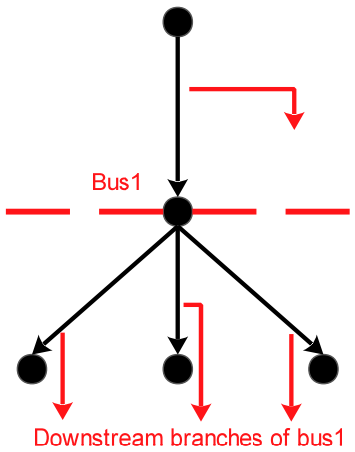

Figure 5.6 The upsteam and downsteam parts of a bus

After generating the busbar's upstream branch information, the path between any two nodes which are connected to the same primary feeder can be found quickly. The Figure 5.7 shows how to find the path between bus3 and bus1 by using upstream branches. Besides being used in path generation, knowledge of each busbar's

upstream and downstream branch is necessary for the upstream and downstream search algorithms introduced in section 5.5.2.

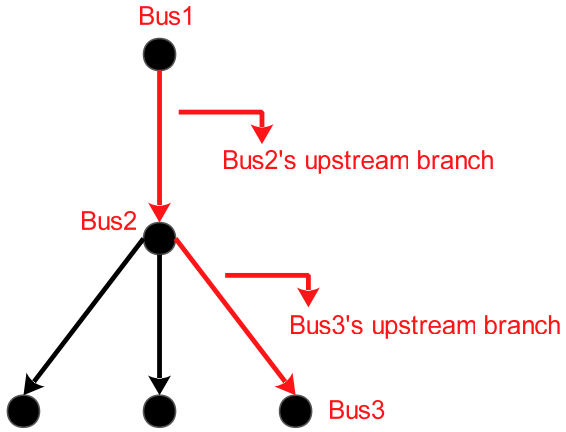

Figure 5.7 The role of the bus's upstream branch in Path search

5.4 Protection Zone Generation

5.4.1 Introduction

Switches and overcurrent protection devices play an important role in system reliability performance. In order to illustrate these effects, the concept of a protection zone is introduced in this section. A feeder can be divided into different protection zones by the positions of the network control points. Network elements between the network control points are in the same protection zone. According to the methods introduced in [166], the protection zone can be divided into two levels:

- **The level 1 zone**

  The boundary of the level 1 protection zone is the protection equipment. If a fault occurs in this zone, the protection device controlling this zone will operate the associated switches to isolate this zone from the feeder. In the example shown in Figure 5.8, the level 1 zone contains:

  - Busbars: b1, b2,b3 b4, b5
  - Branches: br01, br12, br23, br34, br45

  Any fault occurring in this zone will cause the circuit breaker CB to operate.

- **The level 2 zone**

  Since there will be some manual switches in the level 1 zone, the level 1 zone can be divided into subzones which are called the level 2 zone. The type of the network control point that forms the level 2 protection zone's boundary is the manual switch. In the example shown in Figure 5.8, the level 2 zone contains:

  - Busbars: b3, b4, b5
  - Branches: br34, br45

  When a fault has occurred in this zone, supply to busbars b1 and b2 can be restored by opening the manual switch MSW before the fault has been repaired.

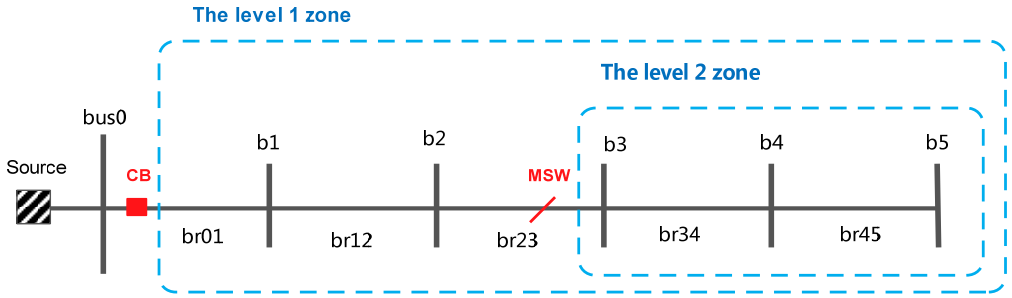

Figure 5.8 Zones of a feeder

The above rules for generating protection zones are designed for a generic network. In order to make these rules more suitable for the characteristics of the SPEN network, the following two modifications are applied to the above rules:

- **Addition of remote controlled switches to devices which form the level 1 zone's boundary**

  The only real difference between a "protection device" (that both detects and isolates a fault condition) and a remote controlled switch is the switching time, but the latter is only a few minutes which, in the terms of a reliability assessment, is still a short time. So the remote controlled switch is considered as the level 1 protection zone's boundary as well as the protection devices. However, the operation of a remote controlled switch depends on the operator knowing that there is a fault condition and so activating the switching action. Thus, the mean time to switch of a remote controlled switch needs to consider the time to determine where the fault is. The algorithm of creating the level 1 protection zone is presented in the next section and both the protection device and remote

controlled switch are named as ‘auto devices’.

- **Elimination of the level 2 zone**

  Due to the high density of manual switches in SPEN 11kV network, if the above protection zone generation rule was applied, a large number of level 2 protection zones will be created, which will complicate the analysis process. In order to solve this problem, the algorithm presented in this thesis only generates level 1 protection zones. Furthermore, the upstream and downstream searches introduced in section 5.5.2 are used to determine the load points affected by manual switch operation instead of creating the level 2 protection zone.

5.4.2 Implementation of the Protection Zone Generation Algorithm

The section introduces the implementation of the protection zone (level 1 zone) generation algorithm. This algorithm is based on breadth-first search (BFS). An initial root node needs to be determined before starting the BFS. Normally, a circuit breaker is installed on the primary feeder. In the single line network diagram, a circuit breaker is installed on the branch directly connected to the grid power source. The receiving busbar of this branch is chosen as the root node of the BFS. If the input data describing the network case does not include a circuit breaker installed on this branch, this algorithm cannot be started. For this condition, the algorithm adds a default circuit breaker on this branch automatically as shown in Figure 5.9.

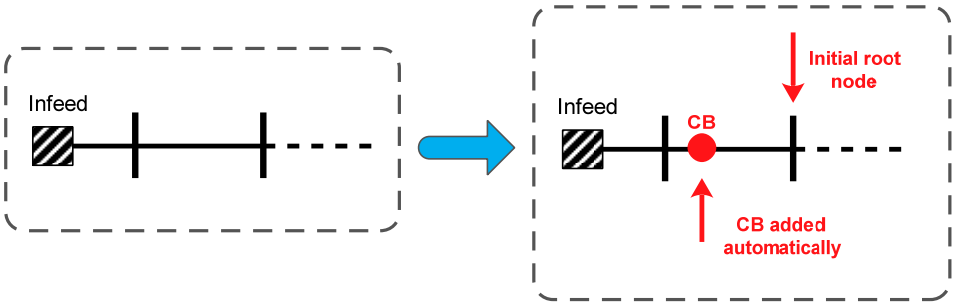

Figure 5.9 Addition of a circuit breaker on the start of the feeder

After determining the initial root node, the BFS search starts from this node and searches its downstream parts. If a busbar connected with an auto device (a protection device or remote controlled switch) is found, the BFS search stops at that busbar and a new root node is determined for the next protection zone search. Unlike

the initial root node, the position relationship between the newly found root node and the newly found auto device needs to be checked before starting to search the downstream elements connected to the new root node. Their position relationship has two cases:

- **Case 1: the auto device is connected to a branch's sending end and the new root node is the receiving end of the branch.**

  In this case, the branch 12 and the new root node (bus 2) shown in Figure 5.10 belong to the protection zone controlled by the auto device (CB1).

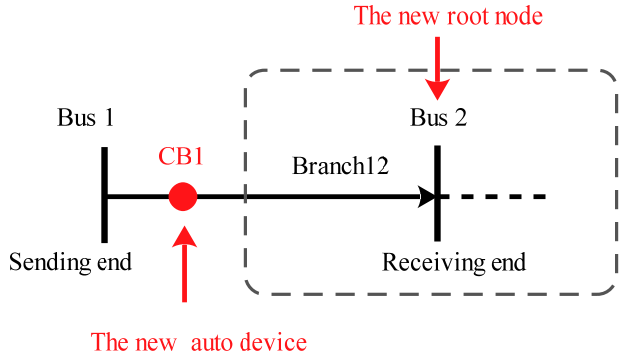

Figure 5.10 The auto device is connected to the sending bus

- **Case 2 the auto device is connected to a branch's receiving end and the new root node is the receiving end of the branch.**

  In this case, only the new root node (bus2) shown in Figure 5.11 belongs to the protection zone controlled by the auto device (CB2).

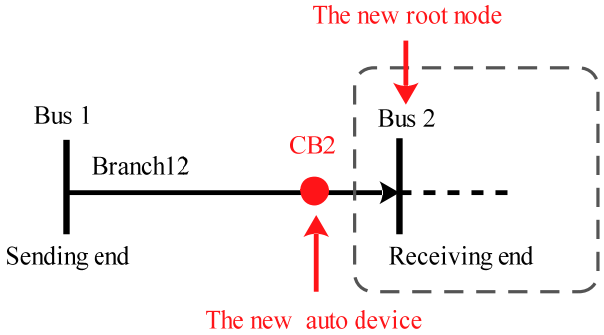

Figure 5.11 The auto device is connected to the receiving bus

When all auto devices installed on the chosen feeder are found, the protection zone generation of this feeder is finished. The application of the protection zones introduced in this section to service restoration is presented in Section 5.5.

5.5 Restoration Process Simulation

The restoration process of a simple network was introduced in section 4.8.3. In this section, the simulation of this process is introduced. The restoration process simulation algorithm has four modules:

- Fault event emulation module
- Network reconfiguration module
- Fault duration calculation module
- Reliability indices calculation module

The flowchart in Figure 5.12 illustrates the relationship between these modules. The details of each module are presented in the following subsections.

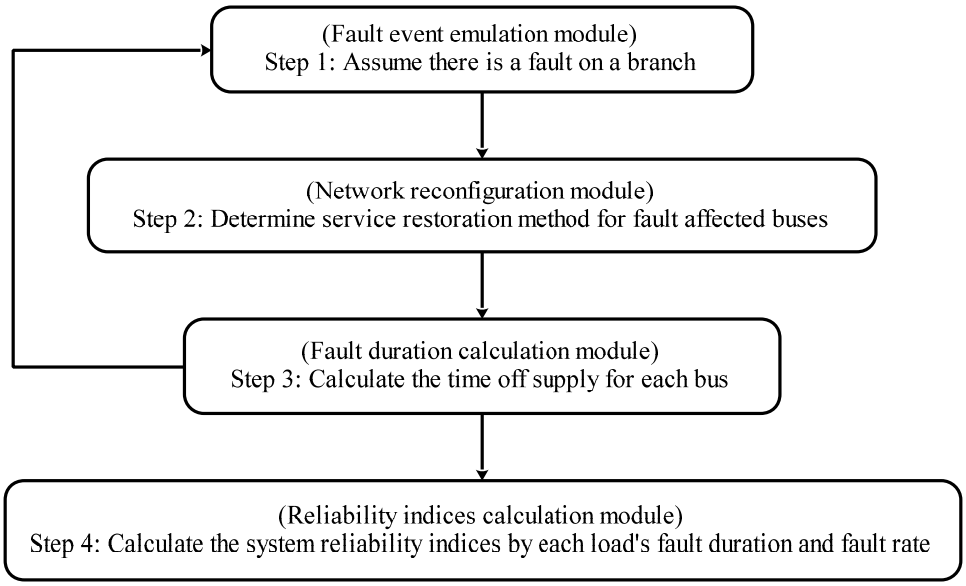

Figure 5.12 Flowchart of the restoration process simulation

5.5.1 Fault Events Emulation Module

The function of the fault events emulation module is to emulate all possible faults in an appropriate way. The protection zone technique introduced in section 5.4 is a widely used fault events emulation technique in the reliability evaluation of radial distribution networks [166, 167]. As introduced in section 4.7.2, only single

independent failures of the branch are simulated. There are two ways to present the relationships between the network and its branches. In relationship 1, the branches belong to the network directly. In relationship 2, the network is divided into feeders and the feeder is further divided into protection zones. So all the branches belong to a protection zone. The Figure 5.13 shows these two ways more clearly. Comparing these two ways, the advantages of using relationship 2 are:

1. For any faults that have occurred in a protection zone, the load points between the source and this protection zone have the same fault duration value which can simplify and speed up the simulation process.
2. Not only the whole system reliability performance but also each feeder's reliability performance can be evaluated.

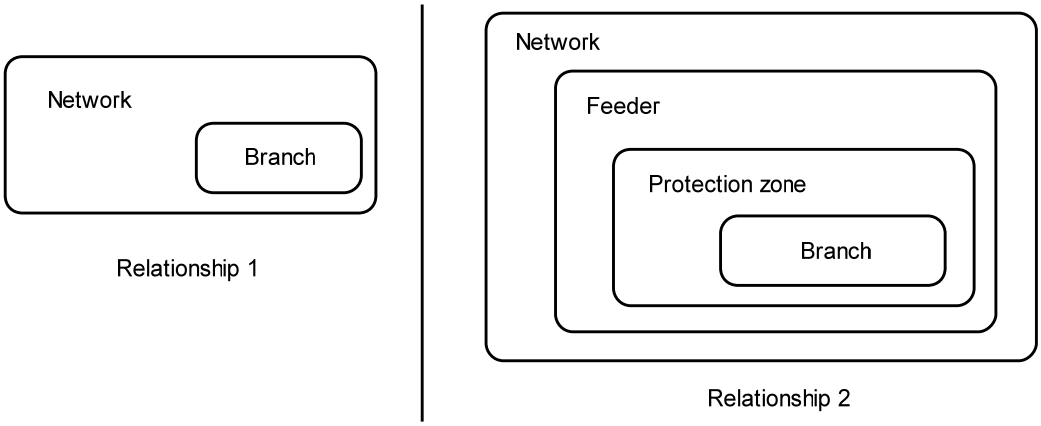

Figure 5.13 Relationships btween the network and branch

5.5.2 Network Reconfiguration Module

When the fault branch is chosen, the next step is to determine which busbars are affected by the fault and how to restore their supply as quickly as possible. How to restore service under fault condition by network reconfiguration is introduced in [168, 169]. Two-stage service restoration and investigation of its impact on distribution reliability is discussed in [88]. A method of determining the area affected by faults and the restoration time of loads in this area by parent-visit, offspring-visit, and breadth-first-search is presented in [167]. In this thesis, a new algorithm of determining the service restoration methods for fault affected load points is developed and implemented. This algorithm, based on network reconfiguration has the following three main steps: upstream restoration, upstream transfer and downstream transfer. Here, "restoration" means that the busbar is reconnected to its

original feeder after network reconfiguration and "transfer" means that the busbar is transferred from the original feeder to another feeder after network reconfiguration. The flowchart of this algorithm is shown in Figure 5.14.

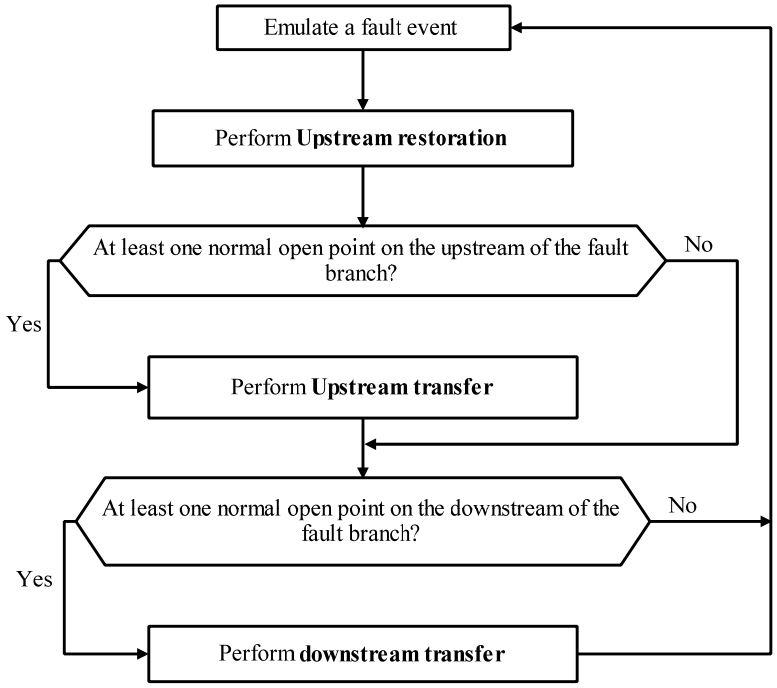

Figure 5.14 Flowchart of the reconfiguration module

When the restoration method has been determined, the restoration duration can be calculated. Its value is equal to either the equivalent switch time or the fault repair time. The following parameters are used in the calculation of restoration duration:

- t_{pr}: the time to reset the protection equipment to the normal operation condition
- t_{rcs}: the switch time of the remote controlled switch
- t_{ms}: the switch time of the manual switch
- t_{nops}: the switch time of the normally open point
- t_{fr}: fault repair time

It should be noted that the restoration time is calculated from when the load point loses power supply to when the supply is restored. The details of how to perform the steps in network reconfiguration are introduced in the following subsections. In the figures in these subsections, a dashed line for a branch means it is isolated and a dashed circle around a switch (e.g. breaker, remote controlled point or manual switch) means it is open.

5.5.2.1 Upstream Load Restoration

The aim of upstream restoration is to find the network control points upstream of the faulted branch and determine which busbars can be reconnected to the original feeder by network control point operation. The upstream restoration has two main stages:

1. Stage 1: Finding the branches of the path from the sending busbar of the fault branch to the receiving busbar of the branch which the nearest upstream protection equipment is installed on. Then finding the nearest remote controlled switch and manual switch to the sending busbar of the fault branch.
2. Stage 2: Determining the restoration method for each busbar on the path found in stage 1.

The implementation of each stage is presented below.

1) <u>Stage 1</u>

The search starts from the sending busbar of the faulted branch. Using the path search algorithm introduced in Section 5.3, the search will stop when the upstream branch has a protection device. The branches found during the search are recorded. Taking the network in Figure 5.15 for example, the start node is busbar b4, which is the sending busbar of the fault branch br45. The nearest protection device upstream of the fault branch is CB installed on branch br01. So the end node is busbar b1 and the required path is branches br34-br23-br12.

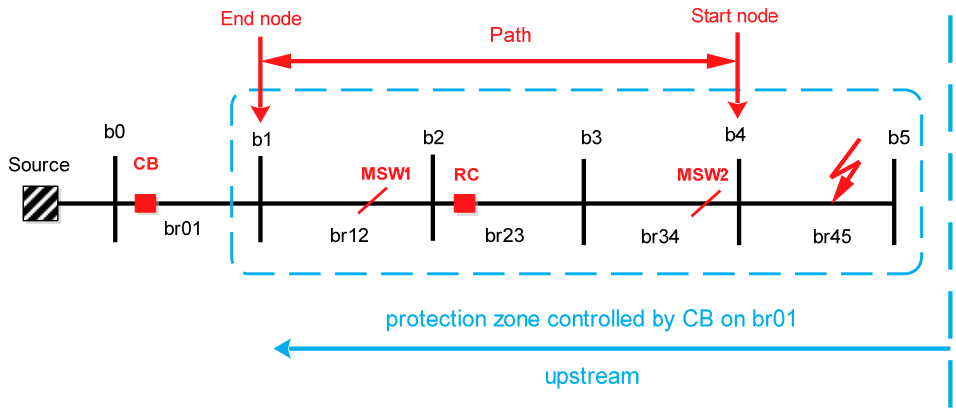

Figure 5.15 Example network used in upstream restoration

When the path has been found, the positions of the nearest remote controlled switch and manual switch to the fault branch on this path can be located. For the example

network in Figure 5.15, the target remote controlled switch is RC installed on branch br23 and the target manual switch is MSW2 installed on branch 45.

1) Stage 2

When stage 1 has been finished, the restoration method for each fault affected busbar on the upstream of the fault branch can be determined in this stage. According to the switch time, the remote controlled switch is the first choice for network reconfiguration and manual switch is the second choice. The switch operation sequence depends on the relative positions of the remote controlled switch and manual switch. The following four scenarios contain all possible device operation sequences:

1. the remote switch's location is farther than the manual switch's location
2. only a remote controlled switch is found or the manual switch's position is further than the remote controlled switch's location
3. only a manual switch is found
4. neither remote controlled switch nor manual switch is found.

The details of how to restore the supply to the busbars upstream of the fault branch under the above scenarios are presented below.

Scenario 1: The remote switch's location is farther than the manual switch's location

In this scenario, the switch sequence contains three steps which are:

1. **Step 1: Open the target remote controlled switch and then reclose the protection device**

   As shown in Figure 5.16(a), after the remote controlled switch RC has been opened, the circuit breaker can be reclosed. When the operations of these two devices have finished, the busbars b1 and b2 are reenergized. Here, the busbars b1 and b2 represent the busbars between the protection device and the remote controlled switch. The restoration duration of these busbars is $(\boldsymbol{t_{pr}} + \boldsymbol{t_{rcs}})$.

2. **Step 2: Open the target manual switch and then reclose the target remote controlled switch**

As shown in Figure 5.16(b), after manual switch MSW has been opened, the remote controlled switch RC can be reclosed. When the operations of these two devices have finished, the busbar b3 is reenergized. Here, the busbar b3 represents busbars between the target remote controlled switch and the target manual switch. The restoration duration of these busbars is $(\boldsymbol{t_{pr}} + \boldsymbol{t_{rcs}}) + (\boldsymbol{t_{ms}} + \boldsymbol{t_{rcs}})$.

3. **Step 3: Close the manual switch when the fault has been repaired**

As shown in Figure 5.16(c), when the fault has been repaired, the manual switch can be closed and the busbar b4 will be reenergized. Here, the busbar 4 represents the busbars between the target manual switch and the fault branch. The restoration duration of these busbars is $\boldsymbol{t_{fr}}$.

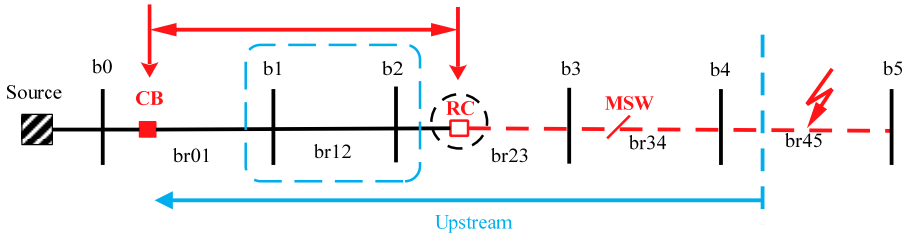

(a) Step 1

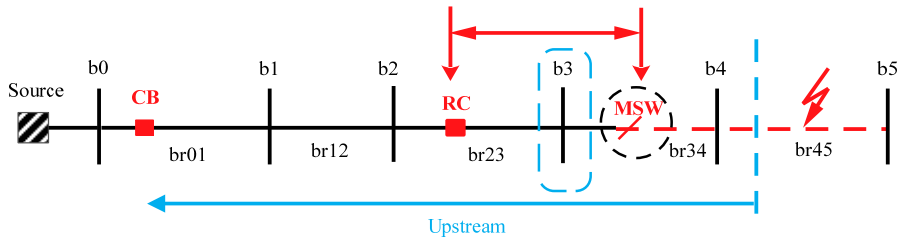

(b) Step 2

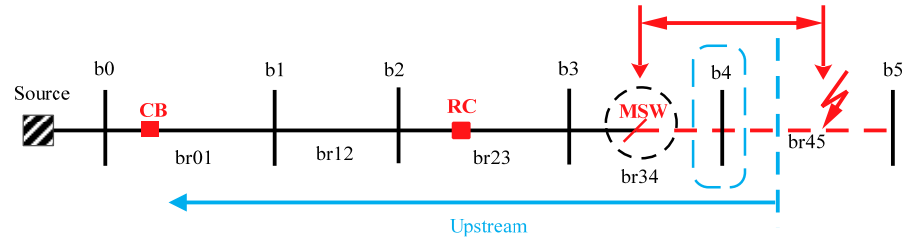

(c) Step 3

Figure 5.16 Steps of the switching sequence in Scenario 1 of upstream load restoration

Scenario 2: Only a remote controlled switch is found or the manual switch's position is farther than the remote controlled switch's location

In this scenario, the switching sequence contains two steps which are:

1. **Step 1: Open the target remote controlled switch and then reclose the protection device**

   As shown in Figure 5.17(a), after the remote controlled switch RC has been opened, the circuit breaker can be reclosed. When the operations of these two devices have been finished, the busbars b1 and b2 are reenergized. Here, the busbars b1 and b2 represent the busbars between the protection device and the remote controlled switch. The restoration duration of these busbars is $(\boldsymbol{t_{pr}} + \boldsymbol{t_{rcs}})$.

2. **Step 2: Close the remote controlled switch when the fault has been repaired.**

   As shown in Figure 5.17(b), when the fault has been repaired, the remote controlled switch can be closed and the busbars b3 and b4 will be reenergized. Here, the busbars b3 and b4 represents the busbars between the target manual switch and the fault branch. The restoration duration of these busbars is $\boldsymbol{t_{fr}}$.

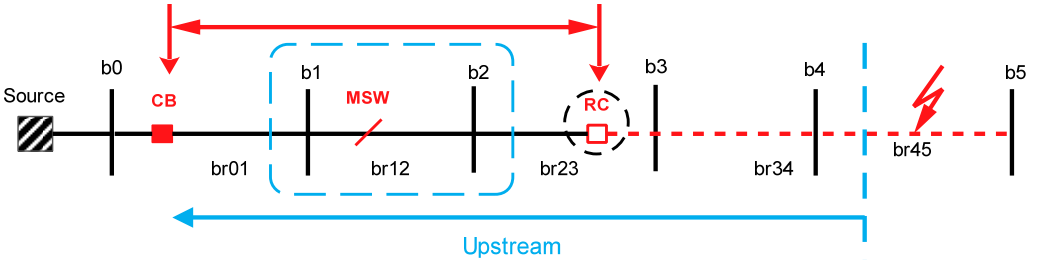

(a) Step 1

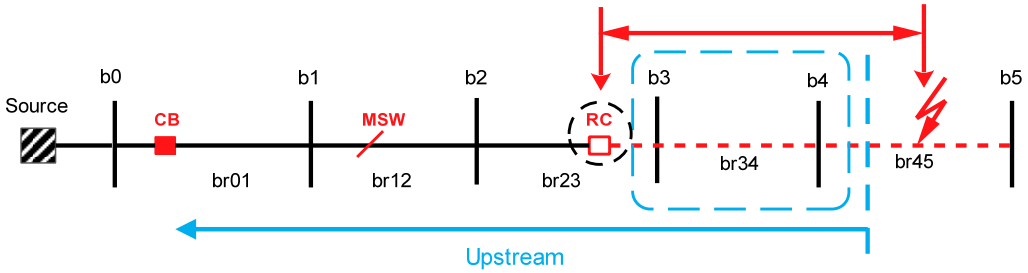

(b) Step 2

Figure 5.17 Steps in the switching sequence in Scenario 2 of upstream load restoration

Scenario 3: Only a manual switch is found

In this scenario, the switch sequence contains two steps which are:

1. **Step 1: Open the target manual switch and then reclose the protection device**

   As shown in Figure 5.18(a), after manual switch MSW has been opened, the protection device CB can be reclosed. When the operations of these two devices have finished, the busbars b1 and b2 are reenergized. Here, the busbars b1 and b2 represent any busbars between the target manual switch and the target protection device. The restoration duration of these busbars is $(\boldsymbol{t_{pr}} + \boldsymbol{t_{ms}})$.

2. **Step 2: close the manual switch when the fault has been repaired**

   As shown in Figure 5.18(b), when the fault has been repaired, the manual switch can be closed and the busbars b3 and b4 will be reenergized. Here, busbars b3 and b4 represent the busbars between the target manual switch and the fault branch. The restoration duration of these busbars is $\boldsymbol{t_{fr}}$

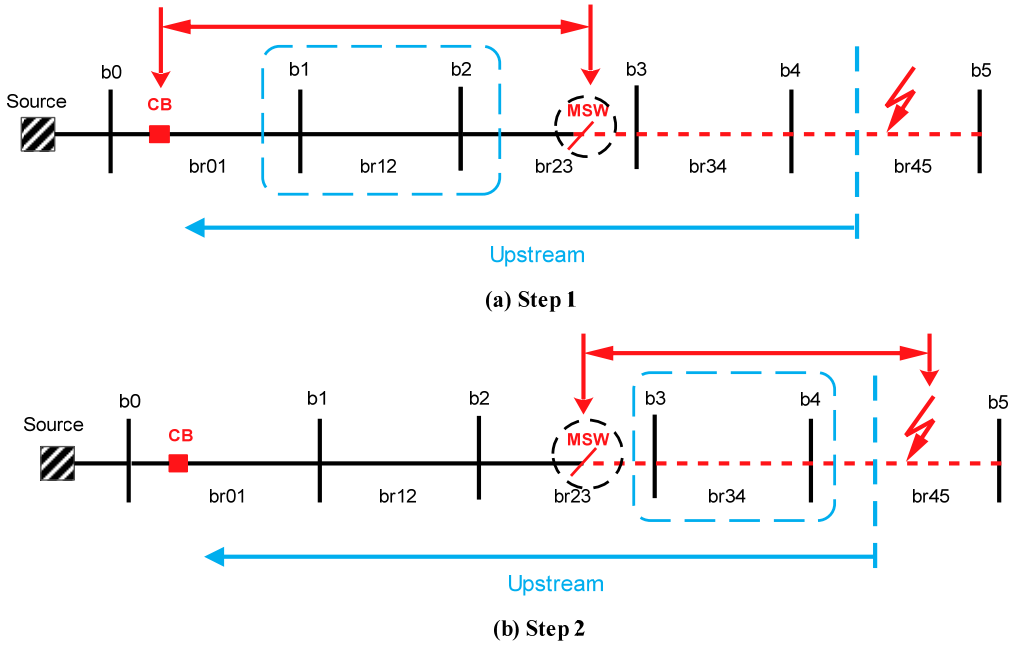

Figure 5.18 Steps in the switching sequence in Scenario 3 of upstream load restoration

Scenario 4: Neither remote controlled switch nor manual switch is found

As shown in Figure 5.19, the power supply of the busbars b1, b2, b3 and b4 which are on the downstream of the fault branch cannot be restored by network reconfiguration before the fault has been repaired. The busbars b1, b2, b3 and b4 represent the busbars between the sending busbar of the fault branch and target protection device. The restoration duration of these busbars is t_{fr}.

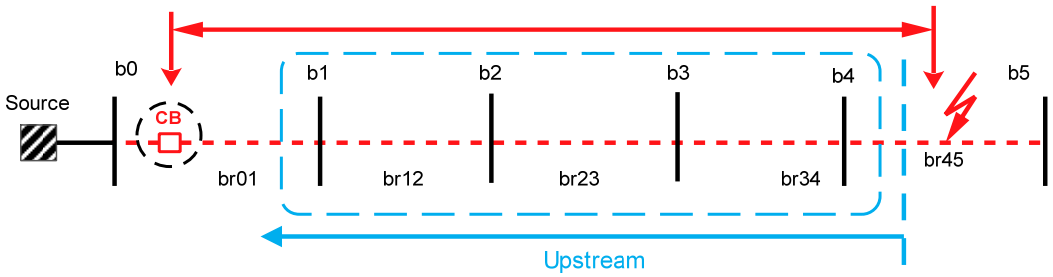

Figure 5.19 Busbars whose power cannot be restored by upstream restoration

5.5.2.2 Upstream Load Transfer

If the network shown in Figure 5.20 is analysed by the method introduced in section 5.5.2.1, the restoration method of busbars b2, b3, b6, b7, b8 and b9 when there is a fault on branch br34 shows that: these busbars cannot be restored by upstream restoration before the fault has been repaired. But in fact, busbars b6, b7, b8 and b9 can be transferred to an alternative feeder so that its power supply can be restored before the fault has been repaired.

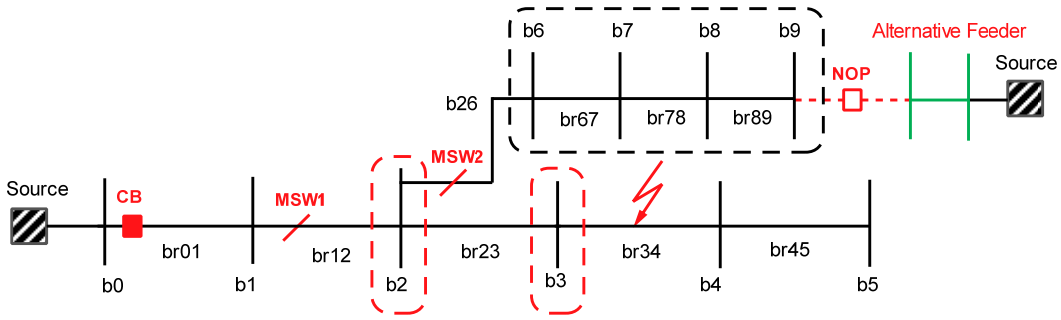

Figure 5.20 The position of the normal point is on the upstream of the fault branch

In order to solve this problem, the method of upstream load transfer is introduced in this section. The upstream load transfer can be executed when the normally open point is on the upstream side of the fault branch. The stages of this method are:

1. Find the edges of the path from the busbar connected to the normally open point to the source and this path is named as path 1.
2. Find the edges of the path from the sending busbar of the fault branch to the source and this path is named as path 2
3. Find the "cross point" (defined below) of the path 1 and path 2. Then find the edges of the path from the normally open point to the cross point. This path is named as path 3
4. Locate the nearest remote controlled switch and manual switch to the cross point and determine the service restoration method for the busbars on path 3.

Taking the network in Figure 5.20 as an example, the details of how to implement the above stages are presented below.

Stage 1

In this stage, the start node of the needed path is the busbar connected to the normally open point and the end node is the busbar connected to the source. As shown in Figure 5.21, the edges of the path from the busbar b9 to the busbar b0 are branches br89-br78-br67-br26-br12-br01.

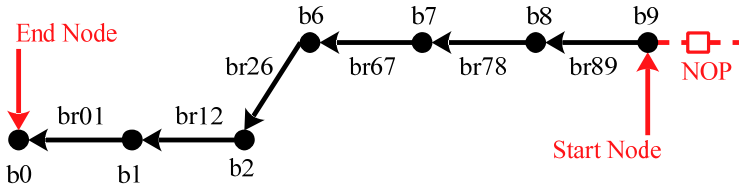

Figure 5.21 Path 1 from the normap open piont to the source node

Stage 2

In this stage, the start node of the needed path is the sending busbar of the fault branch and the end node is the busbar connected to the source. As shown in Figure 5.22, the edges of the path from the busbar b3 to the busbar b0 are branches br23-br12-br01.

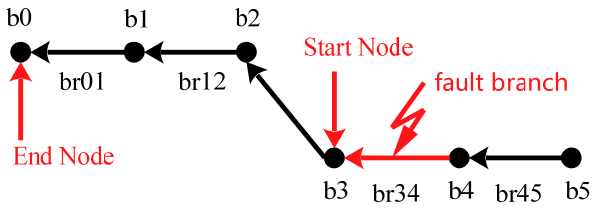

Figure 5.22 Path 2 from the fault branch to the source node

Stage 3

As shown in Figure 5.23, the branches br01 and br12 belong to both of the paths and the branches br23, br34, br45, br26, br67, br78 and br89 belong to one paths from stages 1 and 2 above. The concept of the "cross point" used in this stage is defined such that the branches on the upstream of the cross point belong to both of the paths and the branches on the downstream of it only belong to one path. So busbar b2 is the cross point of these two paths.

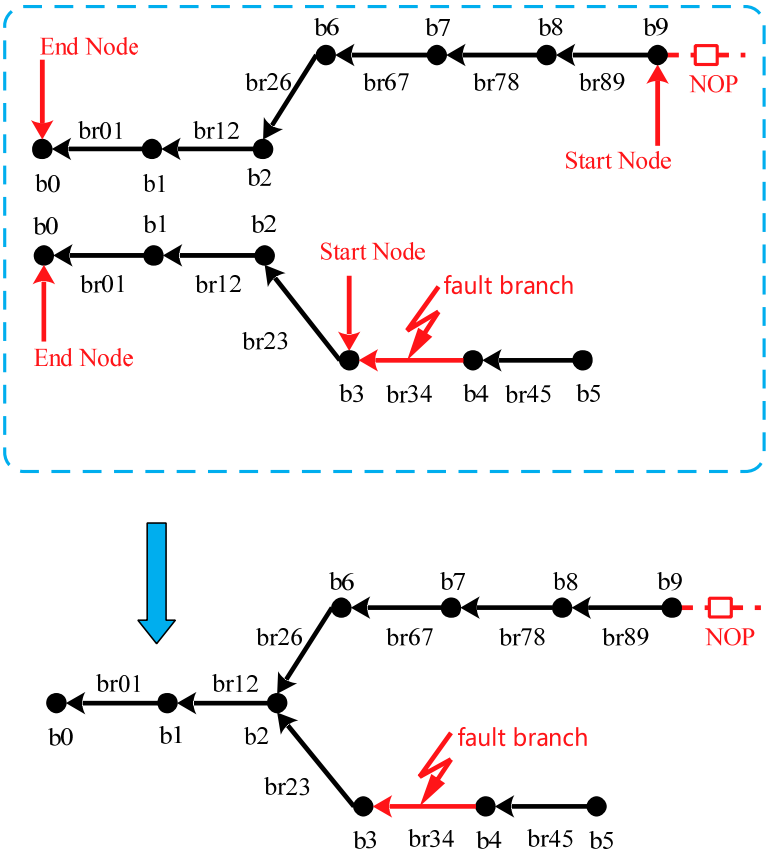

Figure 5.23 Cross point of the path 1 and path2

After the cross point has been found, the edges of path 3 from the busbars connected to the normally open point to the cross point can be determined. The Figure 5.24 shows the edges of path 3 are branches br89-br78-br67-br26.

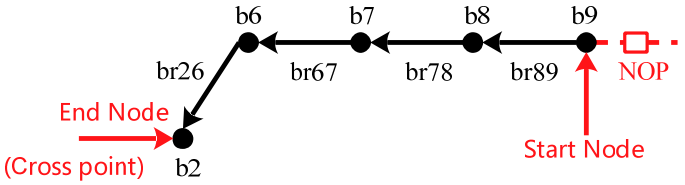

Figure 5.24 Path 3 from the normally open point to the cross point

Stage 4

When path 3 has been found in stage 3, the restoration methods of the busbars on this path are not only affected by the locations of the nearest remote controlled switch and manual switch to the cross point but also the cross point's restoration method which has been generated by the upstream restoration algorithm in advance. For example, the busbars on path 3 only have one restoration choice when the power supply of the cross point cannot be restored by network reconfiguration. But if the cross point is available for network reconfiguration, the busbars on path 3 will have two choices of the restoration method: one is to remain connected to the cross point, the other is to transfer to another feeder using the normally open point and the switches on path 3.

The example network in Figure 5.20 is used to illustrate this scenario of two restoration choices. In this network, the busbar b2 is the cross point. If there is a fault on branch br34, there are two choices for busbar b6's restoration methods:

1. Use the restoration method applied to the cross point: Here, the cross point busbar b2. Its restoration method is to open the manual switch MSW1 and then reset the circuit breaker CB. The restoration duration of this method is t_1.
2. Open the manual switch MSW2 and then close the normally open point NOP. The restoration duration of this method is t_2.

In this thesis, the choice of method to use to restore the power supply is determined by the restoration duration, though more factors may need to be considered in the actual operation (e.g. the cost of the switch operation). In the absence of information regarding these other factors, the method which has the minimum restoration duration is chosen. When the restoration durations are the same, the method requiring minimum device operation times is chosen.

When the power supply of the busbars on path 3 is restored by transferring to the alternative feeder, the sequence of the switch operations is determined by the relative locations of the target manual switches and target remote controlled switches on the path 3. The following four scenarios contain all possible switch operation sequences:

1. The location of the remote switch is farther from the cross point than the manual switch.
2. Only a remote controlled switch is found or the location of manual switch is farther from the cross point than the remote controlled switch
3. Only a the manual switch is found
4. Neither the remote controlled switch nor the manual switch is found.

The details of how to restore the supply to the busbars on path 3 are presented below. Parameter $\boldsymbol{t_{cp}}$ used in the following restoration duration calculation is the restoration duration of the cross point.

Scenario 1

In this scenario, the switch sequence contains two steps which are:

1. **Step 1: Open the target remote controlled switch and then close the normally open point**

   As shown in Figure 5.25(a), after the remote controlled switch RC on branch br34 has been opened, the normally open point NOP can be closed. When the operations of these two devices have been finished, the busbar b9 is reenergized. Here, busbar b9 represents the busbars between the normally open point and the remote controlled switch. The restoration duration of these busbars is $\boldsymbol{t_{nop} + t_{rcs}}$ $(\boldsymbol{t_{nop} + t_{rcs} < t_{cp}})$ or $\boldsymbol{t_{cp}}$ $(\boldsymbol{t_{nop} + t_{rcs} \geq t_{cp}})$

2. **Step 2: Open the target manual switch and then reclose the target remote controlled switch**

   As shown in Figure 5.25(b), after manual switch MSW has been opened, the remote controlled switch RC can be reclosed. When the operations of these two devices have finished, the busbars b7 and b8 are reenergized. Here, the busbars b7 and b8 represent any busbars between the target remote controlled switch and the target manual switch. The restoration duration of these busbars is:

   1) $\boldsymbol{t_{nop} + t_{rcs} + t_{msw} + t_{rcs}}$ when $\boldsymbol{t_{nop} + t_{rcs} + t_{msw} + t_{rcs} < t_{cp}}$**;** or

   2) $\boldsymbol{t_{cp}}$ when $\boldsymbol{t_{nop} + t_{rcs} + t_{msw} + t_{rcs} \geq t_{cp}}$**.**

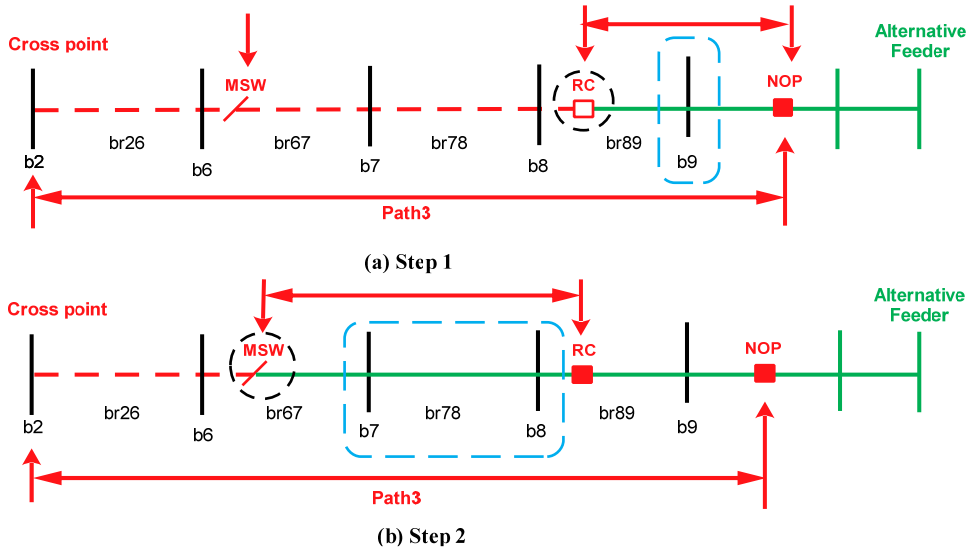

Figure 5.25 Steps in the switching sequence in Scenario 1 of upstream load transfer

Now except for the busbars b2 and b6, all busbars on this path are transferred to the alternative feeder. The busbars b2 and b6 represent all busbars between the cross point and the target manual switch. The restoration duration of these busbars is same as the cross point ($\boldsymbol{t_{cp}}$).

Scenario 2: Only the remote controlled switch is found or the manual switch's position is farther from the cross point than the remote controlled switch's location

In this scenario, the switch sequence contains one step which is:

1. **Step 1: Open the target remote controlled switch and then close the normally open point**

   As shown in Figure 5.26, after the remote controlled switch RC has been opened, the normally open point can be closed. When the operations of these two devices have finished, the busbars b7, b8 and b9 are reenergized. Here, the busbars b7, b8 and b9 represent the busbars between the normally open point and the target remote controlled switch. The restoration duration of these busbars is:

   1) $\boldsymbol{t_{nop} + t_{rcs}}$ when $\boldsymbol{t_{nop} + t_{rcs} < t_{cp}}$; or

   2) $\boldsymbol{t_{cp}}$ when $(\boldsymbol{t_{nop} + t_{rcs} \geq t_{cp}})$.

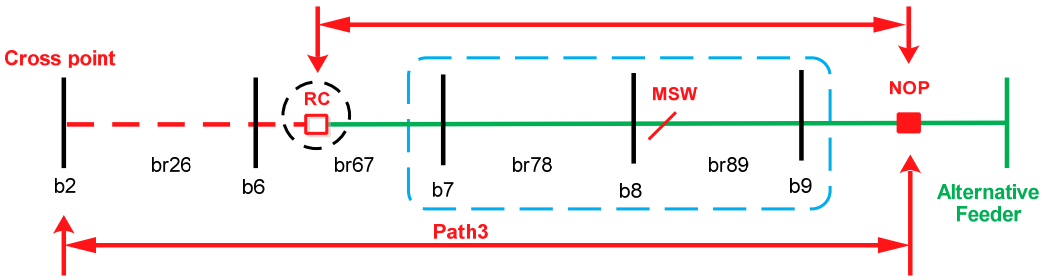

Figure 5.26 Steps in the switching sequence in Scenario 2 of upstream load transfer

Now except for the busbars b2 and b6, all busbars on this path are transferred to the alternative feeder. The busbars b2 and b6 represents all busbars between the cross point and the target remote controlled switch. The restoration duration of these busbars is same as the cross point ($\boldsymbol{t_{cp}}$).

Scenario 3: only a manual switch is found

In this scenario, the switching sequence contains one step which is:

1. **Step 1: Open the target manual switch and then close the normally open point**

   As shown in Figure 5.27, after manual switch MSW has been opened, the normally open point can be closed. When the operations of these two devices have finished, the busbars b8 and b9 are reenergized. Here, the busbars b8 and b9 represent any busbars between the target manual switch and the normally open point. The restoration duration of these busbars is 1) $\boldsymbol{t_{nop} + t_{msw}}$ when $\boldsymbol{t_{nop} + t_{msw} < t_{cp}}$; 2) $\boldsymbol{t_{cp}}$ when $\boldsymbol{t_{nop} + t_{msw} \geq t_{cp}}$

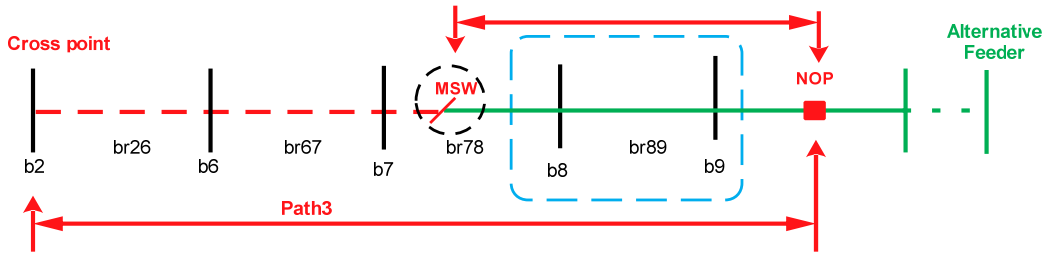

Figure 5.27 Steps in the switching sequence in Scenario 3 of upstream load transfer

Now except for the busbars b2, b6 and b7, all busbars on this path are transferred to the alternative feeder. The busbars b2, b6 and b7 represent all

busbars between the cross point and the target manual switch. The restoration duration of these busbars is the same as the cross point ($\boldsymbol{t_{cp}}$).

Scenario 4: Neither remote controlled switch nor manual switch is found

In this scenario, the busbars between the cross point and the normally open point cannot be transferred to the alternative feeder. The restoration duration of these busbars is the same as the cross point.

5.5.2.3 Downstream Load Transfer

For the busbars on the downstream of the faulted branch, it is impossible to reconnect them to their original feeder. But with an adjacent normally open point, these busbars can be transferred from the original feeder they are connected to in pre-fault conditions to an alternative feeder so that their power supply can be restored. Since information on the feeder's normally open points has already been generated in preprocessing, it is quick to identify whether the load transfer restoration can be executed. The process of the downstream load transfer has two main steps:

1. **Stage 1**: Find the branches of the path from the sending busbar of the branch where the normally open point is located to the receiving busbar or sending busbar of the faulted branch. Then find the nearest remote controlled switch and manual switch to the receiving busbar of the faulted branch.
2. **Stage 2**: Determine the restoration method for every busbar on the path found in stage 1.

The implementation of each stage is presented below:

Stage 1

In order to find the branches of the needed path, the search starts from the branch where the normally open point is located. Using the path search algorithm introduced in section 5.3, the search stops when it reaches the receiving or sending busbar of the faulted branch. When the faulted branch br12 in Figure 5.28 is marked with a "tree" flag, the end node of the path is the receiving busbar of the faulted branch. So the start and end node of are b4 and b2 respectively. Since the fault branch br25 in Figure 5.29 is marked as a lateral, its sending end has neither a protection device nor

a switch. The end node of the path is the sending busbar of the fault branch and the receiving busbar of the fault branch is marked as non-transferable – its fault duration is equal to the fault repair time. So the start and end node of the path are b4 and b2 respectively in both cases. After the path has been found, the positions of the nearest remote controlled switch and manual switch to the faulted branch on this path can be located. The network in Figure 5.28 is used to illustrate the downstream transfer in Stage 2.

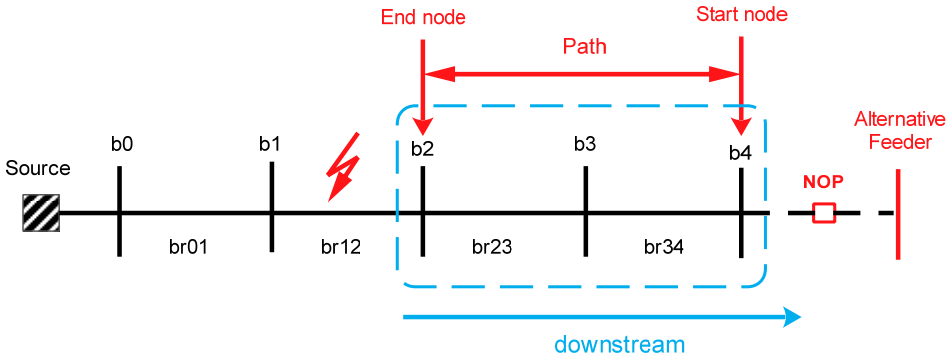

Figure 5.28 Example network used in downstream load transfer

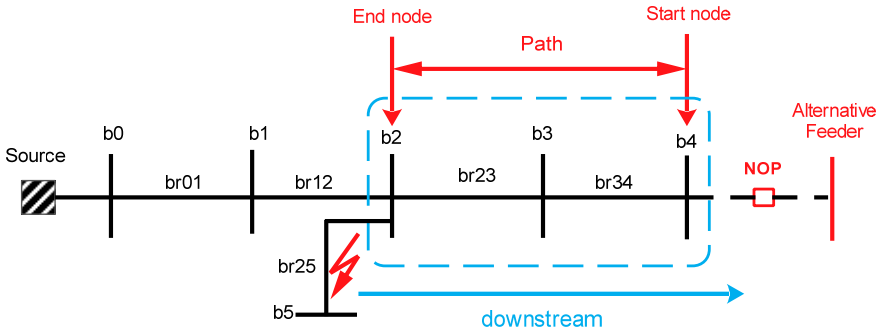

Figure 5.29 Example network whose fault branch is marked as lateral

Stage 2

When stage 1 has been finished, the restoration method for each fault affected busbar downstream of the faulted branch can be determined in this stage. According to the switching time, the remote controlled switch is the first choice for network reconfiguration and manual switch is the second choice. The switching sequence depends on the relative positions of the remote controlled switch and manual switch. The following four scenarios contain all possible device operation sequences:

1. The remote switch's location is farther from the faulted branch than the manual switch's location

2. Only a remote controlled switch is found or the manual switch's position is farther from the faulted branch than the remote controlled switch's location
3. Only a manual switch is found
4. Neither remote controlled switch nor manual switch is found.

The details of how to restore the power supply services of the busbars on the downstream of the fault branch under the above scenarios are presented below.

Scenario 1: The remote switch's location is farther than the manual switch's location

In this scenario, the switch sequence contains three steps which are:

1. **Step 1: Open the target remote controlled switch and then close the normally open point**

   As shown in Figure 5.30(a), after the remote controlled switch RC on branch 34 has been opened, the normally open point NOP can be closed. When the operations of these two devices have finished, the busbar b4 is reenergized. Here, busbar b4 represents the busbars between the normally open point and the remote controlled switch. The restoration duration of these busbars is $(\boldsymbol{t_{nop}} + \boldsymbol{t_{rcs}})$

2. **Step 2: Open the target manual switch and then reclose the target remote controlled switch**

   As shown in Figure 5.30(b), after the manual switch MSW has been opened, the remote controlled switch RC can be reclosed. When the operations of these two devices have finished, the busbar b3 is reenergized. Here, the busbar b3 represents any busbars between the target remote controlled switch and the target manual switch. The restoration duration of these busbars is $(\boldsymbol{t_{nop}} + \boldsymbol{t_{rcs}}) + (\boldsymbol{t_{msw}} + \boldsymbol{t_{rcs}})$.

3. **Step 3: Reset the Feeder to the original operation condition when the fault has been repaired**

   As shown in Figure 5.30(c), when the fault has been repaired and all switches on the upstream of the fault have been closed, the busbar b2 is reenergized by opening the normal point and then closing the circuit breaker (CB) and the

target manual switch. Here, busbar b2 represents the busbars between the target manual switch and the receiving busbar of the fault branch. The power supply of these busbars cannot be restored by network reconfiguration before the fault has been repaired. The restoration duration of these busbars is t_{fr}.

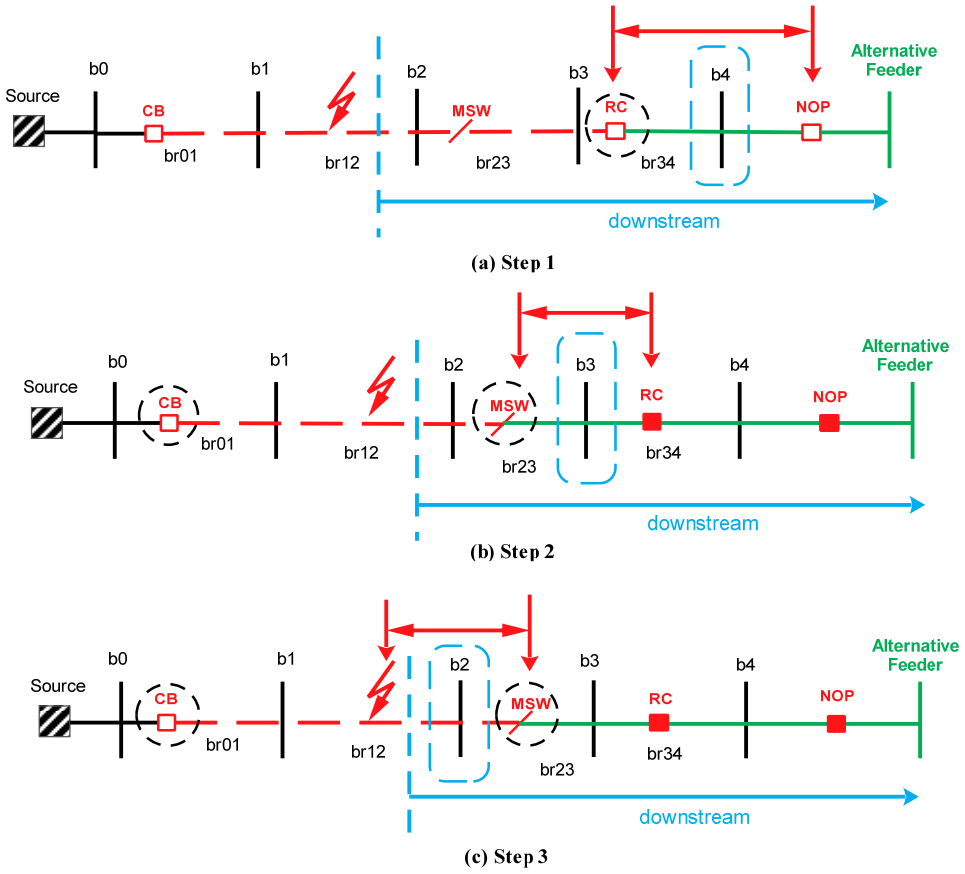

Figure 5.30 Steps in the switching sequence in Scenario 1 of downstream load transfer

Scenario 2: Only the remote controlled switch is found or the manual switch's position is farther from the faulted branch than the remote controlled switch's location

In this scenario, the switching sequence contains two steps which are:

1. **Step 1: Open the target remote controlled switch and then close the normally open point**

   As shown in Figure 5.31(a), after the remote controlled switch RC has been opened, the normally open point can be closed. When the operations of these two devices have finished, the busbars b3 and b4 are reenergized. Here, the busbars b3 and b4 represent the busbars between the normally open point and

the target remote controlled switch. The restoration duration of these busbars is $(\boldsymbol{t_{nop}} + \boldsymbol{t_{rcs}})$.

2. **Step 2: Reset the feeder to the original operation condition when the fault has been repaired**

   As shown in Figure 5.31(b), when the fault has been repaired and all switches on the upstream of the fault have been closed, the busbar b2 is reenergized by opening the normal point and closing the remote controlled switch. Here, busbar b2 represents the busbars between the target remote controlled switch and the receiving busbar of the fault branch. The power supply of these busbars cannot be restored by network reconfiguration before the fault has been repaired. The restoration duration of these busbars is $\boldsymbol{t_{fr}}$.

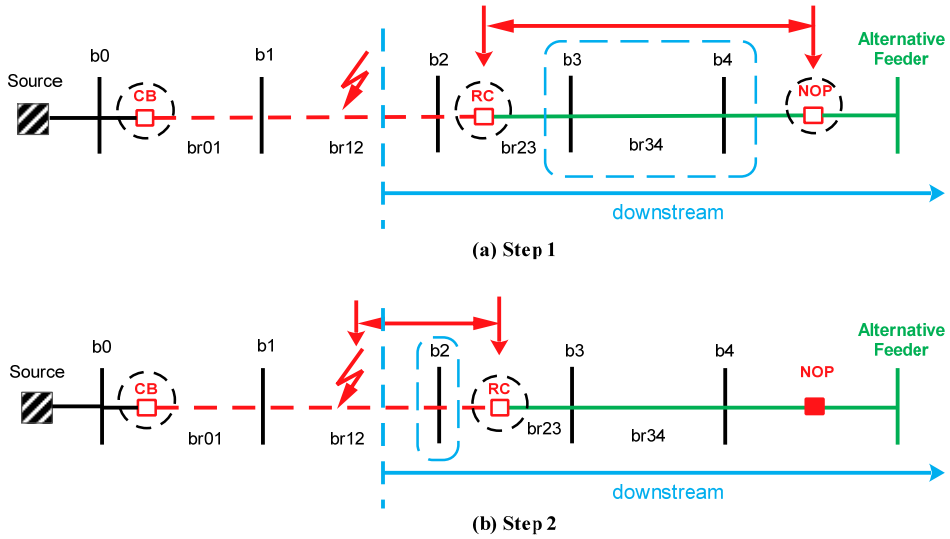

Figure 5.31 Steps in the switching sequence in Scenario 2 of downstream load transfer

Scenario 3: Only a manual switch is found

In this scenario, the switch sequence contains two steps which are:

1. **Step 1: Open the target manual switch and then close the normally open point**

   As shown in Figure 5.32(a), after manual switch MSW has been opened, the normally open point can be closed. When the operations of these two devices have finished, the busbars b3 and b4 are reenergized. Here, the busbars b3 and b4 represent any busbars between the target manual switch and the

normally open point. The restoration duration of these busbars is ($t_{nop} + t_{ms}$).

2. **Step 2: Reset the feeder to the original operation condition when the fault has been repaired**

   As shown in Figure 5.32(b), the busbar b2 is reenergized when the fault has been repaired. Here, the busbar b2 represents the busbars between the target manual switch and the fault branch. The power supply of these busbars cannot be restored by network reconfiguration before the fault has been repaired. The restoration duration of these busbars is t_{fr}.

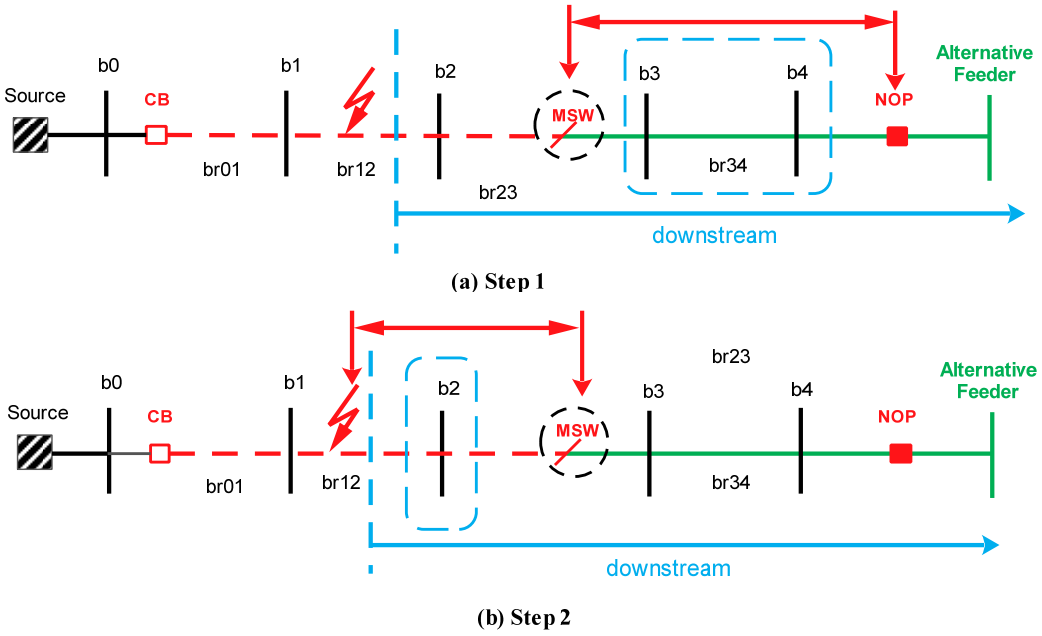

Figure 5.32 Steps in the switching sequence in Scenario 3 of downstream load transfer

<u>Scenario 4</u>: Neither remote controlled switch nor manual switch is found

As shown in Figure 5.33, the power supply of the busbars b2, b3 and b4 which are on the downstream of the fault branch cannot be restored by network reconfiguration before the fault has been repaired. The busbars b2, b3 and b4 represent the busbars between the receiving busbar of the fault branch and the normally open point. The restoration duration of these busbars is t_{fr}.

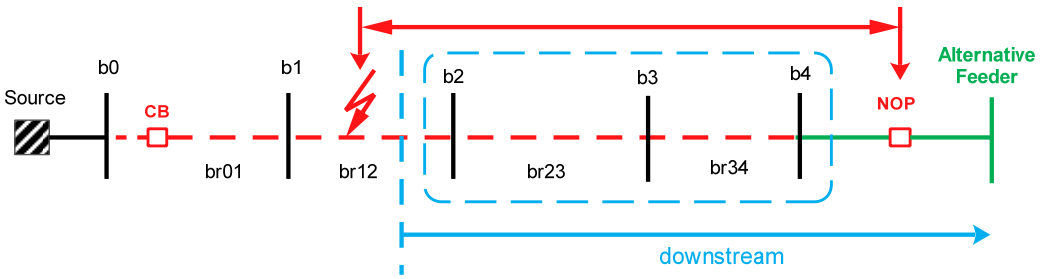

Figure 5.33 Busbars whose power cannot be restored by downstream load transfer

5.5.2.4 Transfer probability

When introducing upstream transfer and downstream transfer in previous sections, transferring the loads to another feeder can be performed only if the switches for performing the transfer exist. But it is restricted by more factors in the actual operation. For example, if the alternative feeder already has a high load and its capacity has insufficient headroom to accept all or part of the transferred loads, it cannot be used. So if the probability of performing the load transfer is considered, the restoration duration of the transferred loads is calculated by the following equation [113]:

$$\begin{aligned} &\text{restoration duration} \\ &\quad = (\text{restoration duration}|\text{transfer}) \\ &\quad \times P_1(\text{of transfer}) \\ &\quad + (\text{restoration duration}|\text{no transfer}) \\ &\quad \times P_2(\text{of no transfer}) \end{aligned} \tag{5.1}$$

For the load transfer algorithms introduced in this thesis, the probability of performing the load transfer (P_1) is assumed to be 100%.

5.6 Calculation of Reliability Indices

When the restoration simulation has been finished, the load points affected by a fault event are recorded. Meanwhile, the fault events that disrupt the power supply of a busbar are known so that the average restoration duration can be calculated. As shown in Figure 5.34(a), each busbar contains the information of all *n* fault events that interrupt its power supply. The information about each fault event shown in Figure 5.34(b) is:

1. Fault rate: λ_i
2. Restoration duration: t_i
3. Fault branch br_q
4. Restoration method of busbar b_j in fault event

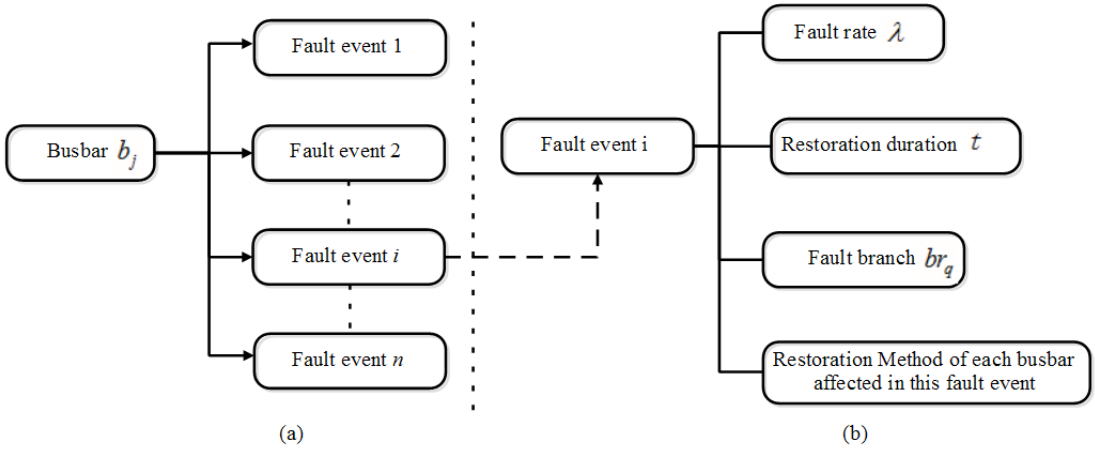

Figure 5.34 Relationship between the fault events and the affected busbars

A fault event needs to be recorded in the *CI* and *CML* calculations when its fault duration lasts 3 minutes or longer [26]. So any fault events whose fault duration is less than three minutes are not used in the following load point and system reliability indices calculation.

Load Point Indices

The load point indices need to be calculated first since the system indices are derived from the load point indices. As mentioned in section 4.3, the average fault rate λ_k, the average annual fault duration T_k and the average fault duration U_k are the main indices for load point k and their equations for a pure series network are shown as follows[107]:

$$\lambda_k = \sum_{i \in C} \lambda_i \ (int./yr.) \tag{5.2}$$

$$T_k = \sum_{i \in C} \lambda_i t_i \ (hr./yr.) \tag{5.3}$$

$$U_k = \frac{\sum_{i \in C} \lambda_i t_i}{\sum_{i \in C} \lambda_i} (hr.) \tag{5.4}$$

where:

λ_i: the fault rate of fault event *i*

t_i: the fault duration of fault event *i*

C: the set of the fault events interrupt the load point *k*

System Indices

When load point indices are calculated and the number of customers connected to each load point is known, the system indices *CI* and *CML* can be obtained as follows [26]:

$$CI = \frac{\sum_{k=1}^{n} \lambda_k N_k}{\sum_{k=1}^{n} N_k} \times 100[int./yr.cust] \tag{5.5}$$

$$CML = \frac{\sum_{k=1}^{n} T_k N_k}{\sum_{k=1}^{n} N_k} [min/yr] \tag{5.6}$$

where:

n: the number of load points

k: the load point *k*

N_k: the customer numbers at the load point *k*

λ_k: the average failure rate of the load point *k*

T_k: the average annual fault duration of the load point *k*

5.7 Validation of Reliability Evaluation Algorithm

The reliability evaluation algorithm introduced in previous sections of this chapter is implemented in DisOPT. In order to validate the accuracy of the algorithm and its implementation, two cases are studied in the following subsections.

5.7.1 Case 1: 10-Bus Network Model

The network model studied in this case is from the widely used text book on 'Reliability Evaluation of Power Systems' by Billinton and Allan [113]. Its network topology and the positions of protection devices and manual switches are shown in Figure 5.35. The reliability data are listed in Appendix A.3. The network model considers the effects of load transfer and protection devices on network reliability performance. In order to allow a comparison with the results given in [4], the assumptions made for this case study are: 1) Operation time of a normally open point

is zero; 2) Only branch faults are considered; 3) Operation failures of protection devices are ignored. The system indices report, bus indices report and report of each bus's fault events are shown in Table 5-1 and Table 5-2 and Figure 5.36 respectively. The results obtained using DisOPT are identical to those reported for the same network and set of component data as given in [97].

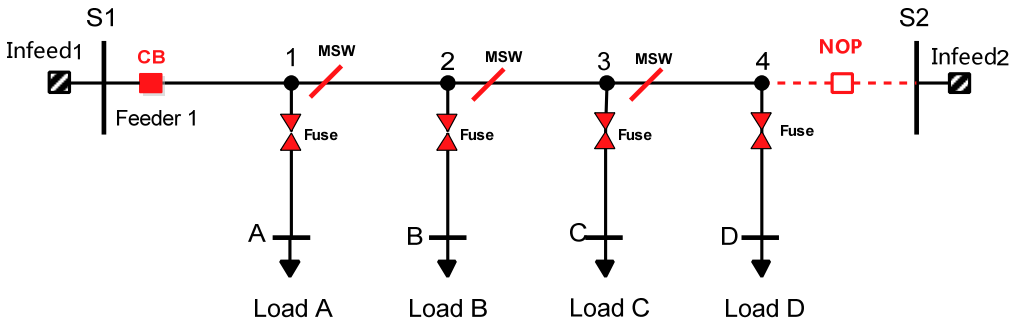

Figure 5.35 Network of case 1

The extra capability of the reliability evaluation developed here, which the method described in [97] does not address, is the ability to determine the restoration method of a fault-affected bus for a specific fault, as shown in Figure 5.37 and Figure 5.38. The groups used in these two figures are introduced in Table 5-3. Consideration of such phenomena would be expected to also represented by *CI* and *CML*, the relationships between *CI* and *SAIFI*, *CML* and *SAIDI* are: 1) $CI=100\times SAIFI$ and 2) $CML=60\times SAIDI$. As shown in Table 5-1 and Table 5-2, this is indeed what is observed.

Table 5-1 The report of system indices

Index	Value	Unit	Description
N	3000	-	Total number of customer served
CI	115.333	int./100cust.yr.	Customers interruptions
CML	107.7	mins./cust.yr.	Customer minutes lost
SAIFI	1.153	int/yr.cust.	System Average Interruption Frequency Index
SAIDI	1.795	h./yr.cust.	System Average Interruption Duration Index

Table 5-2 The report of load indices

Bus Name	Fault duration (h/yr)	Fault rate (int/yr)	Cust Num
A	1.5	1	1000
B	1.95	1.4	800
C	2.25	1.2	700
D	1.5	1	500

Fault Event	fault duration [h/yr] or [mins/yr]	fault rate [int/yr]	Recorded in CI/CML
Feede-S1-1			
[bus: A]	1.5	1	
1-[bran: S1-1]	4	0.2	Y
2-[bran: 1-2]	0.5	0.1	Y
3-[bran: 2-3]	0.5	0.3	Y
4-[bran: 3-4]	0.5	0.2	Y
5-[bran: 1-A]	2	0.2	Y
[bus: B]	1.95	1.4	
1-[bran: S1-1]	0.5	0.2	Y
2-[bran: 1-2]	4	0.1	Y
3-[bran: 2-3]	0.5	0.3	Y
4-[bran: 3-4]	0.5	0.2	Y
5-[bran: 2-B]	2	0.6	Y
[bus: C]	2.25	1.2	
1-[bran: S1-1]	0.5	0.2	Y
2-[bran: 1-2]	0.5	0.1	Y
3-[bran: 2-3]	4	0.3	Y
4-[bran: 3-4]	0.5	0.2	Y
5-[bran: 3-C]	2	0.4	Y
[bus: D]	1.5	1	
1-[bran: S1-1]	0.5	0.2	Y
2-[bran: 1-2]	0.5	0.1	Y
3-[bran: 2-3]	0.5	0.3	Y
4-[bran: 3-4]	4	0.2	Y
5-[bran: 4-D]	2	0.2	Y

Figure 5.36 Fault events of each load point

Fault Branch	Fault Duration(hours/mins)
Feede-S1-1	
S1-1	Circuitbreaker
Repair of fault	branch repair duration
1	4
A	4
DW MSW Transfer Buses	MSW switch time
4	[0.5] [OBr: 4-S2]
3	[0.5] [OBr: 4-S2]
2	[0.5] [OBr: 4-S2]
D	[0.5] [OBr: 4-S2]
C	[0.5] [OBr: 4-S2]
B	[0.5] [OBr: 4-S2]
1-2	Circuitbreaker
UP MSW Restore Buses	MSW switch time
1	0.5
A	0.5
Repair of fault	branch repair duration
2	4
B	4
DW MSW Transfer Buses	MSW switch time
4	[0.5] [OBr: 4-S2]
3	[0.5] [OBr: 4-S2]
D	[0.5] [OBr: 4-S2]
C	[0.5] [OBr: 4-S2]
2-3	Circuitbreaker
UP MSW Restore Buses	MSW switch time
2	0.5
1	0.5
B	0.5
A	0.5
Repair of fault	branch repair duration
3	4
C	4
DW MSW Transfer Buses	MSW switch time
4	[0.5] [OBr: 4-S2]
D	[0.5] [OBr: 4-S2]

Figure 5.37 The restoration time and method of buses affected by specific fault events - Part 1

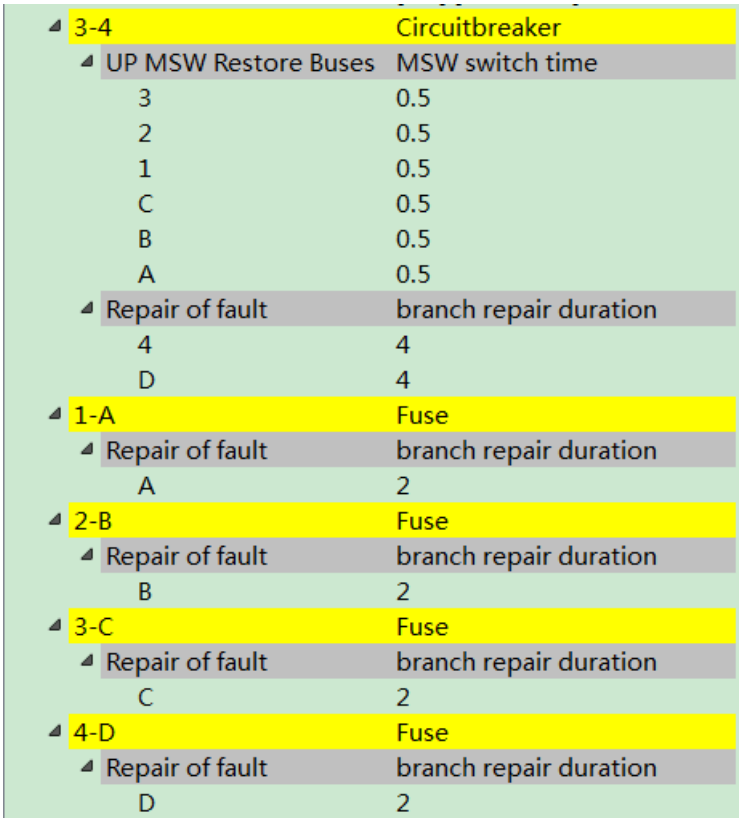

Figure 5.38 The restoration time and method of buses affected by specific fault events - Part 2

Table 5-3 The explanations of the each group

Group name	Restoration method
UP RCS Restore Buses	the upstream buses restored by remote controlled switch
UP MSW Restore Buses	the upstream buses restored by manual switch
ulNOP RCS Transfer Buses	the buses restored by upstream normally open point and remote controlled switch
ulNOP MSW Transfer Buses	the buses restored by upstream normally open point and manual switch
Repair of fault	the buses restored when the fault is repaired
DW MSW Restore Buses	the buses restored by downstream normally open point and manual switch
DW RCS Restore Buses	the buses restored by downstream normally open point and remote controlled switch

5.7.2 Case2: Reliability Evaluation of Network Model used in [142]

As shown in Figure 5.39, the network model used in this case study is published in [142]. Its reliability data are listed in Appendix A.4.1. This network has three circuit breakers CB1, CB2 and CB3. CB1 and CB2 each protect one feeder. When CB1 or

CB2 fails to operate, CB3 will operate to provide backup protection. Besides the circuit breakers, this network has six remote control switches RC1-RC6. The status of RC6 is normally open and others are normally closed. RC6 is connected to an alternative feeder so that load transfer can be performed. There is no restriction on load transfer in this case study.

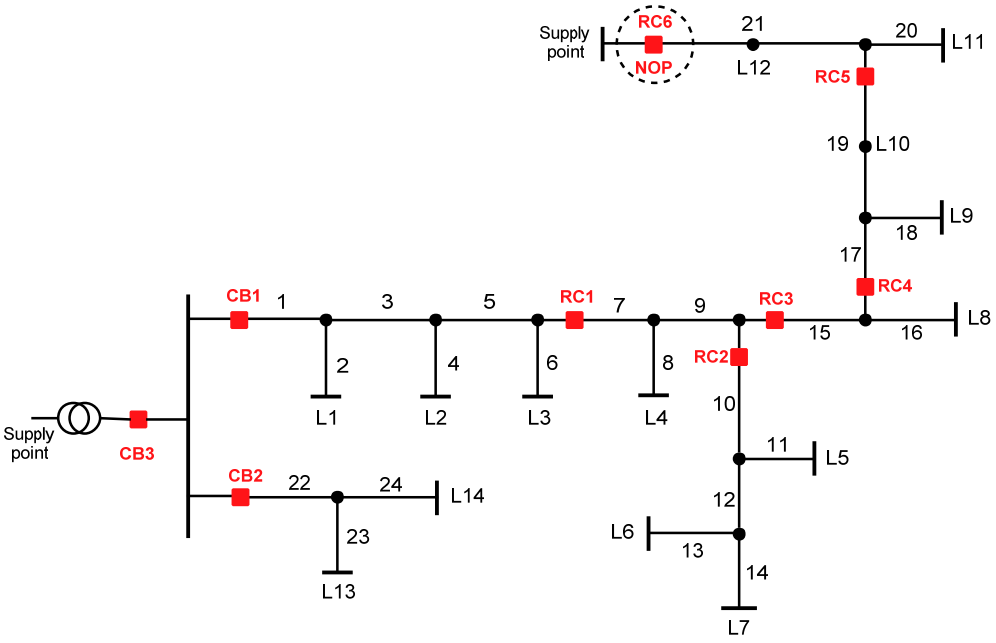

Figure 5.39 Example network used in Case 5 [142]

The load point indices and system indices calculated by DisOPT are shown in Table 5-4 and Table 5-5 respectively. Additionally, the output report of fault events for each load point is shown in Appendix A.4.2, and the restoration time and method of buses affected by specific fault events are shown in Appendix A.4.3.

Table 5-4 System indices calculated by DisOPT

Index	Value	Unit	Description
N	3000	-	Total number of customer served
CI	115.333	int./100cust.yr.	Customers interruptions
CML	107.7	mins./cust.yr.	Customer minutes lost
SAIFI	1.153	int/yr.cust.	System Average Interruption Frequency Index
SAIDI	1.795	h./yr.cust.	System Average Interruption Duration Index

Table 5-5 Load point indices calculated by DisOPT

Load point	Average fault rate (int/yr)	Average annual outage time (h/yr)
LP1	1.805	1.053
LP2	1.805	1.053
LP3	1.805	1.053
LP4	1.805	0.555
LP5	1.805	2.518
LP6	1.805	2.518
LP7	1.805	2.518
LP8	1.805	0.192
LP9	1.805	1.24
LP10	1.805	1.24
LP11	1.805	0.57
LP12	1.805	0.57
LP13	0.133	0.399
LP14	0.133	0.399

Table 5-6 and Table 5-7 compare these results calculated by DisOPT with [142]. According to Table 5-7, the load points' average fault rates are exactly the same, but the average annual outage times are different. The difference in the average annual outage causes the difference in SAIDI and SAIFI.

The main reason of difference in average annual outage time is as follows. DisOPT needs the exact switching time of each switch operation to calculate the restoration time of the buses affected by a fault. But [142] only indicates the total time duration for fault location, isolation, and service restoration. It does not provide the exact switching times of remote control switch and circuit breaker. In order to get the exact switching time of every switch necessary for DisOPT to run the calculation, the following method is applied: In [142], the time of restoration processing which includes fault location, isolation, and service restoration is 40 seconds. In the restoration processing, there are two switch operations: opening a remote control switch and closing a circuit breaker; these will normally be carried out sequentially. The operation times of these two devices are similar, so it is reasonable to consider the operation time of each device is equal to half of the total restoration time. Thus, the time for each switching action is 20 seconds which is 0.011111 hours ($\frac{40}{3600}/2 \approx$

0.011111). The results from DisOPT using these switching times are shown in Table 5.5 alongside a comparison with the results from [126]. The difference in results is small and is due to the rounding error in conversion of seconds to hours for DisOPT.

Table 5-6 Comparison of system indices between the DisOPT and Paper [142]

System indices	Result in DisOPT	Result in [142]	Error	Error %
SAIFI(int/yr.cust)	1.588	1.593	0.005	0.32
SAIDI(h/yr.cust)	1.143	1.142	0.001	0.088

Table 5-7 Compare the load indices results between DisOPT and Paper [142]

Load point	Average fault rate (int/yr)			Average annual outage time (h/yr)			
	Result in DisOPT	Result in [142]	Error	Result in DisOPT	Result in [142]	Error	Error%
LP1	1.805	1.805	0	1.053	1.059	0.006	0.57
LP2	1.805	1.805	0	1.053	1.059	0.006	0.57
LP3	1.805	1.805	0	1.053	1.059	0.006	0.57
LP4	1.805	1.805	0	0.555	0.582	0.027	4.64
LP5	1.805	1.805	0	2.518	2.535	0.017	0.67
LP6	1.805	1.805	0	2.518	2.535	0.017	0.67
LP7	1.805	1.805	0	2.518	2.535	0.017	0.67
LP8	1.805	1.805	0	0.192	0.212	0.02	9.44
LP9	1.805	1.805	0	1.24	1.25	0.01	0.80
LP10	1.805	1.805	0	1.24	1.25	0.01	0.80
LP11	1.805	1.805	0	0.57	0.59	0.02	3.39
LP12	1.805	1.805	0	0.57	0.59	0.02	3.39
LP13	0.133	0.133	0	0.399	0.399	0	0
LP14	0.133	0.133	0	0.399	0.399	0	0

5.8 Network Reliability Optimisation

The algorithm for network reliability optimisation is similar to the loss optimisation algorithm introduced in chapter 3. In loss optimisation, the target function is *P* loss. In reliability optimisation, there are three choices of target function: *CI* reward/penalty, *CML* reward/penalty and *CI*+*CML* reward/penalty. The equations of these improvement indices are shown in (5.7), (5.8) and (5.9) respectively.

$$TF_{CI} = (Ref_{CI} - Perf_{CI}) \times IR_{CI} \tag{5.7}$$

$$TF_{CML} = (Ref_{CML} - Perf_{CML}) \times IR_{CML} \tag{5.8}$$

$$TF_T = \sum_{obj=(CI,CML)} \left(Ref_{obj} - Perf_{obj}\right) \times IR_{obj} \quad (5.9)$$

where:

Ref_{Obj}: the object value (*CI*, *CML* or *CI*+*CML*) of a reference system state which contains topology, load and generation conditions

$Perf_{Obj}$: the object value (*CI*, *CML* or *CI*+*CML*) of a new system state which contains topology, load and generation conditions

IR_{Obj}: the object value (*CI*, *CML* or *CI*+*CML*)'s incentive rate

TF: target function

The reference value and incentive rate are very important since they are the weighted sums of *CI* and *CML*. Inappropriate weights affect the final output results of *CI*+*CML* reward/penalty. In this algorithm, the reference values of *CI* and *CML* are their values in the original network. The incentive rates of *CI* and *CML* can be set by user and the initially assumed value is equal to incentive rate set by Ofgem. The incentive rates are the weights of *CI* and *CI*+*CML* have obvious effects on target function TF_T shown in (5.9). This feature needs to be noticed when the incentive rates are set. According to Table 1-2, the incentive rates set by Ofgem are different for each DNO. Since this study is supported by SPEN, the initially assumed value used in this thesis is the value of SPEN in DPCR5.

Before starting to calculate the *CI* and *CML* of each topology, the load flow of the topology is calculated first. The topologies whose load flow failed, i.e. whose load flow cannot converge, are ignored in reliability optimisation. In some of the failed topologies, the loads are badly balanced among the feeders. The phenomenon indicates that the loads need to be well balanced among the feeders.

5.9 Loss and Reliability Optimisation

The target function of the combined loss and reliability optimisation is shown in (5.10).

$$\sum_{obj=(CI,CML,P\ Loss)} \left(Ref_{obj} - Perf_{obj}\right) \times IR_{obj} \tag{5.10}$$

There are two modes for optimizing both loss and reliability rewards, dependant on the order in which the objectives are considered. Details of these two modes are illustrated as follows:

1) Mode 1: optimize *P* loss first

As shown in Figure 5.40, the *M* output candidate network topologies are generated when the loss optimisation of the network is executed first. Then these *M* topologies are sorted according to the total rewards after the *CI* and *CML* rewards are calculated.

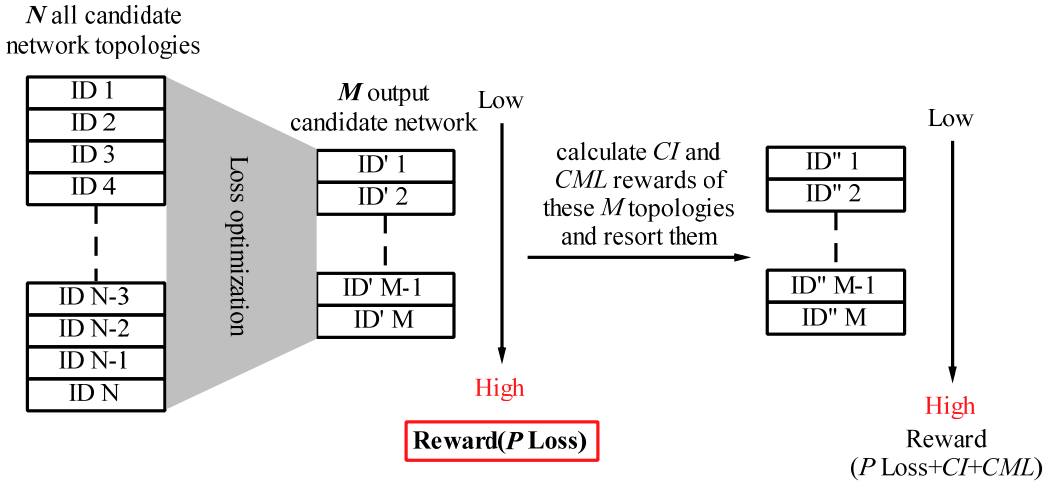

Figure 5.40 Mode 1 of loss and reliability rewards

2) Mode 2: optimize the reliability first

As shown in Figure 5.41, the *M* output candidate network topologies are generated when the reliability optimisation of the network is executed first. Then these *M* topologies are sorted according to the total rewards after loss rewards of them are calculated .

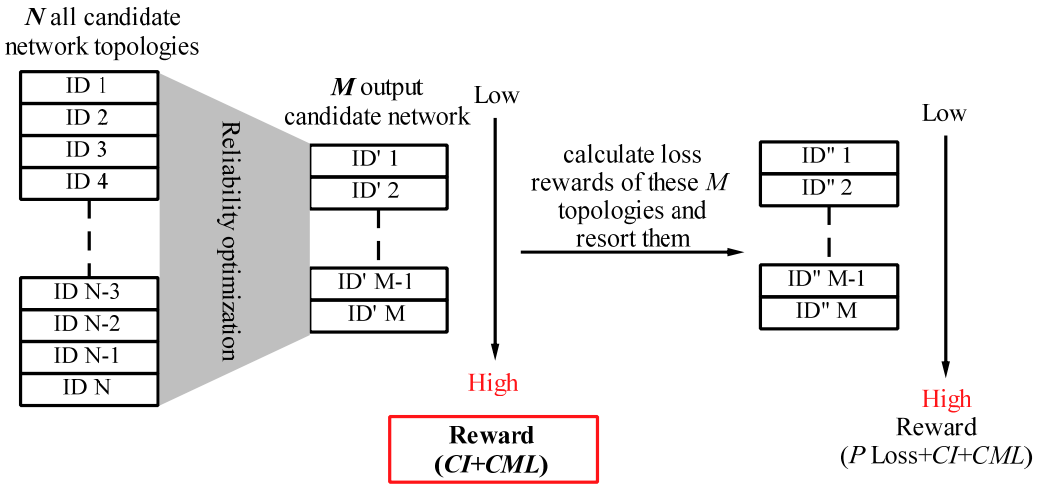

Figure 5.41 Model 2 of loss and reliability rewards

By optimising *P* loss and reliability in two modes, it can be seen which of them is more important and the effects of their weights on the final optimisation results.

5.10 Summary

This chapter has described the details of how to implement the reliability evaluation algorithm. This algorithm considers the effects of the network protection and network reconfiguration. Furthermore, a graphical user interface (GUI) has been built to provide a visual analysis environment. The performance of the described methods is evaluated in Chapter 6.

Chapter 6 Case Studies

The algorithm of *P* loss optimisation was introduced in Chapter 3. The algorithms of reliability evaluation, reliability optimisation and loss-reliability optimisation were introduced in Chapter 5. In this chapter, seven case studies of the application of these algorithms are presented in order to illustrate their performance and value.

In Case study 1, a realistic medium size 11kV distribution network model is examined using the *P* loss optimisation algorithm developed in this thesis. Case study 2 demonstrates how the long term *P* loss optimisation algorithm works by reference to a 16-bus network model. Case study 3 evaluates the effects of normally open points' switching time and service restoration using manual switches on system reliability performance. Case study 4 evaluates the impact of the number and positions of remote control switches on system reliability performance. Case study 5 demonstrates the optimisation of network configuration based on consideration of *CI* and *CML*. Case study 6 demonstrates an optimisation of network configuration based on combined incentives on *P* loss, *CI* and *CML* minimisation. Finally, case study 7 demonstrates the degree of sensitivity of such a combined optimisation to changes in the *P* loss incentive rate. So Case studies 1, 2, 5 are directed towards demonstrating the application of *P* loss optimisation, reliability evaluation and optimisation algorithms, Case studies 3, 4, 5, 7 demonstrate how to apply these algorithms to investigate aspects of distribution system's loss and reliability performance.

The last section of this chapter discusses the Case Study results and describes their significance for DNO engineering practice.

6.1 Case 1: *P* Loss Optimisation by Network Reconfiguration

A small network model was studied in Section 3.7.2 to validate the accuracy of the algorithm of P loss optimisation by network reconfiguration. In the case study described below, a realistic medium size network model is chosen to demonstrate the potential value of loss minimisation. In addition, some aspects of the performance of the algorithm are explored:

1. The effects of a PV edge's status (closed or open) on the computing time and

the final optimisation results

2. A comparison of two ways to calculate the network *P* loss: 1) considering the network as a whole; 2) considering the network as separated zones.

The network model used in this case study is shown in Figure 6.1, and is a small part of the actual SP Manweb 11kV distribution network. It has 4 infeeds, 25 feeders, 221 branches, 195 busbars and 191 loads. 15 normally open points need to be placed in the appropriate positions to make the network radial without unconnected loads. The branch and load data of this network are listed in Appendix A.2.1.

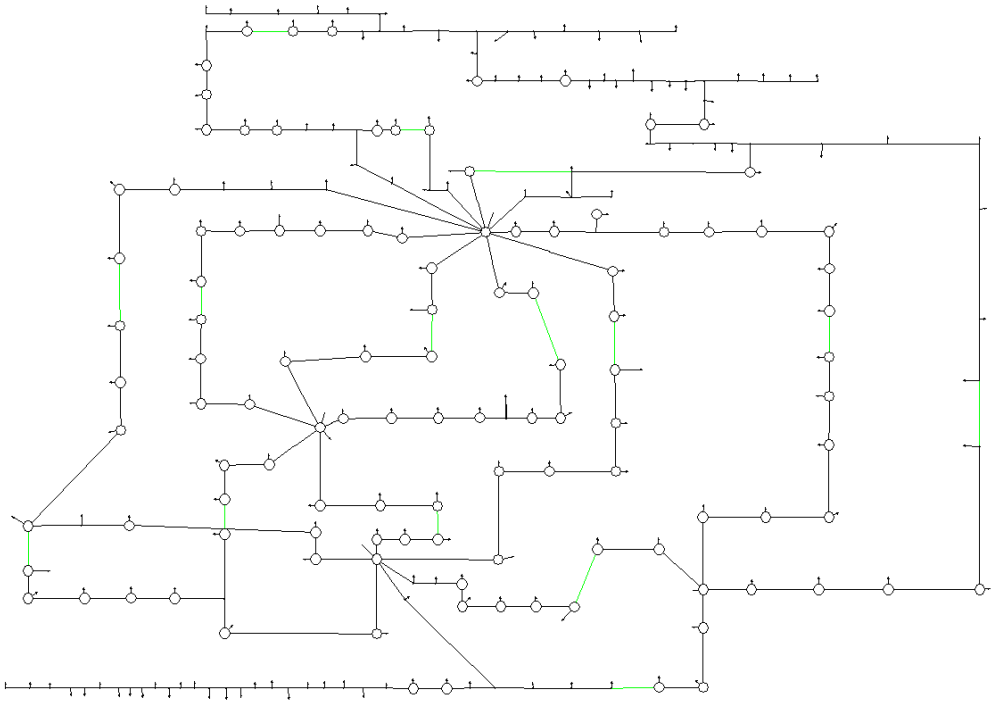

Figure 6.1 Manweb 11kV network model

Based on the zone division algorithm introduced in section 3.4.1, this network model can be divided into 10 zones. The number of feeders, branches and busbars in each is listed in Table 6-1. The concept of the PV edge was introduced in section 3.3. Based on whether PV edges can be opened, two spanning tree generation modes are defined: 1) PVC mode: PV edges (direct connections to infeeds) cannot be opened. 2) PVO mode: PV edges can be opened. The spanning trees of the network model in Figure 6.1 are generated in these two modes. The details of each mode are:

1) Mode 1: PVC

In this mode, the following 25 branches are closed in all generated spanning trees

of each zone: b114-b62, b114-b73, b114-b7, b114-b15, b114-b4, b114-b193 b47-b167, b47-b53, b47-b98, b47-b39, b47-b97, b132-b11, b132-b46, b132-b145, b132-b128, b132-b94, b132-b207, b132-b70, b132-b2, b132-b71, b106-b116, b106-b179, b106-b171 and b106-b63. Number of possible spanning tree topologies for each zone is shown in Table 6-1 and the time taken is 70.363 seconds.

2) Mode 2: PVO

Number of possible spanning tree topologies for each zone is shown in Table 6-1 and the time taken is 336.115 seconds.

Table 6-1 Manweb Network Topologies

Zone ID	Number of possible topologies		Number of feeders in the zone	Number of branches in the zone	Number of busbars in the zone
	Mode 1	Mode 2			
1	6	4	2	6	7
2	1345	788	4	29	29
3	11	9	2	11	12
4	12	10	2	12	13
5	7	5	2	7	8
6	9	7	2	9	10
7	9	7	2	36	37
8	10	8	2	10	11
9	16	14	5	17	18
10	29772	12219	5	84	82

When all spanning trees of the network model have been generated, the network topology with minimum *P* loss can be calculated. In order to observe the features of different output topologies, the number of output topologies is set to 10 in this case study. The output topologies are sorted from the lowest to the highest *P* loss. The *P* loss value of the initial network whose fifteen open branches are listed in Table 6-3 is 0.760 MW. This value is set as the reference value of *P* loss. The *P* loss optimisation results of the PVC and PVO modes shown in Table 6-2 are the same. The open branches of these ten output topologies are listed in Table 6-4. In Table 6-4, each cell coloured in dark grey means that this branch is open in the corresponding topology.

According to the results in Table 6-2, the reduction relative to the initial configuration shows that, as expected, losses can be significantly affected by

topology. However, for this case study, it can be seen that there are a number of different configurations that have approximately the same losses. This suggests a certain degree of flexibility that allows the network operator to choose among these configurations according to other criteria, such as network reliability performance.

Table 6-2 *P* loss optimisation results

TopoID	Original loss (MW)	Final loss (MW)	Saving	
			MW	%
1	0.7597	0.4830	0.2767	36.428
2	0.7597	0.4830	0.2767	36.428
3	0.7597	0.4831	0.2766	36.408
4	0.7597	0.4831	0.2766	36.408
5	0.7597	0.4832	0.2765	36.395
6	0.7597	0.4832	0.2765	36.395
7	0.7597	0.4832	0.2765	36.395
8	0.7597	0.4832	0.2765	36.395
9	0.7597	0.4833	0.2764	36.382
10	0.7597	0.4833	0.2764	36.382

Table 6-3 Open branches of the initial network topology

b110-b203	b122-b130	b124-b75	b150-b17
b69-b25	b9-b37	b10-b113	b133-b198
b18-b66	b184-b169	b206-b156	b210-b123
b139-b168	b36-b11	b43-b131	

Table 6-4 Open branches of output topologies

Open branch	Topo 1	Topo 2	Topo 3	Topo 4	Topo 5	Topo 6	Topo 7	Topo 8	Topo 9	Topo 10
b102-b164	■	■	■	■	■	■	■	■		
b10-b113	■	■	■	■	■	■	■	■	■	■
b133-b198	■	■	■	■	■	■	■	■	■	■
b139-b168	■	■	■	■	■	■			■	■
b161-b50	■	■			■	■	■	■	■	■
b164-b206									■	■
b166-b119	■	■	■	■	■	■	■	■	■	■
b168-b163							■	■		
b185-b68		■		■		■		■		■
b27-b91	■	■	■	■			■	■	■	■
b32-b121	■	■	■	■	■	■	■	■	■	■
b34-b24	■	■	■	■	■	■	■	■	■	■
b36-b11	■	■	■	■	■	■	■	■	■	■
b43-b131	■	■	■	■	■	■	■	■	■	■
b50-b117			■	■						
b68-b58	■		■		■		■		■	
b79-b104	■	■	■	■	■	■	■	■	■	■
b82-b95	■	■	■	■	■	■	■	■	■	■
b87-b210	■	■	■	■	■	■	■	■	■	■
b91-b26					■	■				

According to [55], a distribution network will have low *P* loss when its load is well distributed across it. Spanning trees generated in PVC mode make sure all feeders have at least some load connected. In general, their loads will be more evenly distributed than on networks that have one or more feeders without connected loads. The set of spanning trees generated in PVO mode includes all of the spanning trees generated in PVC mode. Though it cannot be concluded that the results of these two modes will always be the same for every network, the effects of ignoring the spanning trees that have feeders without connected loads (in PVO but not in PVC) can be evaluated which provide a potential way for users to reduce the number of candidate topologies.

It should be noted that the loss reduction in Table 6-2 is around 36% which is high. One reason of this phenomenon is: the original network has some loops since parts of SP Manweb network are unusual in Britain in being run in a partially meshed manner

instead of radial structure. They are designed that way and have protection installed accordingly. To give an initial case for comparison, these loops are opened by choosing branches randomly to make the network purely radial. If the original network is radial and the positions of normally open points are well chosen, the available loss reduction percentage should not be so high.

As introduced in section 3.6, the *P* loss values of a network topology are not exactly the same when considering it as a whole network and as separate zones when running the load flow. The sequences of output topologies are sorted by each topology's $P_{loss-TOG}$. In order to evaluate this effect on the output results, the differences ($\frac{P_{loss-TOG}-P_{loss-SEP}}{P_{loss-TOG}} \times 100\%$) of the first one hundred lowest *P* loss topologies' $P_{loss-TOG}$ and $P_{loss-SEP}$ are calculated and listed in Appendix A2.2. The output topologies are sorted from the lowest to highest *P* loss so the Topo ID *i* means the i^{th} lowest *P* loss topology. The percentage of difference between each topology's $P_{loss-TOG}$ and $P_{loss-SEP}$ is shown in Table 6-5.

Table 6-5 $P_{loss-SEP}$ and $P_{loss-TOG}$ of output topologies

TopoID	$P_{loss-TOG}$ (MW)	$P_{loss-SEP}$ (MW)	Difference (%)
1	0.4830	0.4803	0.0054
2	0.4830	0.4803	0.0054
3	0.4831	0.4804	0.0056
4	0.4831	0.4804	0.0056
5	0.4832	0.4806	0.0054
6	0.4832	0.4806	0.0054
7	0.4832	0.4806	0.0054
8	0.4832	0.4806	0.0054
9	0.4833	0.4807	0.0054
10	0.4833	0.4807	0.0054
11	0.4833	0.4807	0.0054
12	0.4833	0.4807	0.0054
13	0.4833	0.4805	0.0059

Though the difference between $P_{loss-SEP}$ and $P_{loss-TOG}$ is small, in a range between 0.005% and 0.0062%, the $P_{loss-SEP}$ values of output topologies when sorted from lowest to highest $P_{loss-TOG}$ are volatile instead of forming a constantly rising trend. For example, according to Table 6-5, both of $P_{loss-TOG}$ and $P_{loss-SEP}$ have increased

from topology TopoID 1 to topology Topo ID 12 which means the topology with minimum P loss remains same either the output topologies sorted by $P_{loss-TOG}$ or $P_{loss-SEP}$ for this case study. But when the network is changed from topology TopoID 12 to topology Topo ID 13, the $P_{loss-SEP}$ reduces when it should have increased in correspondence with $P_{loss-TOG}$.

6.2 Case 2: Load Curve *P* Loss Optimisation

The algorithm of long period P loss optimisation by network reconfiguration is introduced in Section 3.8. In this case study, the application of this algorithm is demonstrated. The network model used in this case study is shown in Figure 6.2 [68]. The line and load data of this 33-Bus network are listed in Appendix A.6. Based on the load profiles in [104], the load scaling factors at 9 time points through a day in Table 6-6 are applied on this model to perform the long period P loss optimisation.

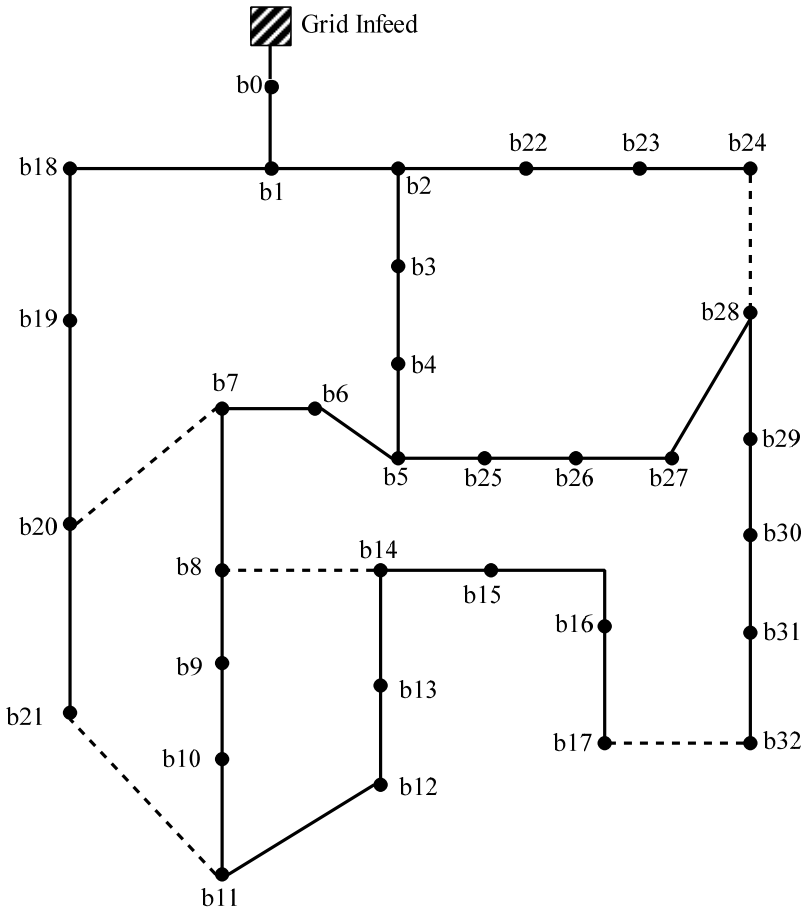

Figure 6.2 33-Bus network model [68]

Table 6-6 Load factors at each time point

Time point	0:30	3:00	5:30	8:00	13:00
Load factor	0.4	0.2	0.2	0.5	0.6

Time point	15:30	18:00	20:30	23:00
Load factor	0.5	0.9	0.8	0.7

Table 6-7 The results of long period *P* loss optimization

Time point	**23:00**	**0:30**	**3:00**	**5:30**	**8:00**
Original loss (MW)	0.083	0.067	0.067	0.095	0.11
New loss (MW)	0.058	0.046	0.046	0.067	0.077
Topology changed					
Open Branches					
14-13					
27-28					
30-31					
6-7					
8-9					
31-32					
24-28					
Time point	**13:00**	**15:30**	**18:00**	**20:30**	
Original loss (MW)	0.095	0.172	0.148	0.128	
New loss (MW)	0.067	0.12	0.104	0.0898	
Topology changed					
Open Branches					
14-13					
27-28					
30-31					
6-7					
8-9					
31-32					
24-28					

The results of long term *P* loss optimisation are shown in Table 6-7. In this table, a coloured cell in the row of branch's name means that this branch is open at the corresponding time points; a coloured cell in the "Topology changed" row means that the network topology at the corresponding time point is different from the topology at the previous time point. As can be seen from this table, the network configuration changes during the day. In this case, 4 different configurations are used,

according to the loading condition, with a total energy saving (assuming that each condition lasts until a new load factor is applied) of 0.783MWh. However, if a DNO knows only the total loading for a particular primary sub-network and not the individual loads at, for example, each secondary substation, it would not be possible for this optimisation to be carried out in that sub-network. This would be the case currently for DNOs in Britain that, to date, lack data on relative loadings of each secondary substation at different points in time. However, a number of current 'Low Carbon Networks Fund' (LCNF) projects are seeking to gain greater information on the loading of networks at and below the secondary substation level [170-172].

6.3 Case 3: The Effect of Switching Time Assumptions on the Apparent System Reliability Performance

Two network models were studied in Sections 5.7.1 and 5.7.2 to validate the algorithm of reliability evaluation developed in this thesis. For the case study in Section 5.7.1, the switching time of a NOP was set to zero which is not realistic. For the case study in Section 5.7.2, the use of manual switches to restore load was not considered. However, on actual distribution networks in Britain, switching time for an NOP is not zero and depends on whether remote control facilities are available. In many cases, they are not and manual actions are required which can take a significant time. In this section, two cases are studied to evaluate the effects of considering the switch time of NOP and the use of manual switches for service restoration on system reliability performance.

Case 3a: Evaluation of the Effect of Switching Time of NOPs on System Reliability Performance

In the network model and data described in Section 5.7.1, an NOP was treated as a manual switch and its switching time was ignored. The switching time of other manual switches in this model was taken as 0.5 hours. In order to evaluate the effects of considering the actual switching time of NOPs on system reliability performance, three scenarios are defined: 1) Scenario 3a-1: the switching time of NOPs is zero which is the same as in section 5.7.1; 2) Scenario 3a-2: the switching time of NOPs is 0.5 hours. 3) Scenario 3a-3: the switching time of NOPs is 1 hour. The network

model used in Section 5.7.1 is reused in this case study, and all other data are the same except the switching time of NOPs. The results of Scenario 3a-1, Scenario 3a-2 and Scenario 3a-3 are compared in Table 6-8. *SAIFI* and average fault rates of each load points remain the same. *SAIDI* and average fault durations of each load points are changed. Compared with results in Scenario 3a-1, the *SAIDI* in Scenario 3a-2 is increased by 6.2%; the *SAIDI* in 3a-3 is increased by 12.4%.

Table 6-8 Results comparison

Load point	Fault duration(h/yr)		
	Scenario 3a-1	Scenario 3a-2	Scenario 3a-3
A	1.5	1.5	1.5
B	1.95	2.05	2.15
C	2.25	2.4	2.55
D	1.5	1.8	2.1
System indices			
SAIDI	1.795	1.907	2.018

Case 3b: Reliability Evaluation of the Network Model used in [142] by Considering the Operation of Manual Switches

The network model used in Section 5.7.2 is reused in this case study. When this network model was studied in [142], manual switches were not used for service restoration under fault conditions. In order to evaluate the impact of manual switch operation on system reliability performance, it is assumed here that all branches of the network model used in Section 5.7.2 can be switched out by manual switches installed on them. Furthermore, these manual switches can be used to restore the service under fault condition. So compared with the model used in Section 5.7.2, all data of the network used in this case study remain the same except for the assumption that all branches can be switched out manually. Besides considering the operation of remote control switches in service restoration by network reconfiguration, the operation of manual switches is considered as well. The manual switching time of remote control switches given in [142] is 1 hour when the remote control process fails. So the switch time of manual switch is assumed to be 1 hour in this case study. The SAIFI and SAIDI calculated by DisOPT are 1.588int/yr.cust. and 0.672h./yr.cust. respectively. In order to evaluate the effects of using manual switches for service restoration on system reliability performance, two scenarios are

defined: 1) Scenario 3b-1: do not use manual switches for service restoration; 2) Scenario 3b-2: use manual switches for service restoration. Comparing with the results in Scenario 3b-1, the value of SAIFI remains the same while the value of SAIDI reduces from 1.143h./yr.cust. to 0.672h./yr.cust., which is 17.8% lower. The fault rate of each load point in Scenario 3b-1 and Scenario 3b-2 is the same. The difference of each load point's average fault duration in these two scenarios is shown in Table 6-9.

Table 6-9 Average fault duration and difference percentage of each load point in Scenario 3a-1 and Scenario 3b-2

Load Point	Average fault duration(hours/year)		
	Scenario 3b-1	Scenario 3b-2	Difference (%)
LP1	1.053	0.501	52.4
LP2	1.053	0.463	56.1
LP3	1.053	0.501	52.4
LP4	0.555	0.349	37.1
LP5	2.518	1.442	42.7
LP6	2.518	1.276	49.3
LP7	2.518	1.724	31.5
LP8	0.193	0.128	33.3
LP9	1.240	0.766	38.2
LP10	1.240	0.434	65.0
LP11	0.573	0.407	29.0
LP12	0.573	0.215	62.5
LP13	0.399	0.311	22.1
LP14	0.399	0.355	11.0

Taking a fault occurred on branch 2, for example, if manual switches are not used to restore service under fault conditions, the power supplies of customers on buses L1, L2, L3 cannot be restored until the fault on branch 2 has been repaired. But if branch 2 has a manual switch, the power supplies of customers on buses L2 and L3 can be restored before the fault has been repaired by opening the manual switch on branch 2. The results of this case study indicate that using manual switches for service restoration under fault conditions can contribute to reducing the number of minutes lost for customers at particular locations, and thus improve the system indices in a significant way, even though the switching time of a manual switch is much longer

than that of a remote control switch. In contrast to what is done in [126], the use of manual switches should therefore not be neglected in a reliability assessment.
The results of Case 3a and Case 3b indicate that the influence of switching times on system reliability performance is significant – restoration time can be reduced by between 10% and 65% depending on fault location – and should be correctly modelled.

6.4 Case 4: Evaluation of the Effects of Remote Control Switches on Reliability Performance

This case study evaluates the effects of different numbers and installation positions of remote control switches. Use of a reliability assessment facility in which switching times are accurately represented for different types of device allows different network design options to be compared in terms of their effect on both system reliability and the reliability of supply at individual load points. This, in turn, can tell a DNO where to place remote control switches. This is particularly important for a network design engineer in helping identify investments in remote control facilities that have an overall positive cost-benefit.

As shown in Figure 6.3, the network model used in this case study is a small part of the Scottish Power Manweb 11kV distribution network. Since the original network model only has branch impedance and load demand data, reasonable assumptions about reliability data, e.g. fault rate, customer numbers, and positions of protection devices, etc., need to be made for reliability evaluation. The assumptions for this model are:

1. Assuming the demand value of an average size UK household is 1.5kW [104], the number of customers at each load point is rounded to the value of total load point demand divided by 1.5kW.
2. Since this is an urban network, all branches are assumed to be underground cables.
3. Since 185mm^2 11kV 3-core XLPE cable is widely used in the SPEN 11kV distribution network and its resistance is 0.21Ω/km [173], the cable length is rounded to the value of cable resistance divided by 0.21Ωm/km.

4. The failure rate and mean time to repair of a cable are assumed to be 0.0122 int/km.yr. and 30 hours respectively [152].
5. The switching time of a manual switch is 2 hours [152], the switching times of circuit breakers and fuses are zero, the switching time of remote control switches is 1 minute ($\approx 0.017\ hour$). The repair time of a fuse is 1.1 hours [152].
6. Each branch can be switched out manually and the switching time is 2 hours.

The other data of this simulation model are listed in Appendix A.4.1. The protection system of this network is: 1) circuit breakers CB1, CB2 and CB3 are installed on branches b0(s)-b55, b0(s)-b52 and b0(s)-b1 respectively for feeder protection; 2) fuses F1, F2 and F3 are installed on branches b15-b16, b42-b43 and b33-b34 respectively for lateral protection. Two normally open points NOP1 and NOP2 are placed on branches b53-b54 and b24-b23 respectively.

In order to analyse the effects of different remote control switch installation scenarios on system reliability performance, three scenarios are studied: 1) Without remote control switches, only using manual switches to restore the service; 2) With 3 remote control switches, one at the middle point of each feeder; 3) With 7 remote control switches, one at each quarter point of each feeder. In scenarios 2 and 3, both remote control switches and manual switches are used to restore the service under fault conditions. The details and performance indices of these three scenarios are presented below.

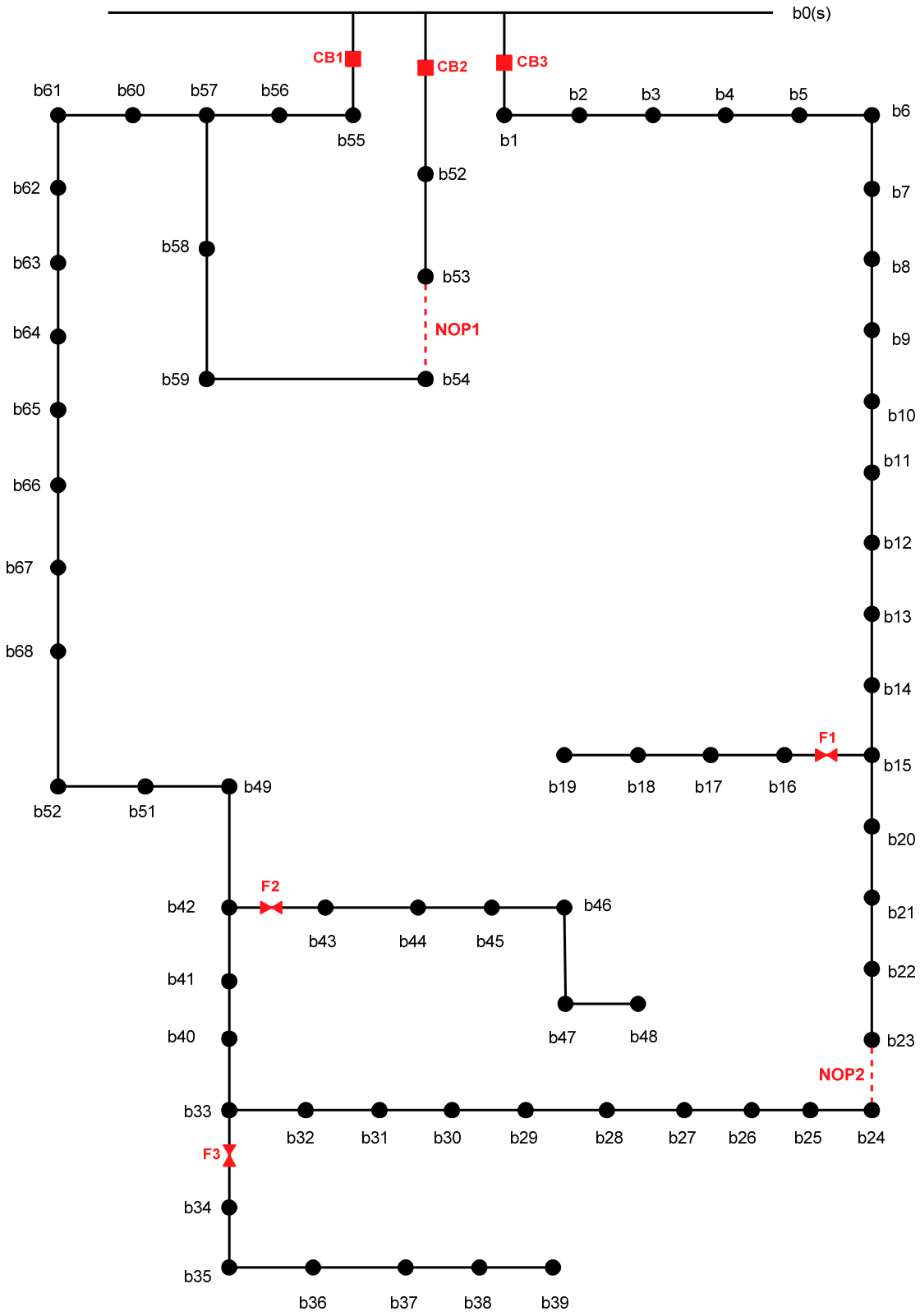

Figure 6.3 Network diagram of model used in Case 4

Scenario 4-1: No remote control switches

In this scenario, each branch can be opened by the manual switch installed on it. Since there are no remote control switches, only manual switches are used to restore the service under fault conditions. The system indices calculated by DisOPT are shown in Table 6-10.

Table 6-10 The system indices of Scenario 4-1

Index	Value	Unit	Description
N	3075	-	Total number of customer served
CI	28.153	int./100cust.yr.	Customers interruptions
CML	56.428	mins./cust.yr.	Customer minutes lost
SAIFI	0.282	int/yr.cust.	System Average Interruption Frequency Index
SAIDI	0.940	h./yr.cust.	System Average Interruption Duration Index

Scenario 4-2: Place remote control switches at the middle point

Customer numbers on each feeder are approximately equal on either side of the middle point. So, nearly half of the customers on the feeder can be restored by operation of the remote control switch after the occurrence of a fault. In this scenario, three remote control switches RC1, RC2, RC3 are installed on branches b64-b65, b53-b54 and b23-b24 respectively. The system indices calculated by DisOPT are shown in Table 6-11.

Table 6-11 The system indices of Scenario 4-2

Index	Value	Unit	Description
N	3075	-	Total number of customer served
CI	28.153	int./100cust.yr.	Customers interruptions
CML	27.971	mins./cust.yr.	Customer minutes lost
SAIFI	0.282	int/yr.cust.	System Average Interruption Frequency Index
SAIDI	0.466	h./yr.cust.	System Average Interruption Duration Index

Scenario 4-3: Place remote control switches at the quarter points

The customers on the feeder are divided approximately equally among the four quarters. In this scenario, seven remote control switches RC1, RC2, RC3, RC4, RC5, RC6, and RC7 are installed on branches b64-b65, b53-b54, b23-b24, b61-b62, b65-b66, b12-b13 and b32-b33 respectively. The system indices calculated by DisOPT are shown in Table 6-12.

Table 6-12 The system indices of Scenario 4-3

Index	Value	Unit	Description
N	3075	-	Total number of customer served
CI	28.153	int./100cust.yr.	Customers interruptions
CML	17.156	mins./cust.yr.	Customer minutes lost
SAIFI	0.282	int/yr.cust.	System Average Interruption Frequency Index
SAIDI	0.286	h./yr.cust.	System Average Interruption Duration Index

Comparing Scenario 4-2's results with Scenario 4-1's, the results of *CI* and *SAIFI* remain the same but the results of *CML* (reduced from 56.428mins./cust.yr. to 27.971mins./cust.yr.) and *SAIDI* (reduced from 0.940h./yr.cust. to 0.466h./yr.cust.) are 101.74% lower. It can be concluded that the installation of remote control points can improve the *CML* significantly.

By comparing Scenario 4-2's results with Scenarios 4-3's, the results of *CI* and *SAIFI* remain the same but the results of *CML* (reduced from 27.971mins./cust.yr. to 17.156mins./cust.yr.) and *SAIDI* (reduced from 0.466h./yr.cust. to 0.286h./yr.cust.) are 38.67% lower. Though a higher density of remote control switches can improve *CML*, a DNO needs to consider the cost of installing new remote control switches against the reward can be gained from the *CML* improvement. However, the results of a reliability analysis can help DNOs to make decisions on remote switch installation by comparing the cost of installing new remote control switches with the extra CML rewards awarded by Ofgem. For example, when the cost of installing remote control switches is *C* and the payback period is *P,* if the annual *CML* benefit is significantly larger than C/P, it is worth making the investment in installing new remote control switches [174].

6.5 Case 5: Reliability Optimisation

The algorithm of reliability optimisation was introduced in Section 5.8. The algorithm optimises the combination of *CI* and *CML*. The weights of *CI* and *CML* are their incentive rates set by Ofgem. In this case study, the reliability optimisation algorithm is illustrated and the effect of *CI* and *CML* on each other is discussed.

The network model used in Section 6.4 is reused in this section. The number of output topologies is set to ten. The candidate output topologies generated by DisOPT

are sorted from highest to lowest *CI*+*CML* rewards. The output results are the ten highest *CI*+*CML* rewards. The *CI* and *CML* values of the initial network topology are listed in Table 6-13 and are set as reference values. The open branches of the output topologies are listed in Table 6-14. The incentive rates of *CI* and *CML* are 90k£/*CI* and 330k£/*CML* respectively. The optimisation results of output topologies calculated by DisOPT are shown in Table 6-15. "R/P" in Table 6-13 and Table 6-15 means Reward/Penalty. According to the results, the best topology is that whose *CI* is 24.051int./100cust.yr. and *CML* is 16.163mins./cust.yr.. Comparing to the original values of *CI* and *CML* which are 28.153int./100cust.yr. and 17.156mins./cust.yr. respectively, this topology reduces *CI* by 17.06% and *CML* by 5.79%. Under the current value of the incentive scheme [24] and assuming that failure and rates and restoration times are constant through a year of operation, this would equate to an average of 0.697m£ per year.

Table 6-13 The system reliability indices of initial topology

Initial Topology				
CI (int./100cust.yr.)	*CML* (mins./cust.yr.)	*CI* R/P (m£)	*CML* R/P (m£)	*CI*+*CML* R/P (m£)
28.153	17.156	0	0	0

Table 6-14 Open branches of output topologies in this case

Topo ID	Open branches	
1	b33-b32	b57-b58
2	b24-b23	b57-b58
3	b33-b32	b56-b57
4	b33-b32	b58-b59
5	b33-b32	b55-b56
6	b24-b23	b56-b57
7	b33-b32	b59-b54
8	b0(s)-b55	b33-b32
9	b24-b23	b58-b59
10	b33-b32	b53-b54

Table 6-15 The report of reliability optimisaiton

Topo ID	New				
	CI **(int./100cust.yr.)**	***CML*** **(mins./cust.yr.)**	***CI*** **R/P (m£)**	***CML*** **R/P (m£)**	***CI+CML*** **R/P (m£)**
1	24.051	16.163	0.369	0.328	0.697
2	25.075	16.016	0.277	0.376	0.653
3	26.085	15.955	0.186	0.396	0.583
4	24.704	16.859	0.31	0.098	0.409
5	26.452	16.386	0.153	0.254	0.407
6	28.515	15.824	-0.033	0.44	0.407
7	25.001	16.911	0.284	0.081	0.365
8	26.652	16.606	0.135	0.182	0.317
9	26.227	16.854	0.173	0.1	0.273
10	25.676	17.217	0.223	-0.02	0.203
Topo ID	**Change**				
	CI **(int./100cust.yr.)**	***CML*** **(mins./cust.yr.)**	***CI*** **R/P (m£)**	***CML*** **R/P (m£)**	***CI+CML*** **R/P (m£)**
1	4.102	0.994	0.369	0.328	0.697
2	3.078	1.14	0.277	0.376	0.653
3	2.067	1.201	0.186	0.396	0.583
4	3.449	0.297	0.31	0.098	0.409
5	1.701	0.77	0.153	0.254	0.407
6	-0.362	1.332	-0.033	0.44	0.407
7	3.152	0.245	0.284	0.081	0.365
8	1.501	0.551	0.135	0.182	0.317
9	1.926	0.302	0.173	0.1	0.273
10	2.477	-0.06	0.223	-0.02	0.203

As can be seen in Figure 6.4 which shows the variation trends of *CI* and *CML*, the variation trends of *CI* and *CML* are not always the same when the topology is changed. For example, when the network topology is changed from Topo 4 to Topo 3, the *CI* increases from 24.704 to 26.085 but the *CML* decreases from 16.859 to 15.955.

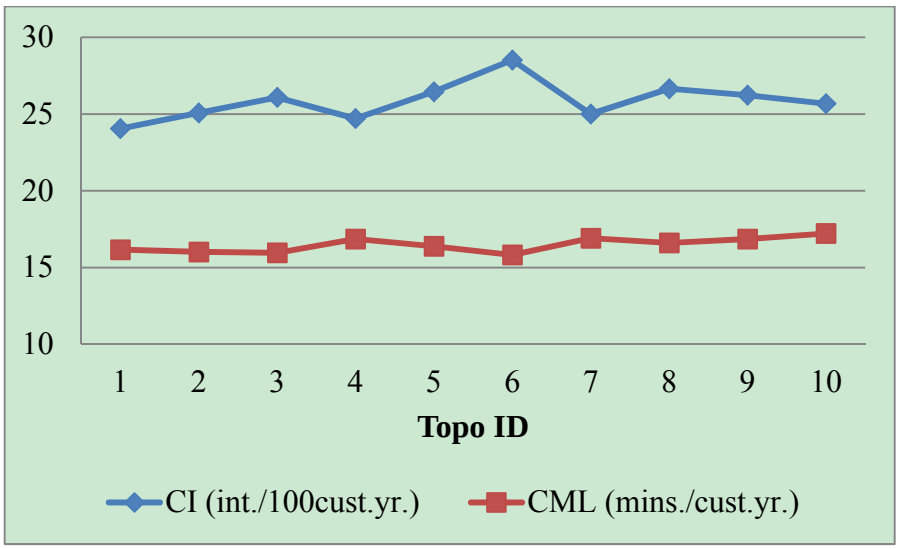

Figure 6.4 The variation trend of *CI* and *CML*

The variation trends of *CI*, *CML* and *CI+CML* rewards are shown in Figure 6.5. From this Figure, it can be seen that the variation trends of *CI+CML* rewards depends on both of the variation trends of *CI* and *CML* rewards. So the network's *CI* and *CML* performances need to be considered together.

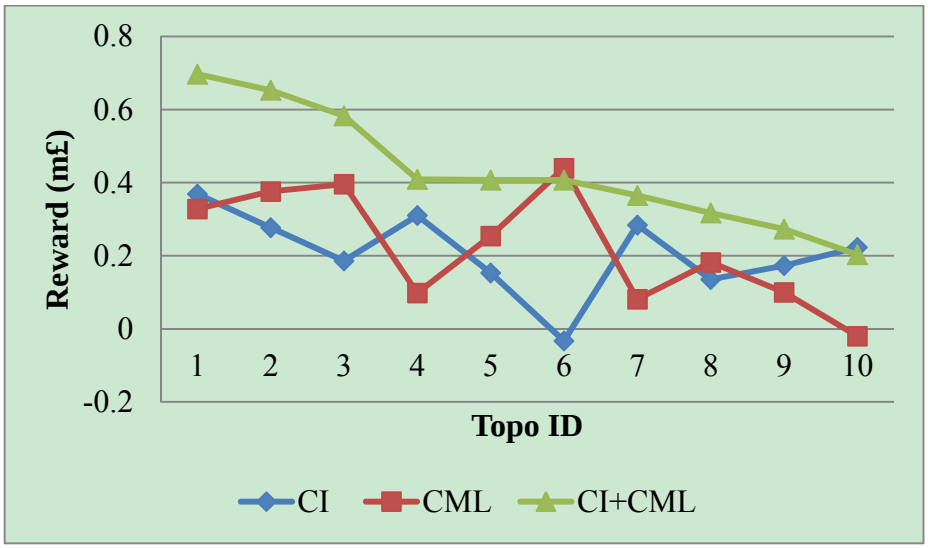

Figure 6.5 The variation trend of *CI*, *CML* and *CI+CML* rewards

6.6 Case 6: Optimisation both of Loss and Reliability by Network Reconfiguration

Based on the loss-reliability optimisation introduced in Section 5.9, this section studies the network behaviour when both loss and reliability are optimised. The mutual impact of loss and reliability is discussed.

The network model used in Section 6.5 is reused in this case study. The positions of normally open points are on branches b24-b23 and b53-b54**.** As introduced in Section 5.9, the function of optimisation both of loss and reliability has two modes: 1) Loss-Reliability: reliability is optimised first, then *P* loss of the candidate topologies is optimised. 2) Reliability-Loss: *P* loss is optimised first, then reliability of the candidate topologies is optimised. Both of these two modes are studied in this case study. The candidate output topologies generated by DisOPT are sorted from highest to lowest *P* loss+*CI*+*CML* rewards. The results of the first ten highest *P* loss+*CI*+*CML* rewards topologies will be outputted. The *P* loss, *CI* and *CML* values of initial network topology are listed in Table 6-16 and are set as reference values.

Table 6-16 The *P* loss, *CI, CML* values of initial topology

Initial Topology						
P loss			*CI*		*CML*	
MW	MWh	Reward (m£)	Performance (int./100.cust.yr.)	Reward (m£)	Performance (mins./cust.yr.)	Reward (m£)
0.235	2054.980	0	28.153	0	17.156	0

The incentive rates of *P* loss, *CI* and *CML* are 60£/MWh, 90k£/*CI* and 330km£/*CML* respectively [24]. The two modes of optimisation results calculated by DisOPT are shown as follows:

- **Mode 1: Loss-Reliability Optimisation**

  In this mode, the duration for loss calculation and reliability evaluation is one year. The load is assumed to be constant over that period of time. The positions of normally open points in the output topologies are listed in Table 6-17. The loss-reliability optimisation results calculated by DisOPT are shown in Table 6-19. In this model, the first *N* (output topology number, defined by user) lowest *P* loss topologies are generated first. The *CI* and *CML* of these *N* topologies are then calculated and the topologies are re-sorted from the highest to the lowest *P* loss+*CI*+*CML* rewards. So the Topo ID *i* in the Table 6-17, Table 6-18 and Table 6-19 is the i^{th} lowest *P* loss (or highest *P* loss reward) topology. In the tables, topologies are listed in order of total rewards.

Table 6-17 The positions of normally open points in output topologies in mode 1

Topo ID	Open branches	
6	b33-b32	b57-b58
2	b30-b29	b57-b58
3	b29-b28	b57-b58
4	b28-b27	b57-b58
1	b31-b30	b57-b58
5	b32-b31	b57-b58
8	b30-b29	b58-b59
9	b29-b28	b58-b59
10	b28-b27	b58-b59
7	b31-b30	b58-b59

The rewards of output topologies in mode 1 are listed in Table 6-18. From this table, it can be concluded that: 1) The *CI*+*CML* reward may be worse than in the initial topology when *P* loss is improved. For example, except the topology whose TopoID is 6, the *CI*+*CML* reward of the other nine topologies are negative which indicates these topologies' *CI*+*CML* reward are worse than the initial network topology; 2) The topology that has the minimum *P* loss may not have the best *CI*+*CML* reward. For example, the topology whose Topo ID is 1 has the minimum *P* loss, but it has the 5th highest *CI*+*CML* reward.

Table 6-18 The rewards of output topologies in mode 1

Topo ID	Total Reward		
	P loss+*CI*+*CML* reward (m£)	*CI*+*CML* reward (m£)	*P* reward (m£)
6	0.836	0.805	0.031
2	-4.164	-4.198	0.033
3	-4.168	-4.201	0.033
4	-4.177	-4.21	0.032
1	-4.196	-4.229	0.033
5	-4.25	-4.281	0.031
8	-4.492	-4.523	0.031
9	-4.502	-4.532	0.03
10	-4.518	-4.547	0.03
7	-4.522	-4.552	0.031

Table 6-19 The report of Loss-Reliability optimisation in mode 1

Topo ID	*P* loss					
	New			Change		
	MW	MWh	Reward(m£)	MW	MWh	Reward(m£)
6	0.176	1539.477	0.031	0.059	515.504	0.031
2	0.171	1500.114	0.033	0.063	554.867	0.033
3	0.172	1503.14	0.033	0.063	551.841	0.033
4	0.173	1513.852	0.032	0.062	541.129	0.032
1	0.171	1500.114	0.033	0.063	554.867	0.033
5	0.175	1534.284	0.031	0.059	520.697	0.031
8	0.176	1545.476	0.031	0.058	509.505	0.031
9	0.177	1549.292	0.03	0.058	505.689	0.03
10	0.178	1561.625	0.03	0.056	493.356	0.03
7	0.176	1545.476	0.031	0.058	509.505	0.031

Topo ID	*CI*			
	New		Change	
	Performance (int./100.cust.yr.)	Reward (m£)	Performance (int./100.cust.yr.)	Reward (m£)
6	24.051	0.369	4.102	0.369
2	23.882	0.384	4.271	0.384
3	24.058	0.369	4.095	0.369
4	24.175	0.358	3.978	0.358
1	23.963	0.377	4.19	0.377
5	22.901	0.473	5.252	0.473
8	24.757	0.306	3.396	0.306
9	24.97	0.286	3.183	0.286
10	25.121	0.273	3.032	0.273
7	24.816	0.3	3.337	0.3

Topo ID	*CML*			
	New		Change	
	Performance (mins./cust.yr.)	Reward (m£)	Performance (mins./cust.yr.)	Reward (m£)
6	15.835	0.436	1.322	0.436
2	31.041	-4.582	-13.885	-4.582
3	31.004	-4.57	-13.848	-4.57
4	30.998	-4.568	-13.842	-4.568
1	31.115	-4.606	-13.959	-4.606
5	31.562	-4.754	-14.406	-4.754
8	31.788	-4.828	-14.631	-4.828
9	31.757	-4.818	-14.601	-4.818
10	31.763	-4.82	-14.606	-4.82
7	31.861	-4.853	-14.705	-4.853

The variation trends of *CI*, *CML*, *CI+CML* rewards are shown in Figure 6.6. The variation trends of *P* loss+*CI*+*CML* and *CI*+*CML* rewards are shown in Figure 6.7. In Figure 6.6, the shape of the *CML* reward's variation is very similar to the shape of *CI*+*CML* reward's variation. In Figure 6.7, the shapes of two variation trends are almost the same. So, in mode 1, the *CML* reward makes the major contribution to the total rewards of *P* loss, *CI* and *CML*.

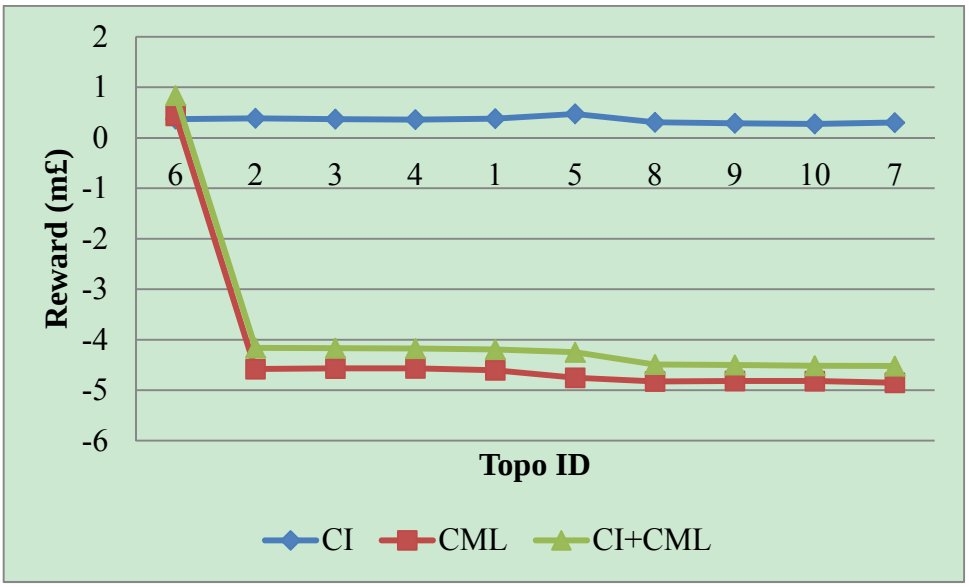

Figure 6.6 The variation trends of *CI*, *CML* and *CI+CML* rewards in mode 1

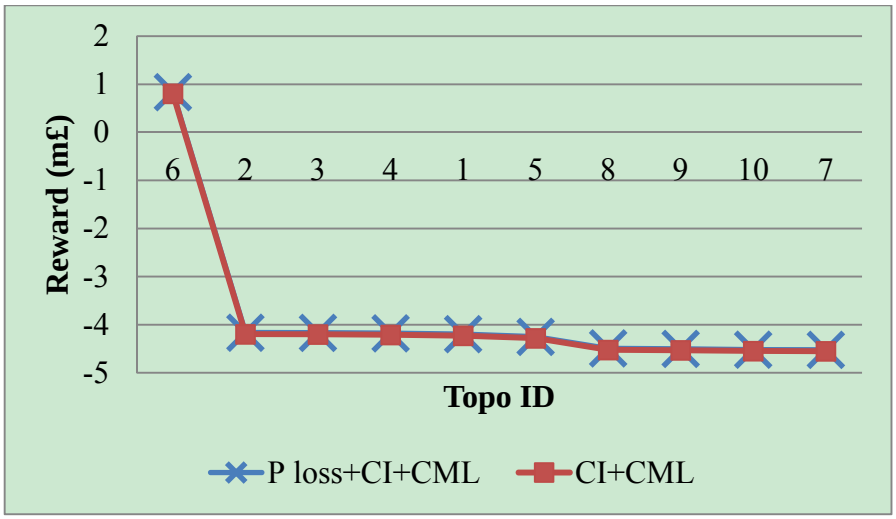

Figure 6.7 The variation trend of *CI+CML* and *P* loss+*CI+CML* rewards in mode 1

- **Mode 2: Reliability-Loss Optimisation**

  In the evaluation of Mode 2, the duration for *P* loss calculation and reliability evaluation are the same as for Mode 1. The positions of the normally open points in the output topologies are listed in Table 6-20. The Reliability-Loss Optimisation results calculated by DisOPT are shown in Table 6-22. The rewards for the output topologies in mode 2 are listed in Table 6-21. In this model, the first *N* (output topology number, defined by user) highest *CI*+*CML* reward are generated first. *P* loss of these *N* topologies is then calculated and they are re-sorted from highest to lowest *P* loss+*CI*+*CML* rewards. So the TopoID *i* in Table 6-20, Table 6-22 and Table 6-21 means the i^{th} highest *CI*+*CML* reward topology. In the tables, topologies are listed in order of total rewards.

Table 6-20 The positions of normally open points in output topologies in mode 2

Topo ID	OPEN BRANCHES	
1	b33-b32	b57-b58
2	b24-b23	b57-b58
3	b33-b32	b56-b57
4	b33-b32	b58-b59
5	b33-b32	b55-b56
6	b24-b23	b56-b57
7	b33-b32	b59-b54
8	b0(s)-b55	b33-b32
9	b24-b23	b58-b59
10	b33-b32	b53-b54

Table 6-21 The rewards of output topologies in mode 2

TopoID	Total Reward		
	P loss+*CI*+*CML* reward (m£)	*CI*+*CML* reward (m£)	*P* reward (m£)
1	0.728	0.697	0.031
2	0.668	0.653	0.014
3	0.6	0.583	0.018
4	0.437	0.409	0.029
5	0.425	0.407	0.018
6	0.399	0.407	-0.008
7	0.39	0.365	0.026
8	0.334	0.317	0.017
9	0.284	0.273	0.01
10	0.224	0.203	0.021

Table 6-22 The report of Reliability-Loss optimisation in mode 2

Topo ID	*P* loss					
	New			Change		
	MW	MWh	Reward(m£)	MW	MWh	Reward(m£)
1	0.176	1539.477	0.031	0.059	515.504	0.031
2	0.208	1818.594	0.014	0.027	236.387	0.014
3	0.201	1758.656	0.018	0.034	296.325	0.018
4	0.18	1578.531	0.029	0.054	476.45	0.029
5	0.201	1760.452	0.018	0.034	294.53	0.018
6	0.25	2193.119	-0.008	-0.016	-138.138	-0.008
7	0.186	1625.331	0.026	0.049	429.651	0.026
8	0.201	1763.533	0.017	0.033	291.448	0.017
9	0.215	1880.558	0.01	0.02	174.423	0.01
10	0.194	1698.961	0.021	0.041	356.02	0.021

Topo ID	*CI*			
	New		Change	
	Performance (int./100.cust.yr.)	Reward (m£)	Performance (int./100.cust.yr.)	Reward (m£)
1	24.051	0.369	4.102	0.369
2	25.075	0.277	3.078	0.277
3	26.085	0.186	2.067	0.186
4	24.704	0.31	3.449	0.31
5	26.452	0.153	1.701	0.153
6	28.515	-0.033	-0.362	-0.033
7	25.001	0.284	3.152	0.284
8	26.652	0.135	1.501	0.135
9	26.227	0.173	1.926	0.173
10	25.676	0.223	2.477	0.223

Topo ID	*CML*			
	New		Change	
	Performance (mins./cust.yr.)	Reward (m£)	Performance (mins./cust.yr.)	Reward (m£)
1	16.163	0.328	0.994	0.328
2	16.016	0.376	1.14	0.376
3	15.955	0.396	1.201	0.396
4	16.859	0.098	0.297	0.098
5	16.386	0.254	0.77	0.254
6	15.824	0.44	1.332	0.44
7	16.911	0.081	0.245	0.081
8	16.606	0.182	0.551	0.182
9	16.854	0.1	0.302	0.1
10	17.217	-0.02	-0.06	-0.02

According to Table 6-21, it can be concluded that: though the sequence of candidate topologies generated by reliability optimisation remains the same after performing *P* loss optimisation since the sequence of TopoID is still from 1 to 10, the *P* loss values of these topologies are not from the lowest to highest. For example, when the network topology are changed from TopoID 3 to TopoID 2, the *CI+CML* reward increases from 0.583m£ to 0.653 m£ but the *P* loss reward decreases from 0.018m£ to 0.014 m£. The *P* loss+CI+CML reward still increases from 0.6m£ to 0.668m£.

The variation trends of *CI*, *CML*, *CI+CML* rewards are shown in Figure 6.8. The variation trends of *P* loss+*CI+CML* and *CI+CML* rewards are shown in Figure 6.9. As can be seen from Figure 6.8, the shape of *CI+CML* reward's variation depends on both the *CI* and *CML* variation trends. In Figure 6.9, the shapes of two variations trends are almost the same. So in mode 2, *CI+CML* reward makes the major contribution to the total rewards of *P* loss, *CI* and *CML*.

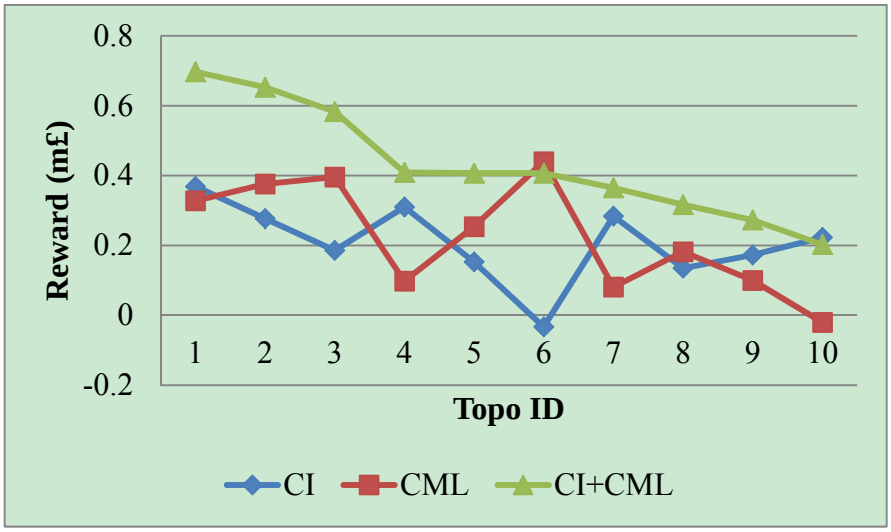

Figure 6.8 The variation trend of *CI*, *CML* and *CI+CML* in Reliability-Loss

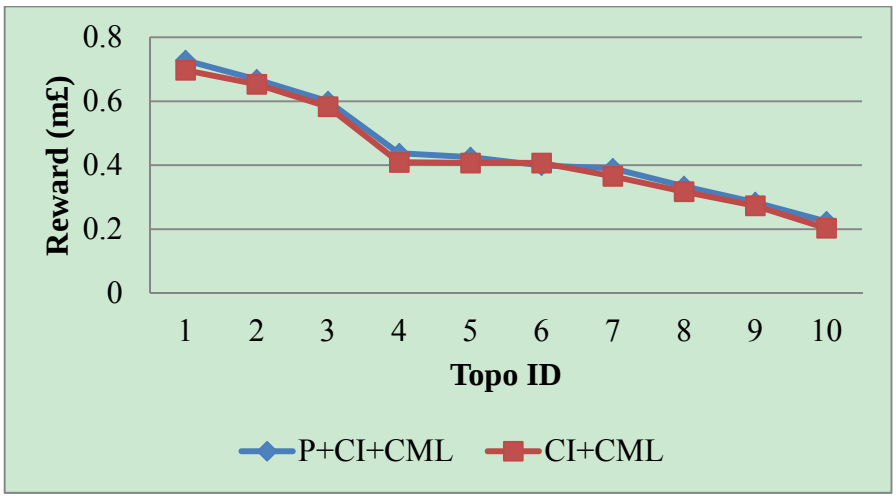

Figure 6.9 The variation trend of *CI+CML* and *P* loss+*CI+CML* loss reward in Reliability-Loss

Based on the results in this case study, it can be concluded that: 1) *CI* and *CML* need to be optimised at the same time; 2) For the urban model used in this case study, the network's *CI* and *CML* performance is much more important than its *P* loss performance under the incentive rate set by Ofgem at the time of this study. But the nature of the network, for example, urban or rural, the distribution of customer, load profile have large impacts on the final results.

As mentioned before, *P* loss and reliability need to be chosen which is optmised first for the *P* loss and reliability developed in this thesis. When P loss is more important than reliability performance, P loss can be chosen to optmised first. Otherwise, reliability performance is optmised first.

6.7 Case 7 Sensitivity analysis of *P* loss's Incentive Rate

The results of Case 6 in Section 6.6 showed that the rewards of *CI+CML* make the major contribution to the rewards of *P* loss+*CI+CML* since the amount of *CI+CML*'s reward is much larger than *P* loss's reward. One reason for this phenomenon is the different weights of *P* loss, *CI* and *CML*. Their weights used in this thesis are the incentive rates of *P* loss, *CI* and *CML* set by Ofgem which, at time of this study, are 0.06k £/MWh, 90k £/*CI* and 330k £/*CML* respectively [24]. This section analyses the sensitivity of *P* loss's incentive rate.

The network model used in Section 6.6 is reused here. The algorithm of loss and reliability optimisation was introduced in Section 5.9. Two modes of loss and reliability optimisation are studied in this section: 1) Mode 1: *P* loss is optimised first, followed by optimisation of reliability (Loss-Reliability); 2) Mode 2: Reliability is optimised first, followed by optimisation of *P* loss (Reliably-Loss). In each mode, four incentive rates of *P* loss are studied which are 0.6k£/MWh, 6k£/MWh, 60k£/MWh and 600k£/MWh. The incentive rates of *CI* and *CML* remain the same at 90k£/*CI* and 330km£/*CML* respectively. The details of the sensitivity analysis of the *P* loss incentive rate are presented below.

- **Mode 1: Loss-Reliability Optimisation**

  The variation trends of *P* loss+*CI*+*CML*, *CI*+*CML* and *P* loss rewards in mode 1 are shown in Figure 6.10- Figure 6.13. The variations of output topologies caused by the change of *P* loss incentive rate are presented in Table 6-23. The summary of the optimal configuration in mode1 is shown in Table 6-24. The Topo ID in each *P* loss incentive rate represents the same topology.

Table 6-23 Output topologies for each *P* loss incentive rate in mode 1

The incentive rate of P loss	0.06k £/MWh	0.6k £/MWh	6k £/MWh	600k £/MWh	6000k £/MWh
Topo ID	6	6	6	6	2
	2	2	2	2	1
	3	3	3	1	3
	4	4	1	3	4
	1	1	4	4	6
	5	5	5	5	5
	8	8	8	8	8
	9	9	7	7	7
	10	7	9	9	9
	7	10	10	10	10

Table 6-24 Summary of the optimal configuration in mode 1

Case	1	2	3	4
P loss incentive rate (k£/MWh)	0.6	6	60	600
CI(int./100.cust.yr.)	24.05	24.05	24.05	23.88
CI(normalize)	100	100	100	99.7
CML(mins./cust.yr.)	15.84	15.84	15.84	31.04
CML(normalize)	100	100	100	196
P loss(*MWh*)	1539.48	1539.48	1539.48	1500.11
P loss(*normalize)*	100	100	100	97.4

In Figure 6.10 and Figure 6.11, the shape of *P* loss+*CI*+*CML* reward's variation is similar to the shape of *CI*+*CML* reward's variation. There are two reasons for this phenomenon: 1) The variation of *P* reward is much smaller than the variation of *CI*+*CML* reward when the network topology is changed; 2) The amount of *CI*+CML reward is larger than the *P* loss reward.

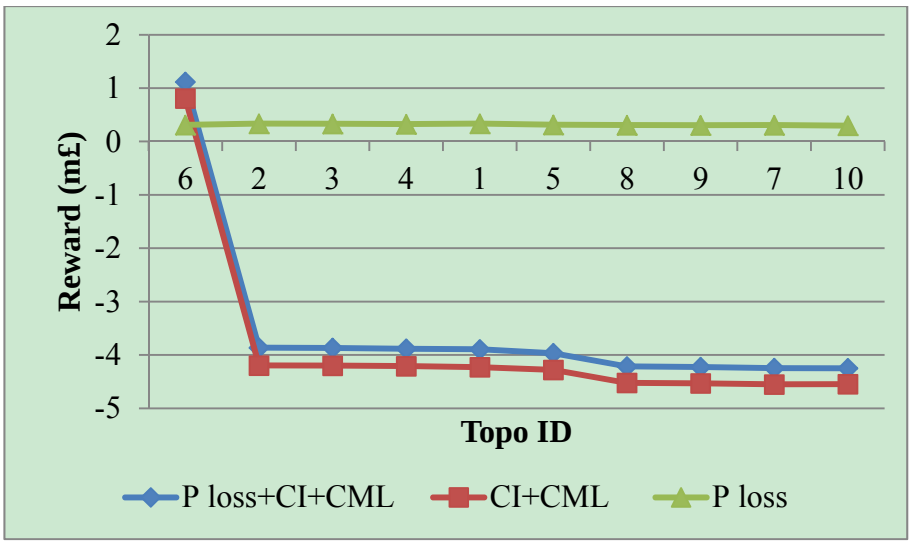

Figure 6.10 *P* loss incentive rate=0.6k£/MWh in Mode 1

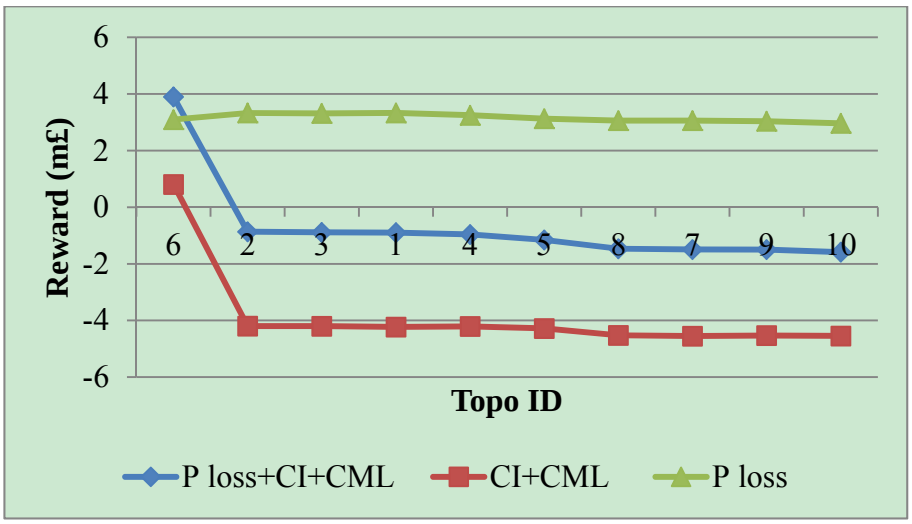

Figure 6.11 *P* loss incentive rate=6k£/MWh in Mode 1

In Figure 6.12, the line of the *P* loss+*CI*+*CML* reward variation is much closer to the line of the *P* loss reward variation. One reason of this phenomenon is that the amount of the *P* loss reward is larger than the amount of the *CI*+*CML* reward.

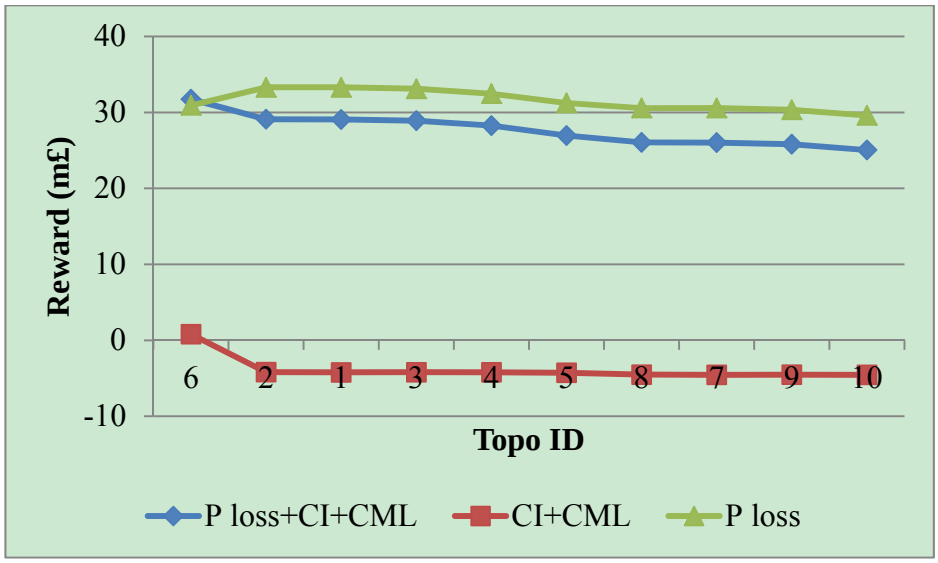

Figure 6.12 *P* loss incentive rate=60k£/MWh in Mode 1

In Figure 6.13, the line of the *P* loss+*CI*+*CML* reward is close to the *P* loss reward variation and far from the *CI*+*CML* reward variation. This phenomenon indicates that the reward of *P* loss is much larger than *CI*+*CML* rewards.

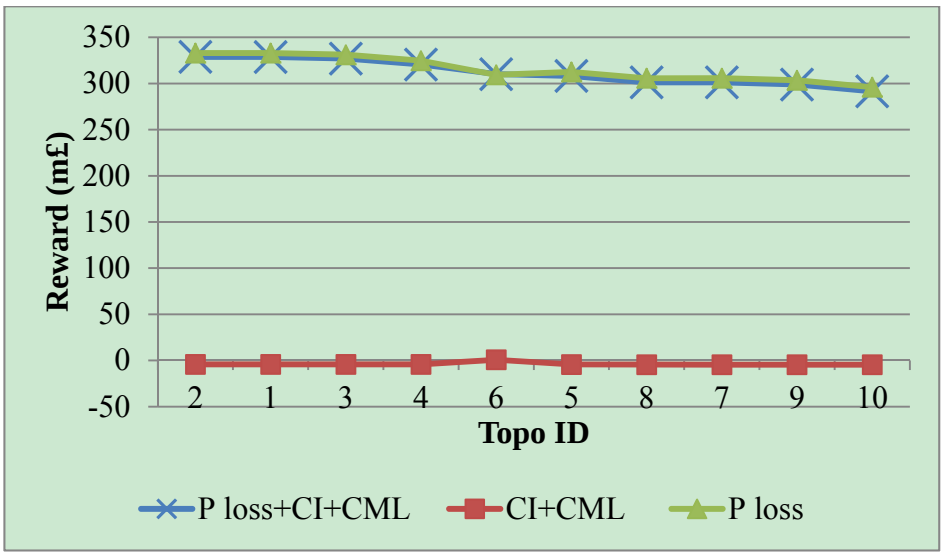

Figure 6.13 *P* loss incentive rate=600k£/MWh in Mode 1

- **Mode 2: Reliability-Loss Optimisation**

  The variation trends of *P* loss+*CI*+*CML*, *CI*+*CML* and *P* loss rewards in mode 2 are shown in Figure 6.14 - Figure 6.17. The variations of output topologies caused by the change of *P* loss incentive rate are presented in Table 6-25. The summary of the optimal configuration in mode1 is shown in Table 6-26.The Topo ID in each *P* loss incentive rate represents the same topology.

Table 6-25 Output topologies for each *P* loss incentive rate in mode 2

The incentive rate of *P* loss	0.06k £/MWh	0.6k £/MWh	6k £/MWh	600k £/MWh	6000k £/MWh
Topo ID	1	1	1	1	1
	2	2	4	4	4
	3	3	7	7	7
	4	4	3	10	10
	5	7	10	3	3
	6	5	5	5	5
	7	8	2	8	8
	8	10	8	2	2
	9	9	9	9	9
	10	6	6	6	6

Table 6-26 Summary of the optimal configuration in mode 2

Case	1	2	3	4
P loss incentive rate (k£/MWh)	0.6	6	60	600
CI(*int./100.cust.yr.*)	24.051	24.051	24.051	24.051
CI(normalize)	100	100	100	100
CML(*mins./cust.yr.*)	16.163	16.163	16.163	16.163
CML(normalize)	100	100	100	100
P loss(MWh)	1539.477	1539.477	1539.477	1539.477
P loss(normalize)	100	100	100	100

Figure 6.14 and Figure 6.15 indicate that the shape of *P* loss+*CI*+*CML* reward depends on both of *P* loss and *CI*+*CML* reward's variation when *P* loss's incentive rates are 0.6k£/MWh and 6k£/MWh in mode 2. It may be interesting to note that the configurations with the lowest losses are not the same as those with the best reliability performance.

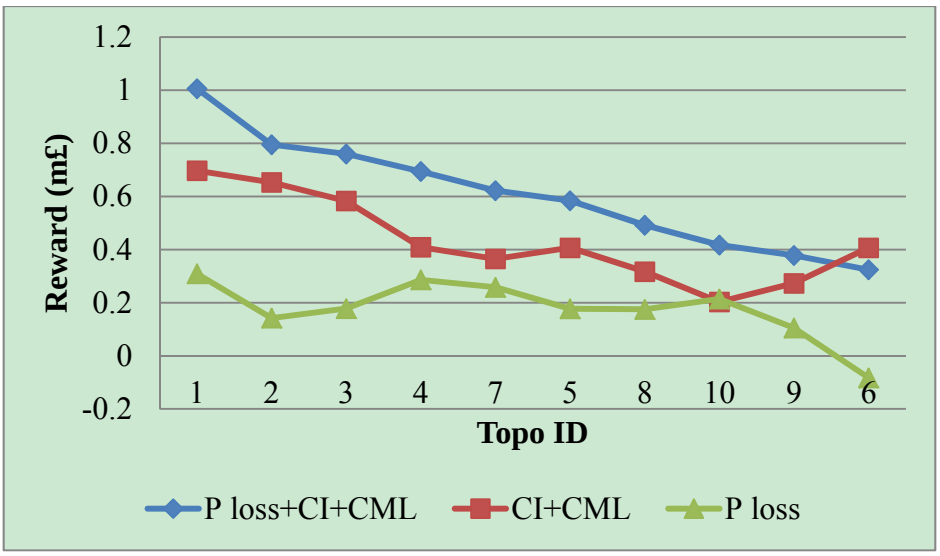

Figure 6.14 *P* loss incentive rate=0.6k£/MWh in Mode 2

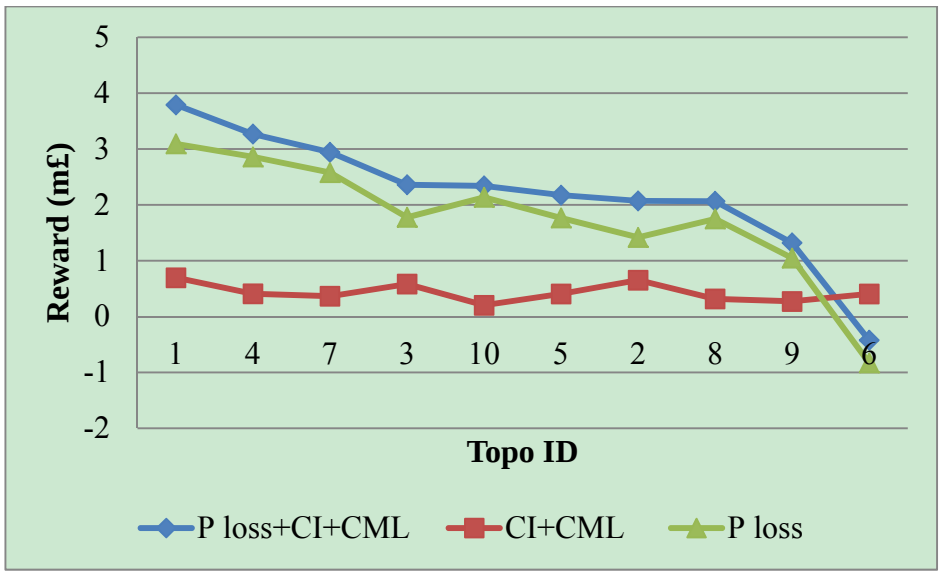

Figure 6.15 *P* loss incentive rate=6k£/MWh in Mode 2

In Figure 6.16 and Figure 6.17, the lines of *P* loss+*CI*+*CML* and *P* loss rewards' variation are almost overlapped which indicate that the reward of *P* loss is much larger than *CI*+*CML* rewards.

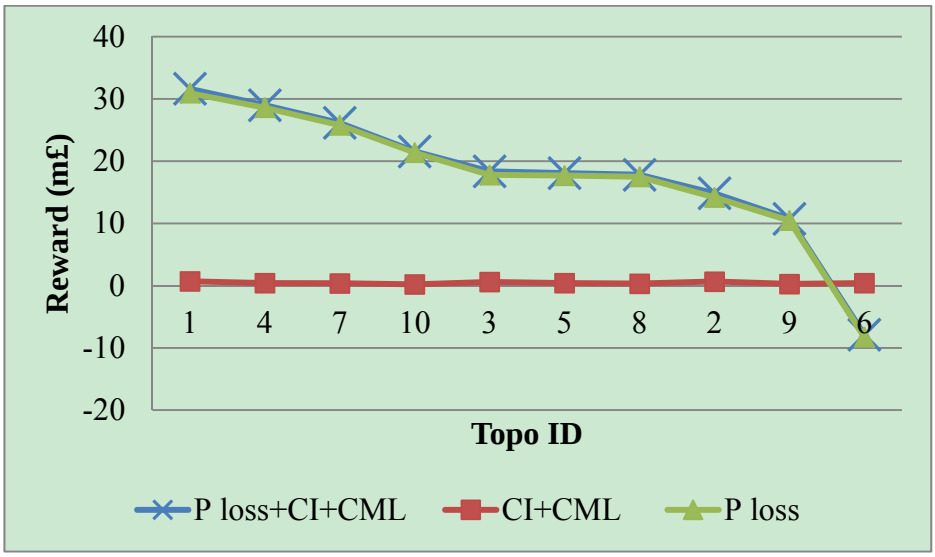

Figure 6.16 *P* loss incentive rate=60k£/MWh in Mode 2

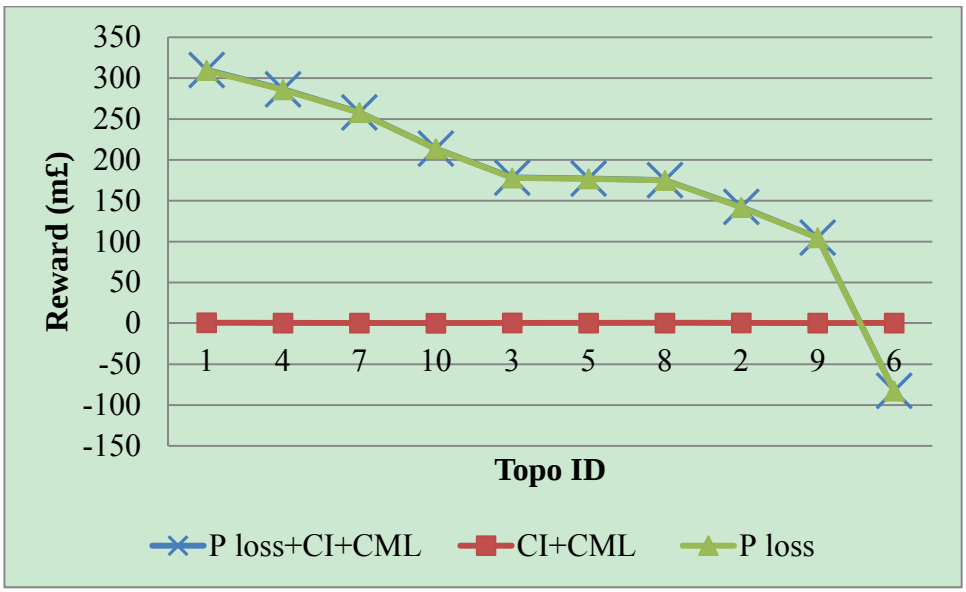

Figure 6.17 *P* loss incentive rate=600k£/MWh in Mode 2

Based on the results in Mode 1 and Mode 2, it can be concluded that: 1) For the urban network used in this case study, the topology whose *P* loss is the lowest does not always have the best *CI+CML* rewards;2) For the urban network used in this case study, the *P* loss incentive becomes significant in determining the optimal topology when the original *P* loss incentive rate (0.06k£/MWh) is multiplied by 100 or larger.

6.8 Discussion of Results

Cases 1 and 2 in sections 6.1 and 6.2 demonstrated optimisation of a network's configuration in respect of branch *P* loss of the network. Case 2 showed that, if the shape of the load profile for different loads on the network is different, different topologies may be optimal at different times of the year. In order to accurately estimate the total reward under Ofgem's Losses Incentive Mechanism (introduced in section 1.2.1), a number of different loading conditions should be assessed and the network reconfigured whenever necessary. This entails the use of a long period mode in the assessment and requires all the relevant load curves to be available. At present, however, this is not generally possible for distribution networks in Britain that only have hourly metering on primary substations and maximum load indicators on secondary substations. It is therefore not currently possible to know the load profiles for secondary substations though this is being addressed in a number of LCNF projects [170-172].

The comparison of PVC and PVO spanning tree generation modes showed that closing all PV edges in the processing of generating spanning trees may not affect the final *P* loss optimisation result. Though it cannot be concluded that the results of these two modes will always be the same for arbitrary networks, these two spanning tree generation modes provide a potential way for users to reduce the number of candidate topologies. In the case study described above, the potential benefit in terms of reduction in computation time is significant.

Case 3a in Section 6.3 evaluated the effects of NOP switching time on system reliability performance. The results of this case study indicate that the switching time of NOPs has a significant effect on the system reliability indices when NOPs are used to transfer the loads from one feeder to another feeder in service restoration. Thus, in contrast to a number of studies reported in the literature, the switching time of NOP needs to be modelled accurately.

Case 3b in Section 6.3 evaluated the effects of using manual switches in service restoration on system reliability performances. The results of this case study indicate that using manual switches in service restoration can improve *CML* even though its switching time is longer than the switching time of remote control switches. This, too, is in contrast with what is assumed in much of the literature.

Case 4 in Section 6.4 evaluated the effects of the number and positions of remote control switches on the system reliability performance. This case study indicates that the reliability evaluation algorithm developed in this thesis can help DNOs to make a decision on whether investment in new switches and remote control is justified, and where to place remote control switches.

Case 5 in Section 6.5 evaluated the effects of *CI* and *CML* on reliability optimisation. The results of this case study indicate that the network topology that has the best *CI* may not have the best *CML*. Thus, *CI* and *CML* need to be optimised together.

Case 6 in Section 6.6 evaluated the effects of *P* loss, *CI* and *CML* incentives on *P* loss and reliability optimisation. The results of this case study indicates that, for the network model used in this case study, the *CI*+*CML* reward is much larger than the reward of *P* loss based on the incentive rates set by Ofgem at the time of this study and for urban cable networks similar to that used in the case study.

Case 7 in Section 6.7 analysed the sensitivity of the incentive rate of *P* loss in loss-reliability. The results indicate that when the *P* loss incentive rate is equal to or larger than 100 times of the current *P* loss incentive rate, the reward of *P* loss becomes as important as *CI*+*CML* rewards, for urban cable networks similar to that used in this case study.

The above case studies, considered together, indicate the value of network reconfiguration in improving network performance and earning rewards under incentive schemes such as those established by Ofgem in Britain. It thus becomes important that analytical facilities exist that can provide advice to a DNO on appropriate configurations under different operating conditions. Moreover, these facilities should:

a) model restoration times accurately, taking adequate account of the different types of switches and where they are located and
b) consider the various performance indicators together, not least *CI* and *CML* since consideration of any one on its own can lead to adoption of a different network configuration when compared with the best for the combination of metrics, weighted by the corresponding incentive.

Chapter 7 Conclusions and Suggestions for Future Work

The conclusions and future work suggestions of spanning tree generation algorithm, *P* loss optimisation algorithm, reliability evaluation and optimisation algorithms, optimisation both of *P* loss and reliability performance and the analytical tool's performance are presented in this chapter.

7.1 Conclusions

The reduction of network losses and improvement of reliability of supply to customers are extremely important for distribution network operators (DNOs) to take into account when designing and operating their networks. They are important because of the need to minimise wasted energy and carbon emissions and to provide customers with an adequate level of service. Moreover, in Great Britain, Ofgem has implemented financial incentives with respect to these things. It is therefore important that a DNO can easily and accurately calculate the impacts of design or operation decisions on losses and reliability. Even better, would be a facility that, given a number of options regarding the configuration of the network, would suggest which are optimal with respect to either incentive or to both of them combined.

Study of the realistic 11kV middle size distribution network indicates that the *P* loss of transformers is the major part of the total *P* loss. But it is generally unrealistic for DNOs to replace old transformers that have high *P* losses by new modern transformers have relative low *P* losses as the early asset write-off cost (equal to the financial value, after depreciation, of the replaced asset at the time at which it is replaced) will often be higher than the value of the reduction in losses. The case studied in Case 1 showed that network reconfiguration can improve a network's *P* loss in a significant way if this network has not been optimized. Currently, remote control and manual switches are mainly used to restore the power supply under fault condition or change network topology for planned outage by DNOs. Using these switching devices for network reconfiguration can not only improve the *P* loss to get extra rewards from Ofgem but also make full use of existing devices. Since each DNO's target *P* loss set by Ofgem is calculated in MWh, a long term *P* loss

optimisation is required rather than optimising *P* loss at one time point. Case 2 showed that, if the shape of the load profile for different loads on the network is different, different topologies may be optimal at different times of the year. In order to accurately estimate the total reward under Ofgem's Losses Incentive Mechanism (introduced in section 1.2.1), a number of different loading conditions should be assessed and the network reconfigured whenever necessary. This entails the use of a long period mode in the assessment and requires all the relevant load curves to be available. At present, however, this is not generally possible for distribution networks in Britain that only have hourly metering on primary substations and maximum load indicators on secondary substations. It is therefore not currently possible to know the load profiles for secondary substations though this is being addressed in a number of LCNF projects [170-172].

The reliability indices set by Ofgem are *CI* and *CML* which indicate the average frequency and duration of interruptions. The cases studied in Cases 3, 4, 5 show that: 1) Restoration times need to be modelled accurately, taking adequate account of the different types of switches and where they are located; 2) Remote control switches can improve the *CML* in a significant way though they cannot improve the *CI*. DNOs need to consider both the cost of installing new remote control switches and the extra benefit that can be gained from the improvement of *CML*; 3) *CI* and *CML* need to be optimised at the same time rather than optimised separately.

When *P* loss, *CI* and *CML* are optimised at the same time against Ofgem's current incentive rates, the performance of *CI* and *CML* are much more important than the *P* loss. A sensitivity analysis of the *P* loss incentive rate in a combined loss-reliability optimisation indicates that when the *P* loss incentive rate is equal to or larger than 100 times of the current *P* loss incentive rate, the reward of *P* loss becomes as important as *CI*+*CML* rewards.

The cases studied in this thesis indicate that current networks still have space for DNOs to improve the *P* loss, *CI* and *CML*. This can not only improve the network's performance but also brings extra profits to DNOs. However, such improvement

require use of analytical facilities such as those described in this thesis, the main innovations in which are (1) the discovery of a globally optimal network configuration in respect of network losses; (2) the automation calculation of a realistic restoration time for each load point following a fault at any location and (3) the provision of a facility to find the optimal network configuration in respect of the combination of regulatory incentives for network losses and reliability.

7.2 Future Work

Potential future work to improve the algorithms presented in this thesis, as well as their software implementation in DisOPT is discussed in following subsections. The future work emphasizes on solving the limitations of the current algorithms and improving the total computational speed.

7.2.1 Future Development of the Spanning Tree Generation Algorithm

The algorithm of finding all spanning trees of a network is the core of the loss and reliability optimisation algorithms described in this thesis. The current version of the spanning tree generation algorithm is implemented by recursion. Recursion is easy to implement but it has a low calculation speed and requires a lot of computer memory. For example, for some complicated networks, more than 1GB of memory is required. Using a stack instead of recursion to control the process of spanning tree growth can solve this problem. Another problem is that it is assumed that all tree edges of the graph introduced in section 3.4 can be opened. But in fact, if a branch doesn't have a switch, the edge representing this branch cannot be opened even if it is marked as tree edge by the preprocessing of network topology introduced in section 3.4. Though it can be solved by checking the results to ignore spanning trees with the open edges which cannot be opened, its efficiency is low. So a new spanning tree generation which can limit the edges is a future requirement. Meanwhile, an algorithm for calculating the number of all spanning tree needs to be developed.

7.2.2 Future Development of *P* Loss Optimisation Algorithm

Since the loss optimisation algorithm developed in this thesis uses an exhaustive search to find the topology with minimum *P* loss, the computation time is very long

when the number of branches in the spanning tree is very large. There are two suggested methods to solve this problem:

1) Instead of performing an exhaustive search of all spanning trees, use other heuristic optimisation methods (e.g. GA [6], evolutionary programming [175, 176], ant colony [74], simulated annealing [71]) to find the topology with the minimum *P* loss without performing an exhaustive search [81].
2) Provide an alternative loss optimisation method introduced in 1). This method may not guarantee a globally optimal result but the percentage of loss reduction may be acceptable and its computation time would be much shorter. If some alternative approach is offered, the user can choose the appropriate loss optimisation method for networks with different spanning tree numbers.

The current network reconfiguration algorithms can only handle radial networks. But the network may be required to operate as a mesh when a distributed generator is connected [5]. How to modify the current algorithm to adapt the impact of DG operating is important. Fault level assessment should be considered further – if the capability of switches to interrupt fault current is exceeded under a particular topology, that topology should not be permitted. Only those topologies that pass a fault level assessment as well as load flow should be considered.

7.2.3 Future Development of the load curve *P* Loss Optimisation Algorithm

The results of load curve *P* loss optimisation are affected by the accuracy of load data during the period being simulated. The best solution to this problem is to read the load data from the network monitoring points directly. The application of smart meters will make this possible [84]. The algorithm as presented here can only handle a single load scaling factor. In order to allow the load profile or load duration evaluation to be done more precisely, the capability of allowing loads (and generation) to be defined for every load bus for multiple points in time needs to be developed.

7.2.4 Future Development of the Reliability Evaluation Algorithm

The current version of reliability analysis algorithm in DisOPT cannot deal with meshed networks, protection failures and the restrictions on load transfer. Though the topology analysis algorithm developed in this thesis cannot handle a meshed network, it can be upgraded to handle protection failures and restrictions on load transfer. In order to handle meshed networks, a new graph algorithm, like minimum cut set [124], is required. Other factors affecting system reliability, like environment, weather, system maintenance, need to be considered as well. The weightings of different fault events need to be considered since Ofgem set different weightings of interruptions included in the Interruption Incentive Scheme, as shown in Table 7-1 [24].

Table 7-1 The weightings of interruptions included in IIS [24]

Source of *CI/CML*	Weighting
Unplanned *CI* and *CML* arising on the distribution network	100 per cent for *CI* and *CML*
Pre-arranged *CI* and *CML* arising on the distribution network	50 per cent for *CI* and *CML*
CI and *CML* arising from distributed generators	100 per cent for *CI* and *CML*

The function of evaluating the effects of passive faults (defined in section 4.7.1) and planned outages on network reliability performance needs to be developed. When considering planned outages and the ability of the in-service branches to support a particular level of load, seasonal rating, i.e. that the capacities of each branch will be different at different times of year, needs to be considered as well. Planned outages are normally taken when demand is low, which is normally in the summer but could be spring or autumn. In those seasons, the overhead line ratings are lower than in winter.

7.2.5 Future Development of the Loss and Reliability Optimisation Algorithm

For optimisation of both loss and reliability together, it is important to set the appropriate weights in the target function to make sure the outputs are exactly what is required. For example, when the topologies of minimum loss and best reliability performance are different, the choice of optimal topology is determined by weights in the target function. At present, the target function only considers the

penalty/rewards set by Ofgem. Whether more factors, like proportion of EHV(33kV and 22kV) distribution network and rural area, should be considered needs to be investigated.

7.2.6 Future Development of the Software

The data of the current version of DisOPT are stored in separate CSV files which makes the processing of data input inconvenient. In order to solve this problem, a graphical network modelling tool would need to be developed. In this tool, a user could draw the network in a visualization environment and all data would be stored in a single file. When DisOPT performs a heavy calculation in the background, the user interface loses response until the calculation is finished. Software performance can be improved by parallel calculation, which is achieved by using multi-threading techniques. The precondition of using this technique is that the computer has a multi-core CPU. This technique can not only solve this particular problem but also could also improve the calculation speed more generally. For example, if the software can execute N threads at the same time, N feeders' reliability evaluations can be executed in parallel and the total calculation time can be reduced N times.

References

[1] D. Hawkins, "The impact of government, regulator, shareholder and customer on the development of utility distribution management systems, SCADA and outage management systems in the 21st Century," in *Electricity Distribution, 2005. CIRED 2005. 18th International Conference and Exhibition on*, 2005, pp. 1-4.

[2] W. D. Stevenson, *Elements of power system analysis*: New York : McGraw-Hill, 1982.

[3] *Electric power engineering handbook : electric power generation, transmission, and distribution*: Boca Raton : CRC Press, 2007.

[4] ScottishPower. (27/01/2013). *SP Long Term Development Statements for the years 2011/12 to 2015/16*. Available: http://www.spenergynetworks.co.uk/lt_statements/default.asp

[5] S. A. M. Javadian and M. R. Haghifam, "Protection of distribution networks in presence of DG using Distribution Automation System capabilities," in *Power and Energy Society General Meeting - Conversion and Delivery of Electrical Energy in the 21st Century, 2008 IEEE*, 2008, pp. 1-6.

[6] P. Prasad, S. Sivanagaraju, and N. Sreenivasulu, "Network Reconfiguration for Load Balancing in Radial Distribution Systems Using Genetic Algorithm," *Electric Power Components and Systems,* vol. 36, pp. 63-72, 2007.

[7] J. J. Burke, *Power distribution engineering : fundamentals and applications*: New York : M. Dekker, 1994.

[8] E.ON. (27/01/2013). *Primary Network Design Manual*. Available: http://www.eon-uk.com/downloads/Primary_Network_Design_Manual.pdf

[9] S. K. Salman and S. F. Tan, "Comparative Study of Protection Requirements of Active Distribution Networks Using Radial and Ring Operations," in *Power Tech, 2007 IEEE Lausanne*, 2007, pp. 1182-1186.

[10] T. E. McDermott, "A heuristic nonlinear constructive method for electric power distribution system reconfiguration," Virginia Polytechnic Institute and State University, 1998.

[11] PIQUE. Liberalisation, privatisation and regulation in the UK electricity sector. Available: http://www.pique.at/reports/pubs/PIQUE_CountryReports_Electricity_UK_November2006.pdf

[12] Ofgem. (27/01/2013). *Ofgem Offical Website*. Available: http://www.ofgem.gov.uk/Pages/OfgemHome.aspx

[13] Ofgem. (27/01/2013). *Electricity Distribution Annual Report for 2010-11*. Available: http://www.ofgem.gov.uk/Pages/MoreInformation.aspx?docid=702&refer=Networks/ElecDist/PriceCntrls/DPCR5

[14] Ofgem. (27/01/2013). *Distribution Price Control Review 4 (DPCR4)*. Available: http://www.ofgem.gov.uk/Networks/ElecDist/PriceCntrls/DPCR4/Pages/DPCR4.aspx

[15] Ofgem. (27/01/2013). *Distribution Price Control Review 5 (DPCR5)* Available: http://www.ofgem.gov.uk/Networks/ElecDist/PriceCntrls/DPCR5/Pages/DPCR5.aspx

[16] Ofgem. (2011, 27/01/2013). *Decision not to activate the Losses Incentive Mechanism in the Fifth Distribution Price Control: Document A* Available: http://www.ofgem.gov.uk/Pages/MoreInformation.aspx?docid=755&refer=Networks/ElecDist/Policy/losses-incentive-mechanism

[17] Ofgem. (27/01/2013). *Electricity Distribution Loss Percentages by Distribution Network Operator (DNO) Area*. Available: http://www.ofgem.gov.uk/Networks/ElecDist/Documents1/Distribution%20Units%20and%20Loss%20Percentages%20Summary.pdf

[18] Ofgem. (27/01/2013). *Losses Incentive Mechanism* Available: http://www.ofgem.gov.uk/Networks/ElecDist/Policy/losses-incentive-mechanism/Pages/index.aspx

[19] Ofgem. Electricity Distribution Allowed Loss Percentages - Representation by ScottishPower EnergyNetworks. Available:

http://www.ofgem.gov.uk/Pages/MoreInformation.aspx?docid=345&refer=Networks/ElecDist/PriceCntrls/DPCR4

[20] Ofgem. (27/01/2013). *Price Controls*. Available: http://www.ofgem.gov.uk/Networks/ElecDist/PriceCntrls/Pages/PriceCntrls.aspx

[21] Ofgem. (27/01/2013). *Electricity Distribution Price Control Review Final Proposals - Financial methodologies*. Available: http://www.ofgem.gov.uk/Networks/ElecDist/PriceCntrls/DPCR5/Documents1/FP_6_DPCR5%20Financial%20methodologies.pdf

[22] Ofgem. (2004, 27/01/2013). *Electricity Distribution Price Control Review*. Available: http://www.ofgem.gov.uk/Networks/ElecDist/PriceCntrls/DPCR4/Documents1/8944-26504.pdf

[23] Ofgem. (2012, 27/01/2013). *Losses Working Group*. Available: http://www.ofgem.gov.uk/Networks/ElecDist/Policy/losses-incentive-mechanism/Documents1/Slide%20pack%20for%20Losses%20Workshop%20March%202012.pdf

[24] Ofgem. (27/01/2013). *Electricity Distribution Price Control Review Final Proposals - Incentives and Obligations*. Available: http://www.ofgem.gov.uk/Networks/ElecDist/PriceCntrls/DPCR5/Documents1/FP_2_Incentives%20and%20Obligations%20FINAL.pdf

[25] Ofgem. (27/01/2013). *2005/06 Electricity distribution quality of service report*. Available: http://www.ofgem.gov.uk/Pages/MoreInformation.aspx?docid=2&refer=Networks/ElecDist/QualofServ/QoSIncent

[26] KEMA and I. College. (2007, 27/01/2013). *Final Report: Review of Distribution Network Design and Performance Criteria* Available: http://www.ofgem.gov.uk/Networks/Techn/TechStandds/Pages/TechStandds.aspx

[27] Ofgem. (27/01/2013). *Information and Incentives Project (IIP): Draft Quality of Service Regulatory Instructions and Guidance (rigs) version 5*. Available:

http://www.ofgem.gov.uk/Networks/ElecDist/QUALOFSERV/GuarStandds/Documents1/9692-49a05.pdf

[28] C. R. Bayliss, *Transmission and distribution electrical engineering*: Oxford : Newnes, 2007.

[29] L. F. Ochoa and A. Padilha-Feltrin, "Distribution line models analysis for loss calculation within three-phase three-wire power flow algorithms," in *Transmission and Distribution Conference and Exposition: Latin America, 2004 IEEE/PES*, 2004, pp. 173-178.

[30] R. M. Ciric, A. P. Feltrin, and L. F. Ochoa, "Power flow in four-wire distribution networks-general approach," *Power Systems, IEEE Transactions on*, vol. 18, pp. 1283-1290, 2003.

[31] W. H. Kersting, *Distribution system modeling and analysis*. Boca Raton: CRC Press, 2007.

[32] Digsilent. (27/01/2013). Available: http://www.digsilent.de/

[33] D. Jiansong, "Report on 11kV model of Glasgow Urban Network Losses."

[34] S. Borlase, *Smart Grids: Infrastructure, Technology, and Solutions* vol. 1: CRC Press, 2012.

[35] G. Quinonez-Varela, K. Bell, and G. Burt, "Automation to optimise network configuration in real time–to optimise DG contribution and reduce losses," *Contract number: DG/CG/00096/REP, URN*.

[36] ALSTOM. (20/05/2010). *ALSTOM DISTRIBUTION TRANSFORMERS*. Available: http://tde.alstom.co.za/images/Final_Distribution-Transformers_10022009.pdf

[37] Ofgem. (27/01/2013). *Electricity distribution losses: a consultation document*. Available: http://www.ofgem.gov.uk/NETWORKS/ELECDIST/POLICY/DISTCHRGS/Documents1/1362-03distlosses.pdf

[38] L. San-Yi and W. Chi-Jui, "On-line reactive power compensation schemes for unbalanced three phase four wire distribution feeders," *Power Delivery, IEEE Transactions on*, vol. 8, pp. 1958-1965, 1993.

[39] C. Wei-Neng and Y. Kuan-Dih, "Design of D-STATCOM for fast load compensation of unbalanced distribution systems," in *Power Electronics and*

Drive Systems, 2001. Proceedings., 2001 4th IEEE International Conference on, 2001, pp. 801-806 vol.2.

[40] A. Pana, A. Baloi, and F. Molnar-Matei, "Experimental Validation of Power Mechanism for Load Balancing Using Variable Susceptances in Three Phase Four Wire Distribution Networks," in *EUROCON, 2007. The International Conference on "Computer as a Tool";*, 2007, pp. 1567-1572.

[41] S. A. N. N. Afshin LASHKAR ARA, "Comparison of the facts equipment operation in transmission and distribution systems," presented at the 17th International Conference on Electricity Distribution, Barcelona, 2003.

[42] M. W. Siti, D. V. Nicolae, A. A. Jimoh, and A. Ukil, "Reconfiguration and Load Balancing in the LV and MV Distribution Networks for Optimal Performance," *Power Delivery, IEEE Transactions on,* vol. 22, pp. 2534-2540, 2007.

[43] J. D. Glover, *Power system analysis and design*: Stamford, CT : Cengage Learning, 2012.

[44] R. C. Luis Ochoa, Antonio Padilha-Feltrin, Gareth Harrison,, "Evaluation of distribution system losses due to load unbalance," presented at the Power Systems Computation Conference (PSCC), Liège, Belgium, 2005.

[45] P. M. Anderson, *Analysis of faulted power systems*. New York: IEEE Press, 1995.

[46] ALSTOM. (27/01/2013). *Alstom Grid's SVC MaxSine*. Available: http://www.alstom.com/Global/Grid/Resources/Facts/Documents/SVC%20MaxSine%20-%20STATCOM%20solution%20for%20the%20future%20Brochure%20ENG.pdf

[47] X.-F. Wang, *Modern power systems analysis*: New York : Springer, 2008.

[48] S. Bhim, A. Adya, A. P. Mittal, and J. R. P. Gupta, "Modeling and control of DSTATCOM for three-phase, four-wire distribution systems," in *Industry Applications Conference, 2005. Fourtieth IAS Annual Meeting. Conference Record of the 2005*, 2005, pp. 2428-2434 Vol. 4.

[49] S. Civanlar, J. J. Grainger, H. Yin, and S. S. H. Lee, "Distribution feeder reconfiguration for loss reduction," *Power Delivery, IEEE Transactions on,* vol. 3, pp. 1217-1223, 1988.

[50] K. Aoki, T. Ichimori, and M. Kanezashi, "Normal State Optimal Load Allocation in Distribution Systems," *Power Delivery, IEEE Transactions on,* vol. 2, pp. 147-155, 1987.

[51] L. S. Czarnecki, H. Shih Min, and C. Guangda, "Adaptive Balancing Compensator," *Power Delivery, IEEE Transactions on,* vol. 10, pp. 1663-1669, 1995.

[52] D. Shirmohammadi and H. W. Hong, "Reconfiguration of electric distribution networks for resistive line losses reduction," *Power Delivery, IEEE Transactions on,* vol. 4, pp. 1492-1498, 1989.

[53] T. E. DcDermott, I. Drezga, and R. P. Broadwater, "A heuristic nonlinear constructive method for distribution system reconfiguration," *Power Systems, IEEE Transactions on,* vol. 14, pp. 478-483, 1999.

[54] G. Raju and P. R. Bijwe, "An Efficient Algorithm for Minimum Loss Reconfiguration of Distribution System Based on Sensitivity and Heuristics," *Power Systems, IEEE Transactions on,* vol. 23, pp. 1280-1287, 2008.

[55] M. A. Kashem, V. Ganapathy, and G. B. Jasmon, "Network reconfiguration for load balancing in distribution networks," *Generation, Transmission and Distribution, IEE Proceedings-,* vol. 146, pp. 563-567, 1999.

[56] S. Ching-Tzong and L. Chu-Sheng, "Network reconfiguration of distribution systems using improved mixed-integer hybrid differential evolution," *Power Delivery, IEEE Transactions on,* vol. 18, pp. 1022-1027, 2003.

[57] S. K. Goswami and S. K. Basu, "A new algorithm for the reconfiguration of distribution feeders for loss minimization," *Power Delivery, IEEE Transactions on,* vol. 7, pp. 1484-1491, 1992.

[58] A. Merlin and H. Back, "Search for a Minimal-Loss Operating Spanning Tree Configuration in an Urban Power Distribution System," in *Proc. 5th Power System Computation Conference (PSCC)*, 1975.

[59] J. T. Boardman and C. C. Meckiff, "A Branch And Bound Formulation To An Electricity Distribution Planning Problem," *Power Apparatus and Systems, IEEE Transactions on,* vol. PAS-104, pp. 2112-2118, 1985.

[60] F. V. Gomes, S. Carneiro, Jr., J. L. R. Pereira, M. P. Vinagre, P. A. N. Garcia, and L. R. Araujo, "A New Heuristic Reconfiguration Algorithm for Large Distribution Systems," *Power Systems, IEEE Transactions on,* vol. 20, pp. 1373-1378, 2005.

[61] R. A. Jabr, R. Singh, and B. C. Pal, "Minimum Loss Network Reconfiguration Using Mixed-Integer Convex Programming," *Power Systems, IEEE Transactions on,* vol. 27, pp. 1106-1115, 2012.

[62] E. R. Ramos, A. G. Exposito, J. R. Santos, and F. L. Iborra, "Path-based distribution network modeling: application to reconfiguration for loss reduction," *Power Systems, IEEE Transactions on,* vol. 20, pp. 556-564, 2005.

[63] H. D. de Macedo Braz and B. A. de Souza, "Distribution Network Reconfiguration Using Genetic Algorithms With Sequential Encoding: Subtractive and Additive Approaches," *Power Systems, IEEE Transactions on,* vol. 26, pp. 582-593, 2011.

[64] J. Mendoza, R. Lopez, D. Morales, E. Lopez, P. Dessante, and R. Moraga, "Minimal loss reconfiguration using genetic algorithms with restricted population and addressed operators: real application," *Power Systems, IEEE Transactions on,* vol. 21, pp. 948-954, 2006.

[65] K. Nara, A. Shiose, M. Kitagawa, and T. Ishihara, "Implementation of genetic algorithm for distribution systems loss minimum re-configuration," *Power Systems, IEEE Transactions on,* vol. 7, pp. 1044-1051, 1992.

[66] H. Ying-Yi and H. Saw-Yu, "Determination of network configuration considering multiobjective in distribution systems using genetic algorithms," *Power Systems, IEEE Transactions on,* vol. 20, pp. 1062-1069, 2005.

[67] K. Prasad, R. Ranjan, N. C. Sahoo, and A. Chaturvedi, "Optimal reconfiguration of radial distribution systems using a fuzzy mutated genetic algorithm," *Power Delivery, IEEE Transactions on,* vol. 20, pp. 1211-1213, 2005.

[68] M. E. Baran and F. F. Wu, "Network reconfiguration in distribution systems for loss reduction and load balancing," *Power Delivery, IEEE Transactions on,* vol. 4, pp. 1401-1407, 1989.

[69] F. V. Gomes, S. Carneiro, J. L. R. Pereira, M. P. Vinagre, P. A. N. Garcia, and A. Leandro Ramos de, "A New Distribution System Reconfiguration Approach Using Optimum Power Flow and Sensitivity Analysis for Loss Reduction," *Power Systems, IEEE Transactions on,* vol. 21, pp. 1616-1623, 2006.

[70] H. P. Schmidt, N. Ida, N. Kagan, and J. C. Guaraldo, "Fast Reconfiguration of Distribution Systems Considering Loss Minimization," *Power Systems, IEEE Transactions on,* vol. 20, pp. 1311-1319, 2005.

[71] H. D. Chiang and R. Jean-Jumeau, "Optimal network reconfigurations in distribution systems. I. A new formulation and a solution methodology," *Power Delivery, IEEE Transactions on,* vol. 5, pp. 1902-1909, 1990.

[72] H. D. Chiang and R. Jean-Jumeau, "Optimal network reconfigurations in distribution systems. II. Solution algorithms and numerical results," *Power Delivery, IEEE Transactions on,* vol. 5, pp. 1568-1574, 1990.

[73] J. Young-Jae, K. Jae-Chul, O. K. Jin, S. Joong-Rin, and K. Y. Lee, "An efficient simulated annealing algorithm for network reconfiguration in large-scale distribution systems," *Power Delivery, IEEE Transactions on,* vol. 17, pp. 1070-1078, 2002.

[74] C. Chung-Fu, "Reconfiguration and Capacitor Placement for Loss Reduction of Distribution Systems by Ant Colony Search Algorithm," *Power Systems, IEEE Transactions on,* vol. 23, pp. 1747-1755, 2008.

[75] H. Kim, Y. Ko, and K. H. Jung, "Artificial neural-network based feeder reconfiguration for loss reduction in distribution systems," *Power Delivery, IEEE Transactions on,* vol. 8, pp. 1356-1366, 1993.

[76] T. Taylor and D. Lubkeman, "Implementation of heuristic search strategies for distribution feeder reconfiguration," *Power Delivery, IEEE Transactions on,* vol. 5, pp. 239-246, 1990.

[77] H. M. Khodr, J. Martinez-Crespo, M. A. Matos, and J. Pereira, "Distribution Systems Reconfiguration Based on OPF Using Benders Decomposition," *Power Delivery, IEEE Transactions on,* vol. 24, pp. 2166-2176, 2009.

[78] D. E. Goldberg, *Genetic algorithms in search, optimization, and machine learning*: Reading, Mass. : Addison-Wesley Pub. Co., 1989.

[79] E. Lopez, H. Opazo, L. Garcia, and P. Bastard, "Online reconfiguration considering variability demand: applications to real networks," *Power Systems, IEEE Transactions on,* vol. 19, pp. 549-553, 2004.

[80] J. Z. Zhu, "Optimal reconfiguration of electrical distribution network using the refined genetic algorithm," *Electric Power Systems Research,* vol. 62, pp. 37-42, 5/28/ 2002.

[81] *Modern heuristic optimization techniques theory and applications to power systems*: Hoboken, N.J. : Wiley ; Chichester : John Wiley distributor, 2008.

[82] D. E. G. a. K. Deb, "A comparative analysis of selection schemes used in genetic algorithms," *Foundations of Genetic Algorithms,* pp. 69--93, 1991.

[83] J. Zhu, *Optimization of power system operation*: Piscataway, N.J. : Wiley-IEEE ; Chichester : John Wiley distributor, 2009.

[84] J. Momoh, *Smart grid: fundamentals of design and analysis*: Hoboken : John Wiley & Sons, 2012.

[85] R. Diestel, *Graph theory*. New York: Springer, 1997.

[86] B. Y. Wu and K.-M. Chao, *Spanning trees and optimization problems*. Boca Raton, FL: Chapman & Hall/CRC, 2004.

[87] A. Gibbons, *Algorithmic graph theory*. Cambridge [Cambridgeshire]; New York: Cambridge University Press, 1985.

[88] R. E. Brown and A. P. Hanson, "Impact of two-stage service restoration on distribution reliability," *Power Systems, IEEE Transactions on,* vol. 16, pp. 624-629, 2001.

[89] D. Jungnickel, *Graphs, networks, and algorithms*: Berlin ; New York : Springer, 2008.

[90] *Introduction to algorithms*: Cambridge, Mass. : MIT Press, 2001.

[91] H. N. Gabow and E. W. Myers, "Finding all spanning trees of directed and undirected graphs," *SIAM J. Comput.,* vol. 7, pp. 280-287, 1978.

[92] S. Hakimi and D. Green, "Generation and Realization of Trees and k-Trees," *Circuit Theory, IEEE Transactions on,* vol. 11, pp. 247-255, 1964.

[93] G. Minty, "A Simple Algorithm for Listing All the Trees of a Graph," *Circuit Theory, IEEE Transactions on,* vol. 12, pp. 120-120, 1965.

[94] K. Seki, "Analysis of no converge networks using the load flow program with complex number state variables," in *Transmission and Distribution Conference and Exhibition 2002: Asia Pacific. IEEE/PES*, 2002, pp. 1124-1127 vol.2.

[95] P. Ravibabu, K. Venkatesh, and C. Sudheer Kumar, "Implementation of genetic algorithm for optimal network reconfiguration in distribution systems for load balancing," in *Computational Technologies in Electrical and Electronics Engineering, 2008. SIBIRCON 2008. IEEE Region 8 International Conference on*, 2008, pp. 124-128.

[96] A. v. Meier, *Electric power systems : a conceptual introduction*: Hoboken, N.J. : IEEE Press : Wiley-Interscience, 2006.

[97] G. M. Masters, *Renewable and efficient electric power systems*: Hoboken, N.J. : Wiley-Interscience, 2004.

[98] N. G. E. T. plc. (27/01/2013). *GB Seven Year Statement*. Available: http://www.nationalgrid.com/uk/sys_06/

[99] T. A. Short, *Electric power distribution handbook*: United Kingdom: CRC Press Inc, 2003.

[100] L. McDonald, R. L. Storry, A. Kane, F. McNicol, G. Ault, I. Kockar, *et al.*, "Minimisation of distribution network real power losses using a smart grid Active Network Management System," in *Universities Power Engineering Conference (UPEC), 2010 45th International*, 2010, pp. 1-6.

[101] A. Mutanen, M. Ruska, S. Repo, and P. Jarventausta, "Customer Classification and Load Profiling Method for Distribution Systems," *Power Delivery, IEEE Transactions on,* vol. 26, pp. 1755-1763, 2011.

[102] G. Gross, N. V. Garapic, and B. McNutt, "The mixture of normals approximation technique for equivalent load duration curves," *Power Systems, IEEE Transactions on,* vol. 3, pp. 368-374, 1988.

[103] A. B. R. Sulaiman, M. S. M. Ai-Hafid, and A. S. A. Al-Fahadi, "Developing annual load duration curve using an intelligent technique," in *Power Systems Conference and Exposition, 2004. IEEE PES*, 2004, pp. 549-552 vol.1.

[104] R. Yao and K. Steemers, "A method of formulating energy load profile for domestic buildings in the UK," *Energy and Buildings*, vol. 37, pp. 663-671, 2005.

[105] R. F. Stapelberg, *Handbook of reliability, availability, maintainability and safety in engineering design*: London : Springer, 2009.

[106] Ofgem. (27/01/2013). *Quality of Service Regulatory Instructions and Guidance version 5*. Available: http://www.ofgem.gov.uk/Networks/ElecDist/QualofServ/QoSIncent/Documents1/10141-9405app.pdf

[107] "IEEE Guide for Electric Power Distribution Reliability Indices," *IEEE Std 1366, 2001 Edition*, p. i, 2001.

[108] J. A. Momoh, *Electric power distribution, automation, protection, and control*: Boca Raton : CRC Press, 2008.

[109] W. Li, *Risk assessment of power systems : models, methods, and applications*: Piscataway, NJ : IEEE Press ; Hoboken, NJ : Wiley, 2005.

[110] J. H. Eto and K. H. LaCommare, "Tracking the reliability of the US Electric Power System: An assessment of publicly available information reported to State Public Utility Commissions," *Sacramento, CA: Ernest Orlando Lawrence Berkeley National Laboratory, Report LBNL-1092E*, vol. 11, 2008.

[111] H. L. Willis, *Power distribution planning reference book*: New York : Marcel Dekker ; London : Taylor & Francis, distributor, 2004.

[112] Ofgem. *Electricity Distribution Annual Report for 2008-09 and 2009-10*. Available: http://www.ofgem.gov.uk/Pages/MoreInformation.aspx?docid=539&refer=Networks/ElecDist/PriceCntrls/DPCR5

[113] R. N. Allan and Billinton, *Reliability Evaluation of Power Systems*: Springer, 1996.

[114] J. Faulin, A. A. Juan, and S. Martorell, *Simulation Methods for Reliability and Availability of Complex Systems*: Springer Verlag, 2010.

[115] R. Billinton, M. Fotuhi-Firuzabad, and L. Bertling, "Bibliography on the application of probability methods in power system reliability evaluation 1996-1999," *Power Systems, IEEE Transactions on,* vol. 16, pp. 595-602, 2001.

[116] M. Rausand and A. Høyland, *System Reliability Theory: Models, Statistical Methods, and Applications*: John Wiley & Sons, 2003.

[117] R. A. Billinton, Ronald N., *Reliability evaluation of engineering systems : concepts and techniques*. New York: Plenum Press, 1992.

[118] P. Camarda, F. Corsi, and A. Trentadue, "An Efficient Simple Algorithm for Fault Tree Automatic Synthesis from the Reliability Graph," *Reliability, IEEE Transactions on,* vol. R-27, pp. 215-221, 1978.

[119] R. Billinton, *Reliability assessment of electric power systems using Monte Carlo methods*: New York : Plenum Press, 1994.

[120] R. Billinton and W. Li, "A system state transition sampling method for composite system reliability evaluation," *Power Systems, IEEE Transactions on,* vol. 8, pp. 761-770, 1993.

[121] R. E. Brown, *Electric power distribution reliability*: Boca Raton, Fla. : CRC ; London : Taylor & Francis distributor, 2008.

[122] M. S. Grover and R. Billinton, "A Computerized Approach to Substation and Switching Station Reliability Evaluation," *Power Apparatus and Systems, IEEE Transactions on,* vol. PAS-93, pp. 1488-1497, 1974.

[123] R. N. Allan, R. Billinton, and M. F. de Oliveira, "Reliability evaluation of electrical systems with switching actions," *Electrical Engineers, Proceedings of the Institution of,* vol. 123, pp. 325-330, 1976.

[124] L. Bertling, "Reliability-centred maintenance for electric power distribution systems," Elektrotekniska system, Stockholm, 2002.

[125] R. E. Brown, S. Gupta, R. D. Christie, S. S. Venkata, and R. Fletcher, "Distribution system reliability assessment: momentary interruptions and storms," *Power Delivery, IEEE Transactions on,* vol. 12, pp. 1569-1575, 1997.

[126] ABB. (27/01/2013). *Section 8.13 Backup Protection-Distribution Automation Handbook.* Available:

http://www05.abb.com/global/scot/scot229.nsf/veritydisplay/d1ef27cd5e3e586fc125795f004356ff/$file/dahandbook_section_08p13_backup_protection_757293_ena.pdf

[127] I. Chilvers, N. Jenkins, and P. Crossley, "Development of distribution network protection schemes to maximize the connection of distributed generation," in *Proc. 2003 CIRED, 17th International Conference on Electricity Distribution, Barcelona*, 2003, pp. 12-15.

[128] J. M. Gers and E. J. Holmes, *Protection of Electricity Distribution Networks (2nd Edition)*: Institution of Engineering and Technology.

[129] E. N. West. (27/01/2013). *Northwest Electrictiy Network Investment Plan 2010-2015*. Available: http://www.enwl.co.uk/docs/about-us/network-investment-plan.pdf

[130] W. P. Distribution. (27/01/2013). *Western Power Distribution Business Plan 2010-2015*. Available: http://www.westernpower.co.uk/getdoc/8b299e6d-3177-43b9-8682-1d3111e48d3a/stake_Wales.aspx

[131] E. Lakervi, *Electricity distribution network design*: London : P. Peregrinus on behalf of the Institution of Electrical Engineers, 1995.

[132] DECC. (27/01/2013). *ABOUT RENEWABLE ENERGY POLICY*. Available: http://www.decc.gov.uk/en/content/cms/meeting_energy/renewable_ener/renewable_ener.aspx

[133] I. M. Chilvers, N. Jenkins, and P. A. Crossley, "The use of 11 kV distance protection to increase generation connected to the distribution network," in *Developments in Power System Protection, 2004. Eighth IEE International Conference on*, 2004, pp. 551-554 Vol.2.

[134] A. Dysko, G. M. Burt, S. Galloway, C. Booth, and J. R. McDonald, "UK distribution system protection issues," *Generation, Transmission & Distribution, IET,* vol. 1, pp. 679-687, 2007.

[135] S. A. M. Javadian and M. R. Haghifam, "Designing a new protection system for distribution networks including DG," in *Developments in Power System Protection, 2008. DPSP 2008. IET 9th International Conference on*, 2008, pp. 675-680.

[136] I. Chilvers, N. Jenkins, and P. Crossley, "Distance relaying of 11 kV circuits to increase the installed capacity of distributed generation," *Generation, Transmission and Distribution, IEE Proceedings-*, vol. 152, pp. 40-46, 2005.

[137] T. Gönen, *Electric power distribution system engineering*. Boca Raton: CRC Press, 2008.

[138] ScottishPower, "Catalogue of ICOND&TroubleCall Symbols."

[139] C. H. Ong and J. B. Royle, "The co-ordination of protection and auto-reclose on 11 kV distribution networks," in *Improving Supply Security on 11kV Overhead Networks, IEE Colloquium on*, 1988, pp. 19/1-19/8.

[140] S. Santoso and T. A. Short, "Identification of Fuse and Recloser Operations in a Radial Distribution System," *Power Delivery, IEEE Transactions on,* vol. 22, pp. 2370-2377, 2007.

[141] A. J. Pansini, *Guide to electrical power distribution systems*. Lilburn, GA; Boca Raton, FL: Fairmont Press ; Distributed by Marcel Dekker/CRC Press, 2005.

[142] Y. He, L. Soder, and R. N. Allan, "Evaluating the Effect of Protection System on Reliability of Automated Distribution System," presented at the Power Systems Computation Conference (PSCC), Seville, Spain, 2002.

[143] Siemens. (27/01/2013). *Protection, Substation Automation, Power Quality and Measurement*. Available: http://www.energy.siemens.com/hq/pool/hq/energy-topics/power%20engineering%20guide/PEG_70_KAP_06.pdf

[144] R. N. Allan and J. R. Ochoa, "Modeling and assessment of station originated outages for composite systems reliability evaluation," *Power Systems, IEEE Transactions on,* vol. 3, pp. 158-165, 1988.

[145] A. Sankarakrishnan and R. Billinton, "Sequential Monte Carlo simulation for composite power system reliability analysis with time varying loads," *Power Systems, IEEE Transactions on,* vol. 10, pp. 1540-1545, 1995.

[146] R. Billinton and A. Sankarakrishnan, "Adequacy assessment of composite power systems with HVDC links using Monte Carlo simulation," *Power Systems, IEEE Transactions on,* vol. 9, pp. 1626-1633, 1994.

[147] R. Billinton and G. Lian, "Monte Carlo approach to substation reliability evaluation," *Generation, Transmission and Distribution, IEE Proceedings C,* vol. 140, pp. 147-152, 1993.

[148] A. M. Rei and M. T. Schilling, "Reliability Assessment of the Brazilian Power System Using Enumeration and Monte Carlo," *Power Systems, IEEE Transactions on,* vol. 23, pp. 1480-1487, 2008.

[149] Y. Xingbin and C. Singh, "A practical approach for integrated power system vulnerability analysis with protection failures," *Power Systems, IEEE Transactions on,* vol. 19, pp. 1811-1820, 2004.

[150] R. Karki, H. Po, and R. Billinton, "Reliability Evaluation Considering Wind and Hydro Power Coordination," *Power Systems, IEEE Transactions on,* vol. 25, pp. 685-693, 2010.

[151] R. Billinton and W. Wangdee, "Reliability-Based Transmission Reinforcement Planning Associated With Large-Scale Wind Farms," *Power Systems, IEEE Transactions on,* vol. 22, pp. 34-41, 2007.

[152] R. E. Brown, S. Gupta, R. D. Christie, S. S. Venkata, and R. Fletcher, "Distribution system reliability assessment using hierarchical Markov modeling," *Power Delivery, IEEE Transactions on,* vol. 11, pp. 1929-1934, 1996.

[153] C. L. Brooks, J. Northcote-Green, T. D. Vismor, W. E. C. A. S. Technology, and E. P. R. Institute, *Development of Distribution System Reliability and Risk Analysis Models*: The Institute, 1981.

[154] G. Kjolle and K. Sand, "RELRAD-an analytical approach for distribution system reliability assessment," *Power Delivery, IEEE Transactions on,* vol. 7, pp. 809-814, 1992.

[155] L. Bertling, M. B. O. Larsson, and C. J. Wallnerstrom, "Evaluation of the customer value of component redundancy in electrical distribution systems," in *Power Tech, 2005 IEEE Russia*, 2005, pp. 1-8.

[156] Setre, x, J. us, Wallnerstro, x, C. J. m*, et al.*, "RACalc - A power distribution reliability tool," in *Probabilistic Methods Applied to Power Systems (PMAPS), 2010 IEEE 11th International Conference on*, 2010, pp. 154-159.

[157] D. O. Koval and R. Billinton, "Evaluation of Distribution Circuit Reliability," *Power Apparatus and Systems, IEEE Transactions on,* vol. PAS-98, pp. 509-518, 1979.

[158] R. P. Broadwater, H. E. Shaalan, A. Oka, and R. E. Lee, "Distribution system reliability and restoration analysis," *Electric Power Systems Research,* vol. 29, pp. 203-211, 5// 1994.

[159] J. J. Meeuwsen, W. L. Kling, and W. A. G. A. Ploem, "The influence of protection system failures and preventive maintenance on protection systems in distribution systems," *Power Delivery, IEEE Transactions on,* vol. 12, pp. 125-133, 1997.

[160] ScottishPower. (27/01/2013). *SECONDARY SUBSTATION INSTALLATION AND COMMISSIONING SPECIFICATION*. Available: http://www.spenergynetworks.co.uk/newconnections/pdf/SUB-02-006%20Issue%205%20Complete.pdf

[161] R. Tarbet, "New distribution control centre-decision making and support," in *Distribution and Transmission Systems (Digest No. 1997/050), IEE Colloquium on Operational Monitoring of*, 1997, pp. 1/1-1/4.

[162] M. T. Skinner, *The C++ primer : a gentle introduction to C++*: New York : Prentice Hall, 1992.

[163] R. E. Barlow, *Statistical theory of reliability and life testing : probability models*: Silver Spring, Md. To Begin With, 1981.

[164] S. Asgarpoor and M. J. Mathine, "Reliability evaluation of distribution systems with nonexponential down times," *Power Systems, IEEE Transactions on,* vol. 12, pp. 579-584, 1997.

[165] C. C. Fong, "Reliability evaluation of transmission and distribution configurations with duration-dependent effects," *Generation, Transmission and Distribution, IEE Proceedings C,* vol. 136, pp. 64-67, 1989.

[166] W. H. Kersting, W. H. Phillips, and R. C. Doyle, "Distribution feeder reliability studies," *Industry Applications, IEEE Transactions on,* vol. 35, pp. 319-323, 1999.

[167] L. Weixing, W. Peng, L. Zhimin, and L. Yingchun, "Reliability evaluation of complex radial distribution systems considering restoration sequence and

network constraints," *Power Delivery, IEEE Transactions on,* vol. 19, pp. 753-758, 2004.

[168] D. Shirmohammadi, "Service restoration in distribution networks via network reconfiguration," *Power Delivery, IEEE Transactions on,* vol. 7, pp. 952-958, 1992.

[169] D. S. Popovic and R. M. Ciric, "A multi-objective algorithm for distribution networks restoration," *Power Delivery, IEEE Transactions on,* vol. 14, pp. 1134-1141, 1999.

[170] Ofgem. (27/01/2013). *Low Carbon Networks Fund* Available: http://www.ofgem.gov.uk/networks/elecdist/lcnf/pages/lcnf.aspx

[171] W. P. Distribution. (27/01/2013). *LV Network Templates for a Low Carbon Future*. Available: http://www.westernpower.co.uk/Renewable-Generation-and-Innovation/Low-Carbon-Networks-Project

[172] S. E. P. Distribution. (27/01/2013). *Thames Valley Vision*. Available: http://www.thamesvalleyvision.co.uk/

[173] ScottishPower. (27/01/2013). *Framework for design and planning for low voltage housing developments underground network installations and associated, new, HV/LV distribution substations*.

[174] V. Detrich, P. Skala, Z. Spacek, and V. Blazek, "Economical Evaluation of Telecontrolled Switches in MV Distribution System Using the Costs of Penalty Payments," in *Probabilistic Methods Applied to Power Systems, 2008. PMAPS '08. Proceedings of the 10th International Conference on*, 2008, pp. 1-6.

[175] A. C. B. Delbem, A. C. P. L. F. de Carvalho, and N. G. Bretas, "Main chain representation for evolutionary algorithms applied to distribution system reconfiguration," *Power Systems, IEEE Transactions on,* vol. 20, pp. 425-436, 2005.

[176] T. Men-Shen and H. Fu-Yuan, "Application of Grey Correlation Analysis in Evolutionary Programming for Distribution System Feeder Reconfiguration," *Power Systems, IEEE Transactions on,* vol. 25, pp. 1126-1133, 2010.

[177] J. Thelin, *Foundations of Qt development*: Berkeley, CA : Apress ; New York : Distributed to the Book trade worldwide by Springer-Verlag New York, 2007.

[178] R. Sedgewick, *Algorithms in C++*: Reading, Mass. : Addison-Wesley, 1998.

[179] IPSA. (27/01/2013). Available: http://www.ipsa-power.com/

[180] *Graphviz*. Available: http://www.graphviz.org/

Appendix A Network model data

Appendix A.1 16-Bus Distribution Network

Appendix A.1.1 Network model Data

Table A-1 Branch impedance data

Branch Name	Bus1 Name	Bus2 Name	Resistance (pu)	Reactance (pu)
1-4	1	4	0.0619835	0.0826446
10-14	10	14	0.330579	0.330579
11-5	11	5	0.0330579	0.0330579
11-9	9	11	0.0909091	0.0909091
13-15	13	15	0.0661157	0.0909091
14-13	13	14	0.0743802	0.0991736
16-15	15	16	0.0330579	0.0330579
2-8	2	8	0.0909091	0.0909091
3-13	3	13	0.0909091	0.0909091
4-5	4	5	0.0661157	0.0909091
4-6	4	6	0.0743802	0.14876
6-7	6	7	0.0330579	0.0330579
7-16	7	16	0.0743802	0.0991736
8-10	8	10	0.0909091	0.0909091
8-9	8	9	0.0661157	0.0909091
9-12	9	12	0.0661157	0.0909091

$S_{base} = 100MVA \;\; V_{base} = 11kV$

Table A-2 Load data

Bus Name	*P*(MW)	*Q*(MVar)
10	1	0.9
11	0.6	0.1
12	4.5	2
13	1	0.9
14	1	0.7
15	1	0.9
16	2.1	1
4	2	1.6
5	3	1.5
6	2	0.8
7	1.5	1.2
8	4	2.7
9	5	3

Appendix A.1.2 Topologies generated in PVO Model

Table A-3 The Open Branches of All PVO Topologies

No.	Open branches		
1	1-4	14-13	2-8
2	1-4	10-14	2-8
3	1-4	2-8	8-10
4	1-4	14-13	8-9
5	1-4	10-14	8-9
6	1-4	8-10	8-9
7	1-4	2-8	8-9
8	1-4	11-9	14-13
9	1-4	10-14	11-9
10	1-4	11-9	8-10
11	1-4	11-9	2-8
12	1-4	11-5	14-13
13	1-4	10-14	11-5
14	1-4	11-5	8-10
15	1-4	11-5	2-8
16	1-4	14-13	4-5
17	1-4	10-14	4-5
18	1-4	4-5	8-10
19	1-4	2-8	4-5
20	14-13	4-6	8-9
21	11-9	14-13	4-6
22	11-5	14-13	4-6
23	14-13	4-5	4-6
24	1-4	14-13	4-6
25	10-14	4-6	8-9
26	10-14	11-9	4-6
27	10-14	11-5	4-6
28	10-14	4-5	4-6
29	1-4	10-14	4-6
30	1-4	4-6	8-10
31	4-5	4-6	8-10
32	11-5	4-6	8-10
33	11-9	4-6	8-10
34	4-6	8-10	8-9
35	14-13	2-8	4-6
36	10-14	2-8	4-6
37	2-8	4-6	8-10
38	2-8	4-6	8-9
39	11-9	2-8	4-6
40	11-5	2-8	4-6
41	2-8	4-5	4-6
42	1-4	2-8	4-6
43	14-13	6-7	8-9
44	11-9	14-13	6-7
45	11-5	14-13	6-7
46	14-13	4-5	6-7
47	1-4	14-13	6-7
48	10-14	6-7	8-9
49	10-14	11-9	6-7
50	10-14	11-5	6-7
51	10-14	4-5	6-7
52	1-4	10-14	6-7
53	1-4	6-7	8-10
54	4-5	6-7	8-10
55	11-5	6-7	8-10
56	11-9	6-7	8-10
57	6-7	8-10	8-9
58	14-13	2-8	6-7
59	10-14	2-8	6-7
60	2-8	6-7	8-10

Continued on next page

…continued from previous page

No.	Open branches		
61	2-8	6-7	8-9
62	11-9	2-8	6-7
63	11-5	2-8	6-7
64	2-8	4-5	6-7
65	1-4	2-8	6-7
66	14-13	7-16	8-9
67	11-9	14-13	7-16
68	11-5	14-13	7-16
69	14-13	4-5	7-16
70	1-4	14-13	7-16
71	10-14	7-16	8-9
72	10-14	11-9	7-16
73	10-14	11-5	7-16
74	10-14	4-5	7-16
75	1-4	10-14	7-16
76	1-4	7-16	8-10
77	4-5	7-16	8-10
78	11-5	7-16	8-10
79	11-9	7-16	8-10
80	7-16	8-10	8-9
81	14-13	2-8	7-16
82	10-14	2-8	7-16
83	2-8	7-16	8-10
84	2-8	7-16	8-9
85	11-9	2-8	7-16
86	11-5	2-8	7-16
87	2-8	4-5	7-16
88	1-4	2-8	7-16
89	14-13	16-15	8-9
90	11-9	14-13	16-15

No.	Open branches		
91	11-5	14-13	16-15
92	14-13	16-15	4-5
93	1-4	14-13	16-15
94	10-14	16-15	8-9
95	10-14	11-9	16-15
96	10-14	11-5	16-15
97	10-14	16-15	4-5
98	1-4	10-14	16-15
99	1-4	16-15	8-10
100	16-15	4-5	8-10
101	11-5	16-15	8-10
102	11-9	16-15	8-10
103	16-15	8-10	8-9
104	14-13	16-15	2-8
105	10-14	16-15	2-8
106	16-15	2-8	8-10
107	16-15	2-8	8-9
108	11-9	16-15	2-8
109	11-5	16-15	2-8
110	16-15	2-8	4-5
111	1-4	16-15	2-8
112	1-4	13-15	2-8
113	13-15	2-8	4-5
114	11-5	13-15	2-8
115	11-9	13-15	2-8
116	13-15	2-8	8-9
117	1-4	13-15	8-10
118	13-15	4-5	8-10
119	11-5	13-15	8-10
120	11-9	13-15	8-10

Continued on next page…

…continued from previous page

No.	Open branches		
121	13-15	8-10	8-9
122	13-15	2-8	8-10
123	10-14	13-15	8-9
124	10-14	11-9	13-15
125	10-14	11-5	13-15
126	10-14	13-15	4-5
127	1-4	10-14	13-15
128	10-14	13-15	2-8
129	13-15	14-13	8-9
130	11-9	13-15	14-13
131	11-5	13-15	14-13
132	13-15	14-13	4-5
133	1-4	13-15	14-13
134	13-15	14-13	2-8
135	1-4	3-13	8-9
136	1-4	11-9	3-13
137	1-4	11-5	3-13
138	1-4	3-13	4-5
139	3-13	4-6	8-9
140	11-9	3-13	4-6
141	11-5	3-13	4-6
142	3-13	4-5	4-6
143	1-4	3-13	4-6
144	3-13	6-7	8-9
145	11-9	3-13	6-7
146	11-5	3-13	6-7
147	3-13	4-5	6-7
148	1-4	3-13	6-7
149	3-13	7-16	8-9
150	11-9	3-13	7-16
151	11-5	3-13	7-16
152	3-13	4-5	7-16
153	1-4	3-13	7-16
154	16-15	3-13	8-9
155	11-9	16-15	3-13

No.	Open branches		
156	11-5	16-15	3-13
157	16-15	3-13	4-5
158	1-4	16-15	3-13
159	13-15	3-13	8-9
160	11-9	13-15	3-13
161	11-5	13-15	3-13
162	13-15	3-13	4-5
163	1-4	13-15	3-13
164	14-13	3-13	8-9
165	11-9	14-13	3-13
166	11-5	14-13	3-13
167	14-13	3-13	4-5
168	1-4	14-13	3-13
169	10-14	3-13	8-9
170	10-14	11-9	3-13
171	10-14	11-5	3-13
172	10-14	3-13	4-5
173	1-4	10-14	3-13
174	1-4	3-13	8-10
175	3-13	4-5	8-10
176	11-5	3-13	8-10
177	11-9	3-13	8-10
178	3-13	8-10	8-9
179	2-8	3-13	4-6
180	2-8	3-13	6-7
181	2-8	3-13	7-16
182	16-15	2-8	3-13
183	13-15	2-8	3-13
184	14-13	2-8	3-13
185	10-14	2-8	3-13
186	2-8	3-13	8-10
187	2-8	3-13	8-9
188	11-9	2-8	3-13
189	11-5	2-8	3-13
190	2-8	3-13	4-5

Appendix A.1.3 Topologies generated in PVC Model

Table A-4 The Open Branches of All PVC Topologies

No.	Open branches		
1	4-5	4-6	8-10
2	11-5	4-6	8-10
3	11-9	4-6	8-10
4	4-6	8-10	8-9
5	10-14	4-5	4-6
6	10-14	11-5	4-6
7	10-14	11-9	4-6
8	10-14	4-6	8-9
9	14-13	4-5	4-6
10	11-5	14-13	4-6
11	11-9	14-13	4-6
12	14-13	4-6	8-9
13	4-5	6-7	8-10
14	11-5	6-7	8-10
15	11-9	6-7	8-10
16	6-7	8-10	8-9
17	10-14	4-5	6-7
18	10-14	11-5	6-7
19	10-14	11-9	6-7
20	10-14	6-7	8-9
21	14-13	4-5	6-7
22	11-5	14-13	6-7
23	11-9	14-13	6-7
24	14-13	6-7	8-9
25	4-5	7-16	8-10
26	11-5	7-16	8-10
27	11-9	7-16	8-10
28	7-16	8-10	8-9
29	10-14	4-5	7-16
30	13-15	14-13	8-9

No.	Open branches		
31	10-14	11-5	7-16
32	10-14	11-9	7-16
33	10-14	7-16	8-9
34	14-13	4-5	7-16
35	11-5	14-13	7-16
36	11-9	14-13	7-16
37	14-13	7-16	8-9
38	16-15	4-5	8-10
39	11-5	16-15	8-10
40	11-9	16-15	8-10
41	16-15	8-10	8-9
42	10-14	16-15	4-5
43	10-14	11-5	16-15
44	10-14	11-9	16-15
45	10-14	16-15	8-9
46	14-13	16-15	4-5
47	11-5	14-13	16-15
48	11-9	14-13	16-15
49	14-13	16-15	8-9
50	13-15	4-5	8-10
51	11-5	13-15	8-10
52	11-9	13-15	8-10
53	13-15	8-10	8-9
54	10-14	13-15	4-5
55	10-14	11-5	13-15
56	10-14	11-9	13-15
57	10-14	13-15	8-9
58	13-15	14-13	4-5
59	11-5	13-15	14-13
60	11-9	13-15	14-13

Appendix A.2 11kV Distribution Network model of Case 2b

Appendix A.2.1 Network model data

Table A-5 Branch impedance data

Branch Name	Bus1 Name	Bus2 Name	Resistance (pu)	Reactance (pu)	Susceptance (pu)
b10-b113	b10	b113	0.122669	0.0359078	2.41E-05
b10-b207	b207	b10	0.0692216	0.0158899	3.98E-05
b100-b123	b100	b123	0.166946	0.0383227	9.59E-05
b101-b175	b101	b175	0.0582589	0.0133734	3.35E-05
b102-b164	b102	b164	0.066128	0.0172326	3.47E-06
b103-b200	b200	b103	0.12347	0.0520628	2.31E-05
b103-b8	b103	b8	0.0573193	0.0131577	3.29E-05
b105-b147	b105	b147	0.178635	0.0489637	0
b106(s)-b116	b106(s)	b116	0.138756	0.0318517	7.97E-05
b106(s)-b171	b106(s)	b171	0.0607647	0.0139486	3.49E-05
b106(s)-b179	b106(s)	b179	0.270309	0.0620497	0.00015534
b106(s)-b63	b106(s)	b63	0.0933396	0.0214262	5.36E-05
b107-b199	b199	b107	0.368097	0.199945	1.01E-05
b108-b112	b108	b112	0.213365	0.0697151	7.24E-05
b109-b87	b109	b87	0.1303	0.0299104	7.49E-05
b11-b132(s)	b132(s)	b11	0.227008	0.0538372	8.96E-05
b110-b203	b110	b203	0.097308	0.068052	0
b111-b110	b111	b110	0.022491	0.015729	0
b113-b14	b14	b113	0.148394	0.0426754	0
b114(s)-b15	b114(s)	b15	0.111381	0.0717138	7.25E-07
b114(s)-b62	b114(s)	b62	0.165847	0.0592327	2.70E-06
b115-b73	b73	b115	0.105242	0.0241584	6.05E-05
b116-b158	b116	b158	0.0927131	0.0212824	5.33E-05
b117-b107	b107	b117	0.0977246	0.0224328	5.62E-05
b118-b44	b118	b44	0.142493	0.0955175	0
b119-b174	b119	b174	0.140685	0.0385617	0
b12-b140	b12	b140	0.229799	0.154041	0
b120-b187	b120	b187	0.0438789	0.0294133	0
b121-b122	b121	b122	0.00281898	0.0006471	1.62E-06
b122-b130	b122	b130	0.0636926	0.0151279	2.46E-05
b124-b174	b174	b124	0.112759	0.0258841	2.53E-05
b124-b75	b124	b75	0.0837606	0.0229587	0
b125-b72	b125	b72	0.129969	0.0748776	0
b126-b76	b76	b126	0.108566	0.0727752	0
b97-b129	b97	b129	0.125418	0.0235883	3.92E-06

Continued on next page

…continued from previous page

b127-b125	b127	b125	0.133446	0.0894529	0
b128-b127	b128	b127	0.228894	0.153434	0
b129-b180	b129	b180	0.0200461	0.0046016	1.15E-05
b13-b202	b13	b202	0.151541	0.101582	0
b131-b35	b35	b131	0.0711009	0.0163213	4.09E-05
b132(s)-b128	b132(s)	b128	0.232945	0.115284	4.94E-06
b132(s)-b145	b132(s)	b145	0.616925	0.150225	0.000335462
b132(s)-b2	b132(s)	b2	0.207352	0.0475978	0.00011916
b132(s)-b46	b132(s)	b46	0.304137	0.0698149	0.00017478
b132(s)-b70	b132(s)	b70	0.0529342	0.0121511	3.04E-05
b132(s)-b78	b132(s)	b78	0.141198	0.0337767	4.96E-05
b132(s)-b94	b132(s)	b94	0.270622	0.0621216	0.00015552
b133-b198	b133	b198	0.272172	0.0953462	0.00164196
b134-b136	b136	b134	0.263726	0.176783	0
b136-b137	b137	b136	0.0235227	0.015768	0
b137-b194	b194	b137	0.296172	0.105304	0
b138-b134	b134	b138	0.341532	0.228939	0
b139-b168	b139	b168	0.0518919	0.0103572	8.57E-07
b140-b205	b140	b205	0.0719252	0.0482136	0
b141-b155	b141	b155	0.165111	0.110679	0
b142-b20	b20	b142	0.0403894	0.0110707	0
b143-b12	b143	b12	0.0796154	0.0533685	0
b144-b133	b144	b133	0.112759	0.025884	6.48E-05
b145-b196	b145	b196	0.048195	0.033705	0
b146-b130	b146	b130	0.19655	0.245684	0
b147-b54	b147	b54	0.00596354	0.0016346	0
b148-b80	b148	b80	0.26248	0.179299	0
b149-b7	b7	b149	0.327282	0.0737793	3.19E-07
b150-b17	b150	b17	0.0680386	0.0186493	0
b151-b64	b64	b151	0.072667	0.0166808	4.18E-05
b152-b95	b152	b95	0.310314	0.0682351	1.05E-07
b156-b201	b201	b156	0.096897	0.0252617	4.99E-06
b157-b84	b84	b157	0.214419	0.143731	0
b158-b108	b158	b108	0.0175403	0.0040264	1.01E-05
b159-b151	b151	b159	0.0306956	0.0070462	1.76E-05
b16-b186	b16	b186	0.191348	0.128266	0
b160-b170	b160	b170	0.0500404	0.0266405	2.46E-06

Continued on next page

…continued from previous page

b190-b9	b190	b9	0.128758	0.035293	0
b191-b90	b191	b90	0.0454169	0.010426	2.61E-05
b160-b59	b59	b160	0.0972574	0.065195	0
b161-b50	b50	b161	0.0820636	0.018838	4.72E-05
b162-b153	b162	b153	0.0900196	0.060343	0
b163-b39	b39	b163	0.0463566	0.010641	2.66E-05
b164-b206	b164	b206	0.0800715	0.023057	0
b165-b111	b165	b111	0.0995192	0.066711	0
b166-b119	b166	b119	0.223013	0.051193	0.00012816
b167-b14	b167	b14	0.0898128	0.023153	6.87E-06
b168-b163	b163	b168	0.121674	0.024729	1.41E-05
b169-b161	b161	b169	0.0617043	0.014164	3.55E-05
b17-b142	b142	b17	0.0786103	0.021547	0
b171-b144	b171	b144	0.122782	0.028185	7.06E-05
b172-b150	b172	b150	0.0601382	0.013805	3.46E-05
b173-b45	b173	b45	0.141375	0.050266	0
b173-b71	b71	b173	0.0319484	0.007334	1.84E-05
b175-b38	b175	b38	0.211704	0.141912	0
b176-b55	b55	b176	0.155695	0.036271	0
b177-b176	b176	b177	0.0966332	0.026264	1.48E-07
b177-b197	b177	b197	0.160702	0.038858	4.81E-05
b178-b33	b33	b178	0.0607197	0.016643	0
b18-b104	b104	b18	0.0651498	0.014955	0
b18-b66	b18	b66	0.171285	0.045972	1.60E-06
b180-b92	b180	b92	0.0675271	0.016581	2.25E-06
b181-b141	b181	b141	0.139155	0.086377	8.35E-07
b182-b138	b138	b182	0.0750918	0.050336	0
b183-b93	b183	b93	0.0859484	0.057614	0
b184-b169	b184	b169	0.111506	0.025596	6.41E-05
b185-b68	b68	b185	0.0927338	0.062162	0
b186-b120	b186	b120	0.0497596	0.033355	0
b187-b189	b187	b189	0.184111	0.123415	0
b188-b89	b188	b89	0.0238047	0.005464	1.37E-05
b189-b208	b189	b208	0.220408	0.135734	1.60E-06
b19-b13	b19	b13	0.184111	0.123415	0
b3-b102	b3	b102	0.127945	0.03507	0
b30-b157	b157	b30	0.0384506	0.025775	0

Continued on next page

…continued from previous page

b30-b85	b30	b85	0.13813	0.0317079	7.94E-05
b31-b143	b31	b143	0.3067	0.20559	0
b192-b139	b192	b139	0.14079	0.0334509	9.60E-07
b193-b114(s)	b114(s)	b193	0.449423	0.102004	0.00012983
b193-b152	b193	b152	0.136723	0.0257926	4.67E-06
b194-b178	b178	b194	0.0560926	0.0376005	0
b195-b99	b195	b99	0.150715	0.0413108	0
b196-b32	b196	b32	0.094554	0.066126	0
b197-b172	b197	b172	0.0830033	0.0190535	4.77E-05
b198-b23	b23	b198	0.103275	0.072225	0
b199-b4	b4	b199	0.231608	0.155254	0
b2-b22	b2	b22	0.25872	0.0593894	0.00014868
b20-b30	b30	b20	0.100876	0.0676203	0
b201-b209	b209	b201	0.160074	0.0426623	2.64E-06
b202-b77	b202	b77	0.090472	0.060646	0
b203-b112	b112	b203	0.323317	0.206834	2.44E-06
b204-b126	b126	b204	0.0603896	0.0257529	3.12E-07
b205-b52	b205	b52	0.0379982	0.0254713	0
b206-b156	b206	b156	0.0713972	0.0206793	0
b207-b132(s)	b132(s)	b207	0.139927	0.0340285	3.90E-05
b208-b101	b208	b101	0.0474978	0.0318391	0
b209-b53	b53	b209	0.0333574	0.00660335	0
b21-b5	b21	b5	0.0520214	0.0348714	0
b210-b123	b210	b123	0.1303	0.0299104	7.49E-05
b22-b29	b22	b29	0.145334	0.0333616	8.35E-05
b23-b67	b67	b23	0.139995	0.097905	0
b24-b21	b24	b21	0.19542	0.130995	0
b26-b25	b26	b25	0.113699	0.0260997	6.53E-05
b27-b91	b27	b91	0.031322	0.00719	0
b28-b15	b15	b28	0.051867	0.036273	0
b28-b200	b28	b200	0.112111	0.0494862	0
b29-b6	b29	b6	0.0410318	0.0094189	2.36E-05
b29-b60	b29	b60	0.0711009	0.0163213	4.09E-05
b50-b117	b117	b50	0.0541871	0.0124387	3.11E-05
b51-b100	b51	b100	0.428815	0.107394	0.000118821
b51-b115	b115	b51	0.172584	0.0396169	9.92E-05
b52-b154	b52	b154	0.0868531	0.0582202	0

Continued on next page

…continued from previous page

b98-b48	b98	b48	0.683328	0.0180044	2.00E-06
b99-b3	b99	b3	0.0498769	0.0136712	0
b31-b61	b61	b31	0.171897	0.115227	0
b32-b121	b32	b121	0.10719	0.0270087	1.51E-05
b32-b81	b32	b81	0.113832	0.079608	0
b33-b41	b33	b41	0.114418	0.055009	0
b33-b42	b42	b33	0.050212	0.0336585	0
b34-b135	b135	b34	0.75811	0.464671	0
b34-b24	b34	b24	0.195872	0.131299	0
b35-b149	b149	b35	0.080858	0.0636288	0
b35-b191	b35	b191	0.14784	0.0339368	8.50E-05
b36-b11	b36	b11	0.0353939	0.0081247	2.03E-05
b36-b135	b36	b135	0.278635	0.0584276	1.53E-05
b36-b173	b173	b36	0.097531	0.0346773	0
b37-b78	b78	b37	0.177362	0.0421268	6.86E-05
b38-b118	b38	b118	0.051569	0.0345682	0
b39-b47(s)	b47(s)	b39	0.117559	0.0221749	4.00E-06
b4-b114(s)	b114(s)	b4	0.0882102	0.0591299	0
b40-b204	b204	b40	0.196132	0.106263	1.10E-05
b41-b181	b41	b181	0.108566	0.0727752	0
b42-b40	b40	b42	0.0591986	0.0135891	3.40E-05
b43-b131	b43	b131	0.1134	0.0242885	0
b44-b162	b44	b162	0.0434266	0.0291101	0
b46-b146	b46	b146	0.228894	0.153434	0
b47(s)-b167	b47(s)	b167	0.0377747	0.0099633	1.16E-06
b47(s)-b53	b47(s)	b53	0.163194	0.0286454	0
b47(s)-b97	b47(s)	b97	0.0645876	0.0160146	1.26E-06
b47(s)-b98	b47(s)	b98	0.046624	0.0127796	0
b48-b43	b48	b43	0.0884916	0.0210741	3.31E-05
b49-b16	b49	b16	0.045236	0.030323	0
b5-b165	b5	b165	0.0465931	0.0312327	0
b84-b31	b31	b84	0.18461	0.105921	9.36E-09
b85-b105	b85	b105	0.0235227	0.015768	0
b86-b166	b86	b166	0.300691	0.069024	0.0001728
b87-b210	b87	b210	0.108061	0.0248055	6.21E-05
b88-b49	b88	b49	0.0217133	0.014555	0
b89-b83	b89	b83	0.0867801	0.020005	4.77E-05

Continued on next page

…continued from previous page

b54-b56	b54	b56	0.020582	0.025728	0
b55-b80	b80	b55	0.272688	0.123012	3.55E-05
b56-b1	b56	b1	0.036189	0.024258	0
b57-b182	b182	b57	0.118066	0.079143	0
b58-b65	b65	b58	0.102686	0.068833	0
b59-b34	b34	b59	0.253774	0.170112	0
b6-b86	b6	b86	0.109314	0.025093	6.28E-05
b61-b185	b185	b61	0.50981	0.34174	0
b62-b192	b62	b192	0.057736	0.022145	0
b63-b184	b63	b184	0.041345	0.009491	2.38E-05
b64-b96	b96	b64	0.105555	0.02423	6.07E-05
b65-b57	b57	b65	0.08821	0.05913	0
b66-b74	b74	b66	0.194383	0.061561	0
b67-b28	b28	b67	0.133569	0.093411	0
b68-b58	b58	b68	0.138875	0.093092	0
b69-b25	b69	b25	0.062844	0.015356	1.61E-05
b69-b70	b70	b69	0.079871	0.018335	4.59E-05
b7-b114(s)	b114(s)	b7	0.291861	0.072757	0
b71-b132(s)	b132(s)	b71	0.170502	0.040274	7.08E-05
b72-b74	b72	b74	0.092164	0.025262	0
b73-b114(s)	b114(s)	b73	0.070788	0.016249	4.07E-05
b75-b159	b159	b75	0.169139	0.038826	9.72E-05
b76-b170	b170	b76	0.047045	0.031536	0
b77-b88	b77	b88	0.04795	0.032142	0
b79-b104	b79	b104	0.288736	0.067911	0.000126
b79-b123	b123	b79	0.408723	0.095358	0.000197
b8-b183	b8	b183	0.097856	0.026822	0
b81-b148	b81	b148	0.063342	0.044298	0
b82-b190	b82	b190	0.145111	0.03831	4.25E-06
b82-b95	b95	b82	0.160373	0.038819	1.87E-05
b83-b19	b83	b19	0.074639	0.050033	0
b9-b37	b9	b37	0.097856	0.026822	0
b90-b109	b90	b109	0.137514	0.038559	1.65E-05
b91-b26	b91	b26	0.091774	0.021067	5.27E-05
b92-b27	b92	b27	0.175532	0.03474	3.84E-06
b93-b188	b93	b188	0.06514	0.043665	0
b94-b195	b94	b195	0.211392	0.04181	2.07E-05
b96-b179	b179	b96	0.078305	0.017975	4.50E-05
b97-b129	b97	b129	0.125418	0.023588	3.92E-06

$S_{base} = 100MVA \quad V_{base} = 11kV$

Table A-6 Load data

Bus	P(MW)	Q(MVAr)
b10	0.447	0.147
b100	0.057	0.019
b101	0.012	0.002
b102	0.219	0.072
b103	0.133	0.044
b104	0.309	0.101
b105	0.168	0.034
b107	0.185	0.061
b108	0.154	0.051
b109	0.059	0.02
b11	2.09	0.69
b110	0.013	0.003
b111	0.015	0.003
b112	0.204	0.067
b113	0.181	0.059
b115	0.131	0.043
b116	0.107	0.035
b117	0.128	0.042
b118	0.022	0.004
b119	0.157	0.052
b12	0.026	0.005
b120	0.004	0.001
b121	0.309	0.063
b122	0.309	0.063
b123	0.458	0.15
b124	0.128	0.042
b125	0.005	0.001
b126	0.387	0.079
b127	0.057	0.019
b128	0.057	0.019
b129	0.257	0.084
b13	0.015	0.003
b130	0.995	0.32
b131	0.38	0.125
b133	0.546	0.18
b134	0.266	0.054
b135	0.899	0.295
b136	0.004	0.001
b137	0.176	0.036
b138	0.001	0
b139	0.114	0.037
b14	0.2	0.066
b140	0.004	0.001
b141	0.029	0.006
b142	0.176	0.036
b143	0.038	0.008
b144	0.392	0.129
b145	0.007	0.001
b146	0.005	0.001
b147	0.071	0.014
b148	0.007	0.001
b149	0.195	0.064
b15	0.014	0.005
b150	0.147	0.03
b151	0.143	0.047
b152	0.368	0.121
b5	0.001	0
b50	0.342	0.112
b51	0.1	0.033
b156	0.47	0.155
b157	0.015	0.003
b158	0.228	0.075
b159	0.029	0.006
b16	0.007	0.001
b160	0.007	0.001
b161	0.423	0.139
b162	0.004	0.001
b163	0.295	0.097

Continued on next page

…continued from previous page

b164	0.162	0.053
b165	0.005	0.001
b166	0.371	0.122
b167	0.75	0.25
b168	0.297	0.098
b169	0.59	0.174
b17	0.088	0.018
b171	0.402	0.134
b172	0.029	0.006
b173	0.057	0.019
b174	0.114	0.037
b175	0.029	0.006
b176	0.142	0.029
b177	0.255	0.052
b178	0.109	0.022
b179	1.254	0.412
b18	0.285	0.094
b180	0.247	0.081
b181	0.029	0.006
b182	0.007	0.001
b183	0.029	0.006
b184	0.114	0.037
b185	0.466	0.095
b186	0.007	0.001
b187	0.007	0.001
b188	0.059	0.012
b189	0.009	0.002
b19	0.009	0.002
b190	0.328	0.108
b191	0.273	0.09
b192	0.062	0.02
b193	0.295	0.097
b194	0.001	0
b195	0.276	0.091
b47(s)	0.485	0.159
b48	0.432	0.142
b49	0.004	0.001
b199	0.007	0.002
b2	0.314	0.103
b20	0.059	0.012
b200	0.004	0.001
b201	0.368	0.121
b202	0.007	0.001
b203	0.101	0.021
b204	0.159	0.032
b205	0.019	0.004
b206	0.314	0.103
b207	0.371	0.122
b208	0.001	0
b209	0.204	0.067
b21	0.015	0.003
b210	0.333	0.109
b22	0.385	0.126
b23	0.029	0.009
b24	0.138	0.028
b25	0.846	0.278
b26	0.261	0.086
b27	0.22	0.073
b3	0.314	0.103
b36	0	0
b37	0.228	0.075
b38	0.005	0.001
b39	0.166	0.055
b4	0.057	0.019
b40	0.184	0.037
b41	0.004	0.001
b42	0.059	0.012
b43	0.47	0.155

Continued on next page

…continued from previous page

b52	0.034	0.007
b53	0.428	0.141
b54	0.007	0.001
b55	0.382	0.078
b56	0.029	0.006
b57	0.368	0.075
b58	0.029	0.006
b59	0.076	0.016
b6	0.399	0.131
b60	0.295	0.097
b61	0.015	0.003
b62	0.185	0.061
b63	0.458	0.151
b64	0.162	0.053
b65	0.059	0.012
b66	0.261	0.086
b67	0.005	0.001
b68	0	0
b69	0.356	0.117
b7	0.233	0.077
b70	0.143	0.047
b71	0.014	0.005
b72	0.119	0.039
b73	0.157	0.052
b74	0.048	0.016
b75	0.114	0.037
b76	0.075	0.015
b77	0.005	0.001
b78	0.273	0.09
b79	0.209	0.069
b8	0.157	0.052
b80	0.201	0.041
b81	0.029	0.006
b82	0.228	0.075
b83	0.029	0.006
b84	0.029	0.006
b85	0.015	0.003
b86	0.119	0.039
b87	0.147	0.048
b88	0	0
b89	0.029	0.006
b9	0.223	0.073
b90	0.1	0.033
b91	0.214	0.07
b92	0.413	0.136
b93	0.169	0.034
b94	0.223	0.073
b95	0.271	0.089
b96	0.214	0.07
b97	0.442	0.145
b98	0.371	0.122
b99	0.166	0.055

Appendix A.2.2 $P_{loss-TOG}$ and $P_{loss-SEP}$ of output topologies

Table A-7 Difference between $P_{loss-TOG}$ and $P_{loss-SEP}$

TopoID	$P_{loss-TOG}$	$P_{loss-SEP}$	Difference%
1	0.48295	0.48034	0.0054
2	0.48295	0.48034	0.0054
3	0.48310	0.48039	0.0056
4	0.48310	0.48039	0.0056
5	0.48320	0.48059	0.0054
6	0.48320	0.48059	0.0054
7	0.48320	0.48059	0.0054
8	0.48320	0.48059	0.0054
9	0.48330	0.48069	0.0054
10	0.48330	0.48069	0.0054
11	0.48334	0.48073	0.0054
12	0.48334	0.48073	0.0054
13	0.48335	0.48049	0.0059
14	0.48335	0.48049	0.0059
15	0.48335	0.48064	0.0056
16	0.48335	0.48064	0.0056
17	0.48335	0.48065	0.0056
18	0.48335	0.48065	0.0056
19	0.48345	0.48084	0.0054
20	0.48345	0.48084	0.0054
21	0.48345	0.48074	0.0056
22	0.48345	0.48074	0.0056
23	0.48349	0.48078	0.0056
24	0.48349	0.48078	0.0056
25	0.48350	0.48055	0.0061
26	0.48350	0.48055	0.0061
27	0.48355	0.48093	0.0054
28	0.48355	0.48093	0.0054
29	0.48355	0.48094	0.0054
30	0.48355	0.48094	0.0054
31	0.48359	0.48098	0.0054
32	0.48359	0.48098	0.0054
33	0.48359	0.48098	0.0054
34	0.48359	0.48098	0.0054
35	0.48360	0.48074	0.0059

Continued on next page

…continued from previous page

36	0.48360	0.48074	0.00590
37	0.48360	0.48075	0.00589
38	0.48360	0.48075	0.00589
39	0.48360	0.48090	0.00560
40	0.48360	0.48090	0.00560
41	0.48369	0.48107	0.00542
42	0.48369	0.48107	0.00542
43	0.48370	0.48084	0.00591
44	0.48370	0.48084	0.00591
45	0.48370	0.48099	0.00561
46	0.48370	0.48099	0.00561
47	0.48370	0.48099	0.00560
48	0.48370	0.48099	0.00560
49	0.48374	0.48088	0.00591
50	0.48374	0.48088	0.00591
51	0.48374	0.48103	0.00561
52	0.48374	0.48103	0.00561
53	0.48374	0.48103	0.00560
54	0.48374	0.48103	0.00560
55	0.48375	0.48079	0.00610
56	0.48375	0.48079	0.00610
57	0.48375	0.48080	0.00609
58	0.48375	0.48080	0.00609
59	0.48380	0.48119	0.00541
60	0.48380	0.48119	0.00541
61	0.48384	0.48123	0.00540
62	0.48384	0.48123	0.00540
63	0.48384	0.48112	0.00562
64	0.48384	0.48112	0.00562
65	0.48385	0.48100	0.00589
66	0.48385	0.48100	0.00589
67	0.48385	0.48089	0.00611
68	0.48385	0.48089	0.00611
69	0.48388	0.48124	0.00546
70	0.48388	0.48124	0.00546
71	0.48389	0.48093	0.00610
72	0.48389	0.48093	0.00610

Continued on next page

…continued from previous page

73	0.48394	0.48132	0.00542
74	0.48394	0.48132	0.00542
75	0.48394	0.48132	0.00541
76	0.48394	0.48132	0.00541
77	0.48395	0.48109	0.00591
78	0.48395	0.48109	0.00591
79	0.48395	0.48109	0.00590
80	0.48395	0.48109	0.00590
81	0.48395	0.48124	0.00560
82	0.48395	0.48124	0.00560
83	0.48399	0.48113	0.00591
84	0.48399	0.48113	0.00591
85	0.48399	0.48113	0.00590
86	0.48399	0.48113	0.00590
87	0.48399	0.48128	0.00560
88	0.48399	0.48128	0.00560
89	0.48399	0.48105	0.00609
90	0.48399	0.48105	0.00609
91	0.48403	0.48129	0.00566
92	0.48403	0.48129	0.00566
93	0.48409	0.48122	0.00592
94	0.48409	0.48122	0.00592
95	0.48409	0.48137	0.00562
96	0.48409	0.48137	0.00562
97	0.48409	0.48138	0.00561
98	0.48409	0.48138	0.00561
99	0.48409	0.48114	0.00611
100	0.48409	0.48114	0.00611

Appendix A.3 10-Bus Network Model Data

Table A-8 Branch reliability data

Branch Name	Bus1 Name	Bus2 Name	Fault rate (int/yr.km)	Repair time (hours)	Length (Km)
1-2	1	2	0.1	4	1
1-A	1	A	0.2	2	1
2-3	2	3	0.1	4	3
2-B	2	B	0.2	2	3
3-4	3	4	0.1	4	2
3-C	3	C	0.2	2	2
4-D	4	D	0.2	2	1
4-S2	4	S2	0.1	4	1
S1-1	S1	1	0.1	4	2

Table A-9 Protection device data

Bus name	Branch Name	Device name	Device type	Mean time to switch (hours)	Mean time to repair (hours)
S1	S1-1	CB	Circuit Breaker	0	1
1	1-A	F1	Fuse	0	1
2	2-B	F2	Fuse	0	1
3	3-C	F3	Fuse	0	1
4	4-D	F4	Fuse	0	1

Table A-10 Manual switch data

Branch Name	Bus1 name	Manual switch connected to bus1	Mean time to switch (hours)	Bus2 name	Manual switch connected to bus2	Mean time to switch (hours)
1-2	1	TRUE	0.5	2	FALSE	-
1-A	1	FALSE	-	A	FALSE	-
2-3	2	TRUE	0.5	3	FALSE	-
2-B	2	FALSE	-	B	FALSE	-
3-4	3	TRUE	0.5	4	FALSE	-
3-C	3	FALSE	-	C	FALSE	-
4-D	4	FALSE	-	D	FALSE	-
4-S2	4	TRUE	0	S2	FALSE	-
S1-1	S1	FALSE	-	1	FALSE	-

Table A-11 Customer Number of each load point

Bus Name	Customer number
A	1000
B	800
C	700
D	500

Appendix A.4 26-Bus Network Model Data

Appendix A.4.1 Network model data

Table A-12 Branch reliability data

Branch Name	Fault rate (int/yr.km)	Repair time (Hours)	Length (Km)
3	0.058	3	1
2	0.064	3	1
20	0.096	3	1
21	0.083	3	1
5	0.026	3	1
4	0.045	3	1
23	0.022	3	1
24	0.044	3	1
7	0.026	3	1
6	0.064	3	1
9	0.077	3	1
8	0.07	3	1
10	0.102	3	1
15	0.032	3	1
12	0.077	3	1
11	0.192	3	1
13	0.032	3	1
14	0.256	3	1
17	0.09	3	1
16	0.019	3	1
19	0.147	3	0.5
18	0.166	3	1
191	0.147	3	0.5
LP12-SP2	0	3	1
1	0.083	3	1
22	0.067	3	1

Table A-13 Protection and remote control devices data

Bus name	Branch Name	Device Name	Device type	Mean time to switch (hours)	Mean time to repair (hours)
3	7	R1	RCSwitch	0.011111	1
5	10	R2	RCSwitch	0.011111	1
5	15	R3	RCSwitch	0.011111	1
8	17	R4	RCSwitch	0.011111	1
11	191	R5	RCSwitch	0.011111	1
LP12	LP12-SP2	R6	RCSwitch	0.011111	1
SP1	1	B1	Circuit Breaker	0.011111	1
SP1	22	B2	Circuit Breaker	0	1

Table A-14 Customer Number of each load point

Bus Name	Customer Number
LP1	20
LP10	11
LP11	7
LP12	6
LP13	24
LP14	4
LP2	4
LP3	9
LP4	4
LP5	15
LP6	11
LP7	25
LP8	43
LP9	33

Appendix A.4.2 Fault Events of Load Points

System Indices | Load indices | Bus fault records

Fault Event	fault duration [hours/minus]	fault rate	Record in CI/CML
Feede-22			
[bus: LP14]	0.399	0.133	
1-[bran: 22]	3	0.067	Y
2-[bran: 24]	3	0.044	Y
3-[bran: 23]	3	0.022	Y
[bus: LP13]	0.399	0.133	
1-[bran: 22]	3	0.067	Y
2-[bran: 24]	3	0.044	Y
3-[bran: 23]	3	0.022	Y
Feede-1			
[bus: LP1]	1.05256	1.805	
1-[bran: 1]	3	0.083	Y
2-[bran: 2]	3	0.064	Y
3-[bran: 3]	3	0.058	Y
4-[bran: 4]	3	0.045	Y
5-[bran: 5]	3	0.026	Y
6-[bran: 6]	3	0.064	Y
7-[bran: 7]	0.0222222	0.026	Y
8-[bran: 8]	0.0222222	0.07	Y
9-[bran: 9]	0.0222222	0.077	Y
10-[bran: 15]	0.0222222	0.032	Y
11-[bran: 16]	0.0222222	0.019	Y
12-[bran: 10]	0.0222222	0.102	Y
13-[bran: 11]	0.0222222	0.192	Y
14-[bran: 12]	0.0222222	0.077	Y
15-[bran: 14]	0.0222222	0.256	Y
16-[bran: 13]	0.0222222	0.032	Y
17-[bran: 17]	0.0222222	0.09	Y
18-[bran: 18]	0.0222222	0.166	Y
19-[bran: 19]	0.0222222	0.0735	Y
20-[bran: 191]	0.0222222	0.0735	Y
21-[bran: 21]	0.0222222	0.083	Y
22-[bran: 20]	0.0222222	0.096	Y

Figure A.1 Fault events of load points-Part 1

Fault Event	fault duration [hours/minus]	fault rate	Record in CI/CML
[bus: LP2]	1.05256	1.805	
1-[bran: 1]	3	0.083	Y
2-[bran: 2]	3	0.064	Y
3-[bran: 3]	3	0.058	Y
4-[bran: 4]	3	0.045	Y
5-[bran: 5]	3	0.026	Y
6-[bran: 6]	3	0.064	Y
7-[bran: 7]	0.0222222	0.026	Y
8-[bran: 8]	0.0222222	0.07	Y
9-[bran: 9]	0.0222222	0.077	Y
10-[bran: 15]	0.0222222	0.032	Y
11-[bran: 16]	0.0222222	0.019	Y
12-[bran: 10]	0.0222222	0.102	Y
13-[bran: 11]	0.0222222	0.192	Y
14-[bran: 12]	0.0222222	0.077	Y
15-[bran: 14]	0.0222222	0.256	Y
16-[bran: 13]	0.0222222	0.032	Y
17-[bran: 17]	0.0222222	0.09	Y
18-[bran: 18]	0.0222222	0.166	Y
19-[bran: 19]	0.0222222	0.0735	Y
20-[bran: 191]	0.0222222	0.0735	Y
21-[bran: 21]	0.0222222	0.083	Y
22-[bran: 20]	0.0222222	0.096	Y
[bus: LP3]	1.05256	1.805	
1-[bran: 1]	3	0.083	Y
2-[bran: 2]	3	0.064	Y
3-[bran: 3]	3	0.058	Y
4-[bran: 4]	3	0.045	Y
5-[bran: 5]	3	0.026	Y
6-[bran: 6]	3	0.064	Y
7-[bran: 7]	0.0222222	0.026	Y
8-[bran: 8]	0.0222222	0.07	Y
9-[bran: 9]	0.0222222	0.077	Y
10-[bran: 15]	0.0222222	0.032	Y
11-[bran: 16]	0.0222222	0.019	Y
12-[bran: 10]	0.0222222	0.102	Y
13-[bran: 11]	0.0222222	0.192	Y
14-[bran: 12]	0.0222222	0.077	Y
15-[bran: 14]	0.0222222	0.256	Y
16-[bran: 13]	0.0222222	0.032	Y
17-[bran: 17]	0.0222222	0.09	Y

Figure A.2 Fault events of load points -Part 2

Fault Event	fault duration [hours/minus]	fault rate	Record in CI/CML
18-[bran: 18]	0.0222222	0.166	Y
19-[bran: 19]	0.0222222	0.0735	Y
20-[bran: 191]	0.0222222	0.0735	Y
21-[bran: 21]	0.0222222	0.083	Y
22-[bran: 20]	0.0222222	0.096	Y
[bus: LP4]	0.555267	1.805	
1-[bran: 1]	0.0222222	0.083	Y
2-[bran: 2]	0.0222222	0.064	Y
3-[bran: 3]	0.0222222	0.058	Y
4-[bran: 4]	0.0222222	0.045	Y
5-[bran: 5]	0.0222222	0.026	Y
6-[bran: 6]	0.0222222	0.064	Y
7-[bran: 7]	3	0.026	Y
8-[bran: 8]	3	0.07	Y
9-[bran: 9]	3	0.077	Y
10-[bran: 15]	0.0222222	0.032	Y
11-[bran: 16]	0.0222222	0.019	Y
12-[bran: 10]	0.0222222	0.102	Y
13-[bran: 11]	0.0222222	0.192	Y
14-[bran: 12]	0.0222222	0.077	Y
15-[bran: 14]	0.0222222	0.256	Y
16-[bran: 13]	0.0222222	0.032	Y
17-[bran: 17]	0.0222222	0.09	Y
18-[bran: 18]	0.0222222	0.166	Y
19-[bran: 19]	0.0222222	0.0735	Y
20-[bran: 191]	0.0222222	0.0735	Y
21-[bran: 21]	0.0222222	0.083	Y
22-[bran: 20]	0.0222222	0.096	Y
[bus: LP8]	0.191978	1.805	
1-[bran: 1]	0.0222222	0.083	Y
2-[bran: 2]	0.0222222	0.064	Y
3-[bran: 3]	0.0222222	0.058	Y
4-[bran: 4]	0.0222222	0.045	Y
5-[bran: 5]	0.0222222	0.026	Y
6-[bran: 6]	0.0222222	0.064	Y
7-[bran: 7]	0.0222222	0.026	Y
8-[bran: 8]	0.0222222	0.07	Y
9-[bran: 9]	0.0222222	0.077	Y
10-[bran: 15]	3	0.032	Y
11-[bran: 16]	3	0.019	Y

Figure A.3 Load points report-Part 3

System Indices | Load indices | Bus fault records

Fault Event	fault duration [hours/minus]	fault rate	Record in CI/CML
12-[bran: 10]	0.0222222	0.102	Y
13-[bran: 11]	0.0222222	0.192	Y
14-[bran: 12]	0.0222222	0.077	Y
15-[bran: 14]	0.0222222	0.256	Y
16-[bran: 13]	0.0222222	0.032	Y
17-[bran: 17]	0.0222222	0.09	Y
18-[bran: 18]	0.0222222	0.166	Y
19-[bran: 19]	0.0222222	0.0735	Y
20-[bran: 191]	0.0222222	0.0735	Y
21-[bran: 21]	0.0222222	0.083	Y
22-[bran: 20]	0.0222222	0.096	Y
[bus: LP5]	2.51762	1.805	
1-[bran: 1]	0.0222222	0.083	Y
2-[bran: 2]	0.0222222	0.064	Y
3-[bran: 3]	0.0222222	0.058	Y
4-[bran: 4]	0.0222222	0.045	Y
5-[bran: 5]	0.0222222	0.026	Y
6-[bran: 6]	0.0222222	0.064	Y
7-[bran: 7]	3	0.026	Y
8-[bran: 8]	3	0.07	Y
9-[bran: 9]	3	0.077	Y
10-[bran: 15]	0.0222222	0.032	Y
11-[bran: 16]	0.0222222	0.019	Y
12-[bran: 10]	3	0.102	Y
13-[bran: 11]	3	0.192	Y
14-[bran: 12]	3	0.077	Y
15-[bran: 14]	3	0.256	Y
16-[bran: 13]	3	0.032	Y
17-[bran: 17]	0.0222222	0.09	Y
18-[bran: 18]	0.0222222	0.166	Y
19-[bran: 19]	0.0222222	0.0735	Y
20-[bran: 191]	0.0222222	0.0735	Y
21-[bran: 21]	0.0222222	0.083	Y
22-[bran: 20]	0.0222222	0.096	Y
[bus: LP9]	1.24016	1.805	
1-[bran: 1]	0.0222222	0.083	Y
2-[bran: 2]	0.0222222	0.064	Y
3-[bran: 3]	0.0222222	0.058	Y
4-[bran: 4]	0.0222222	0.045	Y
5-[bran: 5]	0.0222222	0.026	Y

Figure A.4 Fault events of load points -Part 4

System Indices | Load indices | Bus fault records

Fault Event	fault duration [hours/minus]	fault rate	Record in CI/CML
6-[bran: 6]	0.0222222	0.064	Y
7-[bran: 7]	0.0222222	0.026	Y
8-[bran: 8]	0.0222222	0.07	Y
9-[bran: 9]	0.0222222	0.077	Y
10-[bran: 15]	0.0222222	0.032	Y
11-[bran: 16]	0.0222222	0.019	Y
12-[bran: 10]	0.0222222	0.102	Y
13-[bran: 11]	0.0222222	0.192	Y
14-[bran: 12]	0.0222222	0.077	Y
15-[bran: 14]	0.0222222	0.256	Y
16-[bran: 13]	0.0222222	0.032	Y
17-[bran: 17]	3	0.09	Y
18-[bran: 18]	3	0.166	Y
19-[bran: 19]	3	0.0735	Y
20-[bran: 191]	3	0.0735	Y
21-[bran: 21]	0.0222222	0.083	Y
22-[bran: 20]	0.0222222	0.096	Y
[bus: LP10]	1.24016	1.805	
1-[bran: 1]	0.0222222	0.083	Y
2-[bran: 2]	0.0222222	0.064	Y
3-[bran: 3]	0.0222222	0.058	Y
4-[bran: 4]	0.0222222	0.045	Y
5-[bran: 5]	0.0222222	0.026	Y
6-[bran: 6]	0.0222222	0.064	Y
7-[bran: 7]	0.0222222	0.026	Y
8-[bran: 8]	0.0222222	0.07	Y
9-[bran: 9]	0.0222222	0.077	Y
10-[bran: 15]	0.0222222	0.032	Y
11-[bran: 16]	0.0222222	0.019	Y
12-[bran: 10]	0.0222222	0.102	Y
13-[bran: 11]	0.0222222	0.192	Y
14-[bran: 12]	0.0222222	0.077	Y
15-[bran: 14]	0.0222222	0.256	Y
16-[bran: 13]	0.0222222	0.032	Y
17-[bran: 17]	3	0.09	Y
18-[bran: 18]	3	0.166	Y
19-[bran: 19]	3	0.0735	Y
20-[bran: 191]	3	0.0735	Y
21-[bran: 21]	0.0222222	0.083	Y
22-[bran: 20]	0.0222222	0.096	Y

Figure A.5 Fault events of load points -Part 5

System Indices | Load indices | Bus fault records

Fault Event	fault duration [hours/minus]	fault rate	Record in CI/CML
[bus: LP7]	2.51762	1.805	
1-[bran: 1]	0.0222222	0.083	Y
2-[bran: 2]	0.0222222	0.064	Y
3-[bran: 3]	0.0222222	0.058	Y
4-[bran: 4]	0.0222222	0.045	Y
5-[bran: 5]	0.0222222	0.026	Y
6-[bran: 6]	0.0222222	0.064	Y
7-[bran: 7]	3	0.026	Y
8-[bran: 8]	3	0.07	Y
9-[bran: 9]	3	0.077	Y
10-[bran: 15]	0.0222222	0.032	Y
11-[bran: 16]	0.0222222	0.019	Y
12-[bran: 10]	3	0.102	Y
13-[bran: 11]	3	0.192	Y
14-[bran: 12]	3	0.077	Y
15-[bran: 14]	3	0.256	Y
16-[bran: 13]	3	0.032	Y
17-[bran: 17]	0.0222222	0.09	Y
18-[bran: 18]	0.0222222	0.166	Y
19-[bran: 19]	0.0222222	0.0735	Y
20-[bran: 191]	0.0222222	0.0735	Y
21-[bran: 21]	0.0222222	0.083	Y
22-[bran: 20]	0.0222222	0.096	Y
[bus: LP6]	2.51762	1.805	
1-[bran: 1]	0.0222222	0.083	Y
2-[bran: 2]	0.0222222	0.064	Y
3-[bran: 3]	0.0222222	0.058	Y
4-[bran: 4]	0.0222222	0.045	Y
5-[bran: 5]	0.0222222	0.026	Y
6-[bran: 6]	0.0222222	0.064	Y
7-[bran: 7]	3	0.026	Y
8-[bran: 8]	3	0.07	Y
9-[bran: 9]	3	0.077	Y
10-[bran: 15]	0.0222222	0.032	Y
11-[bran: 16]	0.0222222	0.019	Y
12-[bran: 10]	3	0.102	Y
13-[bran: 11]	3	0.192	Y
14-[bran: 12]	3	0.077	Y
15-[bran: 14]	3	0.256	Y

Figure A.6 Fault events of load points -Part 6

Fault Event	fault duration [hours/minus]	fault rate	Record in CI/CML
16-[bran: 13]	3	0.032	Y
17-[bran: 17]	0.0222222	0.09	Y
18-[bran: 18]	0.0222222	0.166	Y
19-[bran: 19]	0.0222222	0.0735	Y
20-[bran: 191]	0.0222222	0.0735	Y
21-[bran: 21]	0.0222222	0.083	Y
22-[bran: 20]	0.0222222	0.096	Y
[bus: LP12]	0.573133	1.805	
1-[bran: 1]	0.0222222	0.083	Y
2-[bran: 2]	0.0222222	0.064	Y
3-[bran: 3]	0.0222222	0.058	Y
4-[bran: 4]	0.0222222	0.045	Y
5-[bran: 5]	0.0222222	0.026	Y
6-[bran: 6]	0.0222222	0.064	Y
7-[bran: 7]	0.0222222	0.026	Y
8-[bran: 8]	0.0222222	0.07	Y
9-[bran: 9]	0.0222222	0.077	Y
10-[bran: 15]	0.0222222	0.032	Y
11-[bran: 16]	0.0222222	0.019	Y
12-[bran: 10]	0.0222222	0.102	Y
13-[bran: 11]	0.0222222	0.192	Y
14-[bran: 12]	0.0222222	0.077	Y
15-[bran: 14]	0.0222222	0.256	Y
16-[bran: 13]	0.0222222	0.032	Y
17-[bran: 17]	0.0222222	0.09	Y
18-[bran: 18]	0.0222222	0.166	Y
19-[bran: 19]	0.0222222	0.0735	Y
20-[bran: 191]	0.0222222	0.0735	Y
21-[bran: 21]	3	0.083	Y
22-[bran: 20]	3	0.096	Y
[bus: LP11]	0.573133	1.805	
1-[bran: 1]	0.0222222	0.083	Y
2-[bran: 2]	0.0222222	0.064	Y
3-[bran: 3]	0.0222222	0.058	Y
4-[bran: 4]	0.0222222	0.045	Y
5-[bran: 5]	0.0222222	0.026	Y
6-[bran: 6]	0.0222222	0.064	Y
7-[bran: 7]	0.0222222	0.026	Y
8-[bran: 8]	0.0222222	0.07	Y
9-[bran: 9]	0.0222222	0.077	Y
10-[bran: 15]	0.0222222	0.032	Y

Figure A.7 Fault events of load points -Part 7

11-[bran: 16]	0.0222222	0.019	Y
12-[bran: 10]	0.0222222	0.102	Y
13-[bran: 11]	0.0222222	0.192	Y
14-[bran: 12]	0.0222222	0.077	Y
15-[bran: 14]	0.0222222	0.256	Y
16-[bran: 13]	0.0222222	0.032	Y
17-[bran: 17]	0.0222222	0.09	Y
18-[bran: 18]	0.0222222	0.166	Y
19-[bran: 19]	0.0222222	0.0735	Y
20-[bran: 191]	0.0222222	0.0735	Y
21-[bran: 21]	3	0.083	Y
22-[bran: 20]	3	0.096	Y

Figure A.8 Fault events of load points -Part 8

Appendix A.4.3 Restoration Methods of Buses for Relative Fault Events

Fault Event

Fault Branch	Fault Duration(hours/mins)
Feede-22	
22	Circuitbreaker
Repair of fault	branch repair duration
22	3
LP14	3
LP13	3
24	Circuitbreaker
Repair of fault	branch repair duration
22	3
LP13	3
LP14	3
23	Circuitbreaker
Repair of fault	branch repair duration
22	3
LP14	3
LP13	3

Figure A.9 Restoration methods of buses for relative fault events-Part 1

Fault Branch	Fault Duration(hours/mins)
Feede-1	
1	Circuitbreaker
Repair of fault	branch repair duration
3	3
2	3
1	3
LP3	3
LP2	3
LP1	3
DW RCS Restore Buses	
LP12	[0.0222222] [OBr: LP12-SP2]
11	[0.0222222] [OBr: LP12-SP2]
LP10	[0.0222222] [OBr: LP12-SP2]
9	[0.0222222] [OBr: LP12-SP2]
8	[0.0222222] [OBr: LP12-SP2]
5	[0.0222222] [OBr: LP12-SP2]
4	[0.0222222] [OBr: LP12-SP2]
LP11	[0.0222222] [OBr: LP12-SP2]
LP9	[0.0222222] [OBr: LP12-SP2]
LP8	[0.0222222] [OBr: LP12-SP2]
6	[0.0222222] [OBr: LP12-SP2]
LP4	[0.0222222] [OBr: LP12-SP2]
LP5	[0.0222222] [OBr: LP12-SP2]
7	[0.0222222] [OBr: LP12-SP2]
LP7	[0.0222222] [OBr: LP12-SP2]
LP6	[0.0222222] [OBr: LP12-SP2]
2	Circuitbreaker
Repair of fault	branch repair duration
1	3
3	3
2	3
LP1	3
LP3	3
LP2	3
DW RCS Restore Buses	
LP12	[0.0222222] [OBr: LP12-SP2]
11	[0.0222222] [OBr: LP12-SP2]
LP10	[0.0222222] [OBr: LP12-SP2]
9	[0.0222222] [OBr: LP12-SP2]
8	[0.0222222] [OBr: LP12-SP2]
5	[0.0222222] [OBr: LP12-SP2]
4	[0.0222222] [OBr: LP12-SP2]

Figure A.10 Restoration methods of buses for relative fault events -Part 2

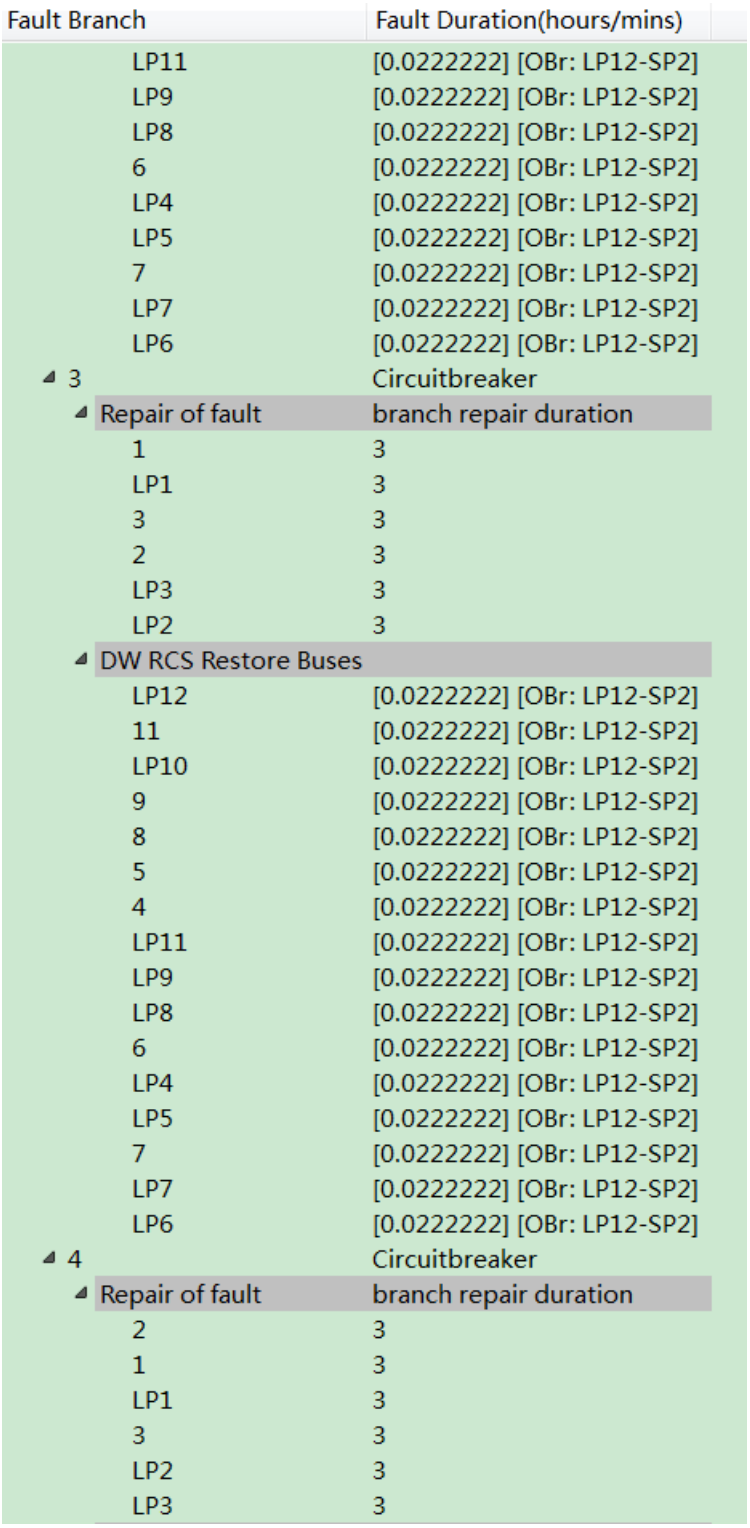

Fault Branch	Fault Duration(hours/mins)
LP11	[0.0222222] [OBr: LP12-SP2]
LP9	[0.0222222] [OBr: LP12-SP2]
LP8	[0.0222222] [OBr: LP12-SP2]
6	[0.0222222] [OBr: LP12-SP2]
LP4	[0.0222222] [OBr: LP12-SP2]
LP5	[0.0222222] [OBr: LP12-SP2]
7	[0.0222222] [OBr: LP12-SP2]
LP7	[0.0222222] [OBr: LP12-SP2]
LP6	[0.0222222] [OBr: LP12-SP2]
3	Circuitbreaker
Repair of fault	branch repair duration
1	3
LP1	3
3	3
2	3
LP3	3
LP2	3
DW RCS Restore Buses	
LP12	[0.0222222] [OBr: LP12-SP2]
11	[0.0222222] [OBr: LP12-SP2]
LP10	[0.0222222] [OBr: LP12-SP2]
9	[0.0222222] [OBr: LP12-SP2]
8	[0.0222222] [OBr: LP12-SP2]
5	[0.0222222] [OBr: LP12-SP2]
4	[0.0222222] [OBr: LP12-SP2]
LP11	[0.0222222] [OBr: LP12-SP2]
LP9	[0.0222222] [OBr: LP12-SP2]
LP8	[0.0222222] [OBr: LP12-SP2]
6	[0.0222222] [OBr: LP12-SP2]
LP4	[0.0222222] [OBr: LP12-SP2]
LP5	[0.0222222] [OBr: LP12-SP2]
7	[0.0222222] [OBr: LP12-SP2]
LP7	[0.0222222] [OBr: LP12-SP2]
LP6	[0.0222222] [OBr: LP12-SP2]
4	Circuitbreaker
Repair of fault	branch repair duration
2	3
1	3
LP1	3
3	3
LP2	3
LP3	3

Figure A.11 Restoration methods of buses for relative fault events-Part 3

Fault Branch	Fault Duration(hours/mins)
DW RCS Restore Buses	
LP12	[0.0222222] [OBr: LP12-SP2]
11	[0.0222222] [OBr: LP12-SP2]
LP10	[0.0222222] [OBr: LP12-SP2]
9	[0.0222222] [OBr: LP12-SP2]
8	[0.0222222] [OBr: LP12-SP2]
5	[0.0222222] [OBr: LP12-SP2]
4	[0.0222222] [OBr: LP12-SP2]
LP11	[0.0222222] [OBr: LP12-SP2]
LP9	[0.0222222] [OBr: LP12-SP2]
LP8	[0.0222222] [OBr: LP12-SP2]
6	[0.0222222] [OBr: LP12-SP2]
LP4	[0.0222222] [OBr: LP12-SP2]
LP5	[0.0222222] [OBr: LP12-SP2]
7	[0.0222222] [OBr: LP12-SP2]
LP7	[0.0222222] [OBr: LP12-SP2]
LP6	[0.0222222] [OBr: LP12-SP2]
5	Circuitbreaker
Repair of fault	branch repair duration
2	3
1	3
LP2	3
LP1	3
3	3
LP3	3
DW RCS Restore Buses	
LP12	[0.0222222] [OBr: LP12-SP2]
11	[0.0222222] [OBr: LP12-SP2]
LP10	[0.0222222] [OBr: LP12-SP2]
9	[0.0222222] [OBr: LP12-SP2]
8	[0.0222222] [OBr: LP12-SP2]
5	[0.0222222] [OBr: LP12-SP2]
4	[0.0222222] [OBr: LP12-SP2]
LP11	[0.0222222] [OBr: LP12-SP2]
LP9	[0.0222222] [OBr: LP12-SP2]
LP8	[0.0222222] [OBr: LP12-SP2]
6	[0.0222222] [OBr: LP12-SP2]
LP4	[0.0222222] [OBr: LP12-SP2]
LP5	[0.0222222] [OBr: LP12-SP2]
7	[0.0222222] [OBr: LP12-SP2]
LP7	[0.0222222] [OBr: LP12-SP2]
LP6	[0.0222222] [OBr: LP12-SP2]

Figure A.12 Restoration methods of buses for relative fault events -Part 4

Fault Branch	Fault Duration(hours/mins)
6	Circuitbreaker
Repair of fault	branch repair duration
3	3
2	3
1	3
LP2	3
LP1	3
LP3	3
DW RCS Restore Buses	
LP12	[0.0222222] [OBr: LP12-SP2]
11	[0.0222222] [OBr: LP12-SP2]
LP10	[0.0222222] [OBr: LP12-SP2]
9	[0.0222222] [OBr: LP12-SP2]
8	[0.0222222] [OBr: LP12-SP2]
5	[0.0222222] [OBr: LP12-SP2]
4	[0.0222222] [OBr: LP12-SP2]
LP11	[0.0222222] [OBr: LP12-SP2]
LP9	[0.0222222] [OBr: LP12-SP2]
LP8	[0.0222222] [OBr: LP12-SP2]
6	[0.0222222] [OBr: LP12-SP2]
LP4	[0.0222222] [OBr: LP12-SP2]
LP5	[0.0222222] [OBr: LP12-SP2]
7	[0.0222222] [OBr: LP12-SP2]
LP7	[0.0222222] [OBr: LP12-SP2]
LP6	[0.0222222] [OBr: LP12-SP2]
7	TeleSwitch
UP RCS Restore Buses	
3	0.0222222
2	0.0222222
1	0.0222222
LP3	0.0222222
LP2	0.0222222
LP1	0.0222222
Repair of fault	branch repair duration
5	3
4	3
6	3
LP4	3
LP5	3
7	3
LP7	3
LP6	3

Figure A.13 Restoration methods of buses for relative fault events -Part 5

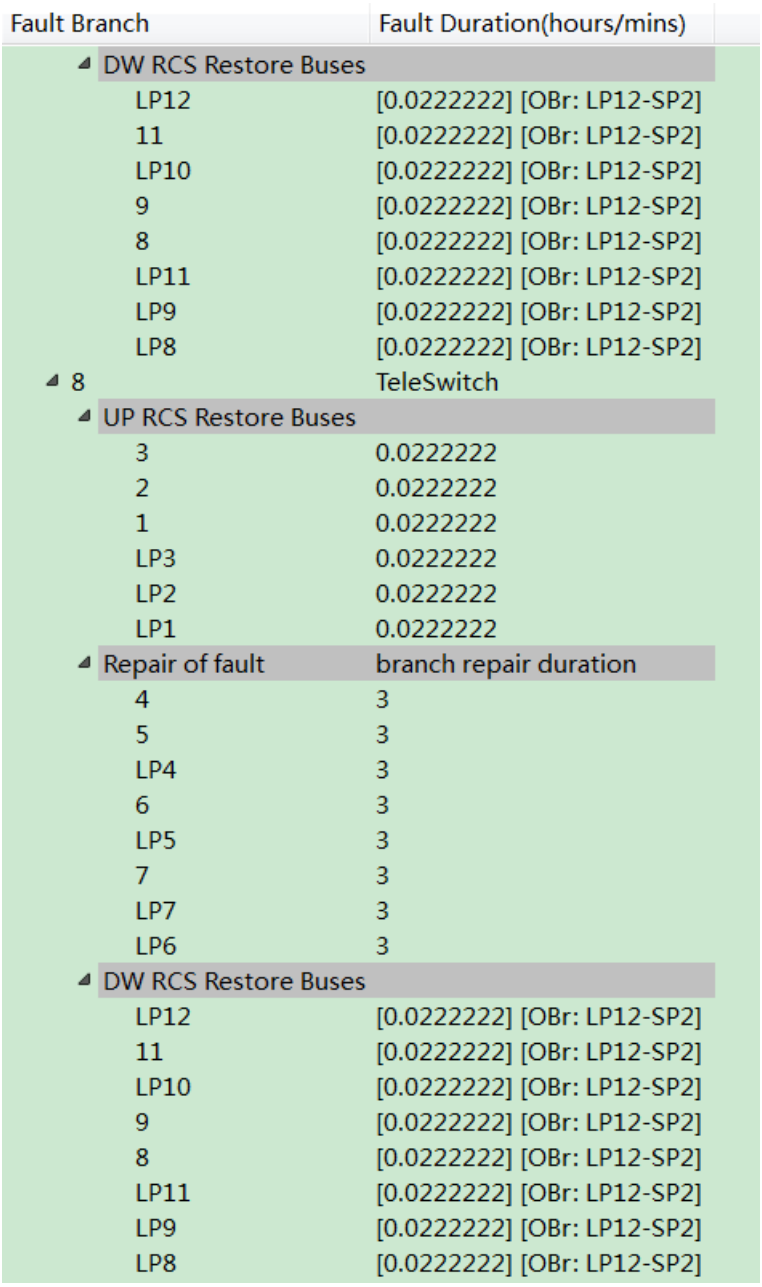

Fault Branch	Fault Duration(hours/mins)
DW RCS Restore Buses	
LP12	[0.0222222] [OBr: LP12-SP2]
11	[0.0222222] [OBr: LP12-SP2]
LP10	[0.0222222] [OBr: LP12-SP2]
9	[0.0222222] [OBr: LP12-SP2]
8	[0.0222222] [OBr: LP12-SP2]
LP11	[0.0222222] [OBr: LP12-SP2]
LP9	[0.0222222] [OBr: LP12-SP2]
LP8	[0.0222222] [OBr: LP12-SP2]
8	TeleSwitch
UP RCS Restore Buses	
3	0.0222222
2	0.0222222
1	0.0222222
LP3	0.0222222
LP2	0.0222222
LP1	0.0222222
Repair of fault	branch repair duration
4	3
5	3
LP4	3
6	3
LP5	3
7	3
LP7	3
LP6	3
DW RCS Restore Buses	
LP12	[0.0222222] [OBr: LP12-SP2]
11	[0.0222222] [OBr: LP12-SP2]
LP10	[0.0222222] [OBr: LP12-SP2]
9	[0.0222222] [OBr: LP12-SP2]
8	[0.0222222] [OBr: LP12-SP2]
LP11	[0.0222222] [OBr: LP12-SP2]
LP9	[0.0222222] [OBr: LP12-SP2]
LP8	[0.0222222] [OBr: LP12-SP2]

Figure A.14 Restoration methods of buses for relative fault events -Part 6

Fault Branch	Fault Duration(hours/mins)
9	TeleSwitch
UP RCS Restore Buses	
3	0.0222222
2	0.0222222
1	0.0222222
LP3	0.0222222
LP2	0.0222222
LP1	0.0222222
Repair of fault	branch repair duration
4	3
LP4	3
5	3
6	3
LP5	3
7	3
LP7	3
LP6	3
DW RCS Restore Buses	
LP12	[0.0222222] [OBr: LP12-SP2]
11	[0.0222222] [OBr: LP12-SP2]
LP10	[0.0222222] [OBr: LP12-SP2]
9	[0.0222222] [OBr: LP12-SP2]
8	[0.0222222] [OBr: LP12-SP2]
LP11	[0.0222222] [OBr: LP12-SP2]
LP9	[0.0222222] [OBr: LP12-SP2]
LP8	[0.0222222] [OBr: LP12-SP2]
15	TeleSwitch
UP RCS Restore Buses	
5	0.0222222
4	0.0222222
3	0.0222222
2	0.0222222
1	0.0222222
6	0.0222222
LP4	0.0222222
LP3	0.0222222
LP2	0.0222222
LP1	0.0222222
LP5	0.0222222
7	0.0222222
LP7	0.0222222
LP6	0.0222222

Figure A.15 Restoration methods of buses for relative fault events -Part 7

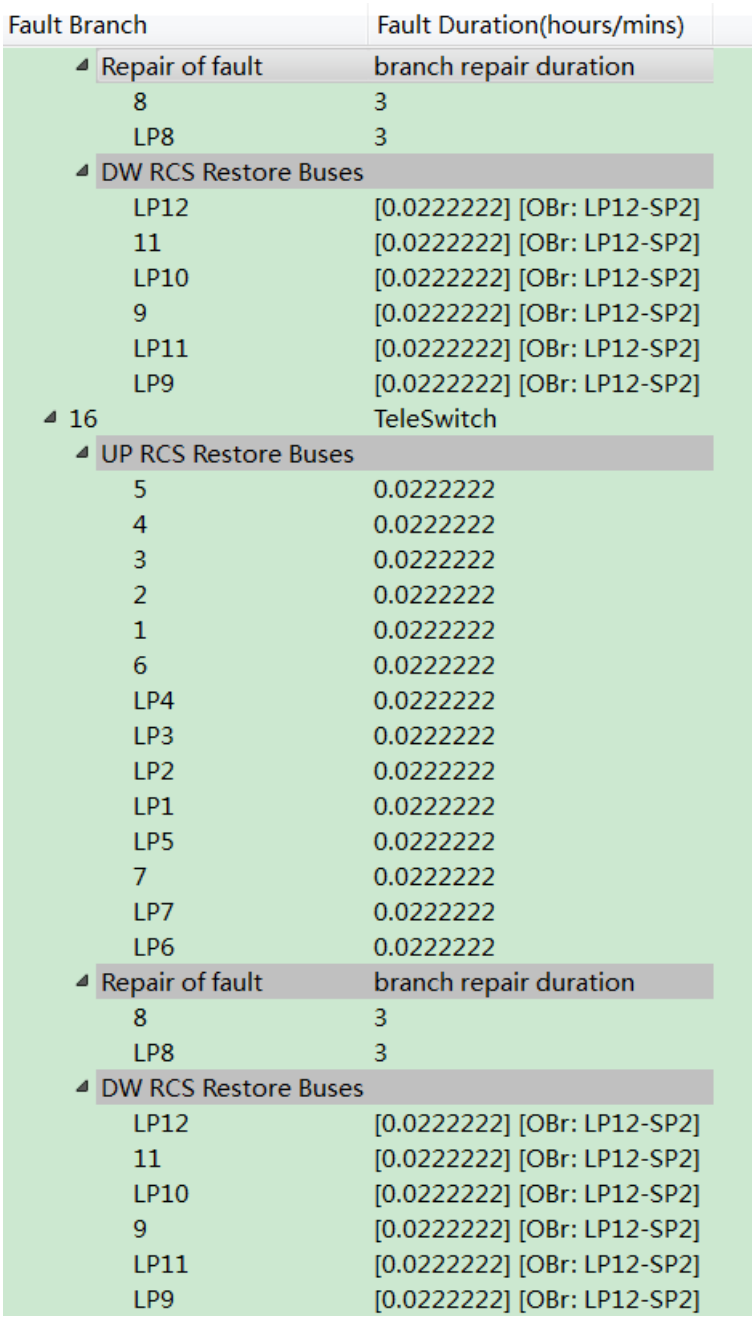

Figure A.16 Restoration methods of buses for relative fault events-Part 8

Fault Branch	Fault Duration(hours/mins)
10	TeleSwitch
UP RCS Restore Buses	
5	0.0222222
4	0.0222222
3	0.0222222
2	0.0222222
1	0.0222222
8	0.0222222
LP4	0.0222222
LP3	0.0222222
LP2	0.0222222
LP1	0.0222222
LP8	0.0222222
9	0.0222222
LP9	0.0222222
LP10	0.0222222
11	0.0222222
LP12	0.0222222
LP11	0.0222222
Repair of fault	branch repair duration
6	3
LP5	3
7	3
LP7	3
LP6	3
11	TeleSwitch
UP RCS Restore Buses	
5	0.0222222
4	0.0222222
3	0.0222222
2	0.0222222
1	0.0222222
8	0.0222222
LP4	0.0222222
LP3	0.0222222
LP2	0.0222222
LP1	0.0222222
LP8	0.0222222
9	0.0222222
LP9	0.0222222

Figure A.17 Restoration methods of buses for relative fault events-Part 9

Fault Branch	Fault Duration(hours/mins)
LP10	0.0222222
11	0.0222222
LP12	0.0222222
LP11	0.0222222
Repair of fault	branch repair duration
6	3
7	3
LP7	3
LP6	3
LP5	3
12	TeleSwitch
UP RCS Restore Buses	
5	0.0222222
4	0.0222222
3	0.0222222
2	0.0222222
1	0.0222222
8	0.0222222
LP4	0.0222222
LP3	0.0222222
LP2	0.0222222
LP1	0.0222222
LP8	0.0222222
9	0.0222222
LP9	0.0222222
LP10	0.0222222
11	0.0222222
LP12	0.0222222
LP11	0.0222222
Repair of fault	branch repair duration
6	3
LP5	3
7	3
LP7	3
LP6	3
14	TeleSwitch
UP RCS Restore Buses	
5	0.0222222
4	0.0222222
3	0.0222222

Figure A.18 Restoration methods of buses for relative fault events-Part 10

Fault Branch	Fault Duration(hours/mins)
2	0.0222222
1	0.0222222
8	0.0222222
LP4	0.0222222
LP3	0.0222222
LP2	0.0222222
LP1	0.0222222
LP8	0.0222222
9	0.0222222
LP9	0.0222222
LP10	0.0222222
11	0.0222222
LP12	0.0222222
LP11	0.0222222
Repair of fault	branch repair duration
7	3
6	3
LP6	3
LP5	3
LP7	3
13	TeleSwitch
UP RCS Restore Buses	
5	0.0222222
4	0.0222222
3	0.0222222
2	0.0222222
1	0.0222222
8	0.0222222
LP4	0.0222222
LP3	0.0222222
LP2	0.0222222
LP1	0.0222222
LP8	0.0222222
9	0.0222222
LP9	0.0222222
LP10	0.0222222
11	0.0222222
LP12	0.0222222
LP11	0.0222222

Figure A.19 Restoration methods of buses for relative fault events-Part 11

Fault Branch	Fault Duration(hours/mins)
Repair of fault	branch repair duration
7	3
6	3
LP7	3
LP5	3
LP6	3
17	TeleSwitch
UP RCS Restore Buses	
8	0.0222222
5	0.0222222
4	0.0222222
3	0.0222222
2	0.0222222
1	0.0222222
LP8	0.0222222
6	0.0222222
LP4	0.0222222
LP3	0.0222222
LP2	0.0222222
LP1	0.0222222
LP5	0.0222222
7	0.0222222
LP7	0.0222222
LP6	0.0222222
Repair of fault	branch repair duration
LP10	3
9	3
LP9	3
DW RCS Restore Buses	
LP12	[0.0222222] [OBr: LP12-SP2]
11	[0.0222222] [OBr: LP12-SP2]
LP11	[0.0222222] [OBr: LP12-SP2]
18	TeleSwitch
UP RCS Restore Buses	
8	0.0222222
5	0.0222222
4	0.0222222
3	0.0222222
2	0.0222222
1	0.0222222

Figure A.20 Restoration methods of buses for relative fault events-Part 12

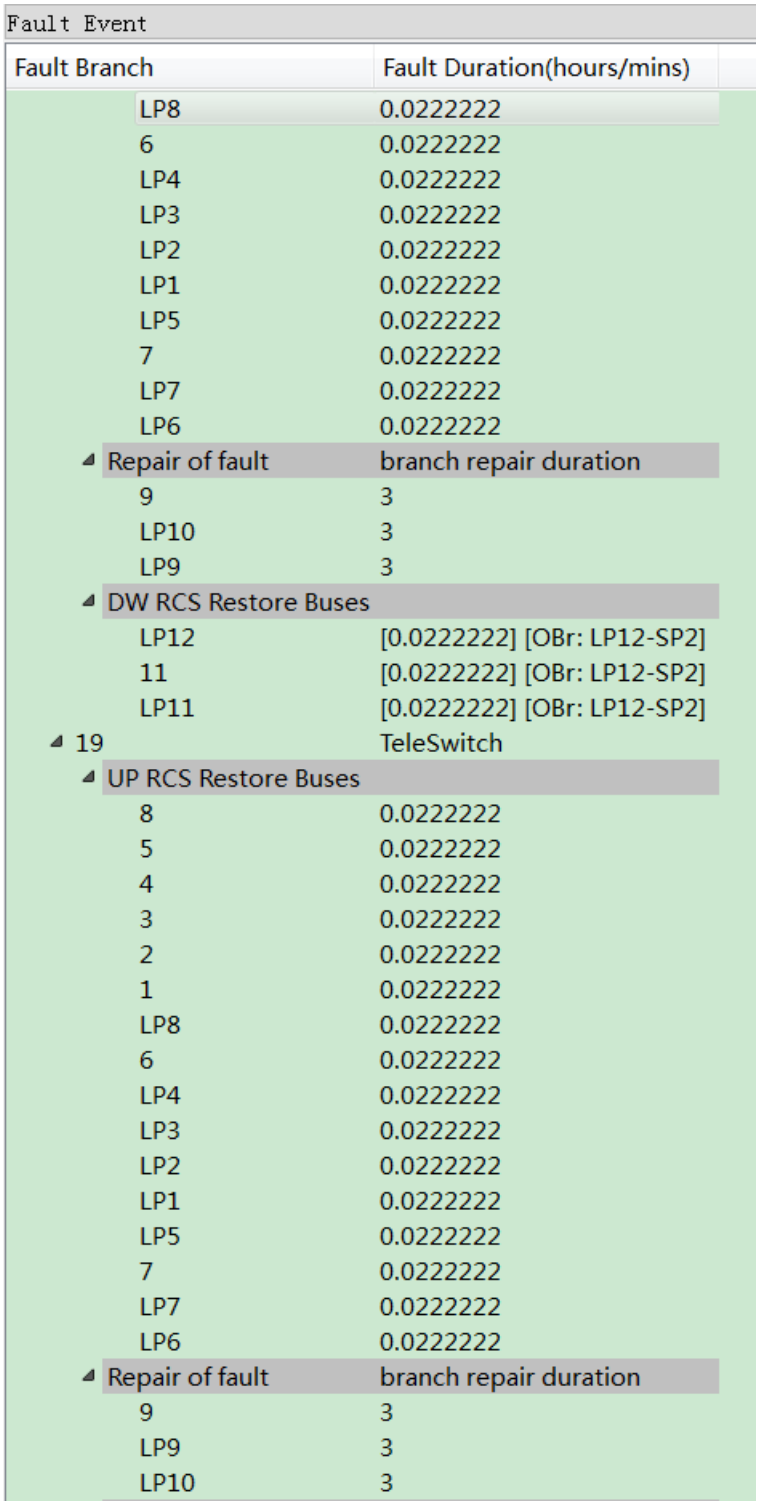

Figure A.21 Restoration methods of buses for relative fault events-Part 13

Fault Branch	Fault Duration(hours/mins)
DW RCS Restore Buses	
LP12	[0.0222222] [OBr: LP12-SP2]
11	[0.0222222] [OBr: LP12-SP2]
LP11	[0.0222222] [OBr: LP12-SP2]
191	TeleSwitch
UP RCS Restore Buses	
8	0.0222222
5	0.0222222
4	0.0222222
3	0.0222222
2	0.0222222
1	0.0222222
LP8	0.0222222
6	0.0222222
LP4	0.0222222
LP3	0.0222222
LP2	0.0222222
LP1	0.0222222
LP5	0.0222222
7	0.0222222
LP7	0.0222222
LP6	0.0222222
Repair of fault	branch repair duration
LP10	3
9	3
LP9	3
DW RCS Restore Buses	
LP12	[0.0222222] [OBr: LP12-SP2]
11	[0.0222222] [OBr: LP12-SP2]
LP11	[0.0222222] [OBr: LP12-SP2]
21	TeleSwitch
UP RCS Restore Buses	
LP10	0.0222222
9	0.0222222
8	0.0222222
5	0.0222222
4	0.0222222
3	0.0222222
2	0.0222222
1	0.0222222

Figure A.22 Restoration methods of buses for relative fault events-Part 14

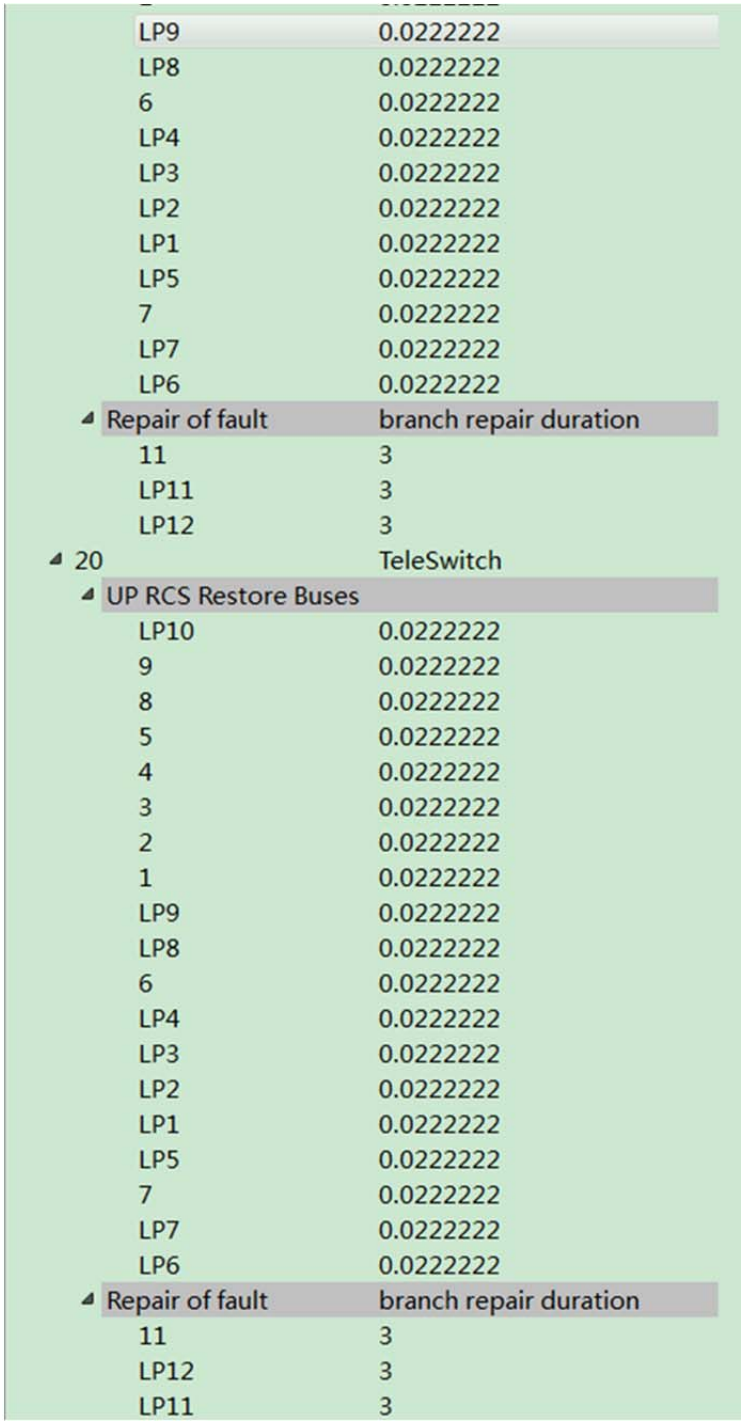

Figure A.23 Restoration methods of buses for relative fault events-Part 15

Appendix A.5 69-Bus Network Model Data

Table A-15 Branch impedance data

Branch Name	Bus1 name	Bus2 name	Resistance (pu)	Reactance (pu)	Susceptance (pu)
b0(s)-b52	b0(s)	b52	0.304137	0.0698149	0.00017478
b0(s)-b55	b0(s)	b55	0.616925	0.150225	0.000335462
b1-b0(s)	b0(s)	b1	0.170502	0.040274	7.08E-05
b10-b9	b9	b10	0.0470454	0.0315359	0
b11-b10	b10	b11	0.108566	0.0727752	0
b12-b11	b11	b12	0.0603896	0.0257529	3.12E-07
b13-b12	b12	b13	0.196132	0.106263	1.10E-05
b14-b13	b13	b14	0.0591986	0.0135891	3.40E-05
b15-b14	b14	b15	0.050212	0.0336585	0
b15-b16	b15	b16	0.114418	0.055009	0
b16-b17	b16	b17	0.108566	0.0727752	0
b17-b18	b17	b18	0.139155	0.0863768	8.35E-07
b18-b19	b18	b19	0.165111	0.110679	0
b2-b1	b1	b2	0.0319484	0.0073338	1.84E-05
b2-b3	b2	b3	0.141375	0.0502661	0
b20-b15	b15	b20	0.0607197	0.0166432	0
b21-b20	b20	b21	0.0560926	0.0376005	0
b22-b21	b21	b22	0.296172	0.105304	0
b23-b22	b22	b23	0.0235227	0.015768	0
b24-b23	b24	b23	0.263726	0.176783	0
b25-b24	b25	b24	0.341532	0.228939	0
b26-b25	b26	b25	0.0750918	0.0503362	0
b27-b26	b27	b26	0.118066	0.079143	0
b28-b27	b28	b27	0.0882102	0.0591299	0
b29-b28	b29	b28	0.102686	0.0688332	0
b30-b29	b30	b29	0.138875	0.0930916	0
b31-b30	b31	b30	0.0927338	0.0621621	0
b32-b31	b32	b31	0.50981	0.34174	0
b33-b32	b33	b32	0.171897	0.115227	0
b33-b34	b33	b34	0.3067	0.20559	0
b34-b35	b34	b35	0.0796154	0.0533685	0
b35-b36	b35	b36	0.229799	0.154041	0
b36-b37	b36	b37	0.0719252	0.0482136	0
b37-b38	b37	b38	0.0379982	0.0254713	0

Continued on next page

…continued from previous page

b38-b39	b38	b39	0.0868531	0.0582202	0
b4-b2	b2	b4	0.097531	0.0346773	0
b4-b5	b4	b5	0.278635	0.0584276	1.53E-05
b40-b33	b40	b33	0.18461	0.105921	9.36E-09
b41-b40	b41	b40	0.214419	0.143731	0
b42-b41	b42	b41	0.0384506	0.0257746	0
b42-b43	b42	b43	0.13813	0.0317079	7.94E-05
b43-b44	b43	b44	0.0235227	0.015768	0
b44-b45	b44	b45	0.178635	0.0489637	0
b45-b46	b45	b46	0.00596354	0.0016346	0
b46-b47	b46	b47	0.0205824	0.0257275	0
b47-b48	b47	b48	0.0361888	0.0242584	0
b49-b42	b49	b42	0.100876	0.0676203	0
b50-b49	b50	b49	0.0403894	0.0110707	0
b51-b50	b51	b50	0.0786103	0.021547	0
b52-b53	b52	b53	0.228894	0.153434	0
b53-b54	b53	b54	0.19655	0.245684	0
b55-b56	b55	b56	0.048195	0.033705	0
b56-b57	b56	b57	0.094554	0.066126	0
b57-b58	b57	b58	0.10719	0.0270087	1.51E-05
b57-b60	b57	b60	0.113832	0.079608	0
b58-b59	b58	b59	0.00281898	0.0006471	1.62E-06
b59-b54	b59	b54	0.0636926	0.0151279	2.46E-05
b6-b5	b5	b6	0.75811	0.464671	0
b60-b61	b60	b61	0.063342	0.044298	0
b61-b62	b61	b62	0.26248	0.179299	0
b63-b62	b62	b63	0.272688	0.123012	3.55E-05
b64-b63	b63	b64	0.155695	0.0362714	0
b65-b64	b64	b65	0.0966332	0.0262638	1.48E-07
b65-b66	b65	b66	0.160702	0.0388579	4.81E-05
b66-b67	b66	b67	0.0830033	0.0190535	4.77E-05
b67-b68	b67	b68	0.0601382	0.0138048	3.46E-05
b68-b51	b68	b51	0.0680386	0.0186493	0
b7-b6	b6	b7	0.253774	0.170112	0
b8-b7	b7	b8	0.0972574	0.0651945	0
b8-b9	b8	b9	0.0500404	0.0266405	2.46E-06

$S_{base} = 100MVA \quad V_{base} = 11kV$

Table A-16 Branch reliability data

Branch Name	Fault rate (int/yr.km)	Repair time (hours)	Length (Km)
b0(s)-b52	0.17	30	1.748
b0(s)-b55	0.17	30	3.546
b1-b0(s)	0.17	30	0.98
b10-b9	0.17	30	0.27
b11-b10	0.17	30	0.624
b12-b11	0.17	30	0.347
b13-b12	0.17	30	1.127
b14-b13	0.17	30	0.34
b15-b14	0.17	30	0.289
b15-b16	0.17	30	0.658
b16-b17	0.17	30	0.624
b17-b18	0.17	30	0.8
b18-b19	0.17	30	0.949
b2-b1	0.17	30	0.184
b2-b3	0.17	30	0.813
b20-b15	0.17	30	0.349
b21-b20	0.17	30	0.322
b22-b21	0.17	30	1.702
b23-b22	0.17	30	0.135
b24-b23	0.17	30	1.516
b25-b24	0.17	30	1.963
b26-b25	0.17	30	0.432
b27-b26	0.17	30	0.679
b28-b27	0.17	30	0.507
b29-b28	0.17	30	0.59
b30-b29	0.17	30	0.798
b31-b30	0.17	30	0.533
b32-b31	0.17	30	2.93
b33-b32	0.17	30	0.988
b33-b34	0.17	30	1.763
b34-b35	0.17	30	0.458
b35-b36	0.17	30	1.321
b36-b37	0.17	30	0.413

Continued on next page

…continued from previous page

b37-b38	0.17	30	0.218
b38-b39	0.17	30	0.499
b4-b2	0.17	30	0.561
b4-b5	0.17	30	1.601
b40-b33	0.17	30	1.061
b41-b40	0.17	30	1.232
b42-b41	0.17	30	0.221
b42-b43	0.17	30	0.794
b43-b44	0.17	30	0.135
b44-b45	0.17	30	1.027
b45-b46	0.17	30	0.034
b46-b47	0.17	30	0.118
b47-b48	0.17	30	0.208
b49-b42	0.17	30	0.58
b50-b49	0.17	30	0.232
b51-b50	0.17	30	0.452
b52-b53	0.17	30	1.315
b53-b54	0.17	30	1.13
b55-b56	0.17	30	0.277
b56-b57	0.17	30	0.543
b57-b58	0.17	30	0.616
b57-b60	0.17	30	0.654
b58-b59	0.17	30	0.016
b59-b54	0.17	30	0.366
b6-b5	0.17	30	4.357
b60-b61	0.17	30	0.364
b61-b62	0.17	30	1.509
b63-b62	0.17	30	1.567
b64-b63	0.17	30	0.895
b65-b64	0.17	30	0.555
b65-b66	0.17	30	0.924
b66-b67	0.17	30	0.477
b67-b68	0.17	30	0.346
b68-b51	0.17	30	0.391
b7-b6	0.17	30	1.458
b8-b7	0.17	30	0.559
b8-b9	0.17	30	0.288

Table A-17 Customer Number of each load point

Bus name	Customer Number	Bus name	Customer Number
b1	9	b44	112
b10	50	b45	47
b11	129	b46	5
b12	106	b47	19
b13	123	b48	0
b14	39	b49	39
b16	3	b5	120
b17	19	b50	117
b18	19	b51	59
b19	0	b52	1
b2	38	b53	3
b20	73	b54	133
b21	1	b55	5
b22	117	b56	3
b23	3	b58	103
b24	117	b59	103
b25	1	b60	19
b26	5	b61	5
b27	123	b62	134
b28	39	b63	127
b29	19	b64	95
b3	38	b65	170
b30	0	b66	127
b31	155	b67	19
b32	10	b68	98
b34	25	b7	51
b35	17	b8	5
b36	3	b39	0
b37	13	b4	0
b38	23	b40	19
b43	10	b41	10

Table A-18 Protection and remote control devices data in scenario 1

Bus name	Branch Name	Device Name	Device type	Mean time to switch (hours)	Mean time to repair (hours)
b0(s)	b0(s)-b52	CB0	Circuit Breaker	0	0
b0(s)	b0(s)-b55	CB1	Circuit Breaker	0	0
b0(s)	b1-b0(s)	CB2	Circuit Breaker	0	0
b15	b15-b16	F1	Fuse	0	1.1
b33	b33-b34	F1	Fuse	0	1.1
b42	b42-b43	F1	Fuse	0	1.1
b64	b65-b64	RC1	RCSwitch	0.017	1
b53	b53-b54	RC2	RCSwitch	0.017	1
b23	b24-b23	RC3	RCSwitch	0.017	1

Table A-19 Protection and remote control devices data in scenario 2

Bus name	Branch Name	Device Name	Device type	Mean time to switch (hours)	Mean time to repair (hours)
b0(s)	b0(s)-b52	CB0	Circuit Breaker	0	0
b0(s)	b0(s)-b55	CB1	Circuit Breaker	0	0
b0(s)	b1-b0(s)	CB2	Circuit Breaker	0	0
b15	b15-b16	F1	Fuse	0	1.1
b33	b33-b34	F1	Fuse	0	1.1
b42	b42-b43	F1	Fuse	0	1.1
b64	b65-b64	RC1	RCSwitch	0.017	1
b53	b53-b54	RC2	RCSwitch	0.017	1
b23	b24-b23	RC3	RCSwitch	0.017	1
b62	b61-b62	RC4	RCSwitch	0.017	1
b65	b65-b66	RC5	RCSwitch	0.017	1
b12	b13-b12	RC6	RCSwitch	0.017	1
b32	b33-b32	RC7	RCSwitch	0.017	1

Appendix A.6 33-Bus Network Model Data

Table A-20 Branch data

Bus 1	Bus 2	Resistance(PU)	Reactance(PU)
0	1	0.0575	0.0293
1	18	0.1023	0.0976
1	2	0.3076	0.1567
10	11	0.2336	0.0772
11	12	0.9159	0.7206
12	13	0.3379	0.4448
13	14	0.3687	0.3282
14	15	0.4656	0.3400
15	16	0.8042	1.0738
16	17	0.4567	0.3581
17	32	0.3120	0.3120
18	19	0.9385	0.8457
19	20	0.2555	0.2985
2	22	0.2815	0.1924
2	3	0.2284	0.1163
20	21	0.4423	0.5848
21	11	1.2479	1.2479
22	23	0.5603	0.4424
23	24	0.5590	0.4374
24	28	0.3120	0.3120
5	25	0.1267	0.0645
25	26	0.1773	0.0903
26	27	0.6607	0.5826
27	28	0.5018	0.4371
28	29	0.3166	0.1613
29	30	0.6080	0.6008
3	4	0.2378	0.1211
30	31	0.1937	0.2258
31	32	0.2128	0.3308
4	5	0.5110	0.4411
5	6	0.1168	0.3861
6	7	0.4439	0.1467
7	20	1.2479	1.2479
7	8	0.6426	0.4617
8	14	1.2479	1.2479
8	9	0.6514	0.4617
9	10	0.1227	0.0406

$S_{base} = 100MVA \quad V_{base} = 12.66kV$

Table A-21 Load Data

Bus	P(MW)	Q(MVar)
1	0.1	0.06
2	0.09	0.04
3	0.12	0.08
4	0.06	0.03
5	0.06	0.02
6	0.2	0.1
7	0.2	0.1
8	0.06	0.02
9	0.06	0.02
10	0.045	0.03
11	0.06	0.035
12	0.06	0.035
13	0.12	0.08
14	0.06	0.01
15	0.06	0.02
16	0.06	0.02
17	0.09	0.04
18	0.09	0.04
19	0.09	0.04
20	0.09	0.04
21	0.09	0.04
22	0.09	0.05
23	0.42	0.2
24	0.42	0.2
25	0.06	0.025
26	0.06	0.025
27	0.06	0.02
28	0.12	0.07
29	0.2	0.6
30	0.15	0.07
31	0.21	0.1
32	0.06	0.04

Appendix B The Algorithm of Spanning Tree Generation

Appendix B.1 Stack and Recursion

- **Stack**

  A stack is an abstract linear data structure [178]. As shown in Figure B.1, an element can be pushed into or popped from the stack only in one direction. So the element pushed into first is on the bottom of stack.

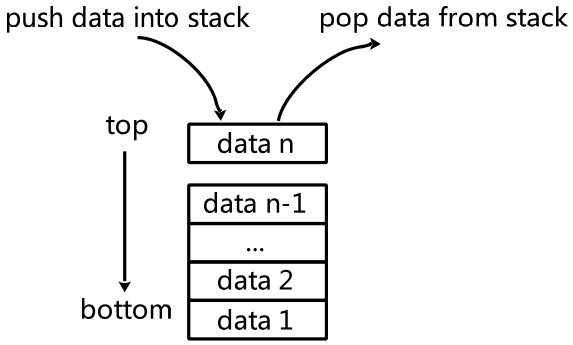

Figure B.1 The structure of stack

- **Recursion**

  Recursion is a programming technique. In C++, it allows a function to call itself [162]. When the function calls itself, the current running position of the program is recorded. When the process of recursion has been finished, the program backtracks to this position and continuous to run the next command.

Appendix B.2 The Processing of Spanning Tree Generation

Take the graph in Figure 3.15 (b) for example. Each step of generating all spanning trees of this graph is illustrated as follows. Figure B.3, Figure B.4 and Figure B.5 visualise the whole processing.

Initial: The root node of G is node 1 and the edges connected to node 1 need to be pushed on to GS. So push edge 1-2 onto it first, then push edge 1-3. [Figure B.3]

The 1st Grow: The top element of G is edge 1-2, so it is popped from G and added to TE. Meanwhile, node 2 is added to TN and marked as "the new added node". G still has edge 1-3, so pop it from G and push it onto L. Now, TN has nodes 1 and 2. Since

it does not contain all nodes of G, push edge 2-4 which is the unsearched edge connects to node 2 onto G. The program starts the next growth stage. [Figure B.3]

The 2nd Grow: The top element of G is edge 2-4, so it is popped from G and added to TE. Meanwhile, node 4 is added to TN and marked as "the new added node". G is empty, so no edge needs to be pushed on to L. Now, TN has nodes 1, 2 and 4. Since it does not contain all nodes of G, push edge 4-5 which is the unsearched edge connected to node 4 onto G. The program starts the next grow. [Figure B.3]

The 3rd Grow: The top element of G is edge 4-5, so it is popped from G and added to TE. Meanwhile, node 5 is added to TN and marked as "the new added node". G is empty, so no edge needs to be pushed on to L. Now, TN has nodes 1, 2, 4 and 5. Since it does not contain all nodes of G, push edge 3-5 which is the unsearched edge connected to node 5 onto G. The program starts the next growth stage. [Figure B.3]

The 4th Grow: The top element of G is edge 5-3, so it is popped from G and added to TE. Meanwhile, node 3 is added to TN and marked as "the new added node". G is empty, so no edge needs to be pushed on to L. Now, TN has nodes 1, 2, 4, 5 and 3. Since it contains all nodes of G, the program backtracks to the previous 3rd grow instead of starting a new grow. [Figure B.3]

Go Back to the 3rd Grow: When the program backtracks to the 3rd grow from the 4th grow, G is empty while L only has edge 1-3 in it. Instead of finding the unsearched edges connected to node 5, push edge 1-3 which is the top element L of onto G then pop it from L. The program starts a new growth since TN does not contain all nodes of G. [Figure B.3]

The 5th Grow: The top element of G is edge 1-3, so it is popped from G and added to TE. Meanwhile, add node 3 which is the new added node to TN. G is empty, so no edge needs to be pushed on to L. Now, TN has nodes 1, 2, 4, 5 and 3. Since it contains all nodes of G, the program backtracks to the previous 3rd grow instead of starting a new grow. [Figure B.3]

Go Back to the 3rd Grow: When the program trackbacks to the 3rd grow from the 5th grow, it is impossible to call a new growth since both of *G* and *L* are empty. The program backtracks to the previous 2nd grow.

Go Back to the 2nd Grow: When the program trackbacks to the 2rd grow from the 3th grow, *G* is empty while *L* only has edge 13 in it. Instead of finding the unsearched edges connect to new added node 5, push edge 13 which is the top element *L* of onto *G* then pop it from *L*. The program starts a new growth since TN doesn't contain all nodes of G. [Figure B.3]

The 6th Grow: The top element of *G* is edge 13, so it is popped from G and added to TE. Meanwhile, add node 3 which is the new added node to TN. G is empty, so no edge needs to be pushed on to *L*. Now, TN has nodes 1, 2, 4 and 3. Since it does not contain all nodes of G, push edge 3-5 which is the unsearched edge connects to node 3 onto *G*. The program starts the next growth stage. [Figure B.3]

The 7th Grow: The top element of *G* is edge 3-5, so it is popped from *G* and added to TE. Meanwhile, add node 5 which is the new added node to TN. G is empty, so no edge needs to be pushed on to L. Now, TN has nodes 1, 2, 4, 5 and 3. Since it contains all nodes of G, the program backtracks to the previous 6th grow instead of starting a new growth. [Figure B.3]

Go Back to the 6th Grow: When the program trackbacks to the 6th grow from the 7th grow, it is impossible to start a new grow since both of G and L are empty. The program backtracks to the previous 2nd grow. [Figure B.4]

Go Back to the 2nd Grow: When the program trackbacks to the 2nd grow from the 6th grow, it is impossible to start a new grow since both of *G* and *L* are empty. The program backtracks to the previous 1st grow. [Figure B.4]

Go Back to the 1st Grow: When the program goes back to the 1st grow from the 2nd grow, G is empty while L only has edge 1-3 in it. Instead of finding the unsearched edges connect to new added node 2, push edge 1-3 which is the top element L of onto G then pop it from L. The program starts a new growth stage since TN doesn't contain all nodes of G. [Figure B.4]

The 8th Grow: The top element of G is edge 1-3, so it is popped from G and added to TE. Meanwhile, add node 5 which is the new added node to TN. G is empty, so no edge needs to be pushed on to L. Now, TN has nodes 1, 2 and 3. Since it does not contain all nodes of G, push edge 35 which is the unsearched edge connected to node 3 onto G. The program starts the next growth stage. [Figure B.4]

The 9th Grow: The top element of G is edge 3-5, so it is popped from G and added to TE. Meanwhile, add node 5 which is the new added node to TN. G is empty, so no edge needs to be pushed on to L. Now, TN has nodes 1, 2, 3 and 5. Since it does not contain all nodes of G, push edge 4-5 which is the unsearched edge connected to node 5 onto G. The program starts the next growth stage. [Figure B.4]

The 10th Grow: The top element of G is edge 4-5, so it is popped from G and added to TE. Meanwhile, add node 4 which is the new added node to TN. G is empty, so no edge needs to be pushed on to L. Now, TN has nodes 1, 2, 4, 5 and 3. Since it contains all nodes of G, the program backtracks to the previous 9th grow instead of starting a new grow. [Figure B.4]

Go Back to the 9th Grow: When the program trackbacks to the 9th grow from the 10th grow, it is impossible to start a new grow since both of G and L are empty. The program backtracks to the previous 8th grow. [Figure B.4]

Go Back to the 8th Grow: When the program trackbacks to the 8th grow from the 9th grow, it is impossible to start a new grow since both of G and L are empty. The program backtracks to the previous 1st grow. [Figure B.4]

Go Back to the 1st Grow: When the program trackbacks to the 1st grow from the 8th grow, it is impossible to start a new grow since both of *G* and *L* are empty. The program backtracks to the initial. [Figure B.4]

When the program trackbacks to the initial stage, *G* needs to be reconstructed by deleting edge 1-2 as shown in Figure B.2 since edge 1-2 is the last edge pushed onto GS and isn't a bridge of *G*.

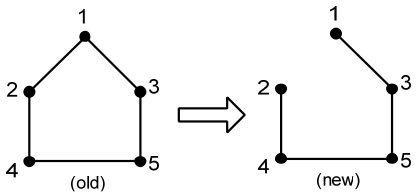

Figure B.2 The new graph

The process of generating all spanning trees of the new graph in Figure B.2 is shown in Figure B.5. After four times grow, a spanning three has been found so the program backtracks to the 3rd grow which is the previous grow of the 4th grow. The stacks *G* and *L* are empty at this stage. Then the program goes back to the 2nd grow whose stacks *G* and *L* are empty as well. Then the program faces the same condition when it goes back to the 1st grow. Now, the program returns to the initial condition. In the initial condition, edge 1-3 is the last edge pushed onto GS at this time. But the graph cannot be reconstructed by deleting edge 1-3 since it is a bridge of G in Figure B.2.

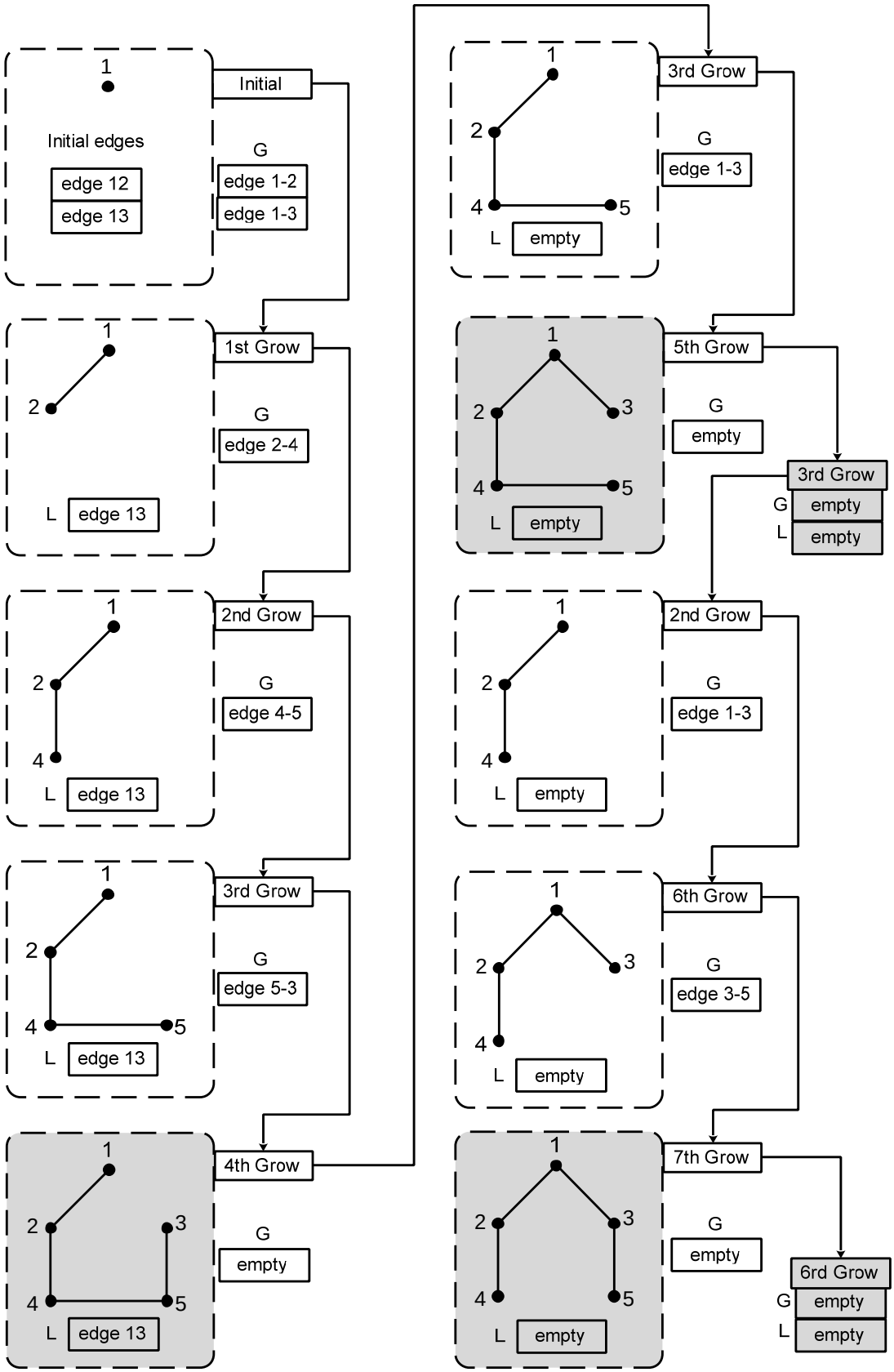

Figure B.3 The processing of generating spanning tree-Part I

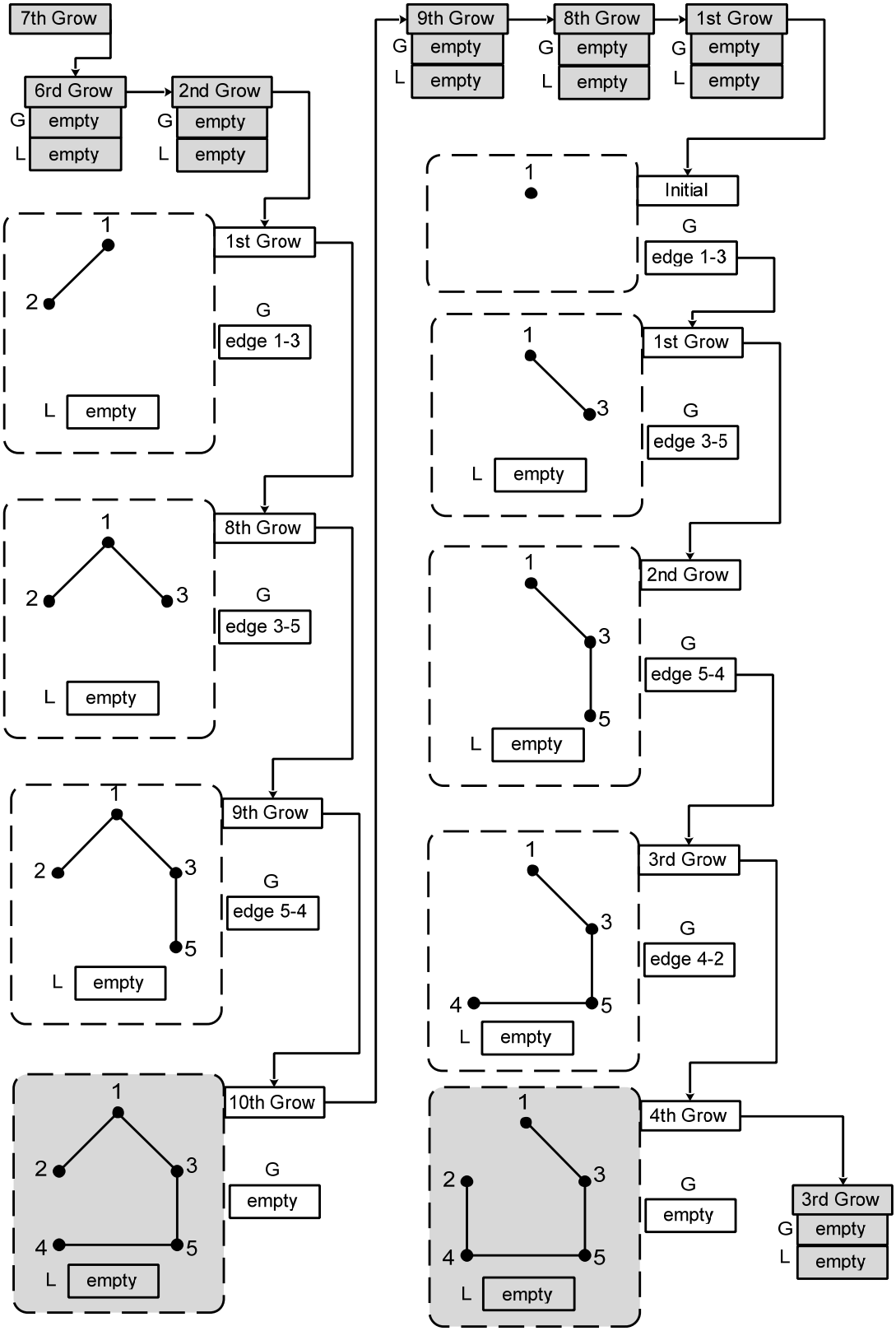

Figure B.4 The processing of generating spanning tree-Part II

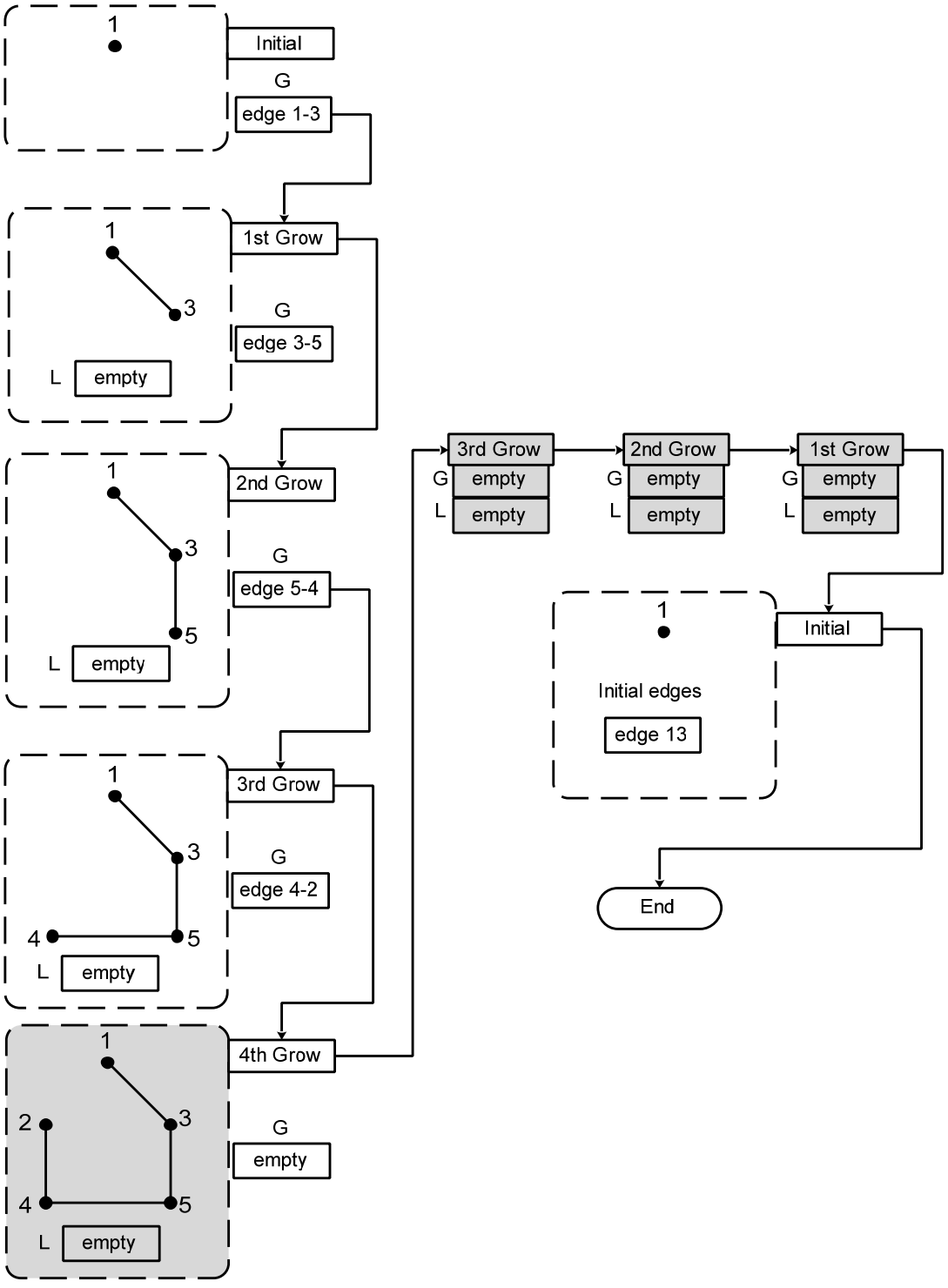

Figure B.5 The processing of generating spanning tree-Part III

Appendix C Distribution Network Optimisation Computer Program - DisOPT

1. Introduction

The *P* loss optimisation, reliability evaluation and optimisation both loss and reliability algorithms are implemented in DisOPT. DisOPT is a distribution network analysis tool which can optimise *P* loss and evaluate the reliability performance. It has the following seven functions implemented in C++ programming language:

1) Topology generation
2) Load flow
3) *P* loss optimisation
4) Load curve *P* loss optimisation
5) Reliability evaluation
6) Reliability optimisation
7) Loss and reliability optimisation

The load flow function of DisOPT is implemented by using IPSA+, LFEngine and scripts which are commercial tools developed by TNEI [179]. IPSA+ is a power system simulation software which can build a network in a graphic view. LFEngine is a load flow engine which provides a header file (.h) and a dynamic link library (.dll). The scripts written in python can read the network model (.iif) built in ISPA+. The python scripts can be embedded into a C++ program which means the C++ program can access the variables of python scripts. So, as shown in Figure C.1, LFEngine and scripts are embedded into DisOPT so that DisOPT has the ability to read the ISPA+ network model (.iif) and perform load flow calculations.

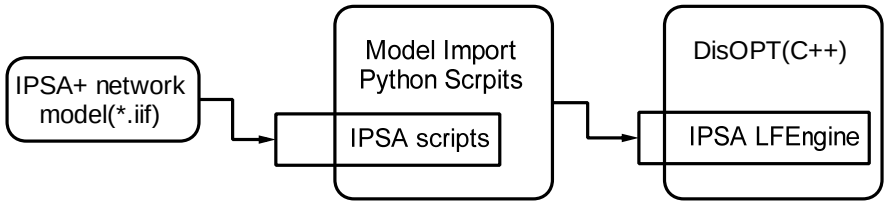

Figure C.1 Relationships among ISPA+. Scripts, LFEngine and DisOPT

Furthermore, its graphic user interface (GUI) shown in Figure C.2 is written in Qt [177]. The details of above seven functions are described in the next sections.

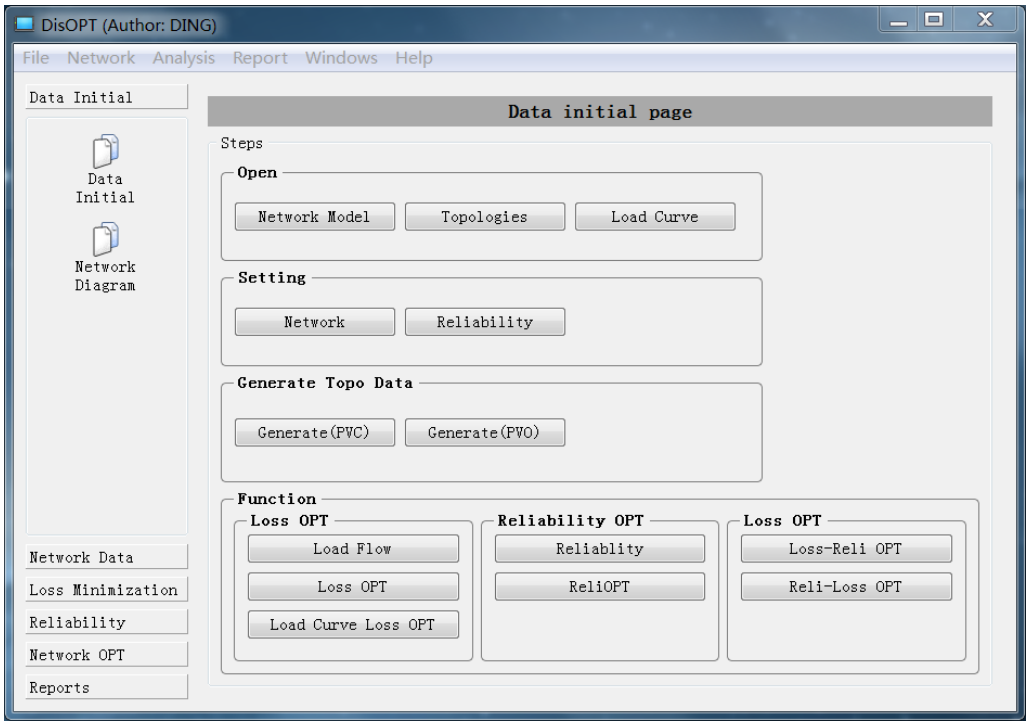

Figure C.2 GUI of the DisOPT

2. Topology Generation Function

The topology generation function can generate all radial topologies of the network by using the spanning tree generation algorithm introduced in Section 3.5. As shown in Figure C.3, this function has two modes: PVC and PVO. In PVC mode, all PV edges of the network, i.e. those connected to a power source or "PV node", are closed in all radial topologies. In PVO mode, PV edges can be either open or closed. The conception of PV edge was introduced in section 3.4.2. The results data of all spanning trees is saved in a CSV file. If the network is not changed after some previous analysis, the spanning tree information only needs to be generated once and the data file can be imported directly instead of generating it again.

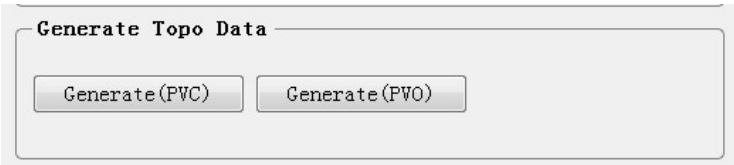

Figure C.3 Two modes of topology generation function

Before clicking the spanning tree generation button, the root nodes of the network topology need to be defined first. When the IPSA model is imported, its root nodes are found by DisOPT and displayed in the dialog shown in Figure C.4. Some system parameters, like nominal voltage, system base, etc., can be set in this dialog as well.

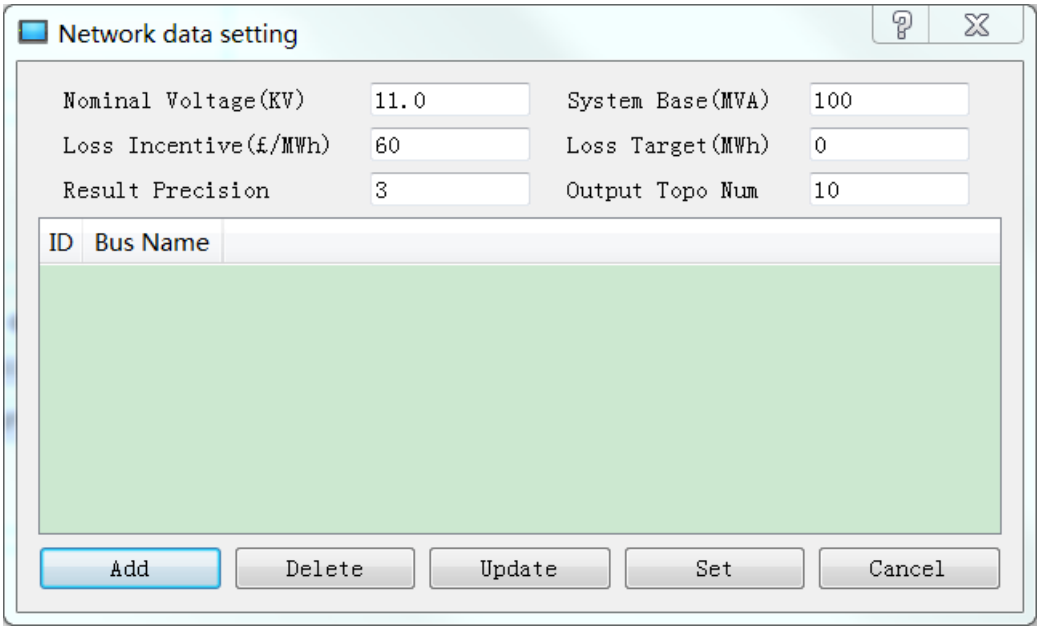

Figure C.4 The dialog of modify root nodes

If the root nodes found by the DisOPT are different from the expected value, user can add or delete nodes. A node is defined as PV nodes by DisOPT in the following conditions:

i) A node has sources (generator, grid infeed) connected to it

ii) A node has transformer(s) connected to it and its voltage rate is 11kV. One side's nominal voltage of this transformer must be higher than 11kV.

But there is no strict rule on building a power system simulation model. The same power system network may be connected in different ways by different users, especially for the connection of substations. Take a substation that has four feeders for example. This substation has two ways to connect in simulation software:

i). As shown in Figure C.5, the substation is represented by node N0 and feeders represented by branches b1, b2, b3 and b4 (cable or overhead line) are connected to this node directly. In this circumstances, N0 is the PV node and

can be automatically found by the software.

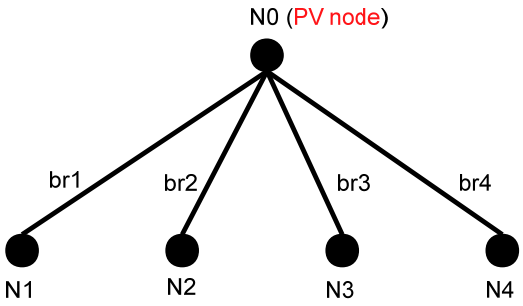

Figure C.5 Connection of feeders-Mode 1

ii). As shown in Figure C.6, the substation is represented by node N0 as well. Instead of connected branches to node N1 directly, four switches SW1, SW2, SW3, SW4 are added to the node N1 then branches br1, br2, br3 and br4 are connected to these four switches. The software will still consider node N1 as PV node since a grid infeed is connected to the node N0. It is better to consider nodes N1, N2, N3, and N4 as PV nodes since it can reduce the total number of spanning trees.

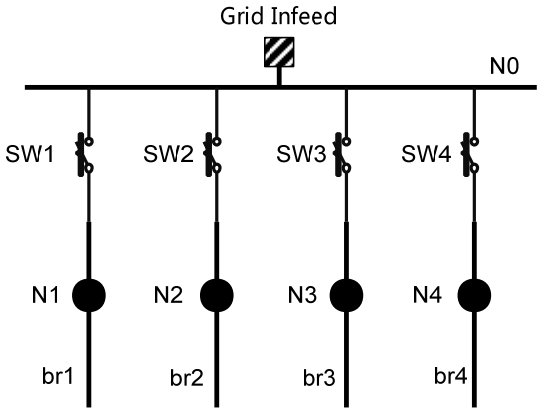

Figure C.6 Connection of feeders-Mode 2

It is hard to find all possible connection ways to make sure the PV nodes can be automatically found by software in the best way. The PV node is the starting node of generating spanning trees and affects the final results of spanning tree directly. This dialog window provides a way for users to check the PV nodes. Users can also customise the PV nodes when they just want to generate part of the network's spanning trees .

3. Load Flow Function

The load flow function of DisOPT is implemented by using IPSA+, LFEngine and scripts which are commercial tools developed by TNEI [179]. IPSA+ is a power system simulation software which can build a network in a graphic view. LFEngine is a load flow engine which provides a header file (.h) and a dynamic link library (.dll). The scripts written in python can read the network model (.iif) built in ISPA+. The python scripts can be embedded into a C++ program which means the C++ program can access the variables of python scripts. So, as shown in Figure C.7, LFEngine and scripts are embedded into DisOPT so that DisOPT has the ability to read the ISPA+ network model (.iif) and perform load flow calculations.

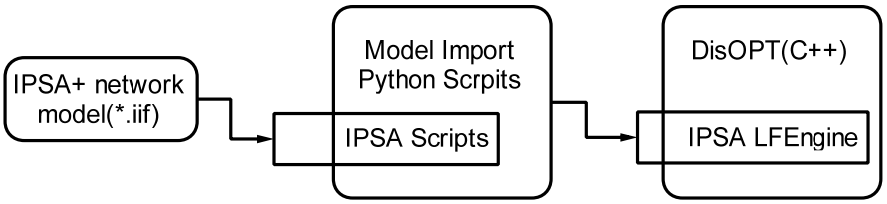

Figure C.7 Relationships among ISPA+. Scripts, LFEngine and DisOPT

When an iif network model is imported, the information of zones and feeders are displayed in feeder view and zone view dock windows respectively. The feeder view window in Figure C.8 displays the buses, branches, normally open points of each feeder analysed by DisOPT in tree view mode. The zone view window in Figure C.9 displays the feeder, branches, buses of each zone analysed by DisOPT in tree view mode as well. The accuracy of zone and feeder information is very important for the following loss optimisation and reliability evaluation analysis. This information can help the user identify and evaluate the details of each feeder and zone.

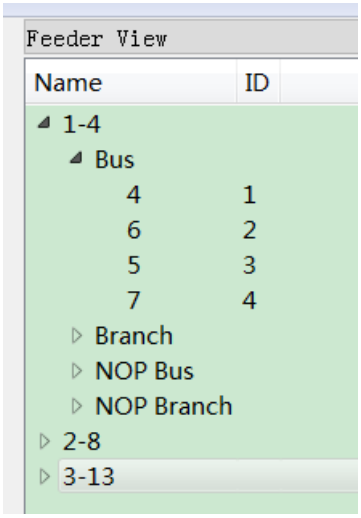

Figure C.8 Feeder View

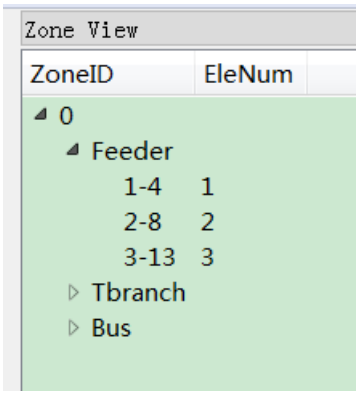

Figure C.9 Zone View

The report of load flow results is shown in Figure C.10. It displays the sending *P*, receiving *P*, and *P* loss of each branch and the total *P* loss of the network.

ID	From Bus	ID	To Bus	Branch Name	Branch ID	Status	SendMW	RecvMW	Loss(MW)
0	1	10	4	1-4	0	1	8.584	8.521	0.063
1	10	5	14	10-14	1	0	0.000	0.000	0.000
2	11	11	5	11-5	2	0	0.000	0.000	0.000
2	11	15	9	11-9	3	1	0.600	0.600	0.000
4	13	6	15	13-15	4	1	3.111	3.102	0.009
5	14	4	13	14-13	5	1	1.000	1.001	0.001
7	16	6	15	16-15	6	1	2.100	2.102	0.002
8	2	14	8	2-8	7	1	15.501	15.206	0.294
9	3	4	13	3-13	8	1	5.147	5.112	0.036
10	4	11	5	4-5	9	1	3.008	3.000	0.008
10	4	12	6	4-6	10	1	3.514	3.501	0.012
12	6	13	7	6-7	11	1	1.501	1.500	0.001
13	7	7	16	7-16	12	0	0.000	0.000	0.000
14	8	1	10	8-10	13	1	1.001	1.000	0.002
14	8	15	9	8-9	14	1	10.208	10.117	0.091
15	9	3	12	9-12	15	1	4.517	4.500	0.017
	Active Power Loss:		0.536	MW					

Figure C.10 Report of load flow results

4. Loss Optimisation Function

The loss optimisation function optimises the network *P* loss by using the network reconfiguration algorithm introduced in Chapter 3. Before starting the loss optimisation, the network model and topology data file need to be imported by the Network Model and Topologies buttons respectively. These two buttons are shown in Figure C.11.

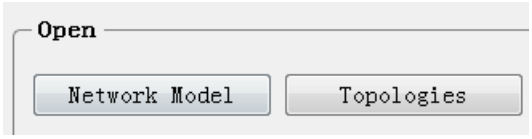

Figure C.11 Network Model and Topologies button

The reports of the loss optimisation contain two parts: an overall report and reports of each candidate topology. The overall report in Figure C.12 shows the loss information and the number of branches that are either opened or closed. If the number of 'no action' branches is equal to the number of open branches in the original network, the line of this topology is marked as light grey to indicate this is the topology of the original network. As introduced in section 3.6, the network *P* loss

are calculated in two ways: the network as whole and the network as zones. The columns “TOG” and “SEP” under “Final Loss” displays the *P* loss of topologies calculated as a whole network and separate zones respectively.

System Report | Overall Report | Topo_1 | Topo_2 | Topo_3 | Topo_4 | Topo_5 | Topo_6 | Top

1	2	3	4	5	6	8	9	10	11
TopoID	Original Loss (MW)	Final Loss(MW)		Saving		Operation branch Num			
		TOG	SEP	(MW)	%	Action(C+O)	Close	Open	No Action
1	0.536	0.501	0.501	0.035	6.553	4	2	2	1
2	0.536	0.518	0.518	0.019	3.488	2	1	1	2
3	0.536	0.518	0.518	0.018	3.366	6	3	3	0
4	0.536	0.518	0.518	0.018	3.348	2	1	1	2
5	0.536	0.528	0.528	0.008	1.566	6	3	3	0
6	0.536	0.530	0.530	0.007	1.279	4	2	2	1
7	0.536	0.536	0.536	0.000	0.000	0	0	0	3

Figure C.12 Overall report of loss optimisation

The report of each topology contains two sub reports in separated tabs: the feeder report and the switch action report. The feeder report in Figure C.13 shows the load and power loss change of each feeder. If the power loss of a feeder increases, the line of this feeder is marked with yellow. The switch report in Figure C.14 shows the details of switch operation.

Feeder | Switch Actions

Feeder	Initial Load				Final Load				Initial Loss	Final Loss	Change Loss	
	MW	MVar	Bus No.	Cust. No.	MW	MVar	Bus No.	Cust. No.	MW	MW	MW	%
1-4	8.500	5.100	5	0	8.500	5.100	5	0	0.084	0.055	0.029	35.064
2-8	15.100	8.700	6	0	14.100	7.800	5	0	0.405	0.948	-0.543	134.202
3-13	5.100	3.500	5	0	6.100	4.400	6	0	0.047	9.620	-9.573	20164.586

Figure C.13 Feeder Report of loss minimization

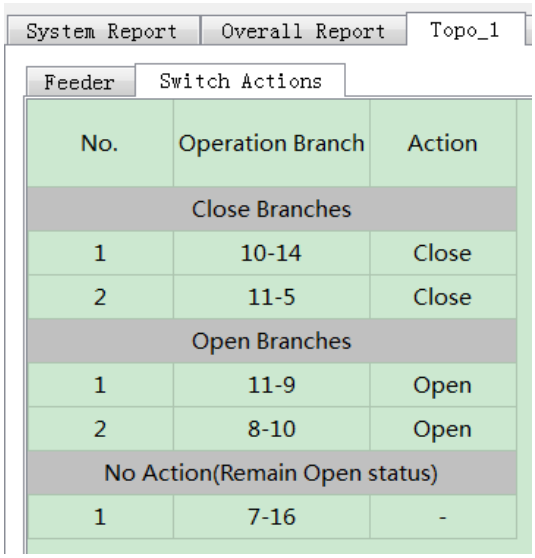

Figure C.14 Switch action report of loss minimization

5. Load Curve *P* loss Optimisation Function

The load curve loss optimisation function uses the loss optimisation algorithm introduced in chapter 3 to find the minimum *P* loss network topology of each point of the load curve and gives advice on how often to perform a network reconfiguration. For each load curve point, the open branches of the topology that has the minimum *P* loss are recorded. In order to show the change of the open branches during the duration of the load curve, the open branches of each time point are put together and shown in the same column of the report. The specific open branches at the specific time point are marked with light grey color. Figure C.15 shows the report of load curve *P* loss optimisation results. If the open branches of the current time point is different from the previous time point, the topology change cell of the current time point is marked as yellow to indicate that the network topology has been changed.

	1	2	3	4	5	6
1	Time Point	Time 1	Time 2	Time 3	Time 4	Time 5
2	Original Loss(MW)	OL 1	OL 2	OL 3	OL 4	OL 5
3	New Loss(MW)	NL 1	NL 2	NL 3	NL 4	NL 5
4	Topology Changed					
5	Open branches					
6	Branch 1					
7	Branch 2					
8	Branch 3					
9	Branch 4					
10	Branch 5					

Figure C.15 Load curve loss optimise report

The purpose of the load curve loss optimisation function is to show how often the network needs to be reconfigured when the loads vary. The accuracy of the result depends on the accuracy of load data during a required time period.

6. Reliability Evaluation Function

The reliability evaluation function of DisOPT uses the algorithm introduced in Chapters 4 and 5. Besides the IPSA network model, the reliability data of the model are required as well. The reliability data input dialog is shown in Figure C.16.

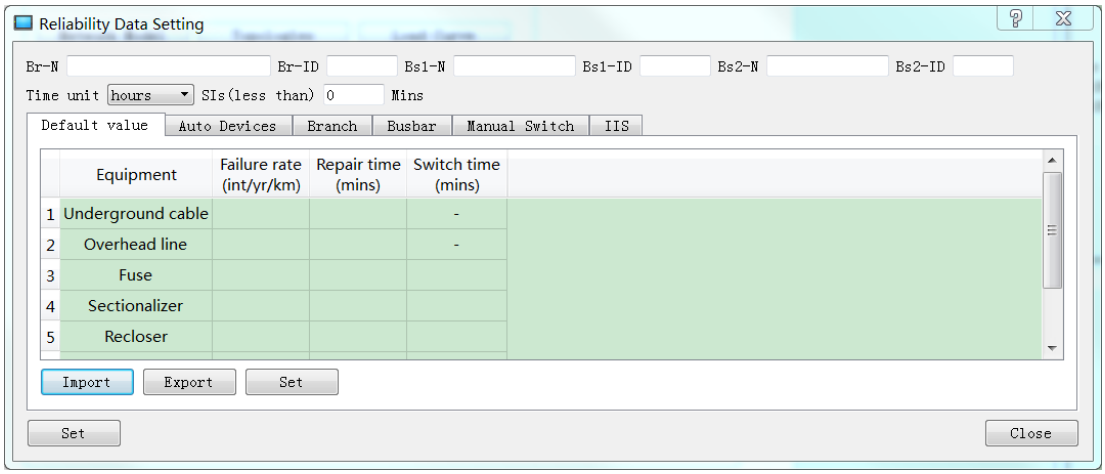

Figure C.16 Reliability data input dialog

The dialog contains the following six separated tab which control the reliability data input of different elements :

1) Default value tab

The default value tab is shown in Figure C.17. The default reliability input data

of underground cable, overhead line, fuse, sectionaliser, recloser, circuit breaker and remote control switch can be set in this tab to avoid much of the input work for a very large network. This tab provides a very simple device library to simplify the data input. A powerful device library will be achieved by a SQLite database in future work.

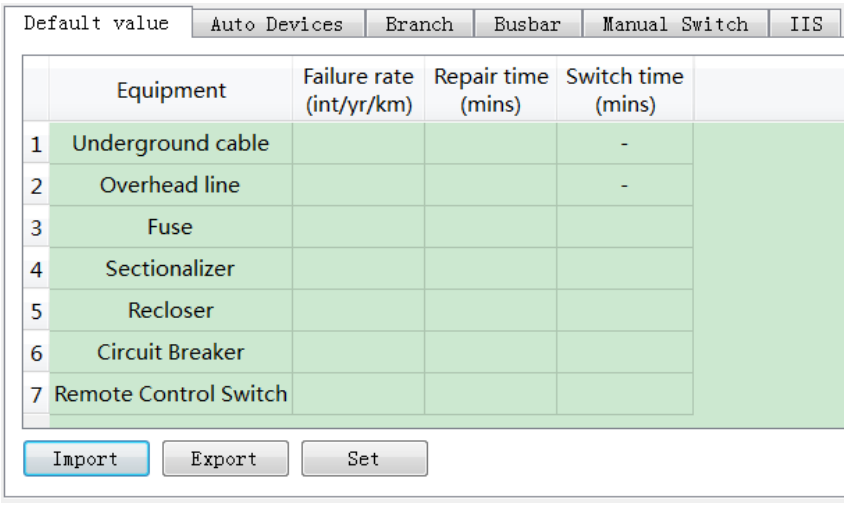

Figure C.17 Dialog of Default value tab

2) Auto Devices tab

The reliability data of protection device and remote controlled can be set in the dialog shown in Figure C.18. The types of the protection device which are modeled in DisOPT are shown in the droplist. And when a branch name or ID is input, the two nodes of this branch are shown in the droplist as well. These designs improve the data input experiences.

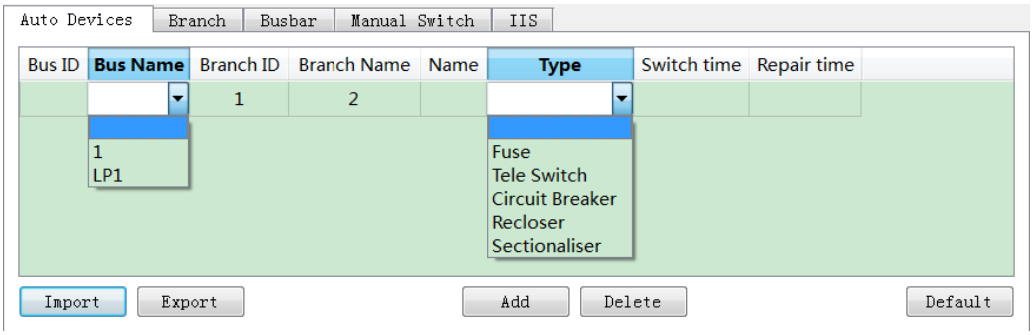

Figure C.18 Dialog of auto devices tab

3) Branch tab

The fault rate and repair time of a branch can be set in the dialog in Figure C.19.

The other data of the branch are read from the ISPA network model directly.

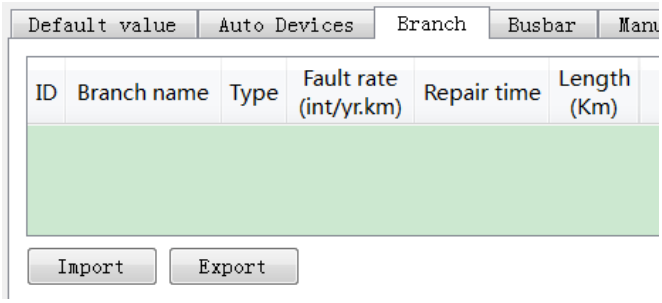

Figure C.19 Dialog of branch tab

4) Busbar tab

The number of customers connected at each busbar can be set in the dialog in Figure C.20. When an IPSA network model is imported, all busbars of this model is shown in this dialog automatically.

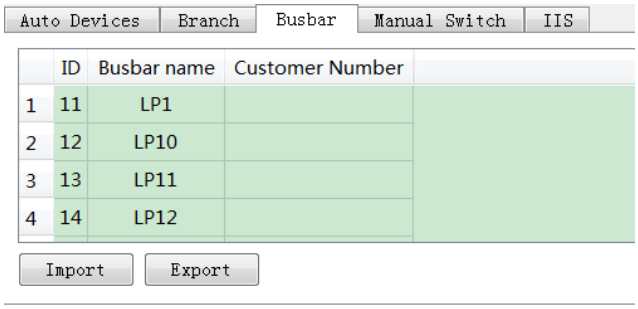

Figure C.20 Dialog of busbar tab

5) Manual switch tab

As shown in Figure C.21, the reliability data of manual switches are integrated in branch data. All branches of the network are displayed in this dialog automatically when a network model is imported. When the network contains a large number of manual switches, the user can click the Add all button to add manual switches to both sides of each branch and then delete the branches without manual switches from the list of manual switches. Or, when the number of manual switches is small, the user can delete all manual switches and then add the branches with manual switches. This feature improves the efficiency of the manual switch data input.

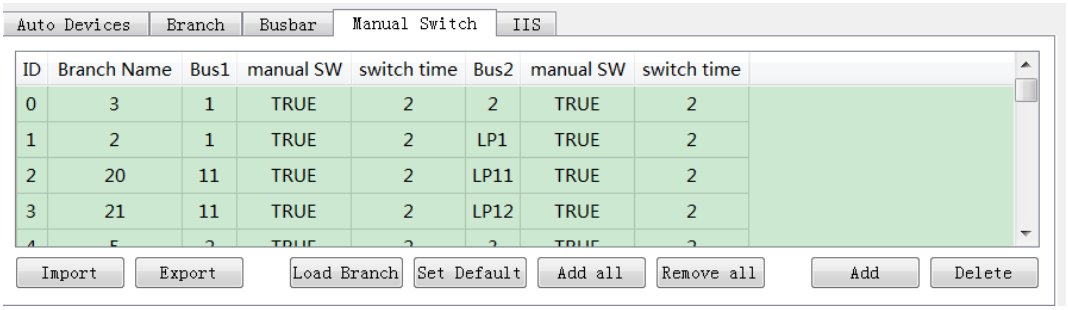

Figure C.21 Dialog in manual switch tab

6) IIS tab

As shown in Figure C.22, the reference value and incentive rate of *CI* and *CML* can be set in this dialog.

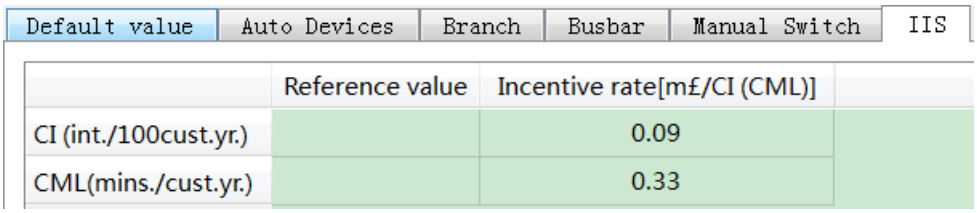

Figure C.22 Dialog in IIS tab

The data in the above tabs can be saved in a CSV file so that they can be imported directly in the next use. DisOPT provides a tree view and a graph to visualize the protection zone information of the network. The tree view in Figure C.23 display the following information of a protection zone:

a) the protection device information: the branch and bus it connects to; device type; switch time; repair time.
b) the downstream protection zones that connect to this protection zone
c) the remote control switches in this protection zone
d) the branches in this protection zone
e) the busbars in this protection zone

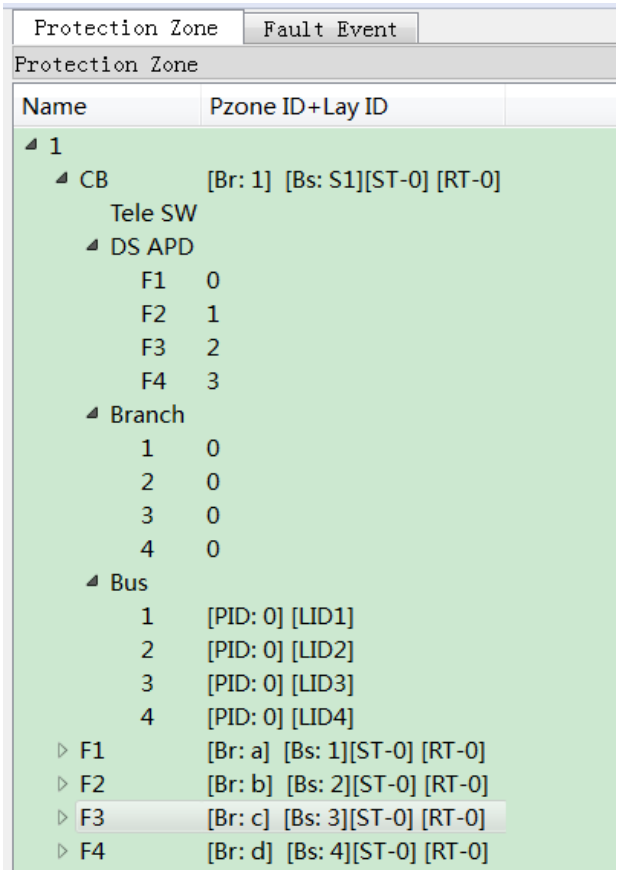

Figure C.23 Tree view of protection zone

In order to generate the graph of the protection zone, DisOPT generates the code of the graph in the dot language. Then the codes are converted to graph by Graphviz. Graphviz is an open source graph tool software developed by AT&T Research Labs [180]. The dot code generation dialog is shown in Figure C.24.

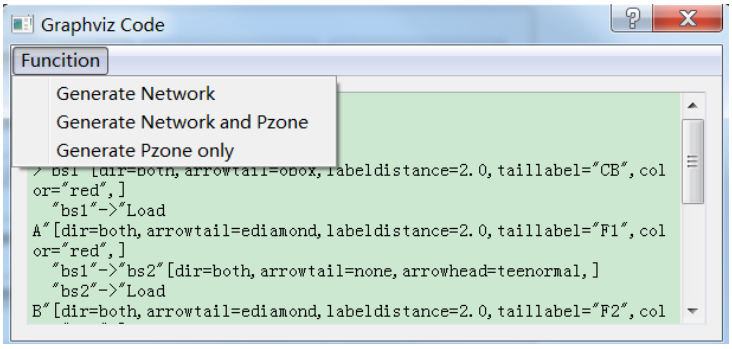

Figure C.24 Dot code generation dialog

DisOPT provides the following three view modes of the protection zone:

1) Network with protection devices and switches

As shown in Figure C.25, the circle represents a busbar; a small red diamond represents a fuse; a yellow rectangular represents a busbar connected with a source; an arrow represents a branch and its normal power flow direction; a red small square represents the circuit breaker; and a short line on the end of a branch represents a manual switch.

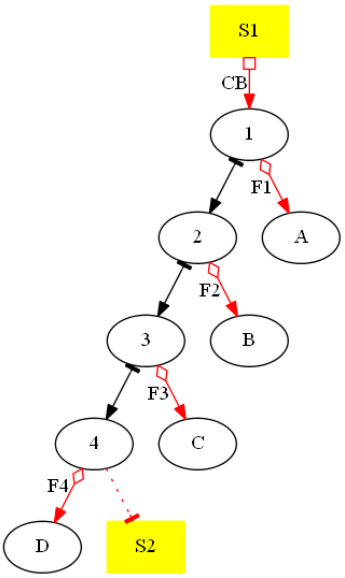

Figure C.25 The positions of protection devices and switches on the network

2) Network with protection zone

As shown in Figure C.26, the symbols used in this graph are the same as the symbols used in Figure C.25. The busbars in the same protection are marked in the same colour and enclosed by a large rectangle.

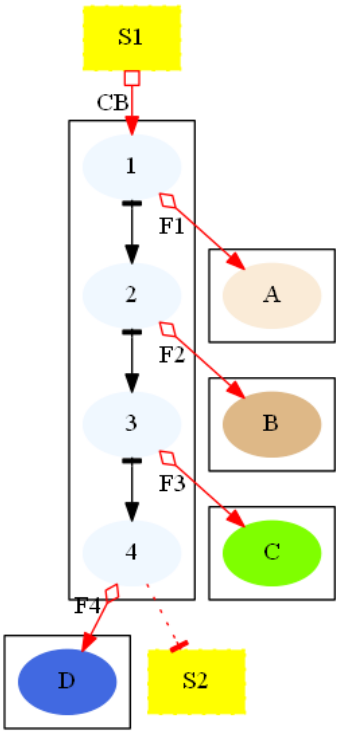

Figure C.26 The protection zones of the network

3) Protection zones position zones relationship

As shown in Figure C.27, a circle represents a protection zone and an arrow points from the upstream protection zone to a neighbouring downstream zone.

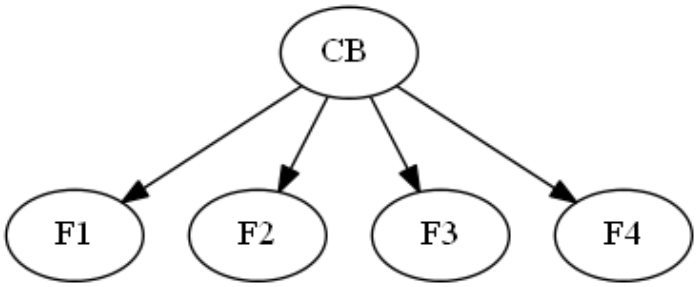

Figure C.27 The position relationships among the protection zones

The reports of reliability load point indices and system indices are shown in Figure C.28 and Figure C.29 respectively. Besides *CI* and *CML*, SAIDI and SAIFI are calculated as well. Since many papers use SAIDI and SAIDI as the system indices, providing these two values makes it easy for the user to compare the results with examples in published papers.

Load data | Bus fault records

	ID	Bus name	f duration[hours/mins]	f rate	Cust Num
1	4	A	1.5	1	1000
2	5	B	1.95	1.4	800
3	6	C	2.25	1.2	700
4	7	D	1.5	1	500

Figure C.28 Report of the load point indices

System Indices | Load indices | Bus fault records

	Index	Value	Unit	Description
1	N		-	Total number of customer sevred
2	CI		int./100cust.yr.	Customers interruptions
3	CML		mins./cust.yr.	Customer minutes lost
4	SAIFI		int/yr.cust.	System average Interruption frequency Index
5	SAIDI		h./yr.cust.	System average Interruption duration Index
6	CI_R/P		m£	CI rewards/penalties
7	CML_R/P		m£	CML rewards/penalties
8	IIS		m£	Interruptions and Incentive Scheme(CML+CI)

Figure C.29 Reliability indices report

Besides outputting the reliability indices, the advantage of DisOPT is that it provides two view modes of fault events. The “Bus fault records” tab in Figure C.30 displays all fault events that affect the chosen load point in tree view. The fault rate and fault duration of each fault event are also shown. The “Fault event” window in Figure C.31 shows which busbars are affected by the chosen fault event and the restoration methods and durations for these busbars. Each fault event has 7 groups which represent the different restoration methods. Busbars in the same group have the same restoration method. The restoration method that each group represents are explained in Table C-1. The group without busbars does not display in “Fault event” window. The advantages of displaying the details of each fault events are:

1) The fault durations and restoration methods calculated by the software can be compared with the real data from the realistic operation so that the accuracy of DisOPT can be evaluated.

2) It can help the distribution network planner to find the method to improve network reliability performance. For example, the effects of different positions of remote control switches can be investigated.

System Indices | Load indices | Bus fault records

Fault Event	fault duration [h/yr] or [mins/yr]	fault rate [int/yr]	Recorded in CI/CML
Feede-1			
[bus: A]	1.5	1	
1-[bran: 1]	4	0.2	Y
2-[bran: 2]	0.5	0.1	Y
3-[bran: 3]	0.5	0.3	Y
4-[bran: 4]	0.5	0.2	Y
5-[bran: a]	2	0.2	Y
[bus: B]	1.95	1.4	
[bus: C]	2.25	1.2	
[bus: D]	1.5	1	

Figure C.30 The tab of bus fault record

Fault Event | Feeder View | Zone View

Fault Event

Fault Branch	Fault Duration(hours/mins)
Feede-1	
1	Circuitbreaker
Repair of fault	branch repair duration
1	4
A	4
DW MSW Transfer Buses	MSW switch time
4	[0.5] [OBr: 4-S2]
3	[0.5] [OBr: 4-S2]
2	[0.5] [OBr: 4-S2]
D	[0.5] [OBr: 4-S2]
C	[0.5] [OBr: 4-S2]
B	[0.5] [OBr: 4-S2]
2	Circuitbreaker
3	Circuitbreaker
4	Circuitbreaker
a	Fuse
b	Fuse
c	Fuse
d	Fuse

Figure C.31 The tab of fault event

Table C-1 The explanations of the each group

Group name	Restoration method
UP RCS Restore Buses	the upstream buses restored by remote controlled switch
UP MSW Restore Buses	the upstream buses restored by manual switch
ulNOP RCS Transfer Buses	the buses restored by upstream normally open point and remote controlled switch
ulNOP MSW Transfer Buses	the buses restored by upstream normally open point and manual switch
Repair of fault	the buses restored when the fault is repaired
DW MSW Restore Buses	the buses restored by downstream normally open point and manual switch
DW RCS Restore Buses	the buses restored by downstream normally open point and remote controlled switch

7. Network Reliability Optimisation

The network reliability optimisation function optimizes the network's CI and CML by using the algorithm introduced in section 5.8. Before starting the reliability optimisation, the reliability evaluation of the initial network topology is run to get the initial CI and CML.

The reports of reliability optimisation contain two parts: overall report, open branches of output topologies report and reports of each candidate topology. The overall report in Figure C.32 shows the reliability indices information and the number of branches with different actions. If the number of no action branches is equal to the open branch number of the original network, the line of this topology is marked as light grey to indicate this is the topology of the original network. The report of output topologies' open branches is shown in Figure C.33. The report of each topology is displayed in separate tabs and contains two sub-reports: system indices report shown in Figure C.34 and switch action report shown in Figure C.35.

System Report | Topology OpenBranch | Topo_1 | Topo_2 | Topo_3 | Topo_4 | Topo_5

		New					Change					Branch Action			
2	TopoID	115.333	102.4	0	0	0									
3		CI (int./100cust.yr.)	CML (mins./cust.yr.)	CI R/P (m£)	CML R/P (m£)	CI+CML R/P (m£)	CI (int./100cust.yr.)	CML (mins./cust.yr.)	CI R/P (m£)	CML R/P (m£)	CI+CML R/P (m£)	Close+ Open	Close	Open	No Action
4	1	65.333	70.200	4.500	10.626	15.126	50.000	32.200	4.500	10.626	15.126	2	1	1	0
5	2	87.000	84.400	2.550	5.940	8.490	28.333	18.000	2.550	5.940	8.490	2	1	1	0
6	3	82.000	87.500	3.000	4.917	7.917	33.333	14.900	3.000	4.917	7.917	2	1	1	0
7	4	105.333	105.100	0.900	-0.891	0.009	10.000	-2.700	0.900	-0.891	0.009	2	1	1	0
8	5	115.333	102.400	0.000	0.000	0.000	0.000	0.000	0.000	0.000	0.000	0	0	0	1

Figure C.32 The system report of reliability optimisation

System Report | Topology OpenBranch | Topo_1

	1	2
1	1	2-3
2	2	3-4
3	3	1-2
4	4	S1-1
5	5	4-S2

Figure C.33 Open branches of output topologies

System Report | Topology OpenBranch | Topo_1 | Topo_2 | Topo_3

System Indices | Switch Actions

Index	Value	Change	Change%
CI(int/yr.cust)	65.333	50.000	43.353
CML(mins/yr)	70.200	32.200	31.445
CI Re/Pe (£m)	4.500	4.500	-
CML Re/Pe (£m)	10.626	10.626	-
CI+CML Re/Pe (£m)	15.126	15.126	-

Figure C.34 System indices report of each output topology

System Report | Topology OpenBranch | Topo_1

System Indices | Switch Actions

No.	Operation Branch	Action
Close Branches		
1	4-S2	Close
Open Branches		
1	2-3	Open

Figure C.35 The switch action report of each output topology